UNIVERSITY OF UDINE

Polytechnic Department of Engineering and Architecture

IN COOPERATION WITH

EURAC research

Institute for Renewable Energy

Doctoral Degree in
Environmental and Energy Engineering Science

XXVIII Cycle

Development of a Dynamic Test Procedure for the Laboratory Characterization of HVAC systems

Author:

Diego Menegon

Supervisor:

Giovanni Cortella

Onorio Saro

Roberto Fedrizzi

Date:

15 April 2016

Abstract

The heating and cooling demand requires about the 40 % of the energy consumptions. This demand is mainly satisfied by means of electricity or fossil fuels driven systems. The alternative is the implementation of renewable sources, whose large market potential has still not been fully reached due to high investment costs, lack of knowledge of designers and installers, lack of reliability, lack of test procedures to characterize systems' performance before marketing.

Hybrid systems implement different energy sources into one system. The interaction of different components, the complex layout required for the implementation of different sources, the working principle of components (continuous or discontinuous modes) and the control strategy affect the performance of those systems. The characterization of system performance is not trivial on account of the influence of those numerous factors. Different standards are available to test single components (chillers or heat pumps) or solar systems but not all the available technologies are covered (i.e. adsorption chillers driven). Most of them foresee only stationary characterization disregarding the effects of dynamic working conditions. The performance evaluation under stationary conditions is not sufficient to perform a reliable evaluation of performance.

The work of this thesis regards the development of a dynamic test procedure for the laboratory characterization of heating and cooling systems. The activity is divided into two mains parts. The first one regards the development and application of the procedure at component level while in the second one the procedure was further developed for the application at system level.

In the procedure developed at component level, the seasonal boundary conditions of the tested component are defined considering its interaction with the system by means of a numerical simulation. From the seasonal boundary conditions, a short sequence is defined by classifying the working conditions and selecting a representative part. From the test results of the sequence, the seasonal performances are extrapolated. Numerous tests have been carried out in order to validate the procedure, according to several criteria. The tests were performed on an adsorption chiller (SorTech ACS 08) and on an electrically driven heat pump (Clivet WSHN-EE 31). The performances evaluated with a short sequence deviate from the seasonal ones about 2 % and the dynamic tests highlight the behaviour of those components under dynamic conditions. Furthermore, the results have been compared with those obtained by two other available test methods. The first is the bin method (EN 14825) that uses stationary tests of the chiller at full and part-load to evaluate its seasonal performance. The second is the Component Testing – System Simulation method that requires a numerical model validated by stationary test; the seasonal performances are evaluated by means of a component simulation. The deviation of developed method with the two mentioned procedures are calculated. For the adsorption chiller, the dynamic test estimates performances 15 % lower than the two methods while for the heat pump the deviation depends from the working mode. In heating mode, the deviation is about 5 % while in cooling is about 29% since the machine is controlled with numerous starts and stops; in this second case the effect of transients becomes important.

The whole system test procedure has been developed with the objective to be at the same time easily implemented, cost attractive for industries and reliable. The adaption of the procedure at system level does not require any more simulations of the system to define the boundary conditions, which are taken directly from the wheatear file simplifying this phase. However, not all the components of the system are installed in the test facility and therefore emulation models are needed. The emulation is performed without commercial software. The selection of a short sequence is performed classifying the days using clustering analysis.

The procedure is applied to a hybrid system (a solar assisted heat pump system) considering four European climates (Bolzano, Zurich, Gdansk and Rome). The seasonal performance figures are extrapolated from the test results and compared with the annual simulation of the system. In all the test cases, the seasonal performance factors are lower than the simulated one up to about 20 % (only one case is 20 %, the others are up to 10 %). The simulation disregards some transient behaviours that are visible during the test. Moreover, the test allows to highlight some limits of the tested system such as the control of storage charge, inefficient use of solar energy for the space heating and control of heat pump. The advantage of the dynamic test is that the test outcome also gives advice for the improvement of the system layout and or control.

At the “Institute for Solar Energy SPF” of the “University of Applied Science of Rapperswil HSR” in Switzerland, a six-day sequence has been developed to perform a direct evaluation of performance in order to reduce the cost of test (from a twelve-days to a six-days test). The sequence has been developed and optimized for a reference solar assisted heat pump system. About one hundred different systems were simulated to verify the representativeness of sequence for different system configurations. The deviation of performance figures extrapolated directly from test (with a 365/6 multiplication factor) and the annual simulation are used as indicators of the representativeness of the six-day sequence. Some independent parameters lead to a predictable deviation in the performance evaluation that can be greatly reduced by simple correction factors. These parameters can be reduced to the nominal collector field power and to storage losses. The deviation is reduced to a maximum value of 5 % and a standard deviation of 21.5 % for the different systems studied. The sequence developed at the SPF-HSR is compared to the sequence defined with the methodology presented in this thesis. The deviation of the total seasonal performance factor evaluated with the two methods is about 1 %.

Acknowledgements

A mê mari, gno pari e.. a la me frute…

The first and most important acknowledgement goes to my parents and my family, for the education and support given me until now and, I know, for the future.

A special thanks to the two external reviewers David Chèze and Ivan Malenković for the time spent for the revision and the precious comments given.

I am grateful to the tutors, the professor Giovanni Cortella and the professor Onorio Saro for their help.

I would thank the Institute for Renewable Energy of EURAC for the experience that allowed me to do during these three year. Especially Roberto Fedrizzi, the coordinator of the research group "Sustainable heating and cooling systems". I thank Alice that has followed me for the first part of my PhD. In addition to them, for the practical work I thank for the collaboration of David, Valentino, Anton, Radko, Simone and Diego. A thank also for the administrative support of the institute staff: Alexa, Laura, Valentina, Cristina, Cristiana.

During this experience I meet a lot of valid people that helped me with some discussions and/or spending free time together: Alessandro, David, Davide B., Davide R., Matteo, Giorgio, Giuseppe, Giovanni and my new neighbours Matteo and Marco and ALL THE OTHERS.

I spent six months abroad that for me has been a double experience of life and working. I would thank to Matthias and Michel that have guested me at the Institute for Solar Energy of the University of Applied Science of Rapperswil. I'm grateful to Michel and Robert for having followed me and to all the great people that I met (Roland, Andrejs, Mihaela, Monica, Patrick, Andreas, Dani and all the others). During this activity I had the possibility to collaborate with two experts as Chris and Tomas I thank them for the collaboration on one paper writing.

And, last but not least, I have in my mind the friends who kept in contact (more or less) during these years of "distance" and all those who have accompanied me during these years (Fabio, Alessandro, Stefano, Mattia, Nicola, Davide, Alberto, Giovanni, Giuseppe, Antino and so on).

Table of contents

Nomenclature, Acronyms and Abbreviations

Nomenclature		Unit
h	Specific enthalpy	J/kg
H	Enthalpy	J
$\dot{m}$	Mass flow rate	kg/s
$\dot{Q}$	Heat Power	kW
$\dot{W}$	Electrical Power	kW
Q	Thermal Energy	kWh
W	Electrical Energy	kWh
E	Energy (generic)	kWh
T	Temperature	K
θ	Temperature	°C
ΔT	Temperature Difference	K
c_p	Specific Heat	J/(kgK)
τ	Time	s
δ	Deviation	-

Table 0-1: Nomenclature.

Subscripts	
in	Inlet
out	Outlet
gen	Generator
cond	Condenser
evap	Evaporator
th	Thermal
el	Electrical
h	Heating
c	Cooling
dhw	Domestic hot water
amb	ambient
max	Maximum
min	Minimum
tot	Total
seas	seasonal
avg	average
amp	amplitude
cy	Cycle
i, j , k	indexes
gf	ground floor
1f	First floor
ref	reference
sys	system
sol	solar
air	air

Table 0-2: Subscripts.

Abbreviation	
IEA	International Energy Agency
SHC	Solar Heating and Cooling
CHP	Combined heat and power
HP	Heat Pump
AdCh	Adsorption Chiller
DC	Dry cooler
SAHP	Solar assisted heat pump system
BC	Boundary conditions
DHW	Domestic hot water
SH	Space heating
SC	Space cooling
FL	Full load
PL	Partial load
SPF	Seasonal Performance Factor
PF	Performance factor
PER	Primary energy ratio
COP	Coefficient Of Performance
SCOP	Seasonal COP
EER	Energy Efficiency Ratio
SEER	Seasonal EER
SF	Solar Fraction
AF	Air Fraction
CTSS	Component test system simulation
WST	Whole system test
DST	Dynamic system testing
CCT	Concise cycle test
SCSPT	Short cycle system performance test
C	Classes
GHI	Global horizontal Irradiation
ITC	Total irradiation on collector
CF	Correction factor
cc	Correction coefficient
N	Dimension of classes matrix
n	Number of

Table 0-3: Acronyms and Abbreviations.

List of Figures and Tables

1 Introduction

In the last years, the needs of limitation of the climate changes has required different measures from different national or international institutions. As indicated by the Renewable Heating & Cooling RHC platform, the main challenges of European Union can be summarized in three principle objectives: the reduction of greenhouse gas emissions, diversification and improvement of security of energy supply and finally maintenance of industry as world leader in clean technologies [1,2]. The renewable energy sources play an important role in achieving these aims due to their large potential, and they will have more space since the governments are incentivising investments in low-carbon technologies with the purpose of achieving their carbon reduction targets [3].

The implementation of renewable sources in HVAC systems[1] of residential sector could be an important action since this sector requires about the 40 % of the overall heat consumption [1]. The reduction of fossil fuels and the increase of efficiency can be performed both in new and existing buildings. For example, different system concepts foresee the implementation of one or more renewable energy sources in one system. When two or more energy sources are implemented in the same system, this is called “hybrid system”.

With the adoption of the European Directive 2010/30/EU [4], all energy-related products should be labelled according to their energy consumption. Following the Directive, different European Regulations for heating and cooling systems have been published, as, e.g., the Regulation N. 626/2011 (specific for heat pumps) [5] and the Regulation N. 811/2013 (generic for heating systems) [6]. These documents establish that, for each system, seasonal performance figures should be provided, declaring its overall energy consumption and allowing the comparison with analogous systems.

The label is a benchmark for the end-consumer which indicates how a product is environmentally friendly and energy saving. The product is classified in a category ranging from A (best) to G (worst). This should help the consumer choosing products that allow to save energy and it incentivizes the industry to develop and design energy efficient products. An example of energy label for an air to air heat pump is showed in Figure 1-1 (Regulation N. 626/2011 [5] - EN 14825 [7]).

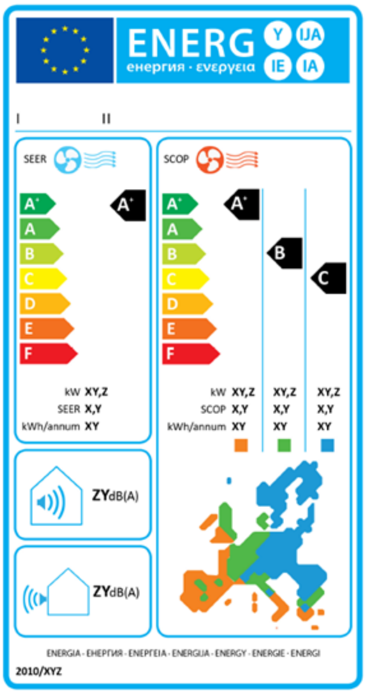

Figure 1-1: Energy label for air-to-air heat pumps.

[1] HVAC: heating, ventilation and air conditioning.

To label a product, a standardized test procedure is needed. This must satisfy different requirements (e.g. comparability and repeatability of results, clarity, simplicity, flexibility, cost effectiveness, etc.) that are usually posed by contrasting involved stakeholders. These are policy makers, customer organizations, test institutes and manufacturers. On the other hand, from a technical point of view it must allow to test a system under realistic and reproducible operating conditions.

The performance assessment of heating and cooling systems currently available on the market is not trivial since their architecture tends to be significantly more complicated than traditional installations, especially when they are exploiting renewable energy contributions, different active components and sophisticated control strategies, all together in a single system. The consequence is that the working conditions of heating and cooling systems are variable in time. Normally, dynamic working conditions are mainly due to the dynamic behaviour of the building, the system layout and its control strategy. In addition, the effect of the unstable nature of the sources has to be considered when the system is driven by a renewable energy source. To characterize the performance of such systems it is necessary to consider all these aspects in order to perform a realistic study of the system' behaviour. A test procedure should represent the system performance as it would be in the real application.

The analysis of standards (chapter 1.1, chapter 1.2 and appendix A) highlights their lacks since the most of them regard test of components under stationary conditions. At opposite, to consider the dynamic working conditions of the system, different whole system test procedures were developed but they present some open points as exhaustively described in chapter 1.3.

From these considerations, the aim of this work is to develop a test method for the laboratory characterization of thermal systems. The development of the procedure is divided in two phases. The first part is the definition of a dynamic procedure for the characterization of components like sorption chiller, heat pump, gas boiler and so on. The procedure is presented in the second chapter which also contains the results of two case studies. The analysis performed highlights how, for a correct evaluation of the seasonal performance of the unit, it is necessary to consider its real operation and include also dynamic and transient effects. Of course, the implementation of a seasonal dynamic test is both costly and time consuming, and therefore it is not an option in a real application. In order to resolve this challenges, it is necessary to perform similar evaluations with a short test sequence, easily reproducible in a laboratory and, at the same time, capable of capturing all important features of the machine operation. To this end, a short dynamic test sequence has been elaborated and the results obtained experimentally have been compared with the whole season tests.

With the promising results obtained in the first phase, the procedure has been further developed to be applied for the characterization of whole system. This procedure evolution allows to overcome some limitations given by the characterization at component level.

The work carried out at system level is divided in three chapters. The third chapter presents the test method while the fourth chapter contains the procedure for the definition of the short sequence; it is demonstrated (4.2.1) that the selection procedure developed in second chapter is not suitable in the whole system application and the clustering method has been adopted instead. The application of the procedure developed in chapter 3 and chapter 4 is presented in the fifth chapter on an example of a solar assisted heat pump system (SAHP). The system has been tested for different climates and for different sequence durations. The climates of Bolzano, Zurich, Gdansk and Rome are considered. Other systems (i.e. adsorption chiller driven by a solar collector) will be studied as further development of the procedure.

In the sixth chapter, the definition of a six-days sequence for the Concise Cycle Test (CCT) method is presented. The aim of this task is to reduce the twelve-days sequence to six-days in a way to perform a direct extrapolation of seasonal performances. A parametric analysis has been performed to verify the validity of the sequence for about one hundred configurations. From these simulations, correction factors are defined to reduce the deviation obtained by a direct extrapolation. This sequence is compared with the sequence defined in the fourth chapter with clustering method and the two methods are compared through the simulation of the case study as introduced in the fifth chapter.

1.1 Methods for the evaluation of seasonal performance

Specific standards for the characterization of complex or hybrid heating and cooling systems are not yet available. On the other hand, a variety of standards for single components, specific combinations of those or particular applications can be accessed. The standards for solar collectors, solar systems and heat pumps (or chillers) are presented in Appendix A.

The analysis of standards has led to the conclusion that:

- Lacks of consistent and common performance figures;
- Not all the technologies present in the market are covered by the standard test methods;
- The test conditions are somehow questionable;
- The inertial effects, control strategies and longtime performances in most cases are not considered.

To evaluate the seasonal performance, different approaches can be identified: the Bin Method [7–9] and the Component-Testing-System-Simulation (CTSS) techniques [10–14] are relatively consolidated, being based on the test of the single components. On the other hand, recent approaches, as the Concise Cycle Test (CCT) [15–17], the Short Cycle System Performance Test (SCSPT) [18–23], the Combitest [24–28] and the Dynamic System Testing (DST) [29,30] move towards the Whole System Testing (WST).

These different procedures are classified in Table 1-1 distinguishing:

- the boundaries considered during the test (component/system);
- test conditions (indoor/outdoor or steady state/dynamic conditions);
- model of the system behaviour (physical model/ performance map);
- method of assessment of long term performance from short test sequence results (simulations, extrapolation or frequency distribution).

Table 1-1: Classification of rating methods for solar heating and cooling systems. Source [31].

Method	Institution	Physical boundary	Measure location	Measure boundary conditions	Description of equipment under test	Calculation of long term performance
Bin method	Fraunhofer-ISE (Germany)	Component	Indoor laboratory	Steady-state conditions	Performance map	Frequency distribution
CTSS	ITW (Germany)	Component	Indoor/Outdoor laboratory	Steady-state/ dynamic conditions	Physical model parameters	Simulation
DST	ITW (Germany)	Whole system	In-situ/Outdoor laboratory	Dynamic conditions	Physical model parameters	Simulation
Combitest	SERC (Sweden)	Whole system	Indoor laboratory	Controlled dynamic conditions	Performance point	Direct extrapolation
CCT	SPF (Switzerland)	Whole system	Indoor laboratory	Controlled dynamic conditions	Physical model parameters	Simulation
SCSPT	CEA-INES (France)	Whole system	Indoor laboratory	Controlled dynamic conditions	Performance point	Direct extrapolation

1.1.1 Performance figures

To characterize the performance of the chillers/heat pumps, the standard EN 14825 [7] describes the performance ratios for electrically driven units. The performance figures identified for the heat pumps, for heating and cooling working modes are respectively the coefficient of performance (COP) and the energy efficiency ratio (EER).

Equation 1-1

$$COP_{el} = \frac{\dot{Q}_{cond}}{\dot{W}_{in}} \quad [-]$$

Equation 1-2 $$EER_{el} = \frac{\dot{Q}_{evap}}{\dot{W}_{in}}$$ [-]

where $\dot{Q}_{cond}$ and $\dot{Q}_{evap}$ are respectively the condenser and evaporator powers while and $\dot{W}_{in}$ is the electrical input power.

For the thermally driven heat pumps or chillers, only the standard EN 12309 [32] considers a performance figure that is limited to the gas fired generators. That standard defines the Gas Utilization Efficiency as the ratio between useful energy and the energy consumed with the combustion. To have a general equation valid for the different sorption chiller or heat pump, the thermal COP or thermal EER could be calculated considering the input thermal power:

Equation 1-3 $$COP_{th} = \frac{\dot{Q}_{cond}}{\dot{Q}_{in}}$$ [-]

Equation 1-4 $$EER_{th} = \frac{\dot{Q}_{evap}}{\dot{Q}_{in}}$$ [-]

For the calculation of the seasonal coefficient of performance (SCOP) or the seasonal energy efficiency ratio (SEER), the standard considers the hourly values of heating power and COP (or cooling power and EER), retrieved from stationary tests, as a function of the external temperature:

Equation 1-5 $$SCOP_{ON} = \frac{\sum_{i=1}^{n}\left(\tau_i \cdot \dot{Q}_{heating,i}(T_{amb})\right)}{\sum_{i=1}^{n}\left(\tau_i \cdot \frac{\dot{Q}_{heating,i}(T_{amb})}{COP_i(T_{amb})}\right)}$$ [-]

Equation 1-6 $$SEER_{ON} = \frac{\sum_{i=1}^{n}\left(\tau_i \cdot \dot{Q}_{chilling,i}(T_{amb})\right)}{\sum_{i=1}^{n}\left(\tau_i \cdot \frac{\dot{Q}_{chilling,i}(T_{amb})}{EER_i(T_{amb})}\right)}$$ [-]

where τ_i is the duration of i-th condition, $\dot{Q}_{heating,i}$ is the heating power and $\dot{Q}_{chilling,i}$ is the chilling power T_{amb} is the external ambient temperature.

The previous equation are easy applicable to the case of the compression heat pump; however, non-continuous operation mode of sorption chillers causes power fluctuations and prevents the use of the EER_{th} in *Equation 1-6* where instantaneous values are needed. A detailed description of adsorption chillers working principles can be found in Peuser et al. [33]. In this case it is better to refer to average conditions defined with reference to one working cycle. The energy is calculated for the different circuits as integration of the power exchanged during the cycle (Equation 1-7). The EER of the cycle is calculated as the ratio of the cycle's energies (Equation 1-8):

Equation 1-7 $$Q_{cy} = \int_{\tau_{cycle,start}}^{\tau_{cycle,end}} \dot{Q}(\tau)\, d\tau$$ [kWh]

Equation 1-8 $$EER_{cy} = \frac{Q_{evap,cy}}{Q_{gen,cy}}$$ [-]

Equation 1-9 $$SEER = \frac{Q_{evap}}{Q_{gen}} = \frac{\sum_{i=1}^{n} \dot{Q}_{evap,cy,i} \cdot \tau_{cy,i}}{\sum_{i=1}^{n} \dot{Q}_{gen,cy,i} \cdot \tau_{cy,i}}$$ [-]

where $\tau_{cy,i}$ is the "i-th" cycle duration.

Considering the whole system, the energies of loads, collector yield, dry cooler, distribution system and so on are calculated from the integration of the discrete measurement of powers (Equation 1-10):

Equation 1-10 $$\mathrm{Q}_i = \int_{\tau_1}^{\tau_2} \dot{\mathrm{Q}}_i(\tau)\, d\tau = \sum_j \dot{\mathrm{Q}}_{i_j} \cdot \Delta\tau_j$$ [kWh]

Where the suffix "i" is valid for the space cooling, space heating, DHW and total loads.

From the calculation of daily (or monthly) energies, the performance factor (PF Equation 1-11) could be calculated with the ratio of "i-th" useful effect with the "i-th" energy input consumption. At the same time, the seasonal performance factor (SPF Equation 1-12) is calculated with the seasonal energies.

Equation 1-11 $$\mathrm{PF}_i = \frac{Q_{out,i}}{E_{in,i}}$$ [-]

Equation 1-12 $$\mathrm{SPF}_i = \frac{Q_{seasonal,out,i}}{E_{seasonal,in,i}}$$ [-]

Where the suffix "i" is valid for the space cooling, space heating, DHW and total loads.

Again, especially in hybrid systems, different energy sources are used for system operation (electrical energy, gas, oil, biomass or heat from the district heating network or waste heat from an industrial process). The exergy content, cost and the environmental impact is different for the different types of energies. Therefore, they should be evaluated separately: for a system with both thermal and electric energy inputs, a thermal and an electrical SPF are provided independently and therefore the consumption could be distinguished into electrical or thermal.

Equation 1-13 $$\mathrm{SPF}_{i,th} = \frac{Q_{seasonal,out,i}}{Q_{seasonal,in,i}}$$ [-]

Equation 1-14 $$\mathrm{SPF}_{i,el} = \frac{Q_{seasonal,out,i}}{W_{seasonal,in,i}}$$ [-]

Where the suffix "i" is valid for the space cooling, space heating, DHW and total loads.

To perform a more in-depth information under economic and environmental point of view, the Primary Energy Ratio (PER) defines the ratio of useful energy output to the primary energy input. In this way, each energy input has to be corrected by a factor ε that represents the conversion efficiency.

Equation 1-15 $$\mathrm{PER}_i = \frac{Q_{out,i}}{\frac{W_{in,i}}{\varepsilon_{el}} + \frac{Q_{in,i}}{\varepsilon_{th}}}$$ [-]

The primary energy ratio can be defined as "overall" or only as "non-renewable". The primary energy factors ε_i depend on the location of the system, time of the year and on local policies. However, some generalized values are given in the national Annexes of the EN 15316 or in EN 15603:2008. If substituted with emission factors (e.g. expressed in $kgCO_{2,eq}$ per kWh energy) or energy price (e.g. expressed in monetary unit per kWh energy), the equivalent CO_2 emissions or the energy costs of the system over the considered period of time can be obtained, respectively.

The primary energy could be compared to the one of a reference system defining the primary energy savings f_{sav}. The comparison is usually performed with conventional technology. The primary energy savings is calculated with the following equation:

Equation 1-16 $$\mathrm{f}_{sav} = 1 - \frac{PER_{ref}}{PER_{sys}}$$ [-]

As well as the SPF and PER, different other performance indicators might be of interest for specific systems. In solar heating and cooling systems different factors could be defied such as renewable energy ratio, solar fraction, fractional energy saving, global warming potential, etc.

The solar fraction (SF Equation 1-17) is calculated with the contribution of solar to the total load. If a backup unit is an air source heat pump, the air fraction could be considered in addition to this factor (AF Equation 1-18). That represents the contribution of air source to the total load.

Equation 1-17 $$\mathrm{SF}_i = \frac{Q_{sol,i}}{Q_i}$$ [-]

Equation 1-18 $$\mathrm{AF}_i = \frac{Q_{air,i}}{Q_i}$$ [-]

Where the suffix "i" is valid for the space cooling, space heating, DHW and total loads.

1.2 Seasonal performance from test on Component Level

In the methods described in this section, each component is tested individually according to the reference standard. The seasonal system performance figures are calculated from these results.

1.2.1 Bin Method

The Bin Method is a handy procedure used to estimate the seasonal performance of heating and cooling systems, taking into account reference operating conditions. The main features of the procedure rely on the evaluation of the cumulative frequency of the outdoor air temperature and the corresponding load variation. Those reference conditions (temperature profile and consequent load profile) are classified in bins which represents an interval of 1°C of external temperature. The cumulative frequency distribution of temperature profiles is used for the calculation of the seasonal performance parameters, along with performance figures retrieved in stationary tests at full and part load conditions.

A description of the method can be found in the standard EN 15312-4-2 [8], which implements the results of the IEA Annex 28 [9] or in the standard EN 14825 [7], for the rating of electrically driven heat pumps. The mentioned standards are used with respect to heat pumps systems, but the application of the method to hybrid system is complicated, as the dynamics of the components and the control influence can hardly be considered since the test are steady state.

Pros/Cons:

- (+) simple test bench can be used for the test of single component;
- (+) simulations are not needed for the seasonal performance assessment;
- (-) the inertial and dynamic conditions are not assessed because the tests are carried out under steady state conditions;
- (-) the effects of the interactions among components and the controller are not taken into account;

The extension of definition of bins as a function of temperature and solar irradiation was made by Schicktanz et al. [34] to consider the effect of solar gains.

1.2.2 Component Testing – System Simulation CTSS

With the Component Testing – System Simulation approach (CTSS), tests made on single components are used to validate a numerical model of the whole system, which is then used for the evaluation of the seasonal performance. The tests are usually performed under stationary conditions, again neglecting their dynamic behaviour.

The flexibility of this method, given by its component oriented approach (i.e. the components can be tested separately), additionally implies that all interactions inside complex systems and with the control are disregarded during the test phase while these factors are accounted for only during the simulation phase.

To overcome this limitation, a possible solution is proposed by use of dynamic tests to identify the parameters required to describe a detailed numerical model with artificial neural networks [35,36], while Uhlmann and Bertsch [37] experimentally investigated the effect of ON-OFF cycles on the performance of air-to-water geothermal heat pumps, to develop a more reliable numerical model of these components.

Kerskes [10] and the standard EN 12977-2 [11] present the application of the procedure to solar thermal systems (space heating and domestic hot water). Based on this application, the procedure has been adopted as Australian Standard for the solar hot water systems (AS/NZS 4234 – 2008) and for solar desiccant based air-conditioners (AS 5389:2013) [12–14]. Results on the effectiveness of this standard for practical applications in solar cooling plants are not available yet.

The dynamic effects introduced by valves and pumps (that are not tested), as well as the losses related to the pipelines are yet disregarded.

Despite the simplicity of test bench for the characterization of single component, the test of each component and the definition of model parameters for each component from test results could require a long work. Moreover, the modelling is affected by the choice of the models, the set parameter that depends from the modeller; this means that from the same test results, the same system modelled by two different people gives different results.

Pros/Cons:

- (+) simple test bench can be used for the test of single component;
- (+) the method is very flexible because the performance for different system configuration can be assessed without additional tests;
- (+) the performance of the system can be predicted for any climate or load;
- (-) the inertial and dynamic conditions are not assessed because the tests are carried out under steady state conditions;
- (-) the real effects of the interactions among components are not taken into account;
- (-) the effort of characterizing each component separately could be more time-consuming and costly, instead of a test of the whole system;
- (-) the control algorithms must be adjusted for each single case if they are not available from manufacturers;

1.3 Seasonal performance from test on System Level

Contrary to previous methods, the Whole System Test approach (WST) includes all interacting and interconnected components (pumps, pipes, sensors, valves, tanks, heating/cooling generator, etc.) into the system boundary. The annual performance can be evaluated through modelling and simulating the system or more simply by direct extrapolation. The WST approach allows to evaluate the performance of the systems taking into account dynamic conditions, inertial effects, control strategies and the controller behaviour under “close to reality” test conditions. These latter are achieved through load file or “hardware in the loop” simulations of the heat sources/sinks. On the other side, these advantages are paid with complex test bench, higher test costs and with the fact that the obtained results are usually valid only for the tested case study conditions of climate, load profiles, system configuration and its size.

The system is set-up almost completely. The exceptions are the solar collector field and the building which response usually is emulated with a real-time and online simulation tools. In the Figure 1-2 the system boundaries of different methods are indicated with different colours. Only the institute SPF considers the pipes from the heat exchangers to the source or the load (solar collector indicated with red; DHW distribution systems indicated in blue; SH distribution system indicated in green).

The basic principles are the same but the procedure differs in important details. The main differences are the definition of the experimental sequence and the post-process of the results. Haller et al. [15] and Papillon et al. [38] compared the three test method for a solar combi application. Further solar heating systems, geothermal heat pump systems’ performance are studied with dynamic tests [39]. In the next paragraphs, the main procedures are presented.

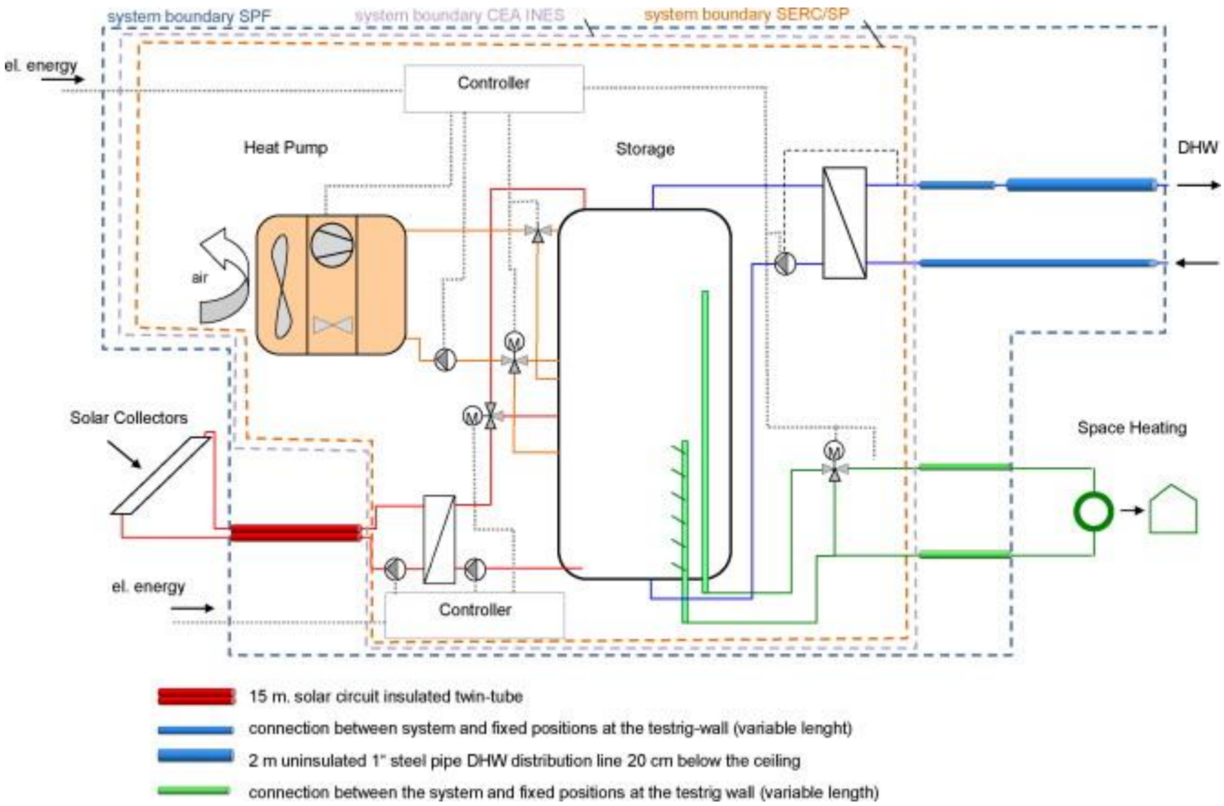

Figure 1-2: System set-up in different procedures. Source [15].

1.3.1 Dynamic System Test method - DST

For the Dynamic System Test method (DST), the system is characterized as a whole with a "black-box" approach. Short outdoor tests are performed in order to identify some parameters with a dynamic computer model. These parameters which describe the characteristics of the tested system are used to obtain the yearly performance prediction by a computer simulation for specific load and climate conditions [29]. The procedure presents some limitations on the system size. The extension of this method for the evaluation of the long term performance of combined SHP hot water systems is proposed by Panaras et al. [30].

This procedure includes only three types of sequences:

- $Ssol_A$ / $Ssol_B$ in order to assess the solar collectors' performance at high/low efficiencies;
- Sstore in order to assess the overall store losses;
- Saux is intended to rate the thermal losses and the contribution of an integrated auxiliary heater.

Pros/Cons:

- (+) dynamic effects and component interaction under realistic operating conditions are assessed;
- (+) less detailed components information compared to the CTSS method can be used to model the system;
- (+) the seasonal performance can be evaluated for different climates and buildings;
- (+) the physical model is built with parameters that have a physical meaning and are easy to understand;
- (-) the test procedure and test facility are more demanding compared to testing each single component;
- (-) for complex hybrid system the prediction of the long-term performance can result less accurately because it is difficult to create an accurate physical model;

1.3.2Concise Cycle Test - CCT

The Concise Cycle Test (CCT) is developed by the Institute for Solar Energy SPF of the University of Applied Science of Rapperswil HSR (Switzerland) [15–17]. The procedure characterizes the system performance with a twelve-days sequence and evaluates the seasonal performance with a numerical model validated with the test results.

About the test sequence, the CCT method foresees a first day for initial conditioning and other twelve-days as core sequence:

- Initial conditioning of the tank at 25-30 °C;
- Cycle conditioning: the last 18 hours of the core phase are run;
- Core phase of 12 days.

The weather data is recorded by MeteoSwiss for Zürich - Fluntern with 10 min measurement resolution. From this annual climatic data, the core sequence is selected in such a way to have:

- Representativeness of the whole cycle's temperature and irradiation average for the whole climatic year;
- Representativeness of each day for the temperature and irradiation average of the corresponding month and with natural fluctuation.

The system is installed by the manufacturer in a designated area in room that is conditioned during the test at 20°C. The insulation of the piping is made by the manufacturer installers and the testing institute do not change anything inside the technical room. The measuring points are defined considering the boundaries defined in Figure 1-2 (indicated with the label "system boundary SPF"). The components included in the system are connected with piping that are part of the tested system without additional piping.

The building model is the TRNSYS Type 56 and its active layer is used for the heat distribution. The thermostatic valves are included in the simulation. For the emulation is used the temperature set point. The flow temperature to heat distribution system is controlled by the tested system. The outdoor air temperature is generated in a small box which contain the system's sensor. Since the load file is not fixed, the heat delivered to the building is depending from the tested system.

The model of solar collector is the Type 301 by Isakson & Eriksson. A 45°C slope and south orientation is used. The collector parameters are calculated on the model chosen by the company. The maximum collector field area is 15 m^2. The power set point is used for the emulation. The fluid in the collector loop is water glycol mixture.

The draw-off profile is based on statistics used in IEA Task 26 [40]. Contrary to other two procedures, there are a distinction between volume type draw offs and energy type draw offs. The set temperature to be reached is depending on the draw off type: none, 30°C, 38°C, 40°C. 40 s is the time limit for reach the set temperature while a variable time limit is defined for reaching the energy set-point. A load file defines the cold water temperature and the number of draw off per day.

The procedure for asses the seasonal performance is described in the Figure 1-3: with all the known parameters from manufacturer's documentation and preliminary test a model is created. The missing parameters are fitted by re-simulating the test days and comparing the measured results. The whole year is simulated with the fitted model. This approach was adopted to evaluate the seasonal performance since they cannot be assessed from the experimental results with a simple proportion because the effects of thermal storages would not be correctly accounted for and the final solar fraction would not be the same. The numerical model is used also to extend the results to different climates and building. The annual performance figures are compared with a reference heating system that uses the same type of main heat source without solar thermal energy.

Pros/Cons:

- (+) dynamic effects and component interaction under realistic operating conditions are assessed;
- (+) the seasonal performance can be evaluated for different climates and buildings;
- (+) the response of the heat distribution system is simulated so that the effect of the thermostatic valves is taking into account;

- (+) the tested system controls the flow temperature to the heat distribution system;
- (±) hardware-in-the loop simulations allow to test the system under a very realistic condition but requirements that regarding the test facility and the efforts for the test procedure are high in demanding and increase the test costs;
- (-) the long-term performances are obtained through simulations;

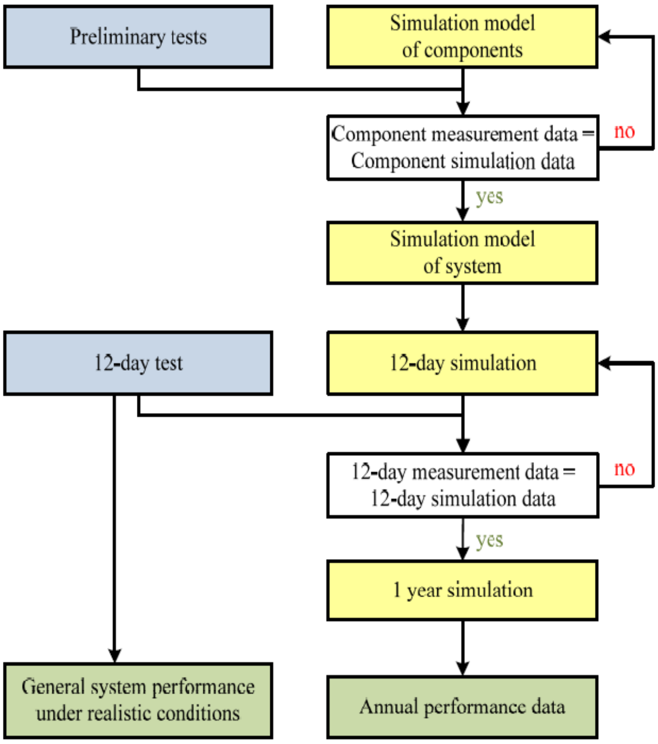

Figure 1-3: Block diagram of CCT method. Source [17].

1.3.3 Short Cycle System Performance Test - SCSPT

The Short Cycle System Performance Test (SCPST) is developed by the National Solar Energy Institute CEA INES in France [18-23]. The approach is similar to the CCT method, since the loads and the sources are emulated. The SCSPT method consists in twelve-days core sequence; the test is carried out with:

- Primary conditioning phase (8 hours) in which upper and lower parts of the storage have to be brought to reasonable temperatures;
- Secondary conditioning phase (1 day) with the simulation of one winter day. This aims to bring the storage to an energy level which corresponds to the last day of the core phase;
- Core phase of 12 days;
- Final discharge of the storage tank (8 hours).

The core twelve-days are selected through an iterative optimization process as indicated in Figure 1-4. These days are chosen such that the following criteria are satisfied:

- Auxiliary energy results that are 12/365 smaller than the annual value;
- Representativeness of the whole cycle's temperature and irradiation average for the whole climatic year;
- Representativeness of each day for the temperature and irradiation average of the corresponding month and with natural fluctuation.
- The selection is optimized in order to have a correspondence between the annual simulation results and the annual result predicted with the test sequence. If the comparison is not good, the twelve-days sequence is changed and the results compared again.

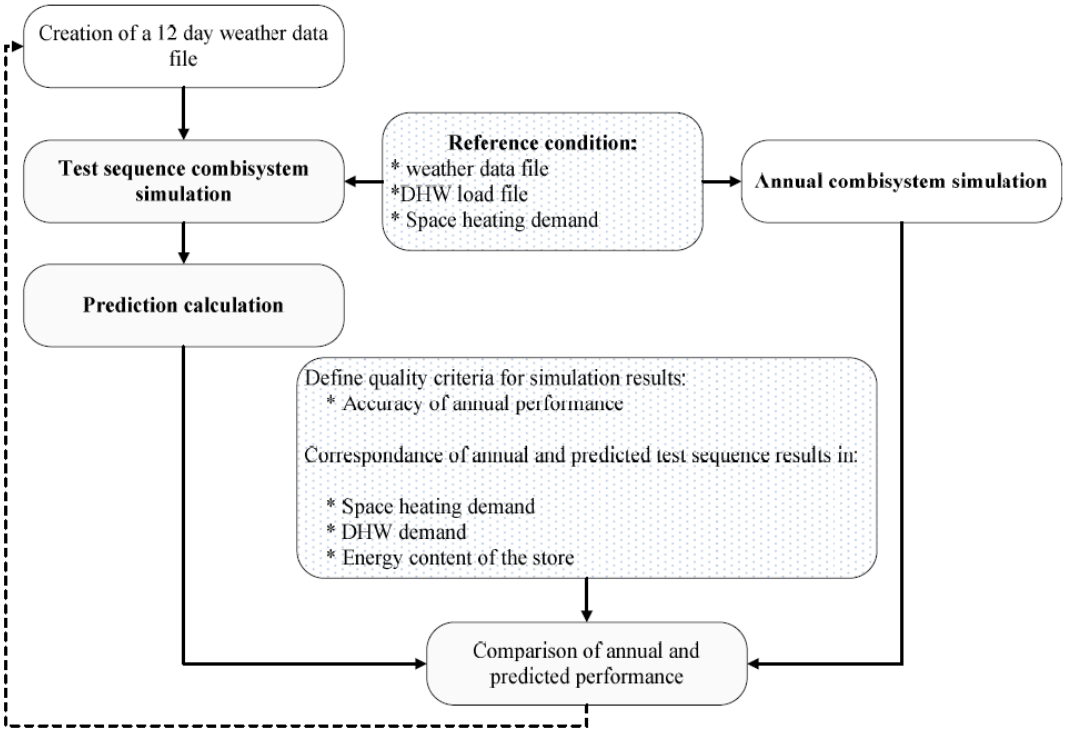

Figure 1-4: Procedure of the SCSPT method for the definition of the twelve-days sequence. Source [21].

The system is installed in a designated area in room that is conditioned during the test at 20°C. To reduce the uncertainty with regard to glycol mixture, only water is used as fluid transfer. Figure 1-2 shows the physical boundaries of the system (indicated with the label "system boundary CEA INES").

The building is simulated with the TRNSYS Type 56 or with a simplified model of building based on standard ISO 13790:2008 [41]. The models of heat distribution are user defined types, and the test could be carried selecting a radiator distribution (Type 262) or heating floor (Type 241). The software does not implement the simulation of thermostatic valves but it is physically possible to emulate them since motorized valves are already installed in the utility.

The model of solar collector is the Type 832 by Bengt Peres [42]. A 45° slope and south orientation is used. The usual field area is 16 m^2 while the limit of the maximum area is 30 m^2 (25 kW).

The draw-off profile is based on statistics used in IEA Task 26 [40]. There are defined only volume-type draw-offs (a certain volume is removed without considering the temperature of the hot water) and the number of draw off per day is variable [43]. The draw-off contains different flow rates and different volumes. The set temperature to be reached is 45 °C and time limit for reaching the set-temperature is not foreseen. A discretization of sine curve is used for the definition of the cold water temperature with temperature varying from 6°C to 14 °C.

From the measured data, the annual energy balances are evaluated by multiplying the ratio 365/12. From the annual values, the fractional energy savings are calculated comparing it with a reference heating system that uses the same type of main heat source without solar thermal energy.

To extrapolate the results to other climates and load, a procedure is currently developed [19]. The measured data is used to identify a dynamic simplified model of the whole system. The model combines simplified physical equation and an artificial neural network.

Pros/Cons:

- (+) dynamic effects and component interaction under realistic operating conditions are assessed;
- (+) the annual performance can be assessed easily with the direct extrapolation;
- (+) different climates and different buildings with various heating loads have been investigated;
- (+) it is not necessary to identify some parameters to model the system or components;
- (+) the tested system controls the flow temperature to the heat distribution system;

- (±) hardware-in-the loop simulations allow to test the system under a very realistic condition but requirements that regarding the test facility and the efforts for the test procedure are high in demanding and increase the test costs;
- (-) the test results are valid only for the set up boundary conditions (such as load and climate) and that determinate system size.

1.3.4 Combitest

The Combitest was developed by the Solar Energy Research Center SERC/SP in Sweden [24–28]. The procedure can be divided in two phases:

- Direct Characterization in which performance indicators of the whole system are obtained from an indoor test sequence;
- Annual Calculation in which the annual performances are predicted with a direct extrapolation from the test results for that fixed climate and load.

The Combitest method consist in 8 days of test where the firsts two are used for preconditioning and the other six-days represent the core test. These days are selected in order to have the possibility to perform a direct extrapolation of performance.

The sequence is defined as:

- Initial condition of tank and boiler at 20°C;
- Two initial days with realistic operation;
- Core sequence of six-days;
- DHW capacity test: discharge of the store until the boiler starts.

The system is installed in a conditioned room (20°C) considering the boundaries are indicated in Figure 1-2 (indicated with the label "system boundary SERC/SP"). All the connections are insulated.

Differently from other procedures, a load file is defined simulating the building and the distribution systems (radiators) TRNSYS with the Type 56; generating a load file. In the simulation also the thermostatic valves are considered. This load file controls the flow temperature to heat distribution system. In this way, emulations of outdoor and indoor temperatures to be feedback to controller are not needed. This permits a direct comparison between different tested systems but this approach has the disadvantage of disregarding the real behaviour of the plant controller.

The draw-off profile is based on the profile defined by Bales [24] recalculated with a set temperature of 40°C. There are defined only energy-type draw-offs (a certain energy is removed). A two-days profile is repeated 3 times: this profile represents bath, shower and short discharges (different flow rates and energies). There are not time limits for reaching the set temperature and the energy set-point. A fixed number of draw offs per day is defined as 6.

The model of collectors is the Type 832 by Bengt Peres [42]. A 45° slope and south orientation is used. The field of solar collectors is between 15 m^2 and 20 m^2. The collector parameters are calculated on the model chosen by the company.

The method does not provide utilization of simulations in the phase of results post-process. The annual performance figures are obtained by multiplying the final energy by the ratio of 365/6 and a correction factor derived by Bales [24]. The performance figures defined as factor of these ones are calculated from the annual value (after the application of the correction factors). The annual DHW load is calculated multiplying the test one by the factor 365/6.

The method does not provide extrapolation procedures for other loads or climates. The test report publishes the annual performance figures and the comparison with a reference pellet boiler without solar store.

Pros/Cons:

- (+) dynamic effects and component interaction under realistic operating conditions are assessed;
- (+) the annual performance can be assessed easily with the direct extrapolation;
- (+) by reducing the test to a six-days sequence, the test cost is reduced;

- (±) on one side, using a fixed load file allows to test different systems in equal conditions, on the other side, the influence of the real behaviour of the distribution system is not considered because a constant mass flow is used and there is not the emulation of thermostatic valves;
- (±) hardware-in-the loop simulations allow to test the system under a very realistic condition but requirements that regarding the test facility and the efforts for the test procedure are high in demanding and increase the test costs;
- (-) the extrapolation to other boundaries conditions is not foreseen.

1.3.5 CCT / SCSPT / Combitest - Definition of a new harmonized procedure

The three institutes of SPF (Switzerland), SERC/SP (Sweden) and CEA INES (France), in the EU project MacSheep have worked to harmonise their test procedures [15,44,45]. The first results of the harmonization of the procedures are described by Chèze et al. [44] and by Haberl et al. [45].

As presented in previous sections, those test methods are based on the same principles but they are different in some important details. The harmonization of the procedures would converge in the same procedure requirements:

- All the tested systems have to deliver the same amount of useful energy;
- All the tested systems have to reach the same comfort level;
- The difference in energy stored in the system at the beginning and the end of the test should be small;
- The extrapolation of annual consumptions has to be done with a factor 365/N where N is the duration of test core sequence expressed in days.

The system's physical boundaries were re-defined (Figure 1-5). Those includes 10 m for the collector pipelines, storage tanks, auxiliary heaters, solar group, controller and so on. Since the control system is part of the boundaries, it has to evolve with its own control strategy; however, it has to be adjusted in a way that the heat demand of the building will be met. Some smart control strategies that could be implemented in the control could not be tested and therefore those functions have to be switched off.

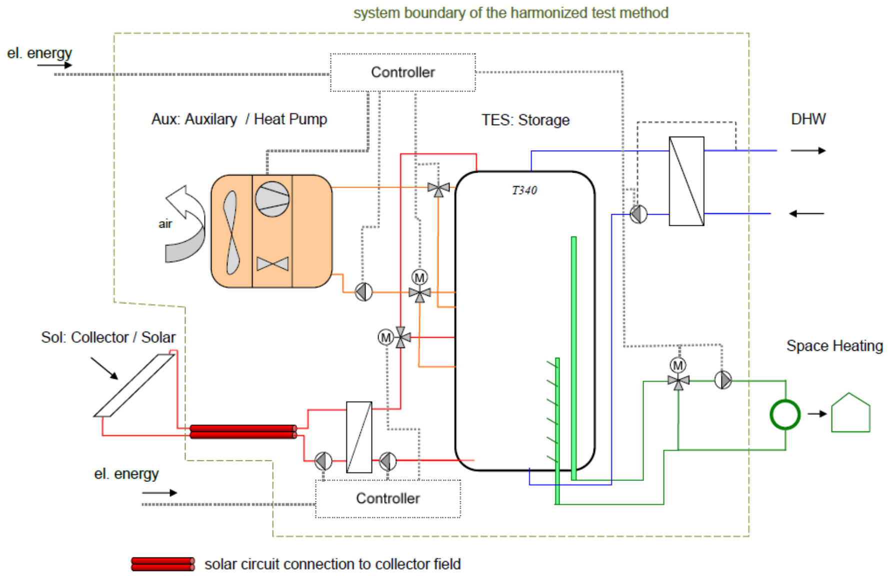

Figure 1-5: System set-up in the new harmonized procedure (CCT/SCSPT/Combitest). Source [45].

The parts that are not installed in the laboratory are emulated. The collector is tested according to EN ISO 9806 and the model has to be defined according to the parameters of the standard.

The building emulation is the point that was changed most. Contrarily to the Combitest method that uses a load file, the SCSPT and the CCT procedures include the emulation of the building with a real-time simulation. In the new harmonized procedure, a "combined approach" is adopted to merge the advantages of both methods. A load file is predefined with the building simulation and it is used to define a maximum energy target. The building is emulated with an online simulation to count the heat delivered by the system and the return temperature. The heat delivered to the building is limited with a mechanic valve that is closing if the energy target is reached during the day (Figure 1-6).

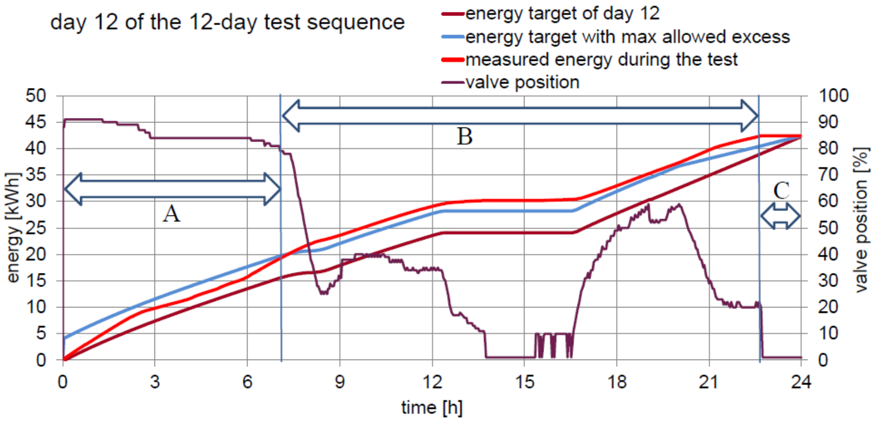

Figure 1-6: Load emulation. Example of "combined approach". Source [45].

Another point is the definition of the test sequence and the consequent post elaboration of results. The sequences are defined with an optimization procedure modifying the profiles in order to have a direct extraction of results from the length of the sequence. Two sequences of six and twelve days were defined.

1.4 Discussion on test methods

A large number of standards are available. However, some lacks are identified:

- Not all technologies or applications are covered;
- Test conditions for discontinuous machines and large system are not clearly defined;
- In the large part of standard, transitory behaviour, inertial effects and control are not considered because all tests are carried out under stationary conditions and for each component individually;
- A consistent and agreed definition of the performance figures and the method for the calculation of the Seasonal Performance Factor (SPF) for a complex hybrid system is missing.

For the definition of system performance, two approaches are identified. The first approach presented concerns component based test procedures; these procedures are flexible but they do not consider effects due to dynamic conditions, control strategies and component interactions. For what concerns the second approach, whole system test methods allow to overcome the lacks of the component based test procedures at the expense of less flexibility in the extension of the results for different conditions and system size. The use of hardware-in-the-loop simulations for emulating the system boundary conditions are high in demanding in terms of knowledge, test bench and costs.

The methods presented in the previous chapters are applied to one fixed climate and their application is quite complicated since online simulations (with a commercial software) are performed to emulate the behaviour of loads and sources. This motivate the development of a new dynamic procedure that simplifies the application without losing in reliability.

To perform a reliable evaluation of the performance, some requirements have been defined during the development of the procedure; some of these are already satisfied by the other test methods:

- The test has to be composed by a small number of consecutive days that represent the annual working conditions;
- The results should represent the annual performances;
- The test should represent the behaviour of the system (or component) in a real installation;
- The system has to be installed in the laboratory with the same configuration used in the real installation;
- The laboratory has to not influence the internal control of the system since it can evolve in according to the manufacturer control;

- The test procedure should be easy to perform and with a short duration to be cost effective in order to be attractive for industry;
- The procedure should be reproducible for different systems (or components), climates and loads;
- Depending from the climate chosen, three different loads should be foreseen as space heating, space cooling and domestic hot water.

To fulfill the requirements described previously, the following questions are analysed:

- Can a load file be used to test different systems with different sizes? Can it be used to have a common base for their comparison?
- Can a factor be defined to realistically represent the on/off cycles of the systems without requiring an on-line building simulation?
- How can the distribution system and the solar collector be emulated without a commercial software?
- How select the boundary conditions? How long should be the sequence?
- Is it possible to directly extrapolate the seasonal performances?

The solution adopted for answering the questions are presented in the chapter 3 and chapter 4.

The concept in the developed method is the simplification of the procedure application and for doing this, a load-file is defined to test different system without require an emulation of the building. The same load file is used to test a range of size of systems. In this way, different systems can be compared on a common base. The idea of not using any commercial software for the emulation of component helps to the simplification and gives the opportunity for a more extended application of the procedure.

2 Test procedure at component level

As broadly discussed in the introduction, dynamic tests are needed to characterize the real performance of the thermal system. A first analysis of dynamic performance has been applied at component level. To validate the procedure, two different components were tested since their working principle is different. The first component analysed is an adsorption chiller (SortTech AG ACS 08) while the second one is a reversible compression heat pump (Clivet WSHN EE 31).

The procedure is described to be applicable to different typologies of components (thermally or electrically driven heat pumps, boilers etc.) and it is described in the first section of this chapter (2.1). The validation of the procedure is presented in the chapter 2.2. After the description of the procedure, it is presented its application: the chapter 2.3 presents the definition of boundary condition of two case studies. Those have been applied to characterize the performance of an adsorption chiller (2.4) and of a reversible heat pump (2.5).

2.1 Test method

The procedure can be explained with the flow chart showed in Figure 2-1 which is taken as a reference in the following sections. The procedure can be divided in three main steps that are indicated with the different colours: the first step, indicated in yellow, is the definition of the working conditions of the component as seasonal boundary conditions. From these, a representative part has to be selected and this is done in the "event selection" step indicated with the green boxes. The last step is the laboratory characterization of the machine and the evaluation of the performance (indicated in red). As better described in the next paragraph, the "events selection" step can be subdivided in other smaller steps. These steps require the output of the previous one and some inputs from the user (indicated in blue).

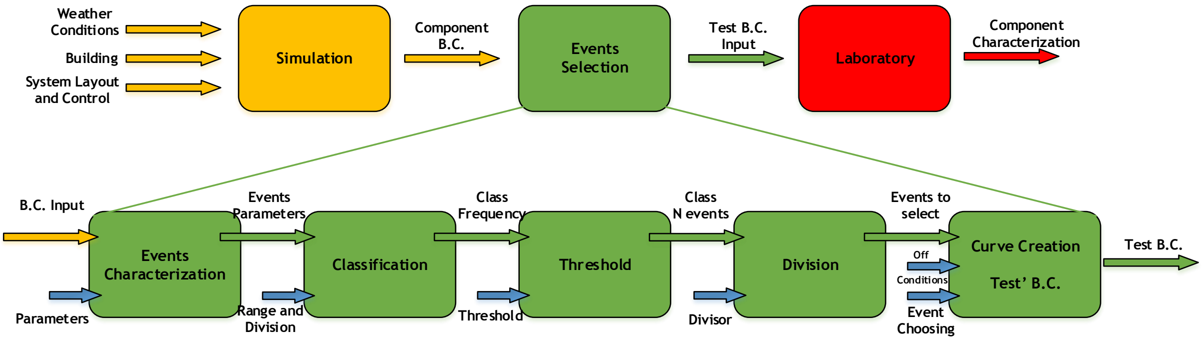

Figure 2-1: Block diagram of the test procedure at component level.

2.1.1 Simulation process

The starting point is the definition of the boundary conditions of the tested component. These boundary conditions are found by means of a numerical simulation of the whole system in TRNSYS [46]. In the model, the building, the control system and the system layout are considered.

Once one typical meteorological year is simulated, the seasonal boundary conditions of the component are found and the events selection starts. The simulation gives as output the inlet and outlet temperature profiles, the power profiles of each component of the system and also other data. From these data, to characterize the performance of the machine, the profiles of inlet temperatures, inlet mass flows and activation are extracted and used to test the component.

2.1.2 Time series selection

The study of the dynamic behaviour for thermal systems and machines offers several analogies with the discipline of fatigue life analysis for mechanical structures. The effect of fatigue processes is the degradation of the structure itself, while the transient and dynamic behaviour of thermal machines affect their overall performance. Fatigue analysis typically deals with random load sequences, which analysis allows the prediction of the structure lifetime [47]. Similarly, thermal components and systems are subject to randomly varying boundary conditions, which influence the system seasonal behaviour and efficiency.

One way to deal with varying amplitude mechanical stresses is to form equivalent load cycles, which allows the use of damage accumulation methods. The rain-flow cycle (RFC) method [48,49] has been developed for this purpose and defines criteria for the identification and the counting of equivalent cycles, starting from the time distribution of a random stress. From a complete load history a shorter and equivalent load is generated to test the component (as showed in Figure 2-2).

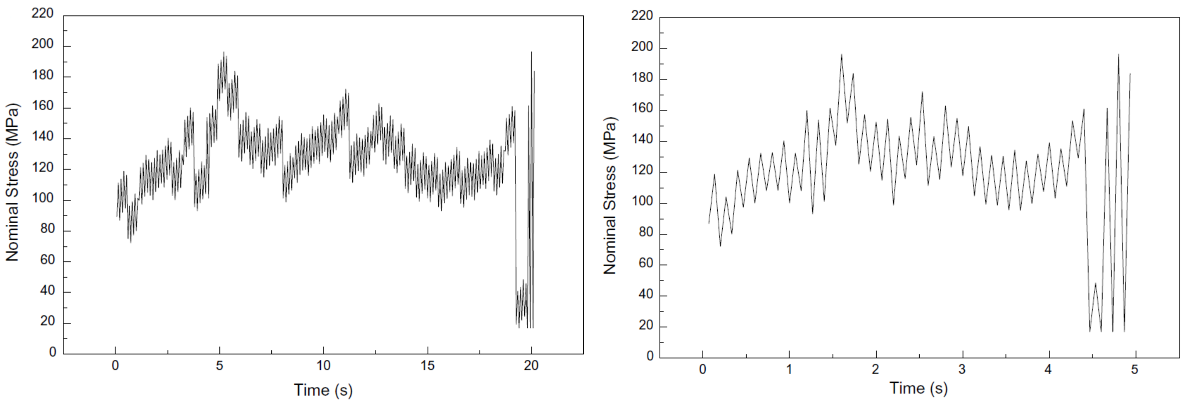

Figure 2-2: Example of generation of short load time-series from original load history.

a) Original load history, b) Generated load history. Source [49].

Each rain-flow cycle is characterized by two stress parameters, typically amplitude (A) and mean (M). The range of variation of both amplitude and mean can be divided into discrete intervals, which constitute the row and column indexes of the so-called rain-flow matrix (Figure 2-3 a). Each element of the matrix represents a class, characterized by a specific pair of amplitude and mean intervals. Each rain-flow cycle is assigned to the corresponding class of the matrix. By counting the number of cycles in each class a 3-D histogram representation of the rain-flow cycles distribution is obtained, where the z-coordinate corresponds to the frequency of the counts (Figure 2-3 b). This data classification allows a quick evaluation of the kind of solicitation in exam, and an estimation of which cycles are more influencing the mechanical behaviour, having a higher statistical frequency.

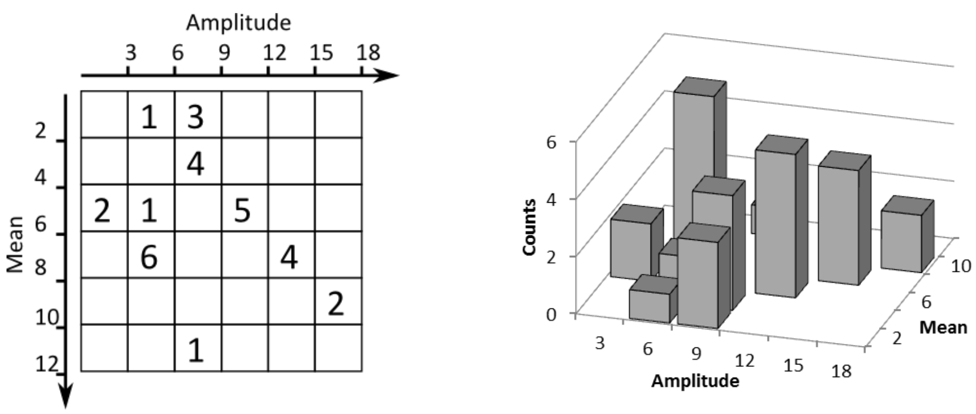

(a) (b)

Figure 2-3: Example of rain-flow cycles classification.

(a) Rain-flow matrix with amplitude (columns) and mean (rows) intervals. (b) Histogram representation of the cumulative frequency from the rain-flow matrix.

Following the analogy with the fatigue analysis, an equivalent procedure to classify the time varying boundary conditions of thermal systems and components has been developed, and criteria to select short experimental sequences, representative of the real-like seasonal working conditions, have been defined. One major difference between the characterization of mechanical stresses and the dynamic behaviour of thermal systems lies on the fact that, whereas mechanical systems present a single stress time-series, heating and cooling systems (and thus their components) are typically dependent on different parameters varying in time (e.g. temperatures, mass flows, solar irradiation, etc.).

The developed procedure takes as input seasonal boundary conditions time series that are extrapolated from a whole system simulation in TRNSYS as indicated in the previous paragraph.

From the boundary conditions time series, different EVENTS are identified. An EVENT corresponds to a period of continuous working between two successive OFF periods, including the initial transient phase. A single day may include none, one or more events.

For every event, amplitude (amp) and average (avg) values are computed for each boundary condition; also the event duration (τ) is considered as a variable of the problem, since it is significant to retrieve energy values. As a result, whereas rain-flow cycles matrices are always bi-dimensional, events matrices are N-dimensional:

Equation 2-1 $$N = 2 \cdot n_p + 1$$ **[-]**

where n_p is the number of boundary conditions.

As a second step of the procedure, considering the entire range of variation of each boundary condition, the amplitude is divided into n_{amp} intervals, the average into n_{avg} intervals and the duration into n_τ intervals. The discretization results in the definition of C classes:

Equation 2-2 $$C = n_\tau \prod_i n_{amp,i} \prod_k n_{avg,k}$$ **[-]**

where the indexes i and k varies from 1 to n_p.

Each class corresponds to a N-dimensional vector, and each element is one of the previously identified intervals. Finally, all the previously identified events are allocated into the corresponding classes and counted.

The number of subdivision for each boundary condition is key: if intervals are too narrow, very few events per class are found; if classes are too wide, some important details might be lost. Therefore, boundary conditions can be assigned different weight (choosing narrower or larger intervals), if it is known that they have a different impact on the performance. For a generic data classification, Barlow [50] suggests that the ideal interval size should result in at least 5 to 10 events per class and the difference between contents of adjacent classes should be small. During the validation phase of the method different possible classifications have been considered and compared.

The selection of a representative part of the seasonal boundary conditions is based on the obtained frequency distribution. However, in order to avoid selecting events marginally influencing the seasonal performance, a threshold to the frequency distributions is applied. All classes characterized by a frequency lower than the threshold are disregarded. Finally, to further reduce the test duration, the event counts in the remaining classes are divided by the minimum count. The remaining events are used to define reduced time-series consistent with the starting one.

<u>*Example*</u>

A simple example could be done considering a component which depends only on one parameter (X); each event will be then 3-dimensional (X_{amp}, X_{avg}, τ). Considering the ranges of variations and choosing the numbers of divisions reported in Table 2-1, *the final number of identified classes will be 4, defined as reported in* Table 2-2.

Table 2-1: Example of parameters classification: range of variation and number of chosen divisions for average, amplitude and duration.

Parameter	Range of variation	Chosen number of subdivisions
X_{amp}	4:6	n_{amp}=1
X_{avg}	3:9	n_{avg}=2
τ	2:8	n_{τ}=2

Table 2-2: Example of Class creation from the divisions defined in Table 2-1.

Class	X_{amp}		X_{avg}		τ	
	from	to	from	to	from	to
1	4	6	3	6	2	5
2	4	6	3	6	5	8
3	4	6	6	9	2	5
4	4	6	6	9	5	8

A possible distribution of 21 events is reported in Table 2-3 on the left. A threshold of 5% for the considered example would cut class 1 out; the minimum number of event in the remaining classes is 2 (class 2). The number of events to be selected after the division are those reported in Table 2-3 on the right.

Table 2-3: Frequency counts and representative selection of events for the proposed classification example.

Class	Events count	Frequency
1	1	4.76 %
2	2	9.52 %
3	12	57.15 %
4	6	25.57 %

Threshold 5 % → Division by 2

Class	No. events to be selected
1	0
2	1
3	6
4	3

As the classes are defined in order to contain equivalent events, the validity of the time sequence reduction should not depend on the selection of the events from the single classes. This has been verified experimentally, after randomly selecting the specific events to define the reduced time-series.

2.1.3 Laboratory set-up

The tests were carried out at the laboratory of the EURAC. The laboratory set-up for the tests on the adsorption chiller is presented by Sparber et al. [51]. The description of the laboratory circuits and the measurement equipment used in the test is presented in the Appendix B.

The laboratory circuits are controlled to reach the flow and temperature set point as defined in the boundary conditions time series calculated in the previous steps. The set points are set up at the measurement frequency from an interpolation of the 1 min resolution data defined from the simulation. During the tests, the electric consumption, the inlet and outlet temperatures and pressures and the volumetric flows of the circuits are measured every 5 seconds.

The thermal powers are calculated from the measurements and the electric power is measured directly. These values are used to retrieve the instantaneous COP and EER.

The seasonal energy of the component is directly extracted from the results of the short dynamic test sequence. This evaluation is obtained by a proportion, considering ON-time during the test:

Equation 2-3

$$Q_{season} = Q_{test}\frac{\tau_{season}}{\tau_{test}} \quad \text{[kWh]}$$

From the Equation 2-3, the SCOP and SEER could be calculated with the Equation 1-5 and Equation 1-6.

2.2 Validation of test procedure

The Figure 2-4 presents the validation procedure. The selection of boundary conditions has been validated with a post process of the results of the test of the whole time series. In the figure, this step is indicated with the red box "Laboratory" which input is the "Test B.C input – whole time series" that comes directly from the simulation (yellow box). This allows a calculation of the seasonal performance through the test of the entire boundary conditions time series.

From the test of the whole time series, the performances of each event are calculated. The "events performance" and the "events selection" are the input of the red box "Extrapolation of Seasonal Performance" that build up the sequence performance and consequently its seasonal extrapolation (output "Extrapolated seasonal performance"). The extrapolated seasonal performances are compared to the one calculated with the test of the whole time series.

Different selection criteria have been defined and the performance of different sequences are compared to the seasonal one in order to identify which classification criterion is valid for the selection of test sequence for different components.

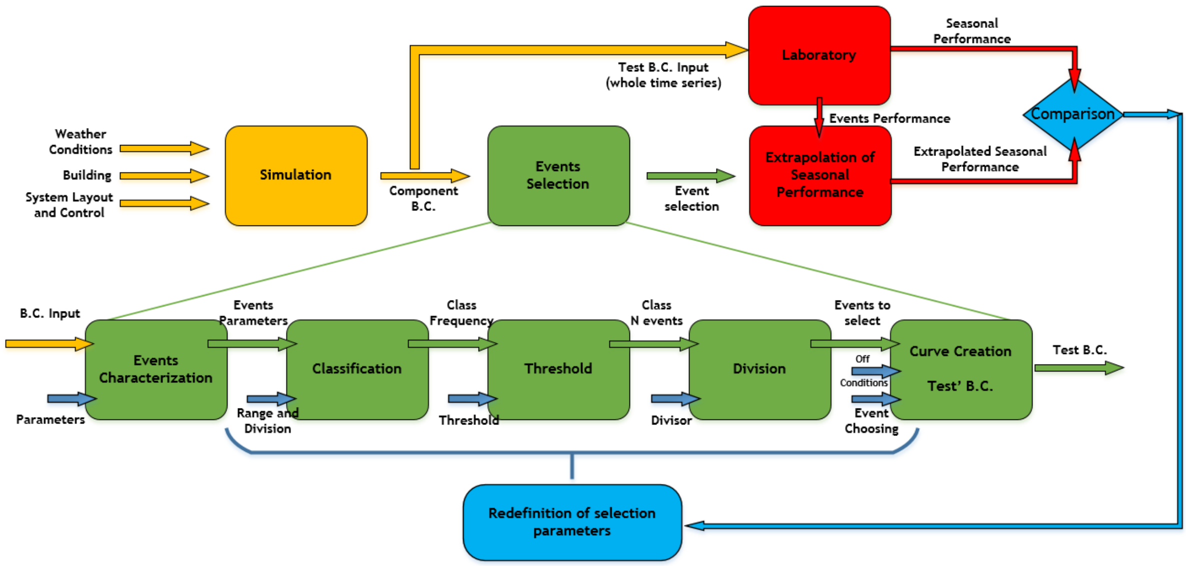

Figure 2-4: Block diagram of the validation of test procedure at component level.

The deviation between the values extrapolated from the short sequence and the seasonal test is calculated with Equation 2-4.

Equation 2-4

$$\delta_E = \frac{E_{short\ test} - E_{seasonal\ test}}{E_{seasonal\ test}} \quad [-]$$

2.3 Definition of the boundary conditions for the tests

The adsorption chiller and the heat pump considered for the application of the procedure are part of a solar combi-plus system. This typology of system uses solar energy to satisfy the load of space heating, space cooling and domestic hot water. In this case specific, the adsorption chiller uses the solar energy for the chilling operation with the reversible compression heat pump that is used as back-up unit. The alternation of these two machines is defined according to a control scheme. The heat pump is also used in heating mode for the preparation of domestic hot water (feeding a hot water storage) and for space heating. The water-to-water heat pump is connected to a dry cooler (air source) and to a solar field (solar source) having the possibility of use one of those two sources.

The system is controlled in a way to manage the energies available from the sources (solar, air and electrical for this case study). In this way, several control schemes have been defined; from these, to manage the operating modes that refer to the adsorption chiller and the heat pump, the following control schemes have been identified:

- SC AdCh: space cooling with adsorption chiller;
- SC HP: space cooling with compression chiller;
- DHW solar: preparation of domestic hot water with solar source;
- DHW air: preparation of domestic hot water with air source;
- SH solar: space heating with solar source;
- SH air: space heating with air source;

The different combinations of schemes throughout the season result in varying boundary conditions for the heat pump and for the chiller, influencing thus the overall performance of the machine. The performances of these systems are strongly influenced by varying boundary conditions and they are a good option to demonstrate the necessity of evaluation of performance with a dynamic test procedure.

Figure 2-5 presents the system scheme. In this scheme, the physical boundaries considered for the test of the chiller and the heat pump are indicated with dotted lines. The red one indicates the compression heat pump while the blue line indicates the adsorption chiller.

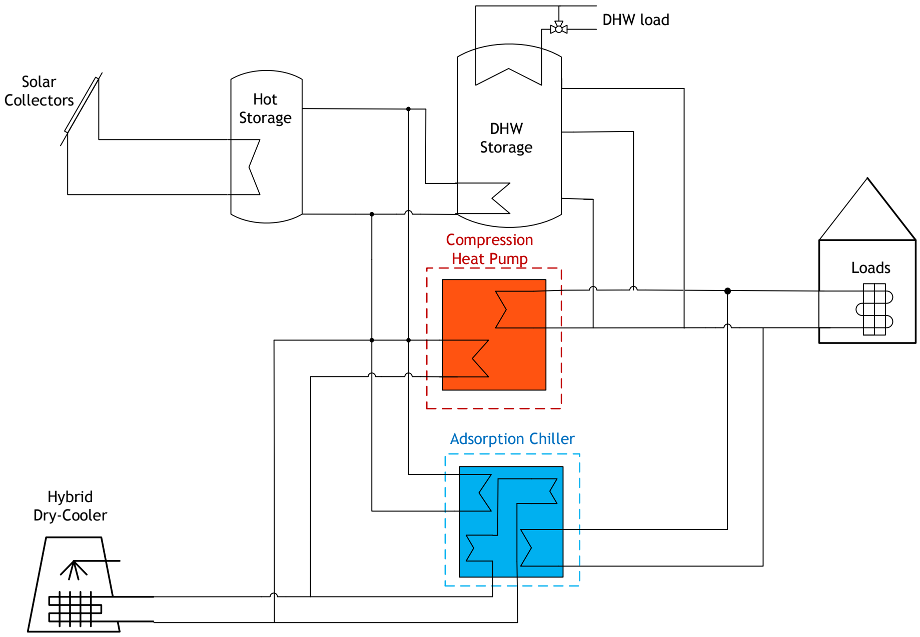

Figure 2-5: Layout of the system for the characterization of the heat pump and chiller.

The numerical model of the whole system was elaborated and validated for the development of the solar combi-plus control system [52]. The details of the simulation can be found in the appendix C.

The weather file is obtained applying Meteonorm dataset. The climate considered is Bolzano. The load is defined by the building selected that has opaque and transparent surfaces transmittance closed to the limits defined in the “DM 26/10/2010”. The building is a single family house of 180 m^2 distributed equally between two floors. The distribution system is a radiant floor (for both space heating and cooling). The total space heating load to satisfy is 50 kWh/m^2 and the space cooling load is 12.6 kWh/m^2. The domestic hot water profile is defined with the statistical method described in the IEA SHC task 26 [53].

From the simulation of the whole system, the boundary conditions of the two components are extracted. For the adsorption chiller, since the control strategy foresees a constant mass flow as recommended by manufacturer, the inlet temperatures in the three circuits (the generator $T_{in,gen}(\tau)$, the evaporator $T_{in,evap}(\tau)$ and the condenser $T_{in,cond}(\tau)$) and the ON/OFF profiles are extracted from the simulation as input of the experimental sequence extraction procedure. The case of the compression heat pump is different since the mass flow of the source circuit is variable. The inlet temperatures of load and source circuits, the mass flow of the source side and the ON/OFF profiles are extracted and used as input for the selection of the sequence procedure. Those profiles and their range of variation are shown in the "time series" sections (2.4.1 for adsorption chiller and 2.5.1 for heat pump).

The working modes are divided in heating mode and cooling mode. The chilling operation mode is defined for the period between the 1st June and the 30th September while the heating mode from the 1st October to the 31th May. Only the compression heat pump works in heating mode. The next two paragraph present the boundary conditions divided in these two modalities.

Note: during the summer season, the heat pump could work in heating mode for the preparation of the DHW. In this case study, the DHW during the summer is totally covered by the solar collector. Therefore, it is possible to identify the cooling season with the summer.

2.3.1 Heating mode

In heating mode, the heat pump works for the preparation of the domestic hot water and for the space heating with the possibility to use solar or air source. The working scheme can give a prior information about the performance. Heat pumps perform better with high evaporation temperatures and low condensation temperatures. When the air source is used, the inlet evaporator temperature is constrained by the external temperature; as a consequence, air source heating schemes result in a better performance during the mid-season months and in worse COPs during the colder months.

With respect to the user side, since during the heating season the heat pump is used both for space heating and for DHW preparation, two different temperature levels are foreseen. In particular, since the set point for DHW preparation is higher, the performance of the heat pump in the DHW schemes is worse than during space heating schemes.

Table 2-4 shows the number of *Events*, the number of schemes' activation and their total duration in the heating season. The control strategy implemented in the system allows changing from one scheme to another (e.g. from space heating to DHW preparation and back to space heating), without requiring the heat pump to be turned OFF. This means that during one *Event* none, one or more changes of schemes could be done. As a consequence, the number of heat pump activations is independent of the sum of schemes activations. For example, considering the whole season (first row of Table 2-4), the heat pump is activated 554 times while the DHW schemes are activated 253 times (6+247) and the space heating schemes are activated 558 times (115+443).

Table 2-4: Activations and durations of heating schemes.

		Scheme Activations [n-times]				Scheme duration [h]			
	n_{ev}	DHW_{sol}	DHW_{air}	SH_{sol}	SH_{air}	DHW_{sol}	DHW_{air}	SH_{sol}	SH_{air}
Seasonal	554	6	247	115	443	1	50	90	785
October	4	0	0	1	5	0	0	1	5
November	93	0	32	16	66	0	7	10	129
December	167	1	95	23	141	0.08	17	22	234
January	130	5	67	33	112	1	14	33	239
February	89	0	36	26	73	0	9	17	144
March	68	0	17	16	43	0	3	7	33
April	3	0	0	0	3	0	0	0	1

To understand how the use of the different loads and sources is distributed throughout the season, the data contained in Table 2-4 can be represented as percentage distributions of the number of activations, as showed in Figure 2-6a, or as percentage distributions of schemes duration, as showed in Figure 2-6b.

From the two figures, it is clear that in October and April the heat pump is not used for the domestic hot water preparation, which is produced directly with the solar energy. The average temperature at the user's side (condenser) is therefore lower than in the other months, and a positive effect on the COP is expected. During the other months, while the percentage of DHW activation schemes ranges between 22% and 37% (the maximum is verified in December), the amount of time in which the heat pump works for the DHW preparation is only 5-6%. This means that DHW schemes are activated frequently and for short periods.

Similar considerations to those done for the loads, can be done also in terms of use of the different sources. The months with the lowest evaporation temperatures are November and December, which also have a low share of solar source use (7% and 8% of the total duration respectively). One particular case is represented by April, where only the air source is employed (but with higher external temperature). For the other months, the share of solar source ranges between 10 and 18% of the working time.

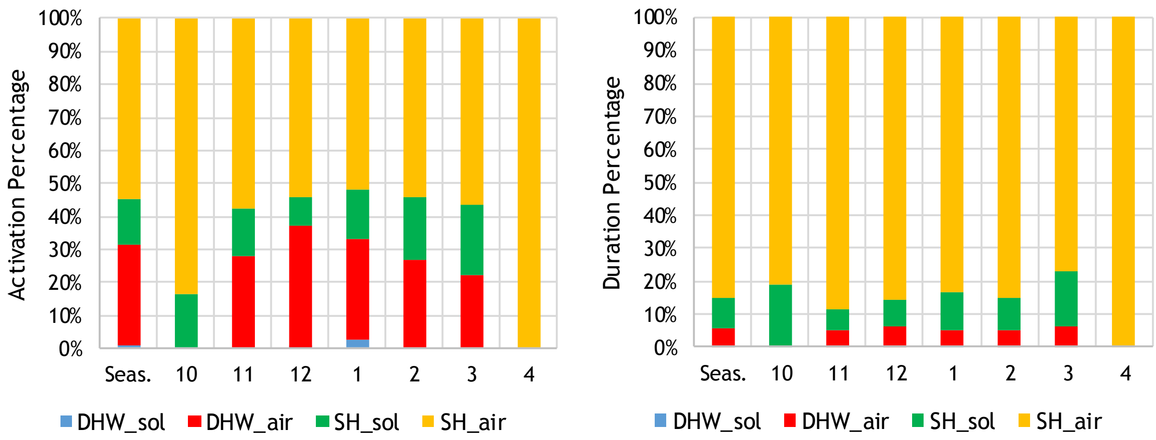

Figure 2-6: Activation of schemes in heating mode.

1a) Percentage of schemes activation. 1b) Percentage of schemes duration.

2.3.2 Cooling mode

In summer, the space cooling load is covered by the adsorption chiller or by the heat pump. The alternation between these two components is decided by the control strategy. In simple terms, the adsorption chiller covers normal load and when it becomes higher, the heat pump covers it.

In Table 2-5 and Figure 2-7, the schemes' activations for the entire cooling season and for the single months are reported. With respect to the heating mode, the cooling season is characterized by shorter and more frequent activations of the heat pump, due to the oversizing of the heat pump capacity compared to the building load and to the alternation with the adsorption chiller. The duration of activation of the adsorption chiller is about 20 times the duration of activation of the heat pump. For the heat pump, the cooling scheme is activated 660 times in 4 months for a total of 79 working hours (versus the 554 times in 7 months with 937 working hours for the heating mode). The average *Event* duration is 7 minutes instead of 100 minutes during the heating mode. Instead, the chiller is activated 97 times with a duration of 240 hours and the consequent average *Event* duration is 148 minutes.

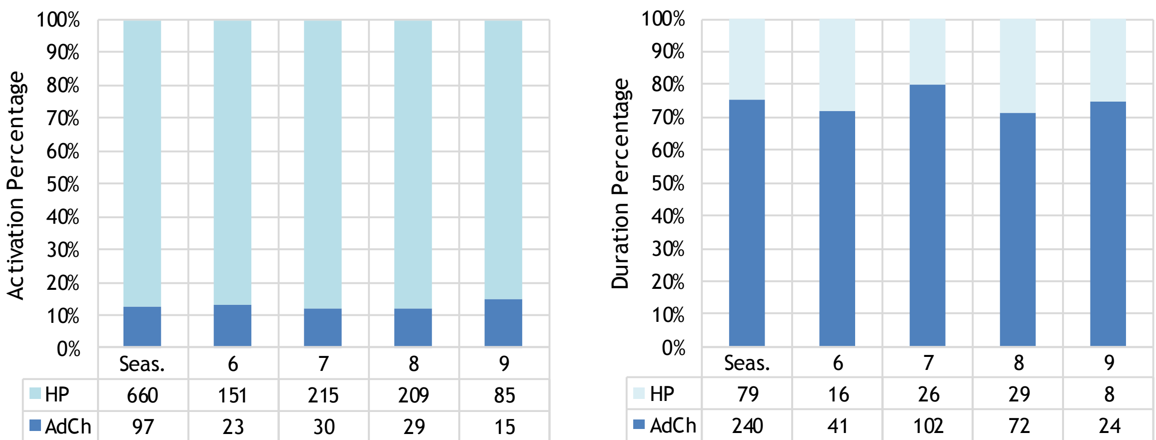

Figure 2-7: Activation of schemes in cooling mode.

1a) Percentage of schemes activation. 1b) Percentage of schemes duration.

Table 2-5: Activations and durations of cooling scheme.

	Adsorption Chiller		Reversible Heat Pump	
	n_{ev}	Duration of activation τ_{on} [h]	n_{ev}	Duration of activation τ_{on} [h]
Seasonal	97	240	660	79
June	23	41	151	16
July	30	102	215	26
August	29	72	209	29
September	15	24	85	8

2.4 Adsorption chiller characterization

The first component considered for the analysis is the adsorption chiller SortTech AG ACS 08 (Table 2-6). The chiller is a water/silica gel with two chambers. The study of the dynamic behaviour of the component was started with the master thesis [54,55] and was used as starting point for the test for the heat pump. This chapter presents a summary of the application of the procedure to this component.

Table 2-6: SorTech ACS 08 characteristics.

Model	Sortech ACS 08		
Cooling capacity	8 kW @ nominal condition		
Max cooling capacity	11 kW		
Declared EER	0.6 @ nominal condition		
Power consumption	7 W_{el}		
	Evaporator	Condenser	Generator
Temperature Range	6-20 [°C]	22-37 [°C]	55-95 [°C]
Nominal Condition	18/15 [°C]	27/32 [°C]	72/65 [°C]
Volumetric Flow	2.0 [m³/h]	3.7 [m³/h]	1.6 [m³/h]
Pressure loss	0.3 [bar]	0.35 [bar]	0.23 [bar]

2.4.1 Time series selection

The boundary conditions considered for the selection are the inlet temperatures of generator, condenser and evaporator. Considering this three mentioned boundary conditions and the event duration (τ), and using *Equation 2-1* the dimension of the resulting class is 7. In Figure 2-8 the time-series for the chiller boundary conditions are showed, including only the ON-time of the machine. From these boundary conditions, 97 events are identified. The range of variation for all boundary conditions is showed in Table 2-7.

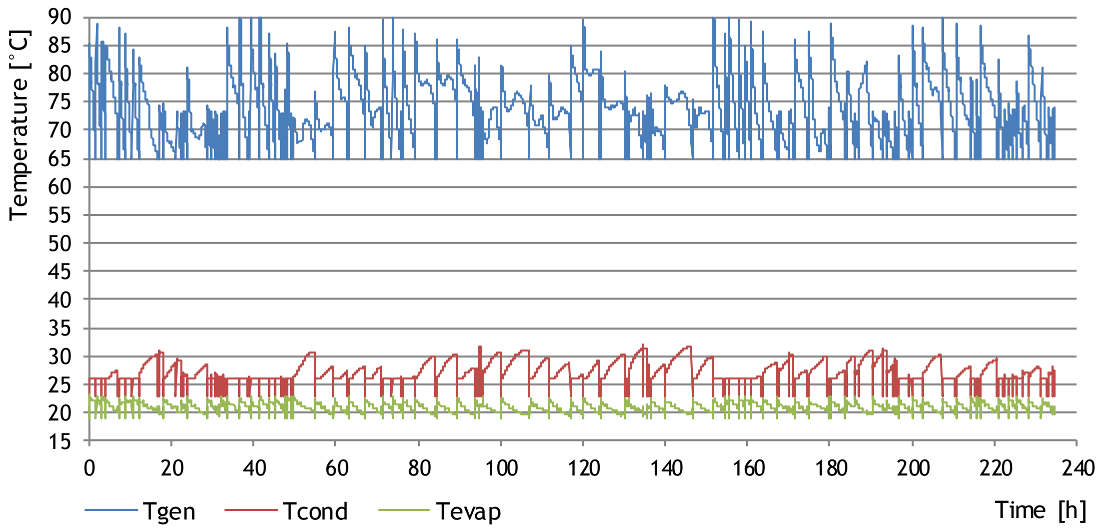

Figure 2-8: Time-series for the boundary conditions of the adsorption chiller, considering only the ON-time of the machine.

Table 2-7: Range of variation of boundary conditions. Adsorption chiller.

	$T_{gen,avg}$	$T_{gen,amp}$	$T_{cond,avg}$	$T_{cond,amp}$	$T_{evap,avg}$	$T_{evap,amp}$	τ [min]
Min	68	4	25	0	18	0	30
Max	81	26	32	6	23	4	410

The subscripts (amp) and (avg) indicate respectively the amplitude and the average, calculated for each event.

Different criteria for the definition of the classes have been experimented but only two of these are reported in Table 2-8; these criteria consider intervals of 2 K or 3 K for the temperature boundary condition and 4 or 8 intervals for the events duration that correspond to a duration of 100 or 50 minutes. in Table 2-8 reports the number of classes created with the chosen intervals (No. Classes) and the number of classes that contain elements (Full Classes). The table also shows the residual number of events and those that are excluded after the application of either a 1% or a 2% threshold and after the division by the minimum number of event counts (divisor). The threshold of 1% excludes from the selection the classes with one element, while the 2% excludes from the selection the classes with two elements.

Table 2-8: Events classification and selection. Adsorption chiller.

	Number of intervals									Threshold			Division		
	$T_{gen,avg}$	$T_{cond,avg}$	$T_{gen,amp}$	$T_{cond,amp}$	$T_{evap,avg}$	$T_{evap,amp}$	duration τ	No. classes	Full classes	Threshold	Residual	Excluded	Divisor	Residual	Test duration [days]
Whole Season	1	1	1	1	1	1	1	1	1	0	97	0	1	97	16.7
2K-8-1	7	4	11	3	3	2	8	44352	78	1	34	63	2	18	2.3
2K-8-2										2	10	87	3	3	0.4
2K-4-1	7	4	11	3	3	2	4	22176	65	1	38	59	2	20	2.6
2K-4-2										2	18	79	3	5	0.7
3K-8-1	4	3	7	2	2	2	8	5376	59	1	55	42	2	29	4.5
3K-8-2										2	37	60	3	13	1.6
3K-4-1	4	3	7	2	2	2	4	2688	53	1	60	37	2	31	4.9
3K-4-2										2	44	53	3	15	2.0

The first column contains the name of the corresponding selection: the number with the "K" letter indicates the temperature step, while the second number indicates the number of intervals for the duration and the third number indicates the threshold. The last column shows the test duration expressed in days.

2.4.2 Dynamic test results

Table 2-9 shows the chiller performance calculated during the cooling season. The SEER obtained during the different months is quite similar each other while the amount of load covered is different. The seasonal SEER is 0.488 quite far from the nominal condition of the machine that is 0.6. This could be explained looking in the detail to the performance with the next two figures.

Table 2-9: Monthly and seasonal results. Adsorption chiller.

	n_{ev}	τ_{on} [h]	SEER [-]	Q_{gen} [kWh]	Q_{cond} [kWh]	Q_{evap} [kWh]
Seasonal	97	240	0.488±0.01	3393±21	4717±71	1659±25
June	23	41	0.478±0.01	598±4	824±12	285±4
July	30	102	0.497±0.01	1388±10	1955±29	690±10
August	29	72	0.483±0.01	1014±7	1396±21	490±7
September	15	24	0.483±0.01	387±3	535±8	187±3

Figure 2-9 shows the detail of the performance during the first hour of one Event. The left axe indicates the temperature and the right indicates the power. The inlet temperature is a fixed boundary condition and the outlet temperature is measured. From this two, the power can be calculated. The area delimitated with the green dotted line indicates the first swap of the machine and this area can be divided in two sub-areas. The first one is the one indicated with a green background: during the first five minutes the machine does not provide any useful effect since the evaporator power is null and the generator absorbs energy. The consequence is that the rejected power is low. After this phase, the chiller continues to heat up the desorption chamber and the cooling power is low. This first phase is long 25 min. Then, as indicated with the area delimitated with the red dotted line, the chiller starts the normal working swap and from this moment it produces a chilling power closed to the nominal one.

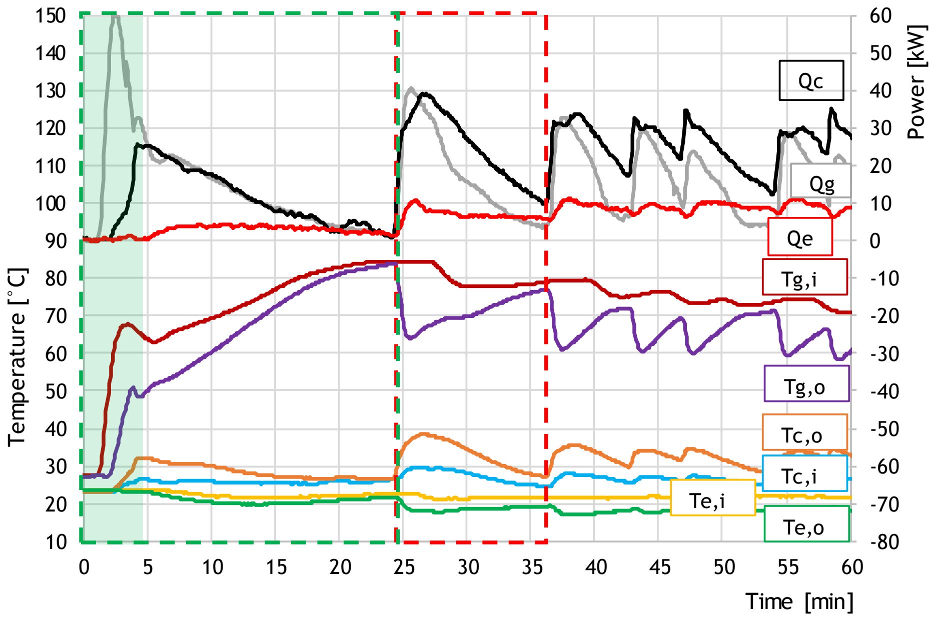

Figure 2-9: Temperature and power profiles during test. Adsorption chiller.

The temperature profiles are indicated with the label "T" while the power profiles are indicated with the label "Q". The first letter of the subscript indicates the circuits (generator "g", condenser "c" and evaporator "e") while the second one indicates the input "i" or the output "o".

The transient phases can be individuated also in the Figure 2-10 where the cycle's EER is indicated as a function of the condenser temperature for different generator temperature series and with a evaporator temperature of 22°C. In the figure, the dynamic points are compared to the stationary points. For each Event, the first 30 min the EER obtained by the machine is large lower to the stationary one, and after this transient phase it will be more closed to the stationary one.

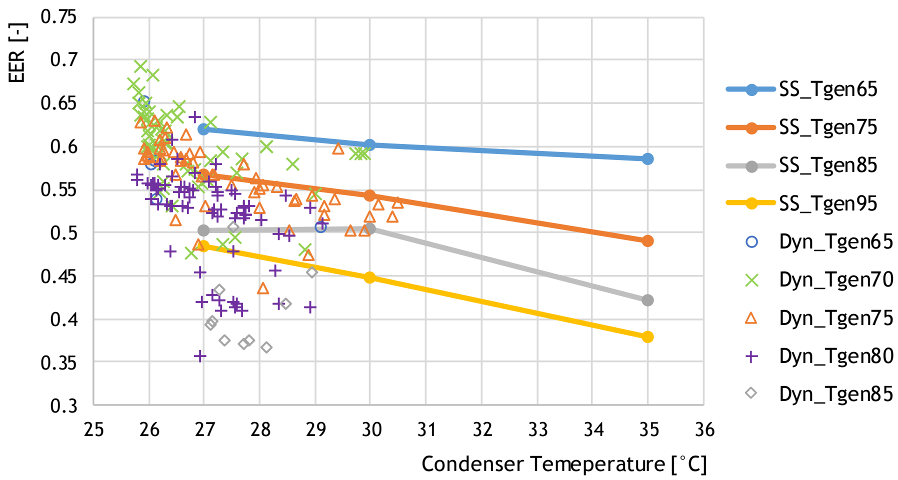

Figure 2-10: EER comparison of dynamic and stationary conditions. Adsorption chiller.

The series are divided by generator temperature respectively for the case of dynamic test and steady-state test. The name of the series indicates the typology of test (dynamic - Dyn or stationary SS) and the generator temperature (i.e. Tgen80). The figure shows the data with evaporator temperature equal to 22°C.

The previous results show the importance of characterize the machine in dynamic condition since the transient phase lasts 25 min. This characterization should be performed with a short test sequence. Table 2-10 shows the results of the test, in terms of SEER and energy flows though the three circuits of the unit obtained with the different short tests. Some test were repeated twice by selecting different events in each classes, to verify that the events' choice does not affects the correctness of the experimental sequence (Table 2-8). The reduced test results are compared with a "Whole Season" test (accounting for all 97 events) in order to verify the effect of applying different thresholds and subdivisions to the events counts and identify the optimal data reduction.

Table 2-10: Result of tests. Adsorption chiller.

Test		Duration	SEER		Q_{gen}	Q_{cond}	Q_{evap}
		[days]	[-]	δ [%]	[kWh]	[kWh]	[kWh]
Whole Season		16.7	0.49±0.01		3393±21	4717±71	1659±25
Test 1	2K-8-1	2.3	0.45±0.01	-8.1	375±2	495±7	169±3
Test 2	2K-8-1	2.3	0.45±0.01	-8.1	379±2	502±8	172±3
Test 3	2K-8-2	0.4	0.46±0.01	-6.1	77±1	103±2	35±1
Test 4	2K-4-1	2.6	0.46±0.01	-6.1	449±3	602±9	207±3
Test 5	2K-4-1	2.6	0.46±0.01	-6.1	450±3	600±9	206±3
Test 6	2K-4-2	0.7	0.47±0.01	-4.1	123±1	166±2	57±1
Test 7	3K-8-1	4.5	0.48±0.01	-2.0	859±5	1179±18	412±6
Test 8	3K-8-1	4.5	0.48±0.01	-2.0	836±5	1146±17	400±6
Test 9	3K-8-2	1.6	0.46±0.01	-6.1	274±2	365±5	126±2
Test 10	3K-4-1	4.9	0.48±0.01	-2.0	965±6	1333±20	465±7
Test 11	3K-4-1	4.9	0.48±0.01	-2.0	924±6	1268±19	442±7
Test 12	3K-4-2	2.0	0.46±0.01	-6.1	363±2	388±6	169±3

The second column contains the name of the corresponding selection: the number with the "K" letter indicates the temperature step, while the second number indicates the number of intervals for the duration and the third number indicates the threshold.

Due to the reduced test duration, the energy flows in test 1 to 12 are lower with respect to the "Whole Season" reference case. The corresponding seasonal energies extrapolated from the tests (with *Equation 2-3*) are reported in Table 2-11. The first result to highlight is that the difference between tests with the same selection criterion and different event choices (Test 1-2, Test 4-5, Test 7-8, Test 10-11) is lower than 1.6%, proving that the defined classification method succeeds at grouping events that are equivalent in terms of effects on the seasonal performance. Starting from the 17-days test for the Whole Season, the maximum duration of the reduced test sequences is five days. The duration of the test is not directly related to the accuracy of the seasonal performance figures evaluation, but, indicatively, the longest tests are the most reliable. The 2K divisions (test 1 to 6) and the 2% threshold (test 9 and 12) remove too many data: these criteria results in short tests (less than three days), but produce a deviation of about 8 % on the SEER evaluation and of about 7 % on the energies estimation with respect to the reference test. Excluding these cases, the difference between tests 7, 8, 10 and 11 and the reference test is about 2 %. In general, the calculated SEER are very similar for all selected test sequences, differing of about 2 % from each other.

Table 2-11: Seasonal energy estimation. Adsorption chiller.

	SEER		$Q_{gen,s}$		$Q_{cond,s}$		$Q_{evap,s}$	
	[-]	δ [%]	[kWh]	δ [%]	[kWh]	δ [%]	[kWh]	δ [%]
Whole Season	0.49±0.01		3393±21	-	4716±71	-	1659±25	-
Test 1	0.45±0.01	-8.1	3625±22	6.8	4788±72	1.5	1638±25	-1.2
Test 2	0.45±0.01	-8.1	3602±22	6.2	4765±71	1.0	1630±25	-1.7
Test 3	0.46±0.01	-6.1	3642±23	7.4	4914±74	4.2	1682±25	1.4
Test 4	0.46±0.01	-6.1	3635±22	7.1	4867±73	3.2	1678±25	1.2
Test 5	0.46±0.01	-6.1	3612±22	6.5	4820±72	2.2	1657±25	-0.1
Test 6	0.47±0.01	-4.1	3685±23	8.6	4978±75	5.5	1720±26	3.7
Test 7	0.48±0.01	-2.0	3463±21	2.1	4756±71	0.8	1660±25	0.1
Test 8	0.48±0.01	-2.0	3415±21	0.7	4683±70	-0.7	1634±25	-1.5
Test 9	0.46±0.01	-6.1	3658±23	7.8	4877±73	3.4	1689±25	1.8
Test 10	0.48±0.01	-2.0	3463±21	2.1	4781±72	1.4	1670±25	0.6
Test 11	0.48±0.01	-2.0	3469±21	2.2	4763±71	1.0	1660±25	0.1
Test 12	0.46±0.01	-6.1	3701±23	9.1	3961±59	-16.0	1721±26	3.7

Besides the seasonal values, the analysis of the distributions of instantaneous performance parameters is key to evaluate the capability of representing the whole season operation with one of the defined selection criterion. Figure 2-11 and Figure 2-12 represent the device performance averaged over working cycle, as computed from test 7 and the reference “Whole Season” test. The figures show a very good agreement between the two cases proving again the reliability of the selection procedure.

The EER (Figure 2-11) presents a bimodal distribution with two distinct peaks around 0.22 and 0.55, respectively. The lower values, between 0.13 and 0.35 correspond to the transient phases at the machine switch on and can be explained looking at the distributions of the powers (Figure 2-12). As explained with Figure 2-9, while the generator is working around its nominal conditions (single peak distribution at 13 kW), the evaporator power distribution presents a maximum at the nominal chilling capacity (8 kW) along with a smaller local maximum at around 3.5 kW: as a consequence of the components inertia and system control, during the switch-on phases, the evaporator is producing a low power while the generator is requiring its nominal power, resulting, thus, in low EER values.

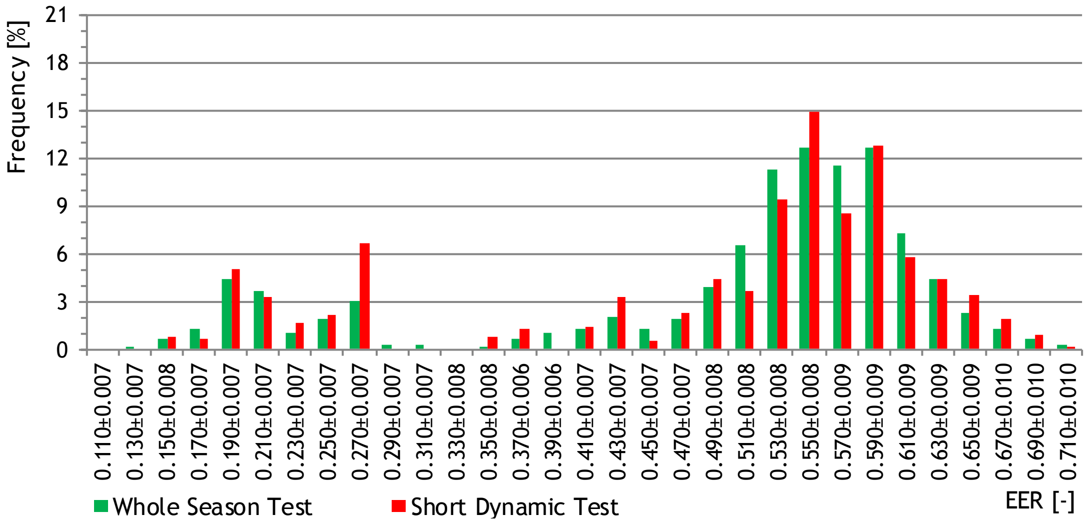

Figure 2-11: EER distribution comparison of whole season and short test. Adsorption chiller.

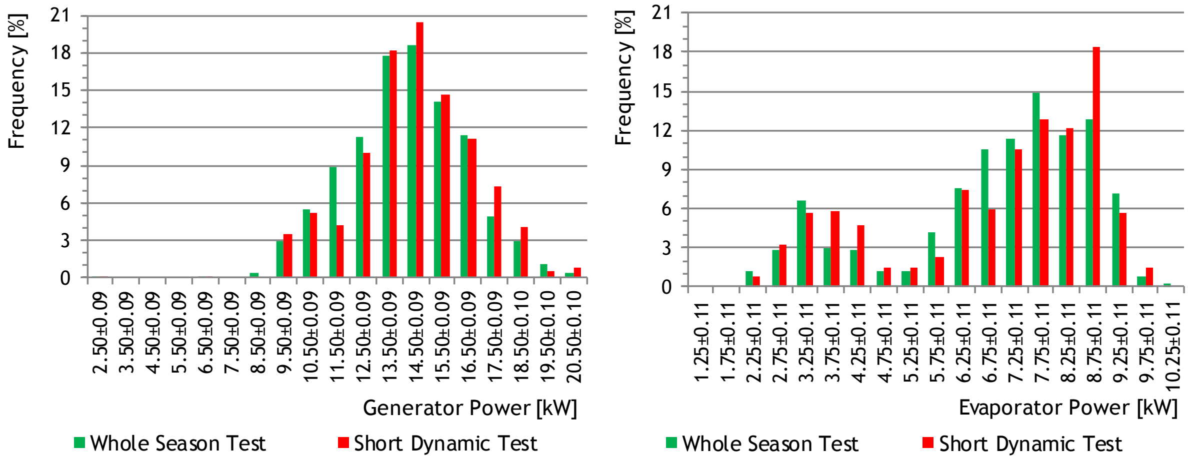

Figure 2-12: Powers’ distributions comparison of whole season and short test. Adsorption chiller.

2.4.3 Comparison with the Bin and CTSS methods

The results obtained with the short dynamic test are compared with the results of the simulations in TRNSYS (CTSS method) and with the Bin Method, as showed in Table 2-12. The Bin Method employed here is similar to the procedure described in EN 14825 [7] (instead of the reference boundary conditions prescribed, the same conditions implemented for the dynamic tests are used). The SEER is calculated with *Equation 1-6*.

Table 2-12: Performance figures comparison of short dynamic test, bin method and simulation. Adsorption chiller.

	SEER		$Q_{evap,s}$		$Q_{gen,s}$	
	[-]	δ [%]	[kWh]	δ [%]	[kWh]	δ [%]
Short Dynamic Test	0.48±0.01	-	1660±26	-	3463±22	-
Bin method	0.55	14.6	1814	9.3	3229	-6.8
Simulation	0.55	14.6	1631	-1.7	2982	-13.9

The simulation and the bin method overestimate the evaluation of the SEER by more than 10% with respect to the short dynamic test. Differences of around 10% are found also for the calculated energy flows. The three methods can be compared as well in terms of EER distribution (Figure 2-13). Both the bin method and the simulations do not show the bi-modal distribution retrieved with the dynamic test. The simulations, however, provides closer values to the dynamic tests, with respect to the bin method, which completely neglects thermal inertia effects.

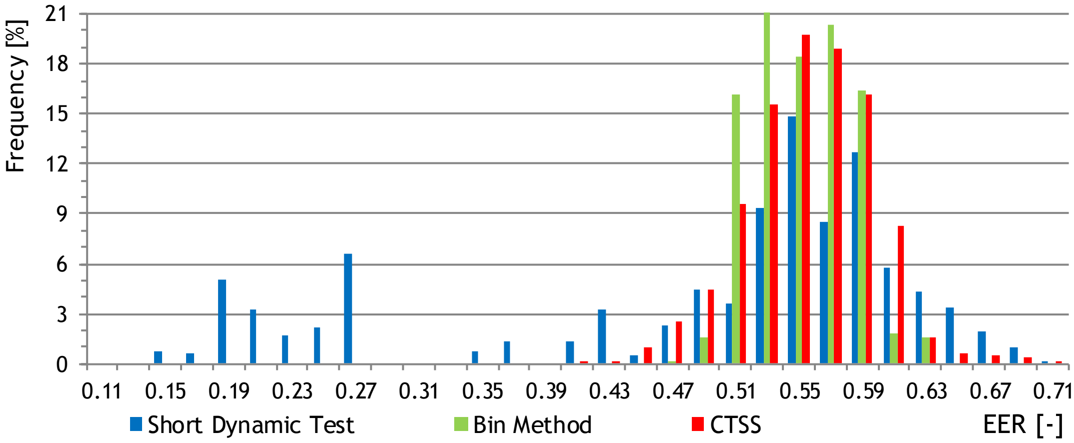

Figure 2-13: EER distribution comparison of short dynamic test, bin method and simulation. Adsorption chiller.

The results obtained from the performed tests show the importance of taking dynamic effects into account and, consequently, the limitations of steady state analysis methods, which ignore some of the intrinsic inefficiencies of the components (or of the systems) under consideration.

2.5 Heat pump characterization

The heat pump is the Clivet WSHN-EE 31 (Table 2-13). This model is an electric driven water to water compression heat pump which uses the refrigerant R-410 A as working fluid. The installed compressor is a scroll-type compressor. An electrical resistance as backup system it is not installed in this unit but could be managed by the heat pump' control system.

Table 2-13: Clivet WSHN-EE31 characteristics.

Compression Heat Pumps	Clivet WSHN-EE 31
Heating capacity	9.42 kW_{th}
Declared COP	5.1
Nominal condition – heating mode	EN14511:2013 30/35°C - 10/7°C
Cooling capacity	10,7 kW_{th}
Declared EER	5.2
Nominal condition – cooling mode	EN14511:2013 23/18°C - 30/35°C
Working fluid	R-410 A
Compressor type	Scroll without inverter

2.5.1 Time series selection

For the vapour compression heat pump, the boundary conditions are the evaporator and condenser inlet temperatures and mass flows. For each *Event*, 9 parameters (*Equation 2-1*) can be identified: duration, amplitude and average of evaporator temperature and mass flow, condenser temperature and mass flow. Since the condenser mass flow is constant, this could be excluded from the classification parameters. From the range of variation of these parameters the *Classes* are created with two criteria. The first one is the identification of intervals of 3 K for temperature, 150 kg/h for mass-flow and 30 minutes for the duration. The second criterion is to consider a constant division of parameters.

The characterization is divided in the two working modes: heating and cooling.

<u>Heating Mode</u>

In Figure 2-14, the time-series for the heat pump boundary conditions are showed, including only the ON-time of the machine. From these boundary conditions, 554 events are identified. The range of variation for all boundary conditions is showed in Table 2-14. The temperatures of condenser and evaporator are quite variable during the season and also during one event. This can be seen with the average values that space out between 22 °C to 44 °C for the condenser and between -5 °C and 13 °C for the evaporator; the amplitude is indication of the variation of the temperature during one event and also this value is high. For the condenser the maximum amplitude is 27.6 °C while for the evaporator is 15 °C. Also the event duration is spacing around a large range (1 min to 719 min).

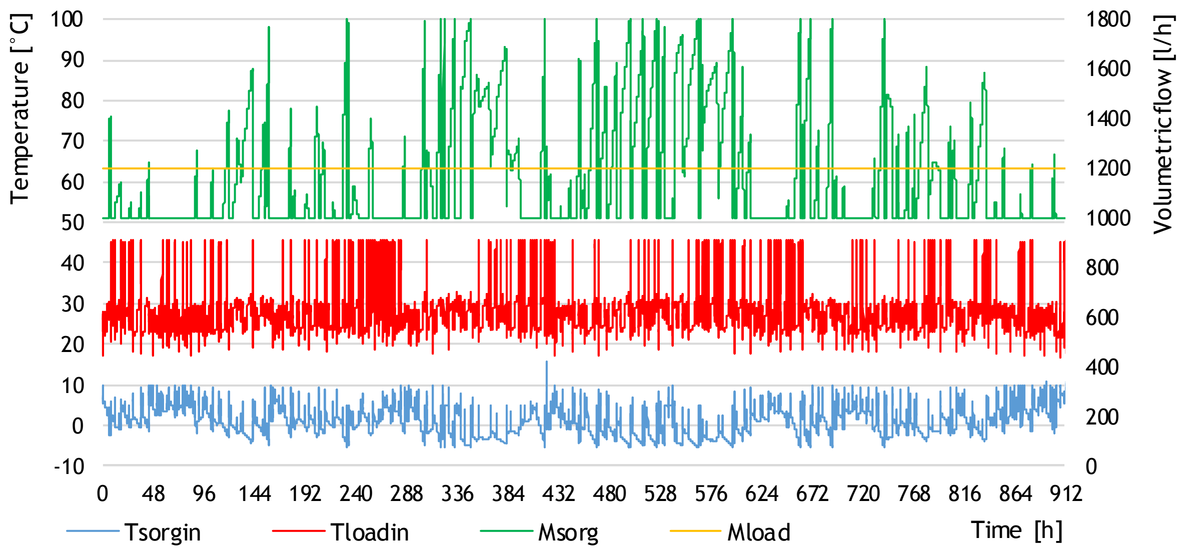

Figure 2-14: Time-series for the boundary conditions of the heat pump in heating mode, considering only the ON-time of the machine.

Table 2-14: Range of variation of boundary conditions. Heat pump - heating mode.

	$T_{cond,avg}$	$T_{cond,amp}$	$T_{evap,avg}$	$T_{evap,amp}$	$\dot{m}_{evap,avg}$	$\dot{m}_{evap,amp}$	τ [min]
Min	22.3	0	-4.6	0	1000	0	1
Max	44.1	27.6	13	14.4	1700	800	719

The subscripts (amp) and (avg) indicate respectively the amplitude and the average, calculated for each event.

Starting from the experience gained with the test performed to the adsorption chiller, different criteria for the definition of the classes are evaluated. Only two different classifications are presented in the Table 2-15; the first one considers intervals of 3 K for the temperature boundary condition and intervals of duration of 30 min while the other one considers a constant division of the intervals (5 interval for each parameter). The table reports the number of classes created with the chosen intervals (No. Classes) and the number of classes with elements (Full Classes). In the same table, the number of events that remain after the threshold and the division is indicated with the “Residual” column. The threshold of 0.2% exclude from the selection the classes with one element, while the 0.4% exclude the classes with two elements and so on.

Table 2-15: Events classification and selection. Heat pump - heating mode.

	Number of intervals									Threshold			Division		
	$T_{cond,avg}$	$T_{cond,amp}$	$T_{evap,avg}$	$T_{evap,amp}$	$\dot{m}_{evap,avg}$	$\dot{m}_{evap,amp}$	duration τ	No. classes	Full classes	Threshold	Residual	Excluded	Divisor	Residual	Test duration [days]
Whole Season	1	1	1	1	1	1	1	1	1	0	554	0	1	554	43
3K-24-1										0.2	297	257	2	161	6
3K-24-2	7	9	6	5	5	5	24	1134000	331	0.4	225	329	3	73	2
3K-24-3										0.6	174	380	4	44	1
5div -24-1										0.2	346	208	2	171	8
5div-24-2	5	5	5	5	5	5	24	375000	286	0.4	230	324	3	73	3
5div -24-3										0.6	194	360	4	51	2

The second column contains the name of the corresponding selection: the number with "K" letter indicates the temperature step while "div" indicates the number of divisions; the second number indicates the number of intervals for the duration and the third number indicates the number of elements excluded with the threshold. The last column shows the test duration expressed in days.

Cooling Mode

In figure the time-series for the chiller boundary conditions are showed, including only the ON-time of the machine. From these boundary conditions, 660 events are identified. The range of variation for all boundary conditions is showed in Table 2-16. In the cooling mode the temperatures are less variable than the one in heating mode. The average temperature of condenser varies between 25 °C and 34 °C while the evaporator between 15.4 °C and 18.2 °C. The maximum amplitudes are 8.3 K for the condenser and 3.8 K for the evaporator. The duration is included in the interval 1 min to 100 min; this lower duration is due to the fact that the heat pump is used as back-up of the chiller.

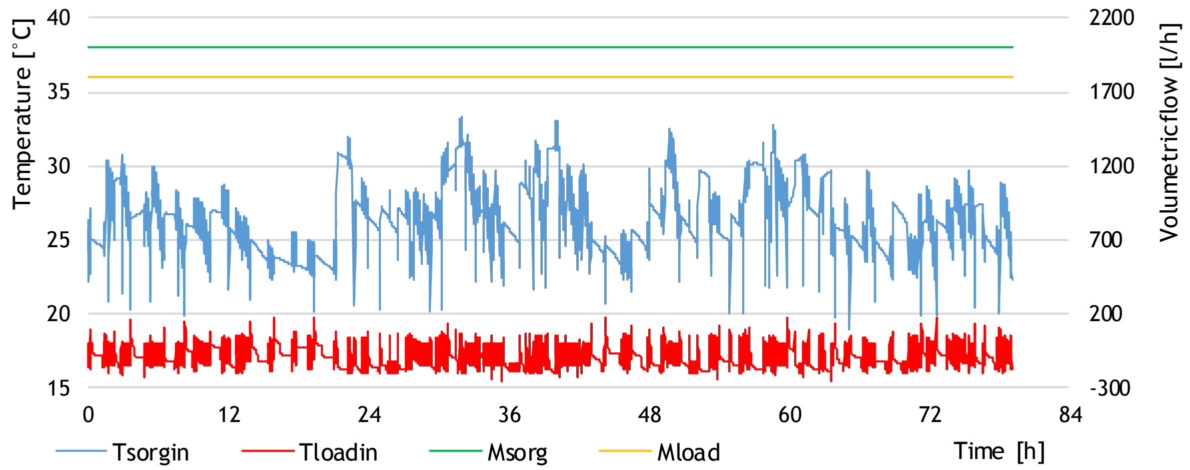

Figure 2-15: Time-series for the boundary conditions of the heat pump in cooling mode, considering only the ON-time of the machine.

Table 2-16: Range of variation of boundary conditions. Heat pump - cooling mode.

	$T_{cond,avg}$	$T_{cond,amp}$	$T_{evap,avg}$	$T_{evap,amp}$	τ [min]
Min	25	0	15.4	0	1
Max	33.6	8.3	18.2	3.8	100

The subscripts (amp) and (avg) indicate respectively the amplitude and the average, calculated for each event.

As the heating mode, different criteria for the classes definition are reported. The same classifications are reported in the Table 2-17. The interval of 3 K requires less divisions since the range are less variable. The consequence is that less classes are created.

Table 2-17: Events classification and selection. Heat pump - cooling mode.

	Number of intervals							Threshold			Division		
	$T_{cond,avg}$	$T_{cond,amp}$	$T_{evap,avg}$	$T_{evap,amp}$	duration τ	No. classes	Full classes	Threshold	Residual	Excluded	Divisor	Residual	Test duration [days]
Whole Season	1	1	1	1	1	1	1	0	660	0	1	660	8
3K-25-1								0.2	649	11	2	330	4
3K-25-2	3	3	1	2	4	72	36	0.4	635	25	3	212	2
3K-25-3								0.6	620	40	4	156	2
5div-25-1								0.2	609	51	2	313	3
5div-25-2	5	5	5	5	4	2500	106	0.4	581	79	3	193	2
5div-25-3								0.6	563	97	4	142	1

The second column contains the name of the corresponding selection: the number with "K" letter indicates the temperature step while "div" indicates the number of divisions; the second number indicates the number of intervals for the duration and the third number indicates the number of elements excluded with the threshold. The last column shows the test duration expressed in days.

2.5.2 Dynamic test results

The characterization of the heat pump performance is separated into the two working modes: heating and cooling.

<u>Heating Mode</u>

Table 2-18 presents the seasonal and the monthly results for the heating season in terms of number of events, total duration, average condenser and evaporator temperatures, SCOP, electric energy consumed by the heat pump and exchanged thermal energies at the condenser and the evaporator.

The considerations streamlined with respect to the schemes distribution help understanding the results in Table 2-18. The SCOP is calculate with Equation 1-5 considering the integration domain on month and seasonal basis. The SCOP varies for the different months between 3.36 and 3.85 while the seasonal value is 3.47. The seasonal value is lower than the mathematical average of the monthly values because the months with a higher SCOP present few working hours. In particular, the months with higher SCOP are, as anticipated, April and October, with one and six working hours respectively. In addition, also March, with a total of 41 working hours, presents a quite high SCOP, because the air source scheme can work with high evaporator temperatures (mild external air temperature). The months with lower SCOP are, as expected, the colder ones, i.e. December, January and February, with respectively 377, 390 and 175 working hours.

Table 2-18: Monthly and seasonal results. Heat pump - heating mode.

	n_{ev}	τ_{on}	$\overline{T}_{cond}$	$\overline{T}_{evap}$	SCOP	W_{hp}	Q_{co}	Q_{ev}
		[h]	[°C]	[°C]	[-]	[kWh]	[kWh]	[kWh]
Seasonal	554	937	27.1	1.9	3.47±0.07	1873.2±18.7	6496.4±103.9	4574.2±73.2
October	4	6	26.1	4.6	3.85±0.07	12.4±0.1	47.9±0.8	35.1±0.6
November	93	147	27.1	1.8	3.59±0.07	291.4±2.9	1046.5±16.7	732.5±11.7
December	167	277	27.8	0.4	3.36±0.06	558.0±5.6	1877.0±30.0	1296.1±20.7
January	130	290	27.7	-0.2	3.44±0.06	580.8±5.8	1998.5±32.0	1387.6±22.2
February	89	175	27.4	0.8	3.49±0.07	348.9±3.5	1217.9±19.5	878.4±14.1
March	68	41	25.9	5.6	3.78±0.07	80.0±0.8	302.2±4.8	239.4±3.8
April	3	1	25.4	5.6	3.71±0.07	1.7±0.0	6.4±0.1	5.0±0.1

Besides the evaluation of the seasonal and monthly SCOPs, dynamic tests also allow a deeper analysis of the behaviour of the heat pump during transients. This can be done by considering a single *Event* as shown in Figure 2-16, where an example of temperature and power times-series for heating operation with air source is reported. The *Event* starts with a space heating scheme at minute 4; at minute 17 the scheme switches to DHW preparation until minute 38, when the scheme is switched back to space heating. The electric power consumption (W_{hp}) is stable from the switch ON and throughout the whole *Event*, while the condenser power ($\dot{Q}_{co}$) and, as consequence, the COP vary. In particular, the condenser power presents two transients moving from zero to a stable value. The first corresponds to the switch ON of the heat pump (green rectangle 1 in Figure 2-16); the second is localized at the switch from space heating to domestic hot water preparation (yellow rectangle 2 in Figure 2-16). In both cases, the outlet condenser temperature ($T_{co,out}$) has to increase and it does so with a certain delay due to the thermal inertia of the machine. Consequently, the instantaneous temperature values are similar (or lower) to the inlet temperature ($T_{co,in}$). This results in a null instantaneous power, which progressively increases towards a stationary value (with a positive temperature difference). During the switch from domestic hot water to space heating, a third transient phase takes place (blue rectangle 3 in Figure 2-16), where the condenser power abruptly increases and then progressively decreases to a new stationary condition. In this case, the inlet condenser temperature decreases, while the outlet temperature follows with some delay caused again by the thermal inertia. The high instantaneous values of the condenser power are a consequence of temperature differences higher than those obtained in stationary operation.

The dynamic behaviour represented in Figure 2-16 could be interpreted as a "storage" effect of the heat pump. In the transient phases with increasing temperatures the heat exchanger of the condenser "stores" energy; this is "released" during the transient phases where the temperatures decrease. If an *Event* stops with a domestic hot water scheme, the energy "stored" in the initial transient is lost most of the times.

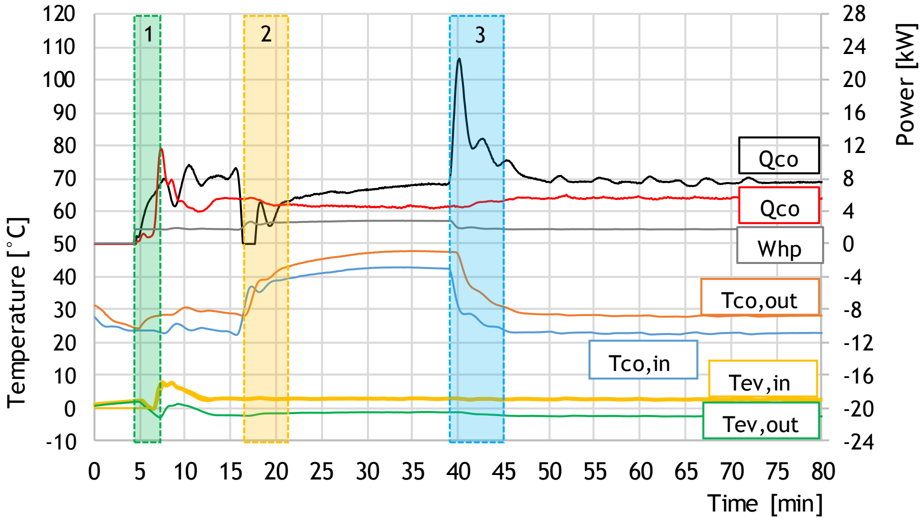

Figure 2-16: Temperature and power profiles during test. Heat pump - heating mode.

The temperature profiles are indicated with the label "T" while the thermal power profiles are indicated with the label "Q" and the electrical power with the letter "W". The first letter of the subscript indicates the circuits (condenser "co" and evaporator "ev") while the second one indicates the input "in" or the output "out".

To understand how these transients affect the seasonal performance of the heat pump, the instantaneous COPs obtained during the dynamic tests for the whole season are reported in Figure 2-17, as a function of the condenser temperature. The curves obtained for different evaporator temperatures under steady state conditions are also plotted as a reference. Different working conditions can be identified in the figure:

- Stationary state operation points corresponding to the cloud of points distributed over the stationary curves; the red points in dynamic condition (those at evaporator temperature of 10°C) are obtained for only short time, as consequence the stationary conditions are not reached.
- Initial transient points (indicated with the two green-arrows - 1a/heating and 1b/DHW - in Figure 2-17). Depending on the scheme with which the heat pump is activated, these points are localized at different condenser temperatures;
- Points corresponding to the switch from space heating to domestic hot water (indicated with the yellow arrow – 2 - in Figure 2-17). During these transients, the temperature of the condenser is increasing and a "storing" effect occurs;
- Points corresponding to the switch from domestic hot water to space heating (indicated with the blue arrow – 3 – in Figure 2-17). During these transients, the condenser temperature decreases and an "energy releasing" effect occurs;

- Area without dynamic COP points (indicated by a black ellipse – 4 – in Figure 2-17). This zone corresponds to the evaporator temperatures between the space heating and the domestic hot water set points (namely 32°C and 40°C for the examined plant). The machine is never working at steady state conditions in this range.

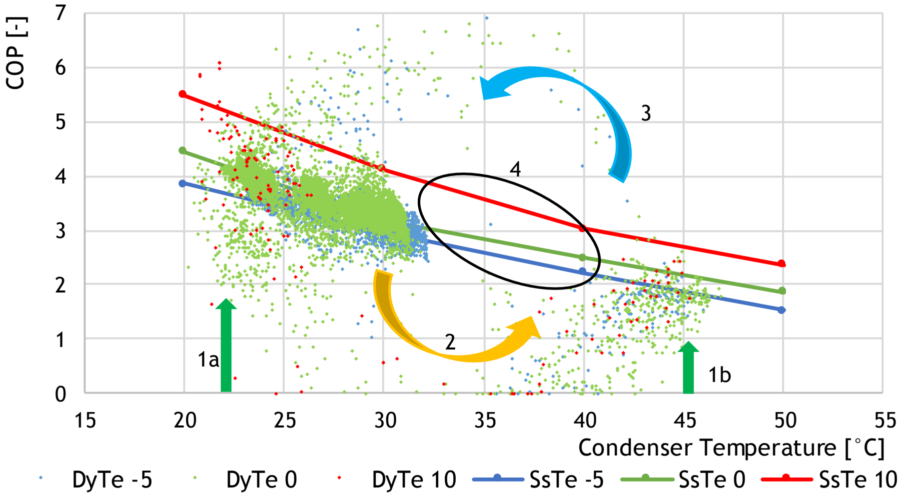

Figure 2-17: COP comparison of dynamic and stationary conditions. Heat pump - heating mode. *The series are divided by evaporator temperature respectively for the case of dynamic test and steady-state test. The name of the series indicates the typology of test (dynamic - Dy or stationary SS) and the evaporator temperature (i.e. Te -5).*

Table 2-19 shows the results obtained with the seasonal test and the results of the short test sequences. The duration of the short test depends from the selection criteria applied in the definition of the sequence. The duration is 6/8 days when a 0.2 % threshold is applied with respect to 43 days needed for the full-length test (and representing the whole heating season). The duration of the test is connected to its cost. The reduction of the test with this classification is huge.

Table 2-19: Result of tests. Heat pump - heating mode.

Test		Test duration [days]	SCOP [-]	SCOP δ [%]	W_{el} [kWh]	Q_{cond} [kWh]	Q_{evap} [kWh]
Whole Season		43	3.47±0.07		1873±19	6496±104	4574±73
Test 1	3K-24-1	5.8	3.36±0.06	-3.15	229.2±2.3	769.7±12.3	569.4±9.1
Test 2	3K-24-1	6.	3.39±0.06	-2.19	238.4±2.4	808.6±12.9	601.9±9.6
Test 3	3K-24-1	5.9	3.39±0.06	-2.24	232.4±2.3	787.9±12.6	584.5±9.4
Test 4	3K-24-2	2.1	3.29±0.06	-5.29	77.0±0.8	253.0±4.0	193.4±3.1
Test 5	3K-24-2	2.1	3.34±0.06	-3.61	76.4±0.8	255.3±4.1	194.6±3.1
Test 6	3K-24-3	1.0	3.16±0.06	-9.00	34.2±0.3	108.0±1.7	85.4±1.4
Test 7	3K-24-3	1.0	3.11±0.06	-10.41	33.5±0.3	104.0±1.7	82.9±1.3
Test 8	5div -24-1	7.5	3.42±0.06	-1.91	304.6±3.0	1036.3±16.6	764.3±12.2
Test 9	5div -24-1	7.7	3.42±0.06	-1.29	315.0±3.2	1078.3±17.3	795.9±12.7
Test 10	5div -24-1	7.6	3.43±0.06	-1.21	307.6±3.1	1053.8±16.9	773.5±12.4
Test 11	5div-24-2	3.1	3.90±0.06	-4.93	119.9±1.2	395.4±6.3	297.8±4.8
Test 12	5div-24-2	2.8	3.28±0.06	-5.44	108.7±1.1	356.6±5.7	270.6±4.3
Test 13	5div -24-3	1.7	3.25±0.06	-6.42	62.7±0.6	203.5±3.3	157.5±2.5
Test 14	5div -24-3	1.6	3.21±0.06	-7.54	58.7±0.6	188.3±3.0	144.6±2.3

The second column contains the name of the corresponding selection: the number with "K" letter indicates the temperature step while "div" indicates the number of divisions; the second number indicates the number of intervals for the duration and the third number indicates the number of elements excluded with the threshold.

Table 2-20 presents the evaluation of the seasonal energy and the deviation from the seasonal energy. The deviation on the evaluation of the SCOP with the selection is lower than 3% in case of exclusion of classes with one event. The increase of the threshold value decreases the test duration but increase the deviation performed. The deviation increases until 10% when classes with 3 elements are excluded from the selection. The outcome is the same of the chiller characterization since the best result is obtained by excluding only the classes with one element. The difference with the selection of the chiller's boundary condition is that a constant division of parameters gives a good correspondence for the heat pump in heating mode while that criterion was excluded for the chiller [54].

Table 2-20: Seasonal energies estimation. Heat pump - heating mode.

	SCOP		$W_{hp,s}$		$Q_{cond,s}$		$Q_{evap,s}$	
	[-]	δ [%]	[kWh]	δ [%]	[kWh]	δ [%]	[kWh]	δ [%]
Whole Season	3.47±0.07		1873±19	-	6496±104	-	4574±73	-
Test 1	3.36±0.06	-3.15	1909±19	1.90	6411±103	-1.31	4743±76	3.69
Test 2	3.39±0.06	-2.19	1899±19	1.39	6442±103	-0.84	4795±77	4.83
Test 3	3.39±0.06	-2.24	1902±19	1.53	6448±103	-0.74	4784±77	4.58
Test 4	3.29±0.06	-5.29	1916±19	2.29	6294±101	-3.11	4812±77	5.19
Test 5	3.34±0.06	-3.61	1898±19	1.33	6345±102	-2.33	4836±77	5.73
Test 6	3.16±0.06	-9.00	1911±19	2.02	6031±97	-7.17	4767±76	4.21
Test 7	3.11±0.06	-10.41	1934±19	3.26	6010±96	-7.49	4788±77	4.68
Test 8	3.42±0.06	-1.91	1904±19	1.65	6477±104	-0.30	4777±76	4.44
Test 9	3.42±0.06	-1.29	1905±19	1.70	6522±104	0.39	4813±77	5.23
Test 10	3.43±0.06	-1.21	1899±19	1.37	6506±104	0.14	4775±76	4.39
Test 11	3.90±0.06	-4.93	1919±19	2.46	6328±101	-2.59	4766±76	4.20
Test 12	3.28±0.06	-5.44	1927±19	2.86	6318±101	-2.74	4794±77	4.82
Test 13	3.25±0.06	-6.42	1918±19	2.40	6226±100	-4.17	4818±77	5.32
Test 14	3.21±0.06	-7.54	1926±19	2.80	6174±99	-4.96	4741±76	3.64

The Table 2-21 completes the previous table; it presents the evaluation of the electric consumption of the circulation pumps due to the pressure drop in the heat pump circuit, the dry cooler fun consumption and the total energy consumption. The SCOP is recalculated considering also these contribution of consumption. The SCOP decreases from 3.47 when it is calculated only for the heat pump until 3.36 when it is considered the whole plant (air unit and circulation pumps).

Table 2-21: Seasonal consumptions estimation. Heat pump - heating mode.

	SCOP		$W_{cond,s}$		$W_{evap,s}$		$W_{dc,s}$		$W_{tot,s}$	
	[-]	δ [%]	[kWh]	δ [%]	[kWh]	δ [%]	[kWh]	δ [%]	[kWh]	δ [%]
Whole Season	3.360	-	5.3	-	9.3	-	45.7		1934	-
Test 1	3.257	-3.05	5.8	8.6	6.3	-32.7	47.4	3.69	1968	1.79
Test 2	3.288	-2.13	5.6	5.8	6.4	-31.4	48.0	4.83	1959	1.32
Test 3	3.287	-2.16	5.5	3.6	6.3	-32.6	47.8	4.58	1962	1.45
Test 4	3.186	-5.18	5.6	5.4	5.9	-36.6	48.1	5.19	1976	2.18
Test 5	3.240	-3.57	6.1	15.4	5.9	-36.9	48.4	5.73	1959	1.29
Test 6	3.060	-8.91	6.1	14.3	5.9	-37.3	47.7	4.21	1971	1.91
Test 7	3.015	-10.3	5.6	5.4	5.8	-38.3	47.9	4.68	1993	3.09
Test 8	3.299	-1.80	5.4	1.6	6.0	-36.1	47.8	4.44	1963	1.53
Test 9	3.319	-1.20	5.6	4.6	6.0	-35.4	48.1	5.23	1965	1.61
Test 10	3.322	-1.13	5.9	10.2	6.0	-35.4	47.8	4.39	1958	1.29
Test 11	3.198	-4.80	5.9	11.2	5.8	-38.2	47.7	4.20	1979	2.33
Test 12	3.181	-5.31	5.6	5.6	5.7	-38.6	47.9	4.82	1986	2.71
Test 13	3.148	-6.31	5.5	4.3	5.8	-38.1	48.2	5.32	1978	2.28
Test 14	3.111	-7.40	5.9	11.2	5.7	-38.7	47.4	3.64	1985	2.64

Besides the evaluation of the seasonal performance figures, the proposed test sequence allows analysing also the frequency distribution of the instantaneous performance figures (COP and powers). In Figure 2-18, the COP distribution obtained during the seasonal and short tests are compared. The COP has a typical normal distribution spanning between 0 to 5.5 with a peak around 3.7. As a consequence of the transients, about 8% of the values are below 2. From Figure 2-18, it is clear that the distribution obtained with the short sequence is comparable to the seasonal one. This is possible because the boundary conditions selection takes into account the statistical distribution of the seasonal boundary conditions.

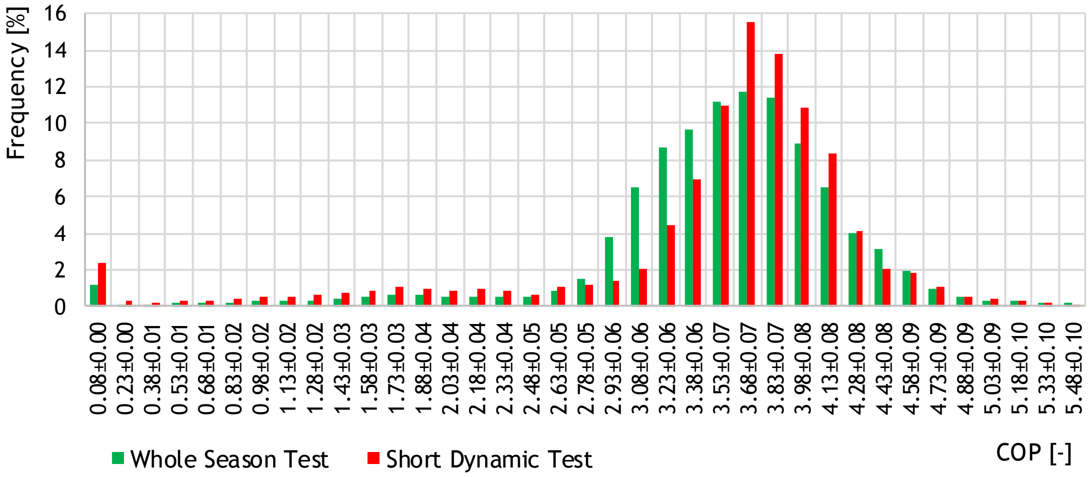

Figure 2-18: COP distribution comparison of whole season and short test. Heat pump - heating mode.

Cooling Mode

Table 2-22 presents the seasonal and the monthly results for the cooling season, similarly to what already presented for the heating season. The SEER is calculated with Equation 1-6 considering the integration domain on month and seasonal basis. The monthly SEER is varying from 3.55 to 3.85 while the seasonal value is 3.75. September is the month with the lowest SEER, and it also presents the lowest average duration of *Events* (about 5 minutes). In this case, the presence of initial transients has a stronger effect on the performance.

Table 2-22: Monthly and seasonal results. Heat pump - cooling mode.

	n_{ev}	τ_{on} [h]	T_{cond} [°C]	T_{evap} [°C]	SEER [-]	W_{hp} [kWh]	Q_{cond} [kWh]	Q_{evap} [kWh]
Seasonal	660	79	28.2	17.0	3.75±0.07	163.7±1.6	709.1±11.3	613.7±9.8
June	151	16	27.8	17.1	3.73±0.07	32.2±0.3	136.6±2.2	120.3±1.9
July	215	26	28.5	16.9	3.73±0.07	55.0±0.6	237.6±3.8	205.2±3.3
August	209	29	28.4	16.9	3.83±0.07	60.8±0.6	273.0±4.4	232.6±3.7
September	85	8	27.8	17.1	3.55±0.07	15.7±0.2	62.0±1.0	55.6±0.9

A deeper insight on the behaviour of the machine during transients can be obtained by looking at the temperature series recorded during a single *Event* in the cooling season, as reported in Figure 2-19. The *Event* starts at minute 1 and ends at minute 19. While the electric consumption (W_{el}) is stable over the whole period, the condenser and evaporator powers present a transient phase of about 3 minutes before reaching the steady state conditions. The temperature difference at the evaporator obtained during the transient is lower than that obtained in steady state and so is the instantaneous EER.

With respect to the heating season, the boundary conditions in cooling mode are less variable (the machine is working with one scheme only) but a larger number of *Events* with short duration is present. For example, the average duration of an *Event* in cooling mode is 7 minutes but many *Events* have a shorter duration. As a consequence, the starting transients have a large impact on the performance. This can be easily observed in Figure 2-20, showing the instantaneous EER as a function of the condenser temperature along with the steady state curves obtained for different evaporator temperatures. Two main areas can be identified in Figure 2-20. The first one (black rectangle) is located near the steady state curves: it includes the working points obtained after the initial transient phases. The second cloud (indicated with a green arrow) has a larger extension and cover the zone from zero EER to the stationary conditions: these points represent the switch ON transient working conditions.

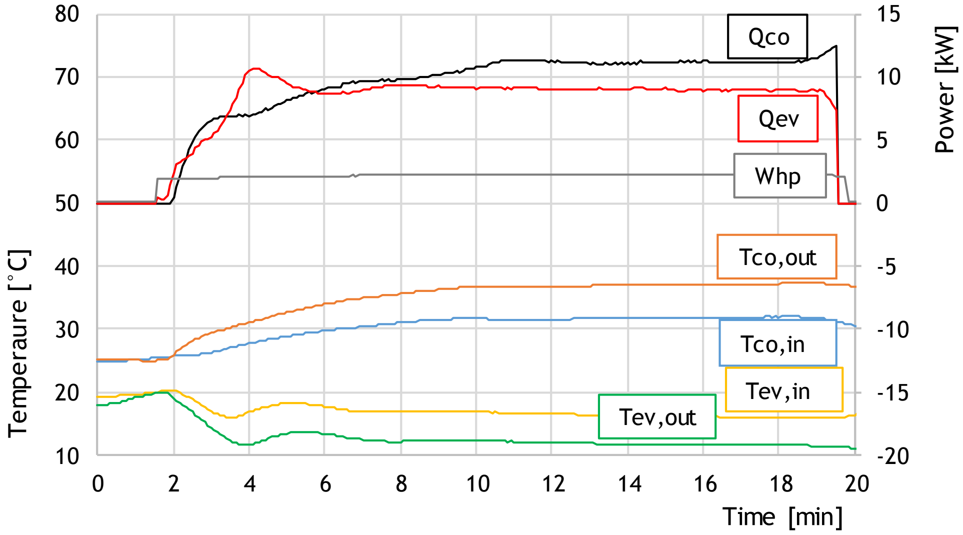

Figure 2-19: Temperature and power profiles during test. Heat pump - cooling mode.
The temperature profiles are indicated with the label "T" while the thermal power profiles are indicated with the label "Q" and the electrical power with the letter "W". The first letter of the subscript indicates the circuits (condenser "co" and evaporator "ev") while the second one indicates the input "in" or the output "out".

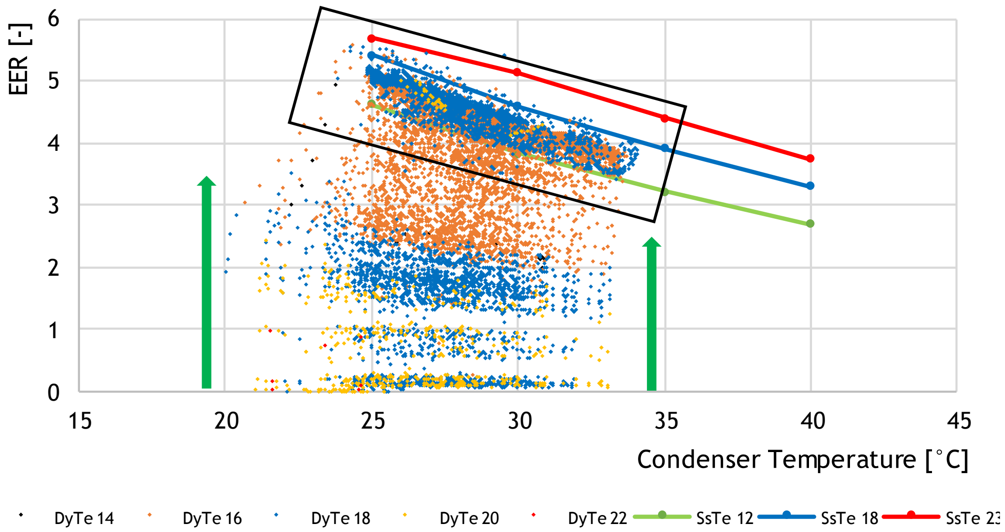

Figure 2-20: EER comparison of dynamic and steady state conditions. Heat pump - cooling mode.
The series are divided by evaporator temperature respectively for the case of dynamic test and steady-state test. The name of the series indicates the typology of test (dynamic - Dy or stationary SS) and the evaporator temperature (i.e. Te 14).

Table 2-23 shows the results obtained in the seasonal test and the results of the short test for the cooling season. The duration of the short test is at least half of the seasonal test. From the short test result, the seasonal energy is extrapolated (Table 2-24). The deviation between the whole season and the test depends from the selection criteria. The constant division of criterion has a large deviation since its range of parameter is small and five divisions create small intervals. This selection criterion was excluded also in the analysis done for the chiller.

The criterion of "3K intervals" gives a small deviation (lower than 2%) for the selection with the threshold of 0.2 %. The reduction of the duration with a higher threshold would involve in a higher deviation (about 5%).

Table 2-23: Result of tests. Heat pump - cooling mode.

Test		Duration	SEER		W_{el}	Q_{cond}	Q_{evap}
		[days]	[-]	δ [%]	[kWh]	[kWh]	[kWh]
Whole Season		7.9	3.75±0.07	-	163.7±1.6	709.1±11.3	613.7±9.8
Test 1	3K-24-1	3.8	3.69±0.07	-1.48	75.2±0.8	318.4±5.1	277.9±4.4
Test 2	3K-24-1	3.8	3.69±0.07	-1.63	75.3±0.8	319.1±5.1	277.8±4.4
Test 3	3K-24-1	3.8	3.68±0.07	-1.75	73.2±0.7	308.4±4.9	269.8±4.3
Test 4	3K-24-2	2.3	3.55±0.07	-5.38	40.9±0.4	163.7±2.6	145.0±2.3
Test 5	3K-24-2	2.3	3.56±0.07	-5.08	41.7±0.4	167.9±2.7	148.4±2.4
Test 6	3K-24-3	1.6	3.31±0.06	-11.61	23.9±0.2	86.2±1.4	79.3±1.3
Test 7	3K-24-3	1.5	3.22±0.06	-14.14	23.0±0.2	80.6±1.3	74.0±1.2
Test 8	5div -24-1	3.2	3.35±0.06	-10.66	51.2±0.5	189.3±3.0	171.5±2.7
Test 9	5div -24-1	3.2	3.38±0.06	-9.88	52.8±0.5	198.6±3.2	178.3±2.9
Test 10	5div -24-1	3.2	3.34±0.06	-10.83	50.9±0.5	187.9±3.0	170.1±2.7
Test 11	5div-24-2	1.8	2.99±0.06	-20.23	24.6±0.2	77.5±1.2	73.6±1.2
Test 12	5div-24-2	1.8	3.00±0.06	-20.03	24.8±0.2	78.3±1.3	74.3±1.2
Test 13	5div -24-3	1.3	2.86±0.05	-23.65	16.6±0.2	48.4±0.8	47.4±0.8
Test 14	5div -24-3	1.3	2.87±0.05	-23.36	16.8±0.2	49.7±0.8	48.3±0.8

The second column contains the name of the corresponding selection: the number with "K" letter indicates the temperature step while "div" indicates the number of divisions; the second number indicates the number of intervals for the duration and the third number indicates the number of elements excluded with the threshold.

Table 2-24 Seasonal energies estimation. Heat pump - cooling mode.

	SEER		$W_{hp,s}$		$Q_{cond,s}$		$Q_{evap,s}$	
	[-]	δ [%]	[kWh]	δ [%]	[kWh]	δ [%]	[kWh]	δ [%]
Whole Season	3.75±0.07	-	163.7±1.6	-	709.1±11.3	-	613.7±9.8	-
Test 1	3.69±0.07	-1.48	163.4±1.6	-0.20	691.4±11.1	-2.48	603.4±9.7	-1.68
Test 2	3.69±0.07	-1.63	163.3±1.6	-0.22	691.9±11.1	-2.42	602.4±9.6	-1.85
Test 3	3.68±0.07	-1.75	162.9±1.6	-0.48	686.0±11.0	-3.25	600.0±9.6	-2.22
Test 4	3.55±0.07	-5.38	163.4±1.6	-0.20	654.1±10.5	-7.76	579.5±9.3	-5.57
Test 5	3.56±0.07	-5.08	162.9±1.6	-0.46	656.1±10.5	-7.47	579.8±9.3	-5.52
Test 6	3.31±0.06	-11.61	162.7±1.6	-0.62	586.5±9.4	-17.28	539.1±8.6	-12.16
Test 7	3.22±0.06	-14.14	163.7±1.6	0.04	574.5±9.2	-18.98	527.1±8.4	-14.11
Test 8	3.35±0.06	-10.66	163.3±1.6	-0.21	604.0±9.7	-14.82	547.1±8.8	-10.85
Test 9	3.38±0.06	-9.88	163.6±1.6	-0.06	615.6±9.8	-13.19	552.8±8.8	-9.93
Test 10	3.34±0.06	-10.83	163.5±1.6	-0.11	604.0±9.7	-14.82	546.7±8.7	-10.92
Test 11	2.99±0.06	-20.23	164.3±1.6	0.37	517.3±8.3	-27.05	491.3±7.9	-19.94
Test 12	3.00±0.06	-20.03	163.8±1.6	0.10	517.9±8.3	-26.96	491.3±7.9	-19.95
Test 13	2.86±0.05	-23.65	163.6±1.6	-0.03	477.6±7.6	-32.64	468.4±7.5	-23.68
Test 14	2.87±0.05	-23.36	164.2±1.6	0.33	485.7±7.8	-31.50	471.9±7.6	-23.11

Table 2-25 presents the calculation of the SEER considering also the estimation of the electric consumption required for the circulation pumps and the rejection of heat with the dry cooler. The electric consumption of the circulation pumps is calculated from the pressure drop measured during the test while the dry cooler consumption is calculated from the energy rejected. The deviation of the dry cooler consumption between the whole season test and the short test is connected to the deviation of the condenser energy since a direct correlation is applied.

In cooling mode, the seasonal electric consumption of the heat pump is about 164 kWh and it is increased of 25 kWh for the auxiliaries. The consequence is that the SEER is reduced from 3.75 to 3.25 when the whole electric consumption is considered.

Table 2-25: Seasonal consumptions estimation. Heat pump - cooling mode.

	SEER		$W_{cond,s}$		$W_{evap,s}$		$W_{dc,s}$		$W_{tot,s}$	
	[-]	δ [%]	[kWh]	δ [%]	[kWh]	δ [%]	[kWh]	δ [%]	[kWh]	δ [%]
Whole Season	3.25	-	0.5	-	3.4	-	21.3	-	188.9	-
Test 1	3.21	-1.2	0.5	-0.13	3.4	-0.06	20.7	-2.48	188.0	-0.5
Test 2	3.20	-1.4	0.5	-0.46	3.4	-0.12	20.8	-2.42	188.0	-0.5
Test 3	3.20	-1.5	0.5	-0.53	3.4	-0.15	20.6	-3.25	187.4	-0.8
Test 4	3.10	-4.6	0.5	-0.93	3.4	-0.38	19.6	-7.76	186.9	-1.1
Test 5	3.11	-4.3	0.5	-0.11	3.4	-0.30	19.7	-7.47	186.5	-1.2
Test 6	2.93	-9.9	0.5	0.54	3.4	-0.65	17.6	-17.3	184.2	-2.5
Test 7	2.85	-12.3	0.5	0.04	3.4	-0.66	17.2	-19.0	184.9	-2.1
Test 8	2.95	-9.2	0.5	-0.36	3.4	-0.76	18.1	-14.8	185.3	-1.9
Test 9	2.97	-8.5	0.5	0.05	3.4	-0.44	18.5	-13.2	186.0	-1.5
Test 10	2.95	-9.3	0.5	-0.65	3.4	-0.72	18.1	-14.8	185.5	-1.8
Test 11	2.68	-17.7	0.5	-0.33	3.4	-1.11	15.5	-27.1	183.7	-2.7
Test 12	2.68	-17.5	0.5	-0.55	3.4	-1.21	15.5	-27.0	183.3	-3.0
Test 13	2.58	-20.7	0.5	-1.52	3.4	-1.45	14.3	-32.6	181.8	-3.7
Test 14	2.58	-20.5	0.5	-0.80	3.4	-0.87	14.6	-31.5	182.7	-3.3

Figure 2-21 reports the comparison of EER frequency distributions as obtained from the whole season tests and from the short test sequence. The EER varies between 0 and 5.3; in particular, about 14% of the values are lower than 2. The large amount of points with low EER is due to the presence of short events, with an overall duration comparable to the initial transient phase duration. The shape of the short test distribution is close to the seasonal test one, validating again the boundary conditions selection procedure.

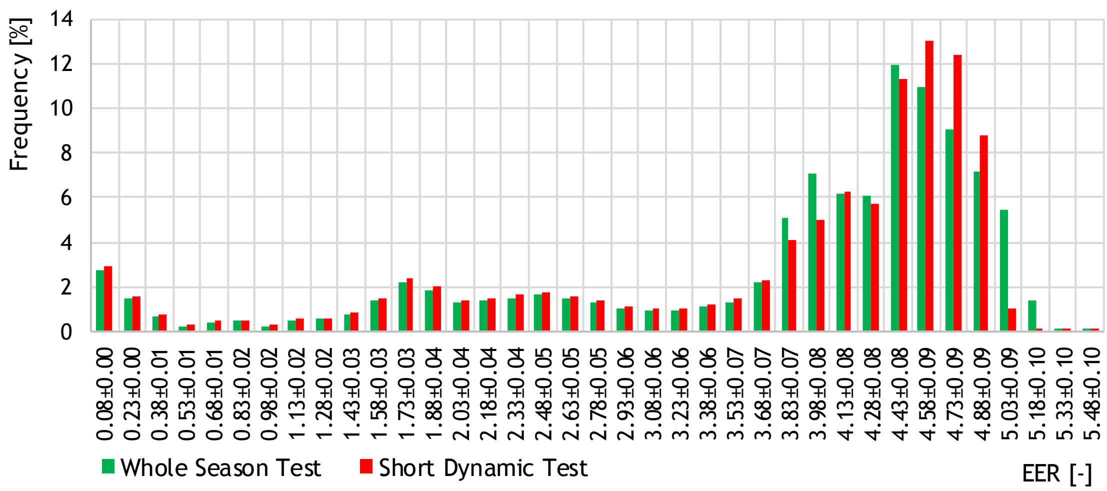

Figure 2-21: EER distribution comparison of whole season and short test. Heat pump - cooling mode.

2.5.3 Comparison with the Bin and CTSS methods

The results obtained with the dynamic test are compared with the Bin Method and with the results of the simulations in TRNSYS (CTSS method) as done for the adsorption chiller. As the previous sections, the heating and cooling modes are distinguished.

The Bin Method employed here considers the boundary condition of the dynamic test instead of the reference climate indicated in EN 14825 [7].

The numerical model used for the CTSS method has been validated with the test performed in accordance to the EN 14511 and it is described in the Appendix C.

Heating Mode

Table 2-26 shows the comparison between CTSS, Bin Method and the dynamic test in terms of SCOP, W_{hp}, Q_{cond}.

The seasonal performance calculated with the Bin Methods is close to the one assessed with the dynamic test. The deviation between the two seasonal coefficients of performance is 2.4 %. At opposite, the CTSS presents a 5.9 % of difference in the evaluation of the SCOP. The electrical energy is assessed with a difference of 0.3% than the dynamic test but the condenser energy of 5.4 %.

Table 2-26: Performance figures comparison of short dynamic test, bin method and simulation. Heat pump - heating mode.

	SCOP		W_{hp}		Q_{cond}	
	[-]	δ [%]	[kWh]	δ [%]	[kWh]	δ [%]
Dynamic Test	3.39±0.06	-	1899±19	-	6442±103	-
Bin Method	3.47	2.4	1864	-1.8	6460	0.3
CTSS	3.59	5.9	1892	-0.3	6792	5.4

The Figure 2-22 shows a good agreement of distribution near the modal peak. However, the Bin and CTSS methods neglect the lowest values of COP due to the initial transient phase.

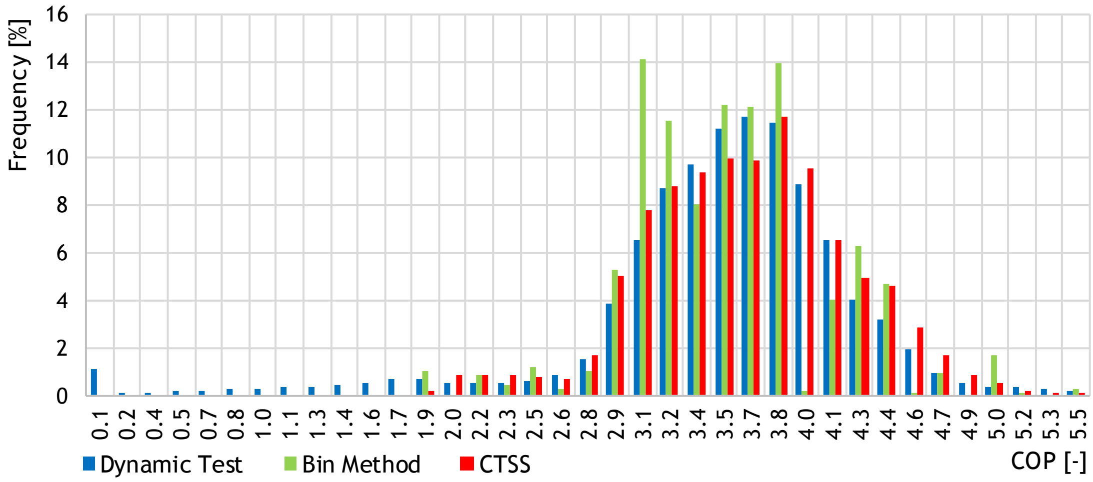

Figure 2-22: COP distribution comparison of short dynamic test, bin method and simulation. Heat pump - heating mode

Cooling Mode

Table 2-27 shows the comparison between CTSS, Bin Method and the dynamic test in terms of SEER, W_{hp}, Q_{evap}.

The Bin and CTSS methods present a large difference with the evaluation done with the dynamic test. These two methods are based on stationary characterization of performance. As the Events are very short, the initial transient phase as a large influence on the final performance. The neglect of this aspect causes a large difference between the dynamic and steady state characterizations.

Table 2-27: Performance figures comparison of short dynamic test, bin method and simulation. Heat pump - cooling mode.

	SEER		W_{hp}		Q_{evap}	
	[-]	δ [%]	[kWh]	δ [%]	[kWh]	δ [%]
Dynamic Test	3.69±0.07	-	163±2	-	604±9.7	-
Bin Method	4.74	28.5	161	-1.2	761	26.0
CTSS	4.87	31.9	163	0	796	31.8

Figure 2-23 shows the distribution of EER obtained with the three methods. The dynamic test evaluates a large number of points with really low values.

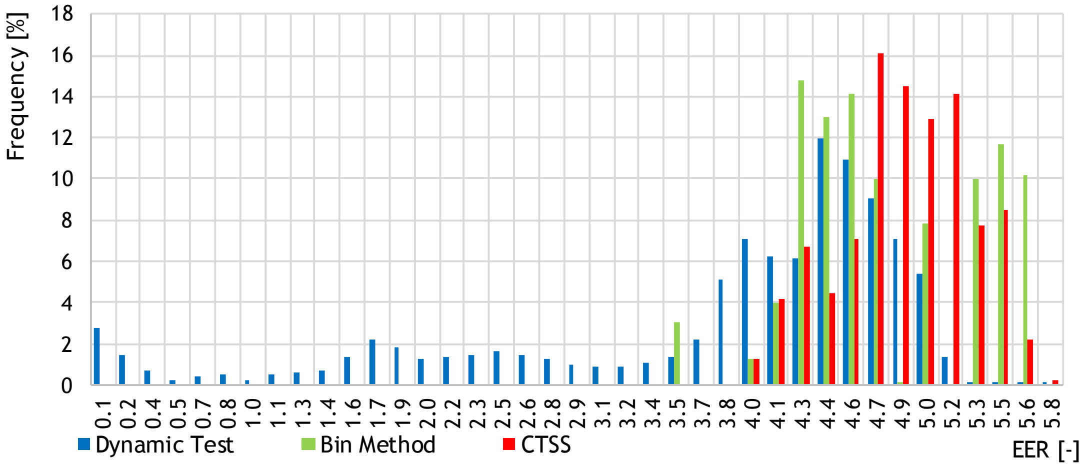

Figure 2-23: EER distribution comparison of short dynamic test, bin method and simulation. Heat pump - cooling mode.

2.6 Conclusions

This chapter has presented the procedure developed for the dynamic characterization of components. The procedure foresees the definition of real-like boundary condition of the component and a selection of a representative part. The sequence is reduced from the whole seasonal boundary conditions to a short test sequence of few days with a classification method developed in analogy with the fatigue analysis. The boundary conditions are divided into intervals that consider their amplitude and average values and from these, classes are created to classify the boundary conditions. The selection is performed by excluding the classes with a frequency lower than a threshold and by selecting a proportional part of the residual one.

The procedure has been applied to an adsorption heat pump and to a compression heat pump. The deviations between the short sequence test and the test of the whole boundary conditions are calculated. With the short tests of the two machines, the deviations obtained are about 3 % when the temperature is divided into intervals of 3 K and only the classes with one element are excluded. Instead, a higher threshold gives a shorter duration but the deviation is increasing. Therefore, the selection of sequence is not suggested with the application of a threshold that exclude classes with two elements. In additions, the classifications that create classes with few elements (with dense intervals) give higher deviation because a large number of classes are excluded from the selection since they contain only one element.

The tests performed on the adsorption chiller and on the heat pump highlight the importance of studying these components under dynamic working condition. During the initial transient phase, the driving energy is consumed without having a useful effect; for the adsorption chiller this phase lasts about 30 min, while for the heat pump a couple of minutes. Moreover, the procedure allows to evaluate the effect of the boundary conditions variation where the most representative case is given by the change of load of the heat pump from space heating to domestic hot water.

A further confirmation of the necessity of characterize the performance with dynamic condition is given by the comparison of stationary methods: test results are compared with the bin method and the simulation of component validated through stationary test; those two methods do not identify the behaviour of transient phases disregarding the worst working conditions. The deviation between the dynamic test and the characterization with stationary methods is higher when the component has high inertia. As example, the adsorption chiller showed a higher deviation than the heat pump.

The mayor limit of the procedure is the necessity of simulation for the definition of the boundary conditions. This limit is overcome in the adaption of the procedure at system level since the boundary conditions are extended to the weather file. Another limit of the procedure is that the strategy of control of the components performed by the system is only simulated; also in this case, in the system level the limit is overcome since the controller is tested with the system.

3 Test procedure at system level

From the good results obtained in the characterization of the components, the procedure was further developed for the application at system level. This evolution allows to overcome the limits of the procedure applied at system level:

- The system boundary conditions are given by the weather data and not anymore from the system simulation.
- The control strategy is part of the system and therefore its behavior is measured and not only simulated.

The following sections present all the part of the procedure that was developed with the aim to satisfy the requirements described in the introduction. As shown in Figure 3-1, the procedure allows to test a system starting from the definition of one building and the weather conditions. With the simulation of the building the load file is defined; from this, the boundary conditions are selected to define a short test sequence. This is used to perform the test and from the results the performance can be analysed.

Figure 3-1: Simplified block diagram of the test procedure at system level.

The procedure can be described with the following phases (each step is referred to a specific section):

I. Selection of the climate and building (paragraph 3.2).

II. Definition of the load file: simulation of the building coupled to the climate (paragraph 3.3).

III. Selection of the boundary conditions (chapter 4).

IV. Installation of the system to the identified physical boundaries (paragraph 3.4).

V. Emulation of distribution system and sources (paragraph 3.5).

VI. Execution of the test. Analysis of results (paragraph 3.6).

3.1 Test method

The method can be described in detail with Figure 3-2 that shows the block scheme. The weather file gives the boundary conditions for the definition of the SH and SC loads. The load file is calculated considering a simulation of a defined building coupled to the weather file. This file contains the power profiles of the space heating and space cooling load distinguished for the different floors of the building. The load file is used to define the heating or cooling requests as described in the section 3.3 and is used in the emulation of the distribution system as described in the section 3.5.1. The other load profile is represented by the DHW request. This is a predefined statistical draw-off profile of the DHW request defined with the program DHWcalc developed within the IEA SHC Task 26 [53] and it is described in the section 3.5.2.

The weather file is used as boundary conditions in the emulations of the components that are not physically present as the solar collector and the external unit of the heat pump. These emulations are described respectively in the 3.5.3 and 3.5.4. The emulations are performed with "concentrate parameter" models. The emulations are run with the same time step of the acquisition of the laboratory. These models are used to calculate the set points of the laboratory circuits in the following way:

- for each time step, the outputs from the tested system are measured, and this data with the time-dependent weather data are passed as input to the model of the component;

- the simulation of the component uses these values to calculate the response of the emulated device. This becomes the set point for the laboratory control;
- the laboratory PID controllers operate to reach the set conditions with the laboratory circuits.

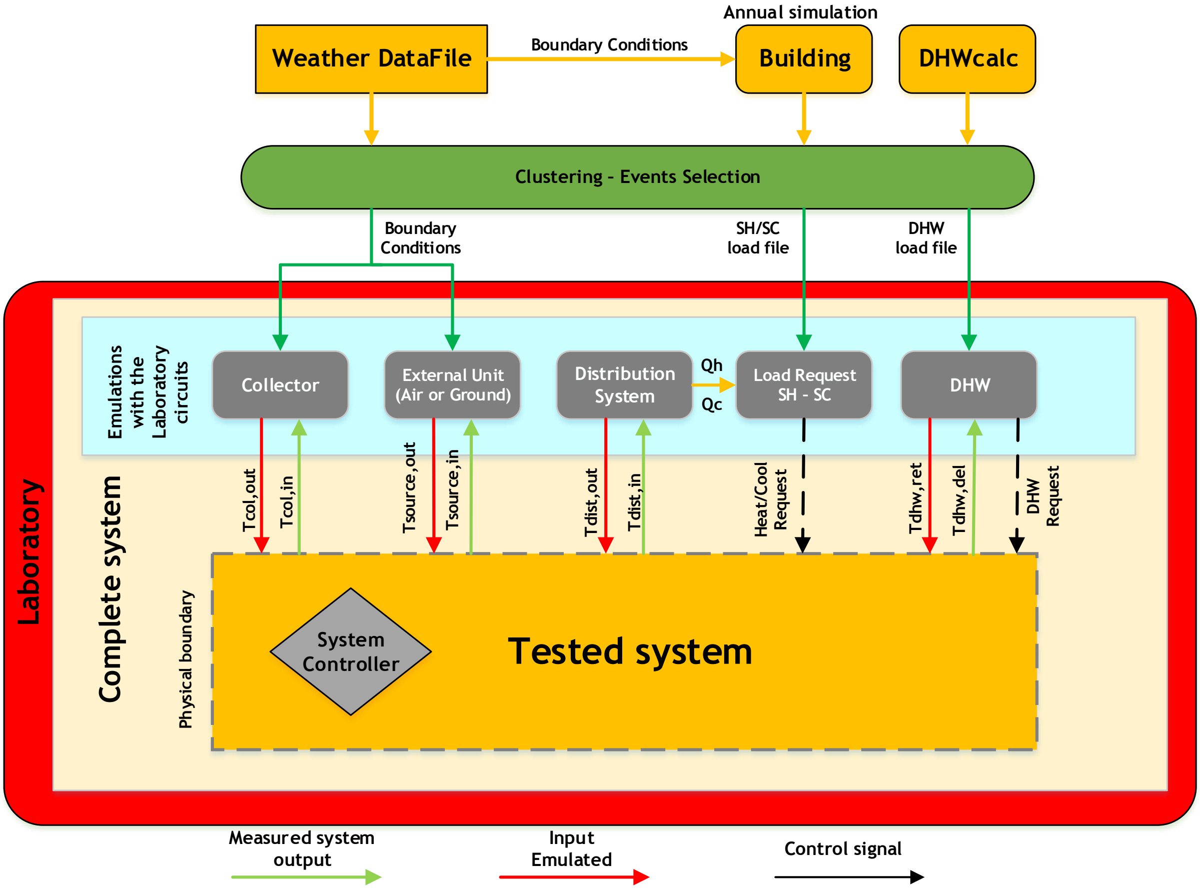

Figure 3-2: Block diagram of the test procedure at system level.

3.2 Selection of climate and building

The weather data file is needed to define the boundary conditions. A test reference year (TRY) with high resolution file should be considered since a high resolution weather data is significant for the emulation of components with low thermal capacity (e.g. dry cooler) and to achieve the transient variations as close as possible to reality. In this case, the weather data has been generated on 1 min resolution using dataset from Meteonorm software. The weather profile is extrapolated from the hourly weather data of Meteonorm with Type 109; unfortunately, the information is not detailed as it would be starting from a high resolution acquisition of weather data.

Figure 3-3 shows the annual average temperature of the world region: there are many different types of climate, and the large span of temperature indicates that one condition could not be representative of all. The selection of one standard climate is important for the comparison between different systems. In fact, two tests made in different climate zones cannot be compared. Therefore, it is advisable to find one or few single standards weather files for all the tests in the considered regions. As example the EN 14825 foreseen 3 regions for the heating and 1 for cooling.

The test procedure was applied to study the same system into different climates. The first climate that was chosen is the weather data of Bolzano because the climate in Bolzano is characterized by hot summer and very cold winter while the second one is the weather of Zurich since it has been used in the other methodologies. Other two climates of Gdansk and Rome are considered for the test.

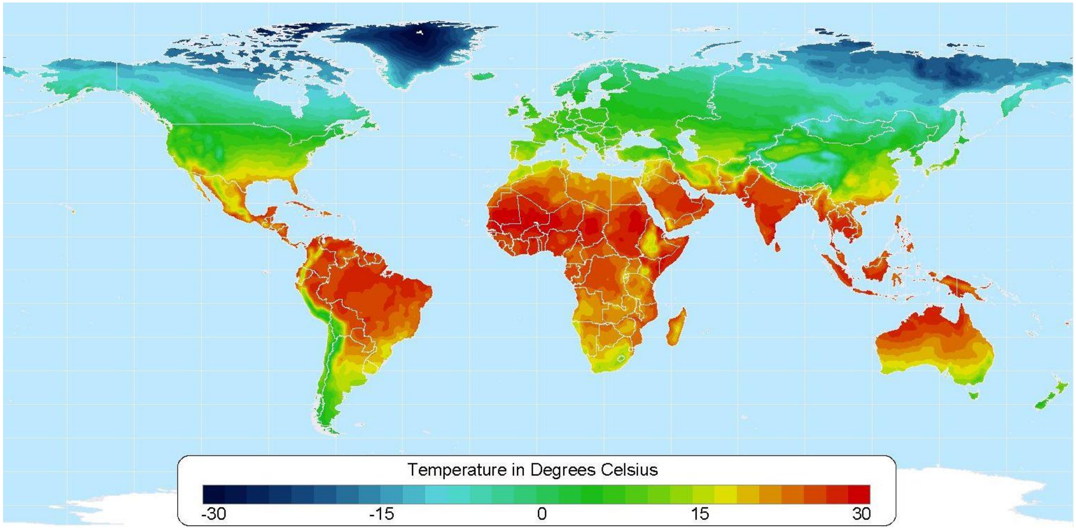

Figure 3-3: Average annual temperature of the world regions.

Figure 3-4 shows the annual temperatures profile of Bolzano while Figure 3-5 shows the annual temperature profiles of Zurich. The figures present the minimum, maximum and average temperature of days. The average annual temperature of Bolzano is 12.01 °C while for Zurich is 9.01 °C.

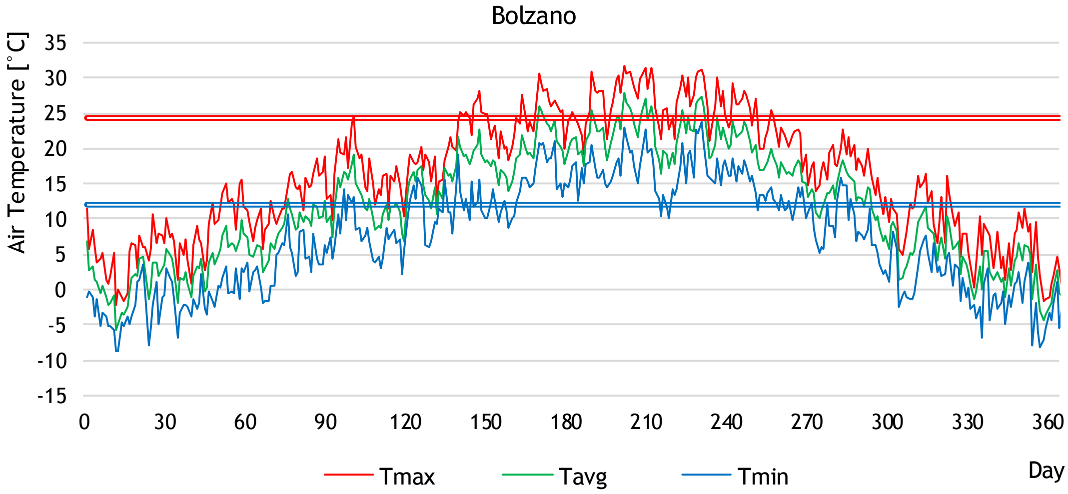

Figure 3-4: Temperatures profiles for the Bolzano climate.

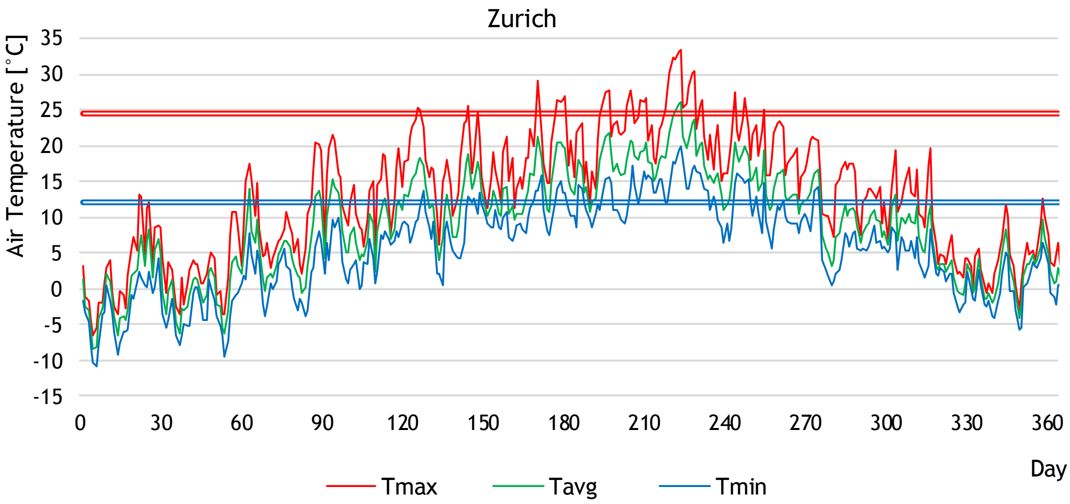

Figure 3-5: Temperatures profiles for the Zurich climate.

The building coupled to the climate, gives the load which have to be satisfied by the system. This building is modelled with TrnBuild and simulated with type 56.

At now, the building selected for the application of the procedure is a single family house with two floors. The internal area is 180 m^2, the external wall components are bricks, plaster, and 10 cm of EPS for insulation and the windows have a double layer with internal air interspace (the transmittance of external wall is about 0.27 W/m^{2}K). With the climate of Bolzano, the heating demand is 52 kWh/m^2 and the cooling demand of 12 kWh/m^2 while with the climate of Zurich the space heating load is 72 kWh/m^2 and the space cooling load is low (2.1 kWh/m^2).

The Table 3-1 summarizes the annual average temperature, annual irradiation and the heating and cooling demands of the four climates considered during the test.

Table 3-1: Climates considered in the test.

	Bolzano	Zurich	Gdansk	Rome
Temperature [°C]	12.05	9.04	7.97	15.54
Irradiation [kWh/m^2]	4504.6	4000.3	3753.9	5618.0
Heating Demand [kWh/m^2]	52.2	72.0	84.0	19.1
Cooling Demand [kWh/m^2]	11.7	2.1	0.6	19.2

3.3 Definition of a load file

To define the building load, two possibilities can be considered. The first one is performing an on-line simulation of the building to have its instantaneous response and the second one is the adoption of a load file defined a priori. The main advantage of using a load file is that it allows to perform tests of different systems with the same load and therefore different systems could be compared on a common load. Furthermore, it avoids the application of a building emulation that is more complicated than other emulations with the consequence of simplifying the procedure. The consequent disadvantage is that since a real-time simulation is not performed, the internal air temperature of the building is unknown. Consequently, the exact behaviour of the thermostatic valves cannot be reproduced. In order to consider the effects of discontinuous operation of a system, a different approach was developed starting from the information included into the load file.

As first step, the ideal load is calculated from the simulation of the building coupled to the weather. Figure 3-6 shows the example of load definition for the climate of Bolzano and the building adopted for the tests (as indicated previously). The Appendix C presents the models used in the simulations.

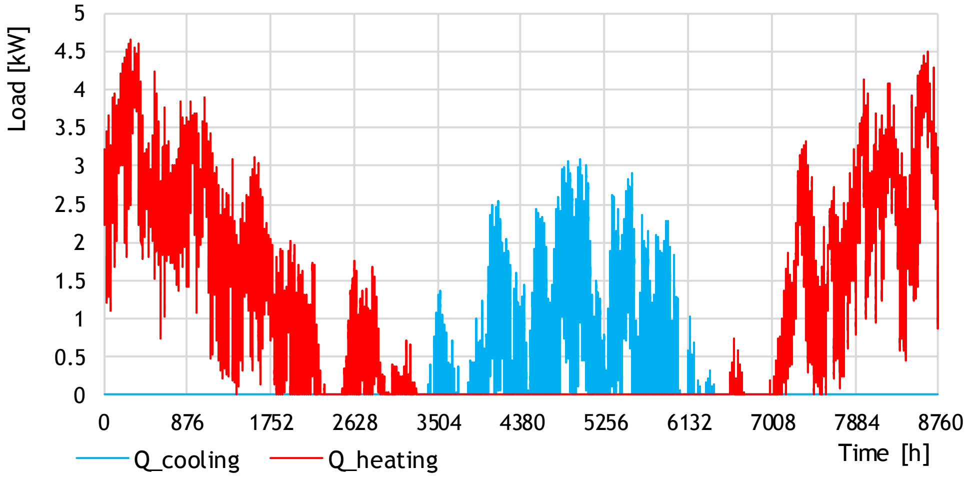

Figure 3-6: Example of load file defined for the Bolzano climate.

To understand if one load file can be used as common file for different systems, a combination of systems with different maximum heating (and cooling) power and different set-point of delivery temperature were simulated. Those systems have to satisfy the comfort of the same building, with the same distribution system (radiant floor), control on internal temperature and on collector temperature of radiant floor. From those different combinations, Table 3-2 shows the simulation of twelve different systems with maximum power from 5 to 20 kW and different set point of the heating/cooling device. The temperature of the building has to be kept at 20°C during the heating season while at 24.5°C during the cooling season. The 5 kW heater does not satisfy the load since the set temperature is not reached: for about 70 hours the temperature is lower than 19°C. By excluding these simulations, the difference of heat delivered to the building between the different system sizes is about 0.5% in heating season and 1.6% in cooling season.

The outcome is that the load file can be used to test different system' sizes since different typologies of systems provide the same energy to the building to satisfy the comfort. The time of activation of heating and cooling schemes shows that the performance is depending from the system. As example, the number of activation (N_{act}) is higher in systems with high power and the duration of activation is shorter.

Table 3-2: Simulation of load as a function of system size.

$\dot{Q}_{cooler}$ [kW]	$\dot{Q}_{heater}$ [kW]	T_{set_cooler} [°C]	T_{set_heater} [°C]	Q_{sc} [kWh]	Q_{sh} [kWh]	N_{actsc} [-]	$N_{act\text{-}sh}$ [-]	onTime$_{sc}$ [h]	onTime$_{sh}$ [h]	Time with T<19 [h]	Time with T>26 [h]
5	5	5	35	2176	9518	304	211	437.2	2233.5	69.8	0.0
5	5	10	40	2176	9518	304	211	437.2	2233.5	69.8	0.0
5	5	15	45	2177	9518	76	211	520.5	2233.5	69.8	0.0
5	6.5	5	35	2176	9673	304	296	437.2	1753.2	0.0	0.0
5	6.5	10	40	2176	9679	304	304	437.2	1748.2	0.0	0.0
5	6.5	15	45	2177	9679	76	304	520.5	1748.2	0.0	0.0
12	13	5	35	2167	9709	2508	1720	181.0	1149.6	0.0	0.0
12	13	10	40	2164	9679	1813	5036	199.5	878.6	0.0	0.0
12	13	15	45	2180	9686	74	5174	488.2	876.0	0.0	0.0
20	20	5	35	2143	9699	4003	4992	107.3	1041.7	0.0	0.0
20	20	10	40	2163	9671	1935	17278	182.8	577.2	0.0	0.0
20	20	15	45	2180	9667	74	18012	488.1	568.3	0.0	0.0

The load file is used for the emulation of the building and it is shown in the section 3.5.1.

3.4 Physical boundary condition and system installation

The boundary conditions influence the thermal system in many ways. In particular, the air temperature and humidity, the solar irradiance and other parameters related to the weather influence the building load demand. The air temperature and the irradiation also influences the performances of the components like the heat pump and solar panels.

Some components in direct contact with the external environmental cannot be installed in the laboratory since it is difficult to achieve reproducible conditions and the test bench required for these component has a high investment and operative costs. Therefore, the test bench should recreate the behaviour of components that are not installed in the laboratory. The test bench has to emulate the effects of the weather boundary conditions on a generic thermal system.

Figure 3-7 shows an example of the system boundary conditions considering the system that is considered in this thesis. The part of the system installed in the laboratory is represented by the grey area. The components outside the boundary are the emulated components:

- Solar panels;
- External unit of heat pump;
- Domestic hot water system;
- Distribution system;
- Other components that are not included yet in the procedure (ground probes, PV field, etc.).

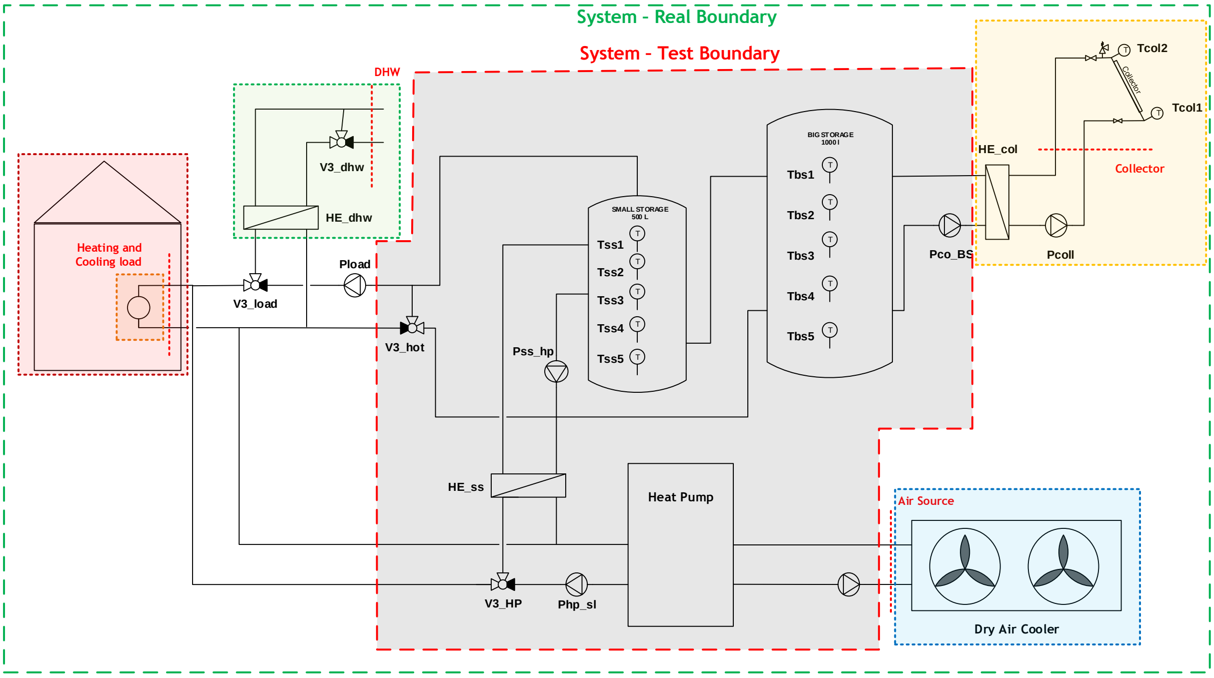

Figure 3-7: System set-up. Example of physical boundaries.

To be a representation of realistic working conditions, the system has to be installed in the laboratory with the same configuration used in the real installation. The laboratory does not have to influence the internal control of the system. Instead it has to evolve in according to the manufacturer control.

3.5 Component emulation

This chapter presents the solutions adopted for the emulation of the component not installed in the laboratory. The description is divided into four sections:

- Load request and distribution system (3.5.1)
- DHW load (3.5.2)
- Collector (3.5.3)
- Air Units (3.5.4)

3.5.1 Load request and distribution system emulation

The emulation of load request is based on the load file defined in the section 3.3. Once the load is fixed, the system activation is based on energetic considerations on this. The aim is to represent the normal behaviour without require an emulation of the building.

The system is activated after that the building exchanged an energy (called energy limit ΔE1) and consequent deactivation of the system after the energy balance is null. More in detail, the approach can be explained Figure 3-8 a formalized with Equation 3-1 to Equation 3-4. At time τ_0, a counter starts to count the cumulative energy of the load. When it reaches the “energy limit”, at time τ_1 Equation 3-1, the system is activated. This “energy limit” is represented by the area highlighted under the red curve with the orange dotted lines. After the activation, the calculation of the cumulative load continues (Equation 3-2), while the energy given by the system starts to be counted (Equation 3-3). When these two energies are equal, at time τ_2, the system is deactivated. This balance (Equation 3-4) is represented by the area highlighted under the red curve with the dotted red lines and the area highlighted with the green lines. The green and red areas are equal. When those two areas become equal, the counter is restarted. The cumulative energy can be seen in the Figure 3-8 b where the red line indicates the red area, the green line indicates the green area. The difference between these two is indicated with the blue line while the energy limit is indicated with the yellow line.

Equation 3-1
$$\int_{0}^{\tau 1} \dot{Q}_{load}\, d\tau = \Delta E_{0-1} = \Delta E_{1} \quad \text{[kWh]}$$

Equation 3-2
$$\int_{\tau 0}^{\tau 2} (\dot{Q}_{load})\, d\tau = \Delta E_{0-1} + \Delta E_{1-2} \quad \text{[kWh]}$$

Equation 3-3
$$\int_{\tau 1}^{\tau 2} (\dot{Q}_{sist,distr})\, d\tau = -(\Delta E_{0-1} + \Delta E_{1-2}) \quad \text{[kWh]}$$

Equation 3-4
$$\int_{\tau 0}^{\tau 2} (\dot{Q}_{load} + \dot{Q}_{sist,distr})\, d\tau = 0 \quad \text{[kWh]}$$

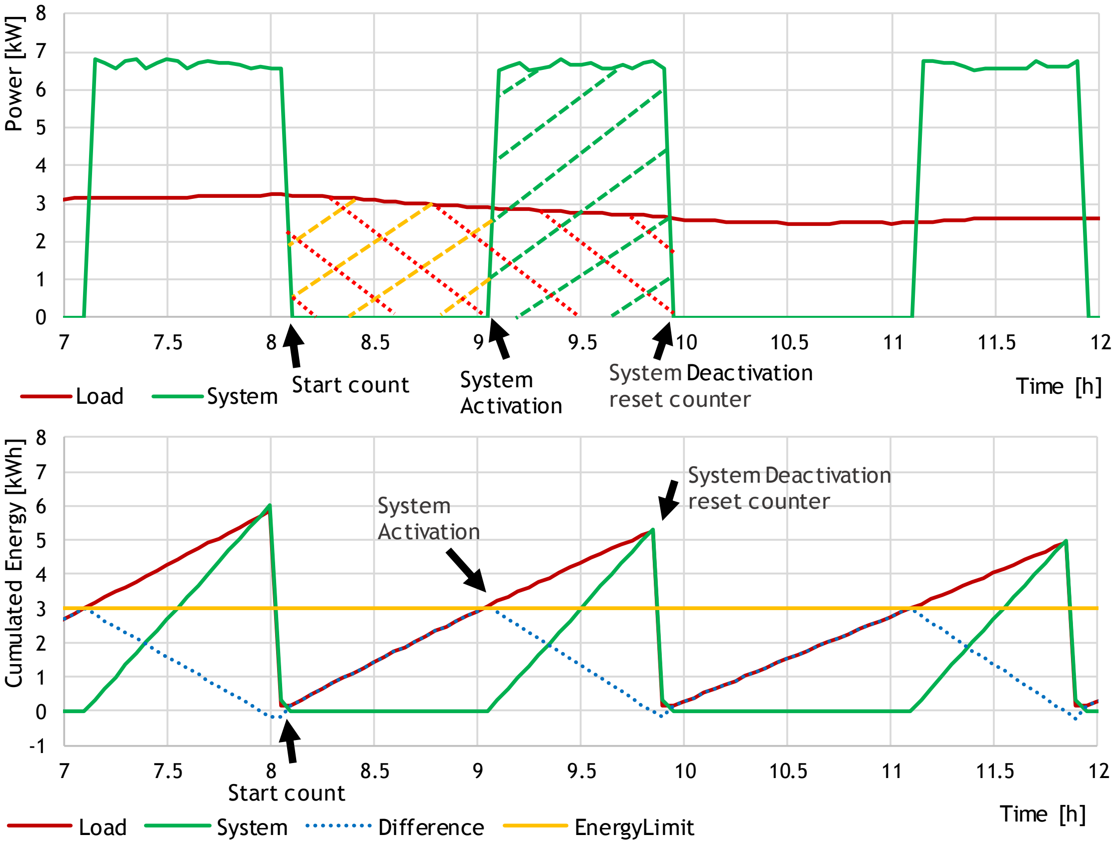

Figure 3-8: Load File. Activation principle.

Energy limits are calculated for different systems as indicated in the Table 3-2. In Figure 3-9, the energy limits are shown as a function of the distribution system power. The power emitted by the distribution system is depending from the delivery temperature set-point. For different systems, the “energy limit” is closed to a constant value. In the cooling, the energy limit is about 9 kWh while in the heating it is 7 kWh. Some points obtained in the first floor are higher than 10 kWh.

The application of the energy limit identified with the Figure 3-9 is not possible when a short sequence of few days (e.g. 6 or 12) is used since a lower limit is required. The necessity of using a lower limit is given by the duration of the test: considering the daily load, during the mid-season, some days present a load lower than the energy limit; in this way, the system would not be activated during those days while during the year the load is satisfied the following days. The consequence is that the load foreseen by the file would not be fully covered during the sequence. As example, if the sequence considers a heating load of 150 kWh, a maximum of 9 kWh could be not satisfied: the method would introduce a deviation of 6 % on the total load. Therefore, the emulation considers an energy limit of 3 kWh; this reduction is corresponding to the reduction of the capacity of the radiant floor performed in the other procedures [45]. The adoption of an energy limit lower than the one identified in Figure

3-9, does not affect the energy delivered to the building and the consequent comfort; however the number of activations increases.

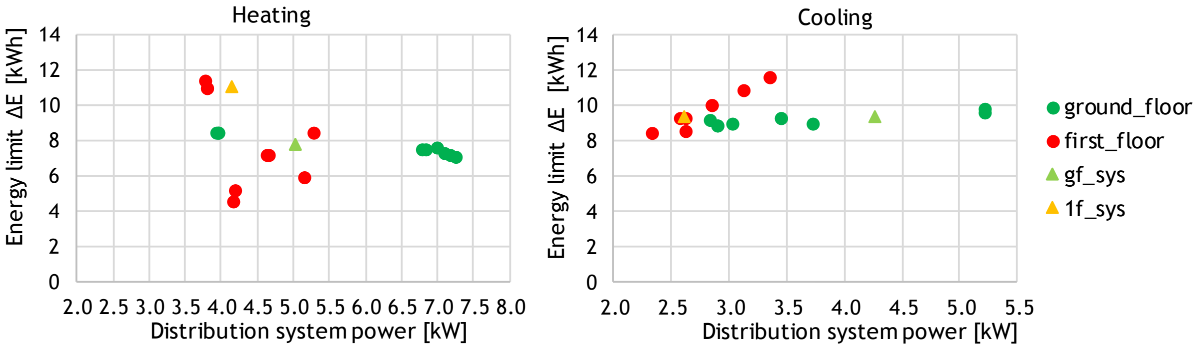

Figure 3-9: Energy limits before the activation of the system.

The series "ground floor" and "first floor" are calculated with the simulation of systems indicated in Table 3-2. The series "gf_sys" and "1f_sys" indicate respectively the ground and first floors of the SAHP system.

The concept of system activation has been verified replacing the building model with this calculation (fixed load file and activation thought energy limit). Both energy limits of 9 kWh and of 3 kWh were applied for the systems indicated in Table 3-2. Activating the systems with the energy limit, the building temperature does not drop out the lower limit of building set temperature. The same substitution of models was done with the model of the tested system (the model is presented in Appendix C); again the internal temperature is kept as the set point and the influence on seasonal performance factors can be seen in Table 3-3. The deviation on the performance (SPF) is lower than 2%.

Table 3-3: Performance factors calculated with the reference model and with the load file.

	SPF_{cool}	SPF_{heat}	SPF_{DHW}	SPF_{tot}
Load file and activation with "energy limit"	4.11 (+1.9%)	3.82 (-1.5%)	9.08 (1.0%)	4.32 (-0.1%)
Reference (No Load File)	4.03	3.88	8.99	4.35

Distribution system

For the energy delivered to the building needed in the emulation of the load request above described, a reference heat distribution system is chosen. It includes the radiant panels and a hydraulic junction (Figure 3-10). Since the building considers two independent floors, the hydraulic junction is connected to two radiant panels. The figure presents the scheme highlighted with the same coloured area of Figure 3-7.

The behaviour of the distribution system is modelled with concentrated parameter models. The thermal capacity of the simulated heat distribution system is reduced to the thermal capacity of the hydraulic junction. Unfortunately, this does not allow to investigate its inertial effects on the system behaviour. As it is discussed by Haberl et al. [45] this assumption is necessary to avoid problems for the repeatability of the results of the short test sequence. This is due to the fact that the heat delivered on one day could be consumed in the next days of the sequence because of the thermal inertia typical of this distribution system.

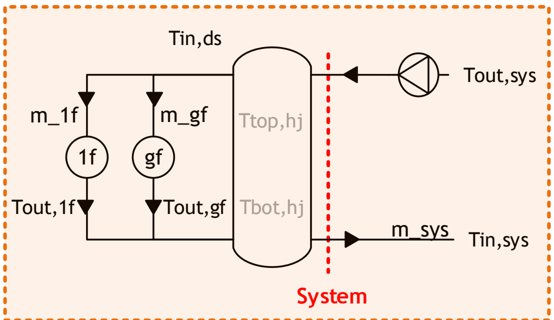

Figure 3-10: Distribution system scheme.

Figure 3-11 shows the emulation principle. When the system is activated, it delivers the heat-transfer fluid at a flow ratio and temperature according to its control. From the measure of the mass flow (m_{sys}) and temperature ($T_{out,sys}$), the emulation calculates the heat delivered to the building and the consequent return temperature. This heat is used to calculate the activation of the system as previously described while the return temperature is used as set point of the laboratory.

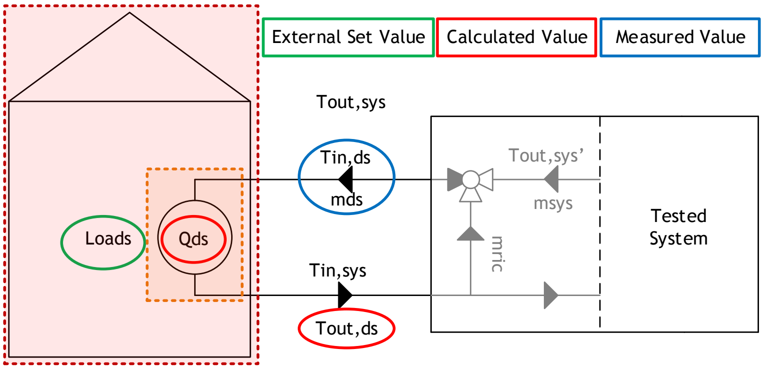

Figure 3-11: Distribution system. Scheme of the emulation principle.

The thermal power of the radiant panel is calculated as a function of the delivery temperature. Four different equations are defined for the two floors and the modality of operation. The equations are valid for a constant internal temperature in the heating season (20 °C) and in the cooling season (24.5°C). This condition is respected if the system activation control is applied as indicated previously.

Equation 3-5 $$\dot{Q}_{heat,gf} = -13.294 + 0.6186 \cdot T_{in,ds}$$ [kW]

Equation 3-6 $$\dot{Q}_{heat,1f} = -12.299 + 0.5314 \cdot T_{in,ds}$$ [kW]

Equation 3-7 $$\dot{Q}_{cool,gf} = 15.526 - 0.8026 \cdot T_{in,ds}$$ [kW]

Equation 3-8 $$\dot{Q}_{cool,1f} = 14.6998 - 0.6764 \cdot T_{in,ds}$$ [kW]

The outlet temperature from the radiant panels of the two floors are calculated from the inlet temperature. The ß parameter indicates the activation of the panel in the heating or cooling conditions.

Equation 3-9 $$T_{out,gf} = T_{in,gf} + \frac{\dot{Q}_{cool,gf} \cdot \beta_{c,gf} - \dot{Q}_{heat,gf} \cdot \beta_{h,gf}}{630 \cdot cp}$$ [°C]

Equation 3-10 $$T_{out,1f} = T_{in,1f} + \frac{\dot{Q}_{cool,gf} \cdot \beta_{c,1f} - \dot{Q}_{heat,1f} \cdot \beta_{h,1f}}{630 \cdot cp}$$ [°C]

The hydraulic junction is modelled with two nodes:

Equation 3-11 $$T_{top,hj}(t) = T_{top,hj}(t-1) \cdot \left(1 - m_{sys}{}^{*} - m_{ric,up}{}^{*}\right) + T_{out,sys} \cdot m_{sys}{}^{*} + T_{bot,hj}(t-1) \cdot m_{ric,up}{}^{*}$$ [°C]

Equation 3-12 $$T_{bot,hj}(t) = T_{bot,hj}(t-1) \cdot \left(1 - m_{gf}{}^{*} - m_{1f}{}^{*} - m_{ric,dwn}{}^{*}\right) + T_{out,gf} \cdot m_{gf}{}^{*} + T_{out,1f} \cdot m_{1f}{}^{*} + T_{top,hj}(t-1) \cdot m_{ric,dwn}{}^{*}$$ [°C]

The masses (m*) are normalised by considering the control mass of the node.

Again, a new model of the system has been built from the one simulated in the Table 3-3 where the distribution model have been replaced by those equations. The Table 3-4 shows the difference between the simulation of the system with the simplified emulation and the traditional types. This difference is lower than 3.2%.

Table 3-4: Performance factors calculated with the reference model and with the load file and distribution system simplified emulation.

	SPF_{cool}	SPF_{heat}	SPF_{DHW}	SPF_{tot}
Simplified Emulation	3.92 (-2.7%)	3.83 (-1.2%)	9.12 (1.4%)	4.21 (-3.2%)
Reference (No Load File)	4.03	3.88	8.99	4.35

3.5.2 DHW load emulation

The annual profile of DHW is defined in advance with a statistical profile with the program DHWcalc developed within the IEA SHC Task 26 [53]. The total annual energy consumption is 2550 kWh of useful heat. The hot water has to be delivered at 40°C. From the annual sequence, the day that has a consumption of 7 kWh, - that is the daily average consumption – is used as draw off for the sequence. In this way, the days in the sequence have the same energy extraction.

A dedicated laboratory circuit is used to reject the equivalent useful heat in order to get the return temperature from the measured supply water temperature. The emulated DHW distribution system is presented in the Figure 3-12. The figure presents the scheme highlighted with the same coloured area of Figure 3-7.

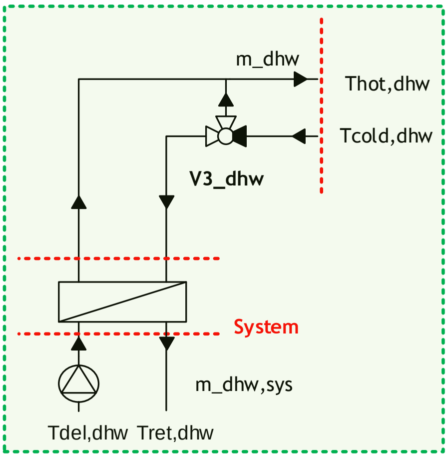

Figure 3-12: Domestic hot water. Scheme for the calculation of temperature.

The heat to reject is defined by the DHW file:

Equation 3-13 $$\dot{Q}_{DHW} = \dot{m}_{dhw} \cdot cp \cdot \Delta T = \dot{m}_{dhw} \cdot cp \cdot (T_{hot,dhw} - T_{cold,dhw}) \quad [kW]$$

Considering the equation, the return temperature is calculated as consequence of the delivery temperature and the fixed draw-off:

Equation 3-14 $$T_{ret,dhw} = T_{del,dhw} - \frac{\dot{Q}_{DHW}}{\dot{m}_{dhw,sys} \cdot cp} \quad [°C]$$

Note: the heat exchanger is not part of the test. In case of the V3_dhw system could be included in the boundaries, the emulation for the calculation of $T_{ret,dhw}$ is not required since the laboratory circuit have to deliver the flow m_{dhw} at the temperature $T_{cold,dhw}$ (usually 10°C).

The system has to deliver the water at 40°C ($T_{hot,dhw}$). Usual practice is to circulate the fluid until the outlet temperature reaches the set point. In this way, some energy is wasted during the circulation. An example of DHW extraction could be seen in Figure 3-13. The blue dotted line represents the request of DHW while the light blue dotted line represents the condition which the set point is reached. In this way, during the extraction two energies can be identified. The yellow one is the energy extracted with a temperature lower than 40°C while the light blue area represents the energy extracted at temperature higher than 40°C.

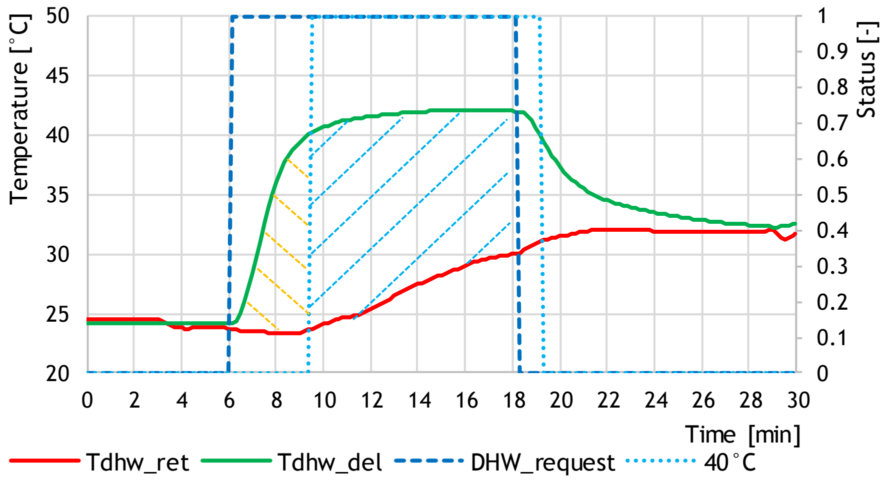

Figure 3-13: Example of DHW extraction.

During the test, the system is activated by the DHW load file and the return temperature is calculated with Equation 3-13 and Equation 3-14. The point is how to manage the effect explained in Figure 3-13. Two solutions are considered:

- Useful Heat: A control on the delivery temperature checks if the set point is reached. If the temperature is lower than the set point, the energy is counted as “not-useful” (yellow area). When the temperature reaches the set point, the energy is counted as “useful” energy (blue area). The draw-off ends when the “useful energy” is equal to the one set in the draw-off. This additional “not-useful” heat is measured but is not counted for the DHW tapping. Different systems can reach the set-point with different timing and therefore the wasted energies are different.
- Constant Energy: in this case, the draw-off is increased to consider a constant “not-useful” energy for all the systems. The energy is counted without considering if is “useful” or “not-useful”. For example, during the test 11 kWh are defined of draw-off, considering a useful heat of 7 kWh and a not-useful of 4 kWh. In this way the energy extracted is the same for different system. However, the control of the useful heat is not done during the test.

The adoption of a constant energy draw-off allows to test different system with the same extraction of energy.

A first test was carried out considering the method of “Useful Heat”. From this, the “not-useful” energy is quantified in 4 kWh and the “useful heat” is 7 kWh. A second test was done with the method “Constant Energy” with a total energy extracted of 11 kWh. The Figure 3-14 shows the comparison of the two methods: the results showed that the method “Constant Energy” is similar to the other since about 4 kWh of energy with temperature lower than 40 C was measured. In detail, the Figure 3-14 distinguishes the different energy level at 30°C, from 30°C to 35°C, from 35°C to 40°C and from 40°C.

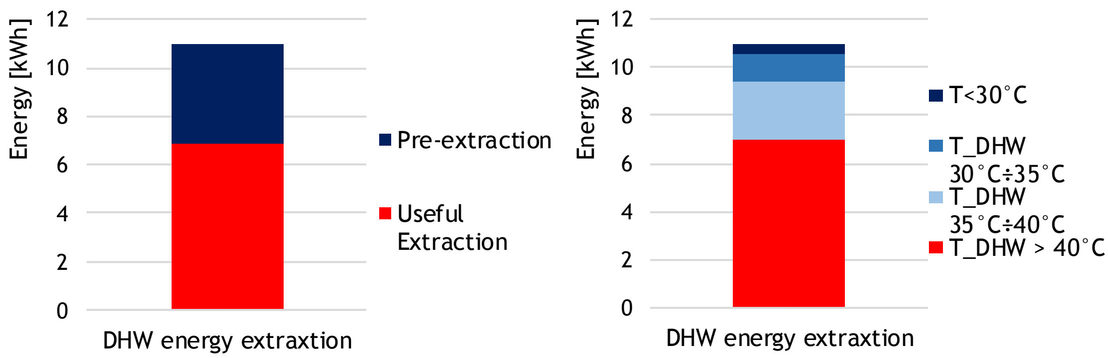

Figure 3-14: Domestic hot water energy extracted. Comparison of scheme of pre-extraction and constant draw-off.

3.5.3 Collector emulation

The collector field is not part of the tested system because it is difficult to install it physically and to achieve reproducible conditions in terms of ambient temperatures and irradiance profiles. Moreover, a solar simulator requires a huge investment and high operative costs (specially to achieve a good spectral content).

The collector output power and temperatures are reach with a dedicated laboratory circuit that uses a thermo-regulator. For the emulation of the collector field, the model requires the data of Table 3-5. This information is given by the collector test certificate according to the reference standard (e.g. EN 12975-2).

Table 3-5: Collector parameters considered in the solar field emulation.

Number of collector modules	-	[-]
Hydraulic configuration of the solar field	-	[-]
Gross area of collector	A	[m^2]
Zero loss efficiency	η_0	[-]
linear heat loss coefficient	a_1	[W/m^2K]
quadratic heat loss coefficient	a_2	[W/m^2K^2]
specific heat capacitance of the collector	C_{col}	[kJ/m^2K]

The collector emulated is presented in the Figure 3-15. The figure presents the scheme highlighted with the same coloured area of Figure 3-7.

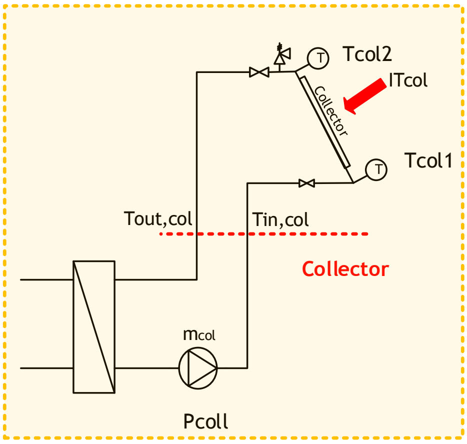

Figure 3-15: Collector. Scheme for the calculation of temperature.

For each time step the collector efficiency is assessed with a quadratic correlation with respect to the reduced temperature difference T_m^*:

Equation 3-15 $$\eta = \eta_0 - a_1 \cdot T_m^* - a_2 \cdot IT_{col} \cdot {T_m^*}^2$$ [-]

Equation 3-16 $$T_m^* = \frac{T_m - T_a}{IT_{col}}$$ [K m^2/W]

To consider the incidence angle modifier IAM, a constant factor corrects the efficiency. The losses for the not orthogonal incidence are quantified in 7%. The IAM_{cor} is 0.93.

Equation 3-17 $$\eta_{corr} = \eta * IAM_{cor}$$ [-]

When the collector circuit is activated, the outlet temperature is calculated from the inlet temperature and the total irradiance incident on the collector surface.

Equation 3-18 $$T_{out,col} = T_{in,col} + \frac{\eta \cdot A_{col} \cdot IT_{col}}{\dot{m}_{col} \cdot c_p}$$ [°C]

If the collector circuit is not activated, the temperature is calculated considering the collector capacity with the solar contribution and the thermal losses. The calculation is made considering the temperature at the previous time step $(\tau - 1)$.

Equation 3-19 $$T_{out,col}(\tau) = T_{out,col}(\tau - 1) + \frac{(\dot{Q}_{gain} - \dot{Q}_{loss}) \cdot \Delta\tau}{C_{col}}$$ [°C]

To introduce an inertia effect, a moving average is applied to the outlet temperature.

To verify the equation, during the debug test, the efficiency and outlet temperature of the collector were simulated with TRNSYS. The Figure 3-16 shows the comparison between the adoption of a constant angle modifier as indicated in the Equation 3-17 and the application of a incidence angle modifier as described in the mathematical reference of type 1 [46].

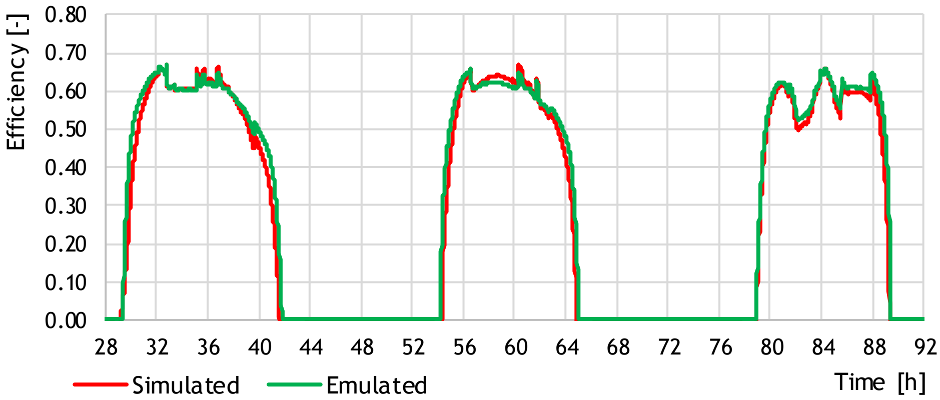

Figure 3-16: Efficiency of collector. Comparison of simulation model and model used for the emulation.

3.5.4 Air-unit emulation

Usual practice is to install the air units in a climatic chamber that reproduces the ambient condition of external air units. In case of not availability of a climatic chamber, also the air unit is emulated. The emulated air unit is presented in the Figure 3-17. The figure presents the scheme highlighted with the same coloured area of Figure 3-7.

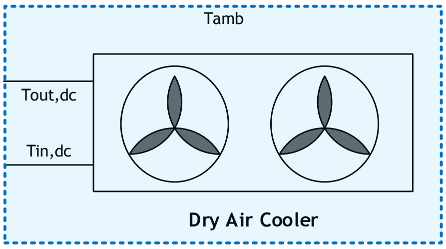

Figure 3-17: Air-unit. Scheme for the calculation of temperature.

The thermal power and the electric consumption are calculated as a function of the air temperature and the inlet temperature. Two different equations are defined for the working mode (heat rejection and heat source).

Equation 3-20 $$\dot{Q}_{DC,source} = 1.3987 - 0.6416 \cdot T_{in,dc} + 0.622 \cdot T_{amb}$$ [kW]

Equation 3-21 $$\dot{Q}_{DC,rejection} = -(19.1493 - 1.6325 \cdot T_{in,dc} + 1.0396 \cdot T_{amb})$$ [kW]

These two relations are defined with a linear regression of the working condition of the unit. The type of the air unit is presented in Appendix C.

The source mode used for the space heating and the domestic hot water preparation is shown in Figure 3-18 and Figure 3-19. The first figure shows the thermal power as a function of inlet temperature for different series of ambient temperatures. The second figure shows the thermal power as a function of the ambient temperature for different series of inlet temperatures. In the graphs, the series are selected with a tolerance of 0.5 K. The subscript “em” represent the powers calculated with Equation 3-20 and Equation 3-21. The figures show a good agreement between the simplified emulation of the air unit and the detailed model ad exception of few points. These equations are really easy to be implemented in the laboratory control software instead of the utilization of a commercial software like TRNSYS that requires skilled personnel.

In the Figure 3-18, there are some points of the simulated power far from the linear regression. The motivation is that the model foresees the effect of condensation of the air humidity as a function of the external temperature (not continuous function) while the linear regression disregards this effect.

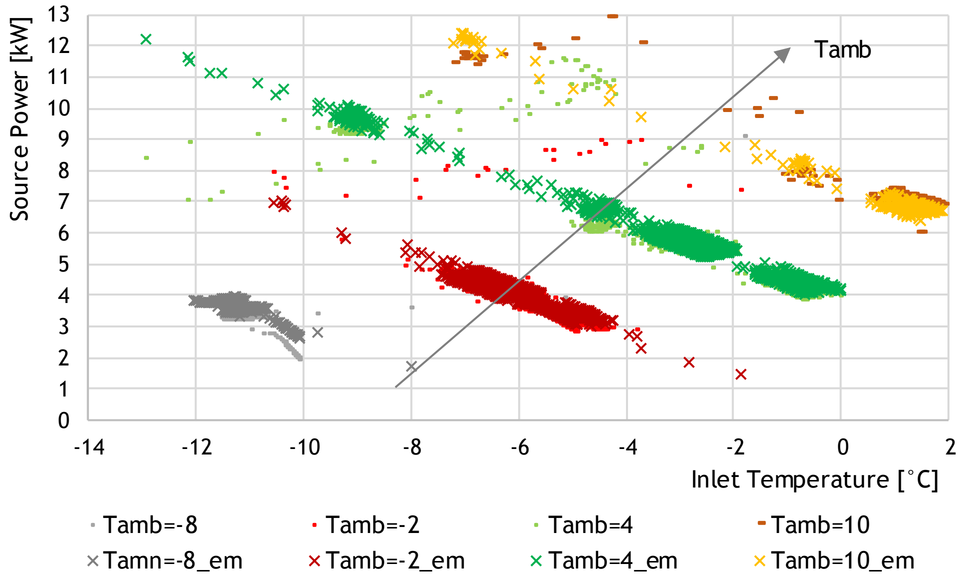

Figure 3-18: Air unit power - heat source mode. Power as a function of inlet temperature.

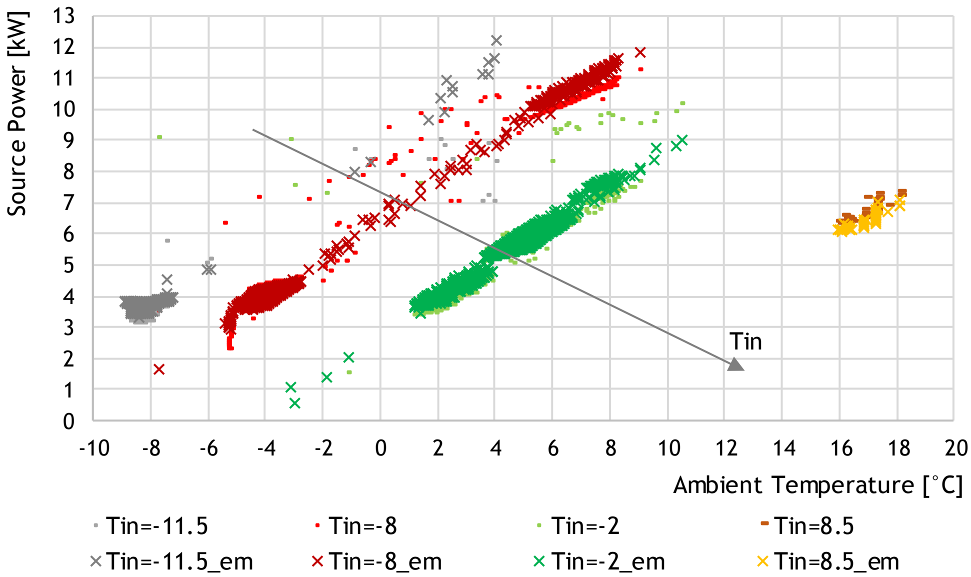

Figure 3-19: Air unit power - heat source mode. Power as a function of ambient temperature.

At the same time, the rejected power is shown in the Figure 3-20 and Figure 3-21. As the previous case, the first figure shows the thermal power as a function of inlet temperature for different series of ambient temperatures. The second figure shows the thermal power as a function of the ambient temperature for different series of inlet temperatures. In the graphs, the series are selected with a tolerance of 0.5 K.

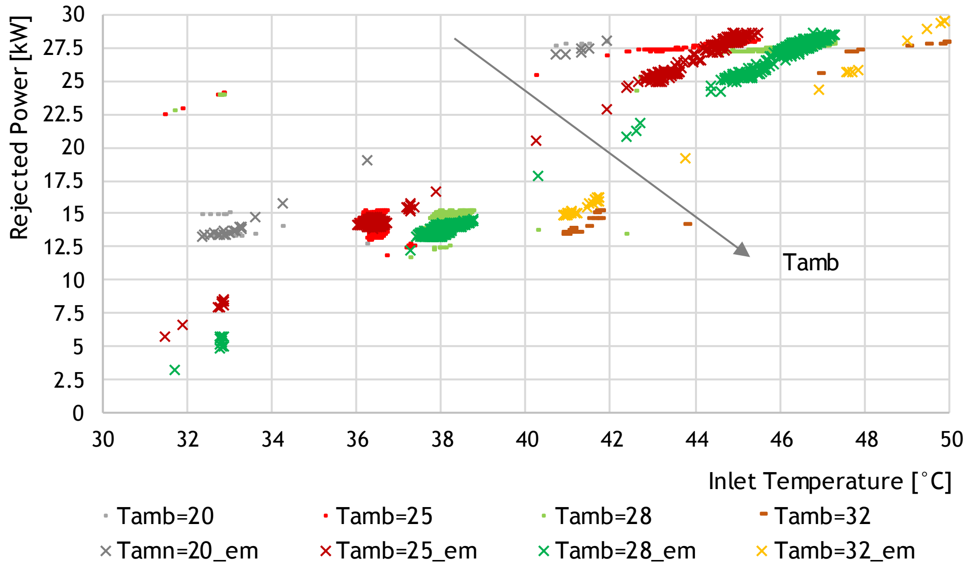

Figure 3-20: Air unit power - heat rejection mode. Power as a function of inlet temperature.

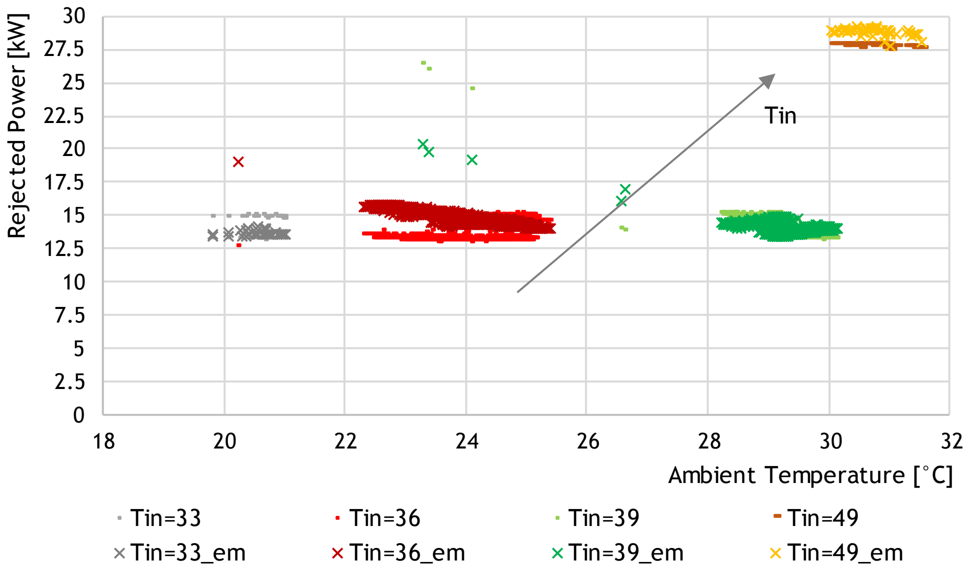

Figure 3-21: Air unit power - heat rejection mode. Power as a function of ambient temperature.

The thermal power considered depends from the scheme that activates the air unit. The heat should be rejected when the building is cooled while the dry cooler is used as source when the heat is produced.

Equation 3-22

$$T_{out,dc} = T_{in,dc} + \frac{\dot{Q}_{DC,source} \cdot HeatingMode - \dot{Q}_{DC,rejection} \cdot ChillingMode}{\dot{m}_{dc} \cdot cp} \quad [^\circ C]$$

To evaluate the electrical consumptions of the fans, an empiric equation is used. This relates the electric consumption to the heat extracted from (or rejected into) the air.

Equation 3-23

$$\dot{W}_{el,fan} = k \cdot \dot{Q}_{th} \quad [kW]$$

In the equation, it is important to distinguish whether the operation condition is heat extraction or rejection. The coefficient k is equal to 0.03 or 0.01, respectively.

These values refer to one specific air unit model. As per the solar collectors, the operational features of this components shall be known by the manufacturer if the devices cannot be tested directly.

3.6 Test execution and data analysis

The test has two preconditioning phases: in the first one the test bench brings the storage to a predetermined temperature; after that, the last 24 hour of the sequence are used as second preconditioning. The last phase of the procedure concerns the analysis of the results.

The test bench software creates a file with a large number of vectors also called channels. Each channel is acquired with a time step of 5 seconds. The channels acquire the values of temperatures and mass flows of the ports considered for the calculation of the power exchanged by the system. Moreover, the values of positions of the valves, pumps' speed, electrical powers are measured.

The Figure 3-22 shows the ports considered to calculate the powers exchanged by the system (and into the system when it is possible to introduce sensor inside the system). From these, on a daily base, the energies are calculated through integration and the performance ratio are calculated. The performances calculated in the test are:

- Space heating, space cooling and DHW loads.
- Collector yield and air yield.
- Direct measure of electrical consumptions (heat pump, circulation pumps, valves, control system).
- Direct measure of other back-up consumptions (natural gas, LPG, biomass etc.).
- Calculation of consumptions of emulated components (from emulation).
- Calculation of performance ratios as seasonal performance factor, solar fraction, air fraction, SCOP/SEER.

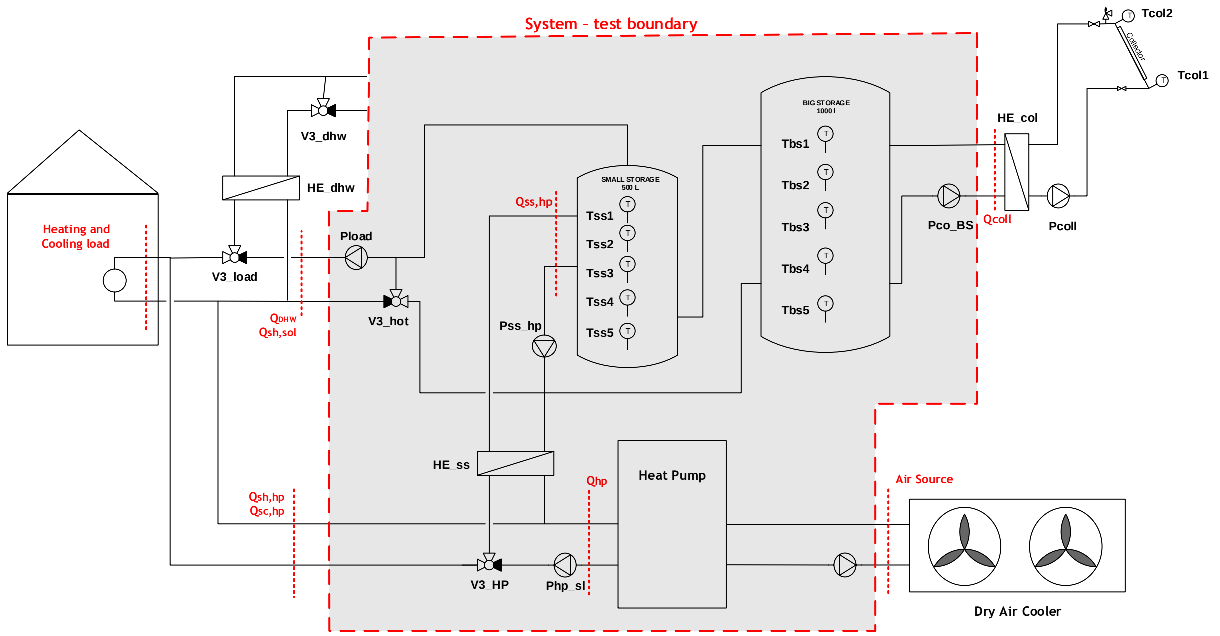

Figure 3-22: Boundaries for the calculation of system performances.

3.7 Validation of test procedure

The procedure was applied to different climates and system configurations. The results are compared with the simulation of the sequence and the simulation of the year. The models of the components are validated with experimental results or with monitored data (Appendix C).

The simulations have been used for the improvement of the emulations described in the chapter 3.5.

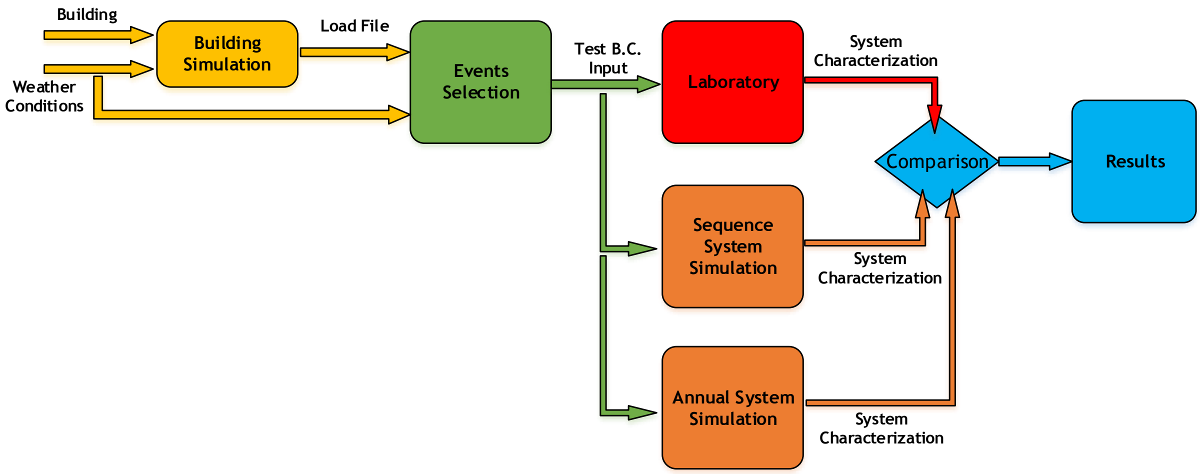

Figure 3-23: Block diagram of the validation of test procedure at system level.

The deviation between the values extrapolated from the short sequence and the annual simulation is calculated with Equation 3-24 while the deviation between the extrapolated from short simulation and annual simulation is calculated with Equation 3-25.

Equation 3-24
$$\delta_E = \frac{E_{short\ test} - E_{annual\ simulation}}{E_{annual\ simulation}} \quad [-]$$

Equation 3-25
$$\delta_{E,sim} = \frac{E_{sequence\ simulation} - E_{annual\ simulation}}{E_{annual\ simulation}} \quad [-]$$

3.8 Conclusions

This chapter has presented the test procedure at system level. The aim was to develop a benchmark test with a procedure that is at the same time reliable and easy to be implemented in order to be attractive for industries.

Differently to the procedure at component level, the boundary conditions are given directly from the weather data and not from simulation anymore. Beyond this advantage, the procedure has been developed to be applicable for different climates.

A reference building is considered to define the load but this choice is not binding for the validity of the method. The decision of the application of a load file gives the advantage of testing different system under the same load condition in a way to have a common base for the performance comparison. Moreover, this simplifies the adaption of the procedure since the alternative would be an on-line simulation of the building.

Since the installation of the whole system could not be performed, the physical boundaries of the tested system have been defined and emulation models for the components not installed have been developed. Again, to have an easy implementation of the procedure, the models do not foresee the adoption of commercial software but consider simplified equations. This is motivated by the fact that the focus of the dynamic characterization is the system and not the components not installed (i.e. collector, distribution system).

4 Selection of a sequence

The previous chapter has described the test method without explaining how create a short test sequence. The procedure has to evaluate the system annual performance testing only a few events caught from a list of 365 days, each one with its own irradiance profile, temperature profile, humidity profile, load profile etc. This is a delicate stage of the procedure and there are many discussions underway about it. Two approaches are identified in literature: the first one is an iterative procedure for selecting the sequence in order to have a proportionality with the annual performance while the second method is to select days with temperature and radiation profiles corresponding to the monthly average conditions. The first approach is complicated and the optimization requires decisions from the user (different users involves in a different optimum); moreover, a new optimization should be carried out when a different weather condition would be used. The second method is more easy to be implemented but it could not be able to perform a direct evaluation of performance [17]. This chapter debates about the procedure for the definition of the short sequence.

Before defining the method, the procedure for the selection of the short sequence has to satisfy the following requirements:

- The sequence has to represent the performance through the entire year operation;
- The seasonal performance should be directly extrapolated from the short test results;
- The procedure should be applicable for different climates;
- The procedure has not to allow the influence of operator choice (from one set of boundary conditions, the output should be univocal).

To understand how the selection has to be done, these three points have to be discussed:

- Duration of the event (4.1);
- Duration of the sequence (4.2 and 4.3);
- How select the events (4.2 and 4.3).

The first question is answered with the section 4.1 while the second two questions are analysed with two methodologies in the sections 4.2 and 4.3.

The validation of the selection procedure has been done with simulations since a work similar to the component level would be time and cost consuming: the same work would require a test of the whole season (1 year) plus the tests of the different selections (1 or 2 weeks each).

4.1 Event duration

The first step is the definition of “Event”. In the procedure developed at component level, the “Event” is defined as continuous working phase (from switch on to switch off). With this definition, the duration of Event is variable. At system level, the event has to be defined since the activation of the system could not be defined in advance. “Event” is defined as the continuous period considered to divide the entire boundary conditions. Usual practice is to consider days, but the aim was to understand if also shorter periods could be considered. This question is answered with a spectral analysis of the boundary condition to identify the length of the event.

The essence of the spectral estimation problem is to assess how the intensity of a signal (power) is distributed over frequency from a finite record of data sequence. This analysis, which is widely applied in different fields, may reveal hidden periodicities in the studied data which are to be associated with cyclic behaviour or recurring processes. In addition, it could help in characterizing the dynamical behaviour of a generic system. The function that is investigated is the Power Spectral Density (PSD) of some signals of the weather file and later of the studied system. This name comes from the study of random variations of the power absorbed in an electrical circuit. This is computed from the Discrete Fourier Transform (DFT) and provides a useful way to characterize the amplitude versus frequency content of a signal. For a finite-duration, discrete-time signal x(m) of length N samples, the Discrete Fourier transform (DFT) is defined as N uniformly spaced spectral samples.

Equation 4-1

$$X(k) = \sum_{m=0}^{N-1} x(m)\ e^{-j\left(\frac{2\pi}{N}\right)m\,k} \qquad k = 0{:}\,N-1 \qquad [-]$$

For stochastic signals, the Power-Spectral Density is defined as the Fourier transform of the autocorrelation function:

Equation 4-2

$$PSD = P_{XX}(f) = \sum_{m=-\infty}^{\infty} r_{XX}(m)\ e^{-j\,2\pi f\,m} \qquad [-]$$

In practice, the autocorrelation function is useful for analysing how a signal changes in time by comparing the influence of the signal value at the instant k and its value at the instant k+m. If a signal is sufficiently periodic, this function has a maximum each time the delay m is a multiple of the signal period. It is estimated from a signal record of length N samples as:

Equation 4-3

$$r_{XX}(m) = \frac{1}{N-|m|} \sum_{k=0}^{N-|m|-1} \mathrm{x}(k)\cdot\mathrm{x}(k+m) \qquad k = 0{:}\,N-1 \qquad [-]$$

The analysed signals are the annual weather data, the building load and other internal parameters of the system obtained through the annual simulation of the whole system in TRNSYS with a time resolution of one minute. In this chapter, it is reported the results of the spectral analysis of the dynamic boundary conditions. This analysis is valid in general since it is not dependent from the system.

As shown from Figure 4-1 to Figure 4-4, the irradiance on horizontal surface, the temperature and the loads are characterized by two main components at frequencies corresponding to 24 h and 12 h. Other weekly, monthly or seasonal periodicities are identified. The component at 24 h have a higher PSD. As consequence of the spectral analysis, the events are defined with the days. The analysis tells that also the adaption of events corresponding to half days could be reasonable.

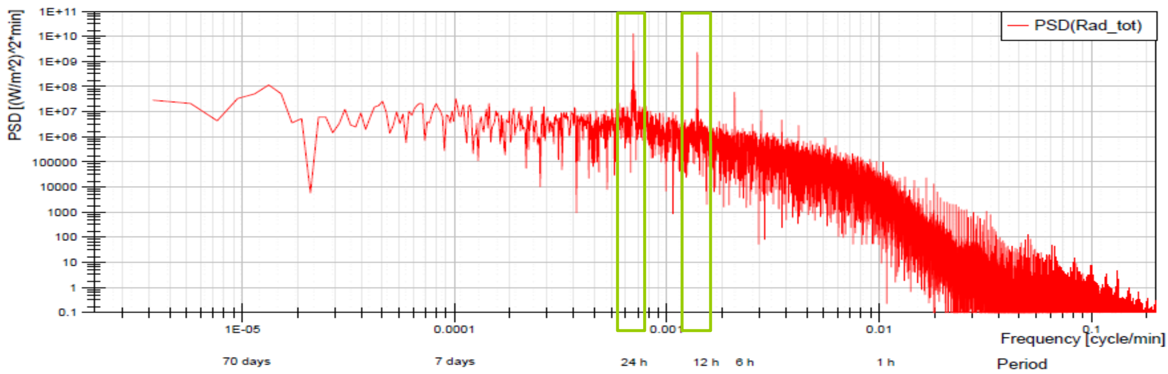

Figure 4-1: Spectral analysis of global horizontal irradiance.

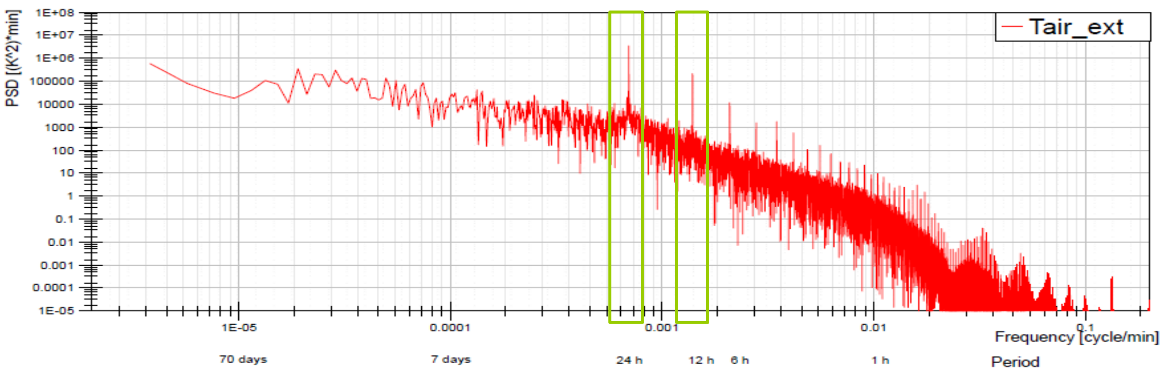

Figure 4-2: Spectral analysis of external temperature.

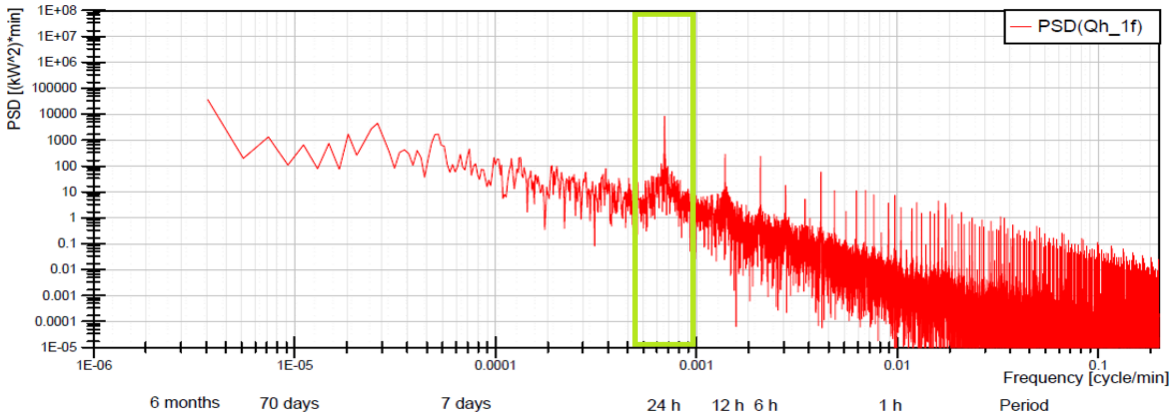

Figure 4-3: Spectral analysis of heating load.

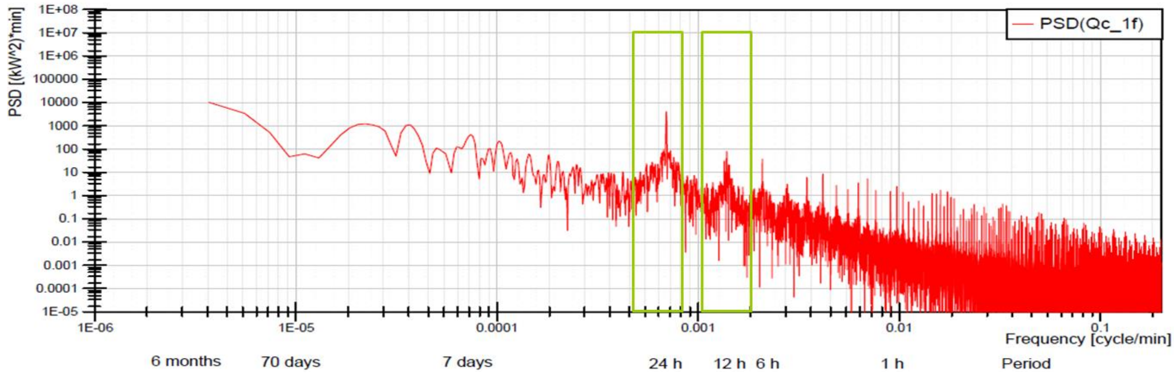

Figure 4-4: Spectral analysis of cooling load.

4.2 Selection by "class"

Since the Events are identified by days, the boundary conditions are divided in 365 events. The first selection has been performed applying the classification described in the chapter 2.1.2. In this section, the analysis considers the climate of Bolzano.

As indicated in the chapter 2.1.2, the classes are built identifying intervals of amplitude and average of the boundary conditions and intervals of the duration. In this case, since the duration of event is constant, it does not require a specific classification. As consequence, the dimension of the event matrices is reduced by 1 parameter (Equation 4-4) and the number of classes created does not depend from the division on the duration (since it is 1 - Equation 4-5).

Equation 4-4 $$N = 2 \cdot n_p$$ [-]

Equation 4-5 $$C = \prod_i n_{amp,i} \prod_k n_{avg,k}$$ [-]

where the indexes i and k varies from 1 to n_p.

As for the component test method, each class corresponds to a N-dimensional vector.

Once the boundary conditions are identified and their average and amplitude is calculated, the classification proceeds as described in the chapter 2.1.2. A threshold is applied to exclude from the selection the Events which effect is negligible and the remaining classes are divided by the minimum number of events.

For the whole system, several boundary conditions can be identified since it is connected with the external ambient. These could be the temperature, irradiance (and its different component), humidity, wind (speed and direction) and so on. From these boundary conditions, only the ones that have the highest influence on performance should be considered. For this motivation, the boundary conditions considered for the selection are the profiles of temperatures and irradiance on horizontal surface. The classes are four-dimension vector (Equation 4-4). The calculation of the average and amplitude of the irradiance is corresponding to give the information of the daily irradiation[2] and of the maximum peak of irradiance[3]. These values give a direct information instead of the average and amplitude of irradiance. The Table 4-1 shows the range of average external temperature, amplitude of external temperature, the daily irradiation and the maximum irradiance. Those parameters are used to classify the Events.

Table 4-1: Range of variation of boundary conditions. Bolzano climate. Whole system.

	$T_{amb,avg}$	$T_{amb,amp}$	GHI	GHI_{max}
	[°C]	[K]	[Wh/m^2]	[W/m^2]
Min	-5.621	1.9395	212.0	50.358
Max	28.017	16.55	7846.8	908.27

The subscript (amp) and (avg) indicate respectively the amplitude and the average, calculated for each event.

The ranges indicated in Table 4-1 are divided into intervals of 2K or 3K for the temperature or into intervals of 50 W/m^2 or 150 W/m^2 for the irradiance. The result of this classification is visible in Table 4-2 which indicates the number of classes created and the number of classes that contain elements. The column threshold shows the number of events remaining after its application and the number of events excluded. Then, a divisor is applied and the residual number of events is indicated. The test duration considers this value plus one day of preconditioning. As first outcome from these classifications, a high value of threshold should be applied to reduce the sequence to a reasonable duration. It is not logic for cost motivations to test a system for a long duration; E.g. 36 or 65 days as indicated with the criteria 2K-50-1 and 2K-150-1. The table indicates that having a duration of a fixed number of days is not possible: as example the criterion 2K-50 gives duration of 7 or 4 days depending from the threshold but intermediate durations could not be defined with this criterion.

Table 4-2: Events classification and selection. Bolzano climate. Whole system.

	Number of intervals						Threshold			Division		
	$T_{amb,avg}$	$T_{amb,amp}$	GHI	GHI_{max}	No. classes	Full classes	Threshold	Residual	Excluded	Divisor	Residual	Test duration [days]
Whole Season	1	1	1	1	1	1				1	365	366
2K-50-1	17	7	6	17	12138	170	1	139	226	4	35	36
2K-50-1.5							1.5	48	317	6	7	8
2K-50-1.75							1.75	30	335	7	4	5
2K-150-1	17	7	2	6	1428	110	1	247	118	4	64	65
2K-150-1.5							1.5	153	212	6	24	25
2K-150-1.75							1.75	105	260	7	14	15
2K-150-2							2	63	302	8	8	9
3K-50-1	11	5	6	17	5610	103	1	249	116	4	63	64
3K-50-1.5							1.5	149	216	6	22	23
3K-50-1.75							1.75	125	240	7	17	18
3K-150-2.5	11	5	2	6	660	60	2.5	171	194	10	19	20
3K-150-2.75							2.75	161	204	11	14	15
3K-150-3.5							3.5	139	226	12	10	11
3K-150-3.75							3.75	115	250	15	7	8

The first column contains the name of the corresponding selection: the number with the "K" letter indicates the temperature step; the second number indicates the number of intervals for the irradiation and the third number indicates the threshold percentage.

[2] The calculation of average irradiance during the day multiplied by 24h correspond to the irradiation of that day.

[3] The minimum irradiance is always 0. The amplitude corresponds to the difference between maximum and minimum.

The results of the sequences obtained at component level showed that a high value of threshold would involve in a large uncertainty of the results. In the classification of the 365 days, a high value of threshold should be adopted to reduce the sequence to a duration of one or two weeks. Moreover, the different classifications require different levels of threshold to obtain similar durations.

Some sequences defined with those criteria were simulated considering the system model as indicated in Appendix C. The results are presented in the following section.

4.2.1 Simulation of sequences

Sequences from 5 to 12 days were created from the selection indicated in Table 4-2. The sequences were simulated considering the SHP system indicated in the Appendix C. The short sequences defined are compared with the simulation of the whole year in terms of seasonal extrapolated performance figures. The performance figures here reported are the heating and cooling loads, and the seasonal performance factors for the space heating, space cooling, domestic hot water and total load.

The results show a high deviation between the sequence extrapolation and the annual simulation. Figure 4-5 shows the seasonal performance factors (cooling, heating, DHW and total) and the loads (heating and cooling) obtained with the simulations of different sequences. The DHW load is not reported in the figure since it is equal for all the sequence (fixed extraction).

The sequences individuated with the "classification" method, present higher total performance factor than the annual simulation.

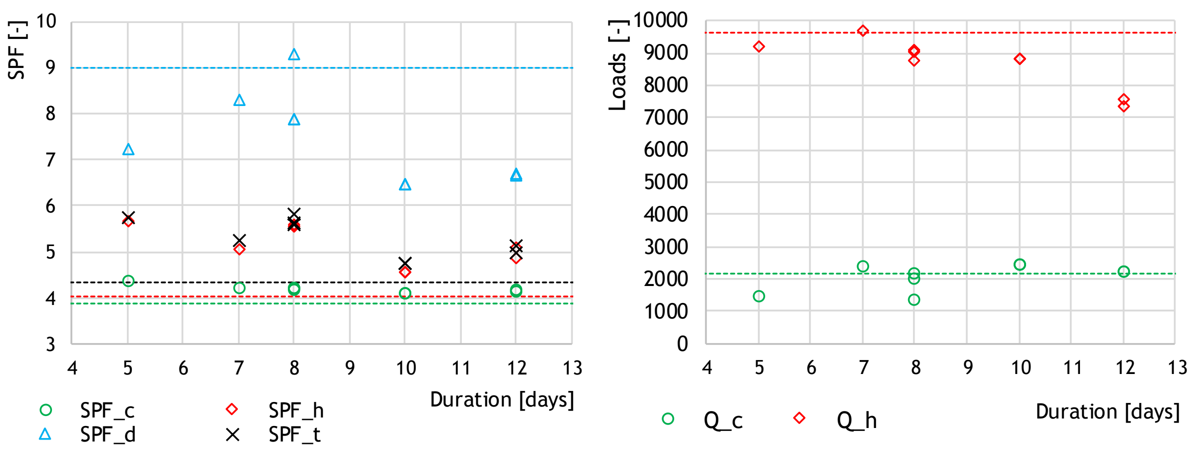

Figure 4-5: Results of sequences defined with classification method.

Table 4-3: Results of sequences defined with classification method.

Seq.	SPF_c [-]	SPF_h [-]	SPF_d [-]	SPF_{tot} [-]	Q_c [kWh]	Q_h [kWh]	Q_{dhw} [kWh]	W_c [kWh]	W_h [kWh]	W_{dhw} [kWh]
Annual	4.03	3.88	8.99	4.35	2151	9624	2569	534	2479	286
5 days	4.38	5.65	7.23	5.75	1439	9211	3027	328	1630	419
7 days	4.23	5.06	8.31	5.27	2379	9663	2707	562	1911	326
8 days	4.17	5.55	9.28	5.83	1345	9050	2689	322	1631	290
8 days	4.21	5.57	7.90	5.64	1976	9064	2682	469	1626	339
8 days	4.21	5.59	7.90	5.58	2154	8753	2367	511	1567	300
10 days	4.12	4.57	6.47	4.74	2415	8801	2601	586	1927	402
10 days	4.12	4.57	6.47	4.74	2415	8801	2601	586	1927	402
10 days	4.12	4.57	6.47	4.74	2415	8801	2601	586	1927	402
12 days	4.18	5.11	6.65	5.14	2229	7323	2413	534	1432	363
12 days	4.13	4.87	6.70	4.97	2225	7574	2401	538	1556	358

The results obtained in this selection have a huge deviation from the annual simulation. Since to obtain a short sequence, a high value of threshold is applied, the Events selected are representative of the distribution peaks of the weather data (classified with temperature and radiation). The representation of only few peaks disregard the behaviour of other events that are more diffused and that their influence is not negligible. The conclusion is that the selection is not applicable when a high threshold is needed. At component level, a threshold that exclude classed with one element gives a short test duration (and therefore justifiable in terms of test cost and effort require) while at system level the same threshold gives long durations.

4.3 Selection by Clustering

The selections performed in the previous section showed that the classification depends from the choice of the user and the data reduction to be performed requires the exclusion of a large number of days. The results do not justify the application of this procedure. For this motivation, a new approach is adopted. The representative days must be selected to replicate the different seasonal working condition of the tested system with an objective approach that gives a univocal output. To select a representative part of the events, a clustering approach is used.

4.3.1 Method

Clustering is task of grouping a set of objects in such a way that objects in the same group (cluster) are more similar to each other than to those in other groups. The clustering can be formulated as multi-objective optimization problem. Different algorithms are defined to solve this task. To classify the days to select, the Partitioning Around Medoids (PAM also called k-medoids) algorithm is used. The *k*-medoids method was also used by Dominguez et al. [56] to reduce a full year of demand data (power, heating, and cooling) to a few representative days for combined heat and power (CHP) optimization.

The method creates a number of groups which elements are described by M-dimensional coordinates The number of groups is chosen by the user. Different sequence of 6, 8, 10, 12 and 24 days were created. For each groups, the method selects a representative element.

More in detail, the Partitioning Around Medoid (PAM) algorithm is defined as follow: the clusters outline is calculated minimizing for every cluster the overall Euclidean distance between the cluster points. The coordinates are normalized with its standard deviation across all observations. The idea is to create “N” groups (cluster) and assign every points in the cloud to a group. The boundary of the cluster is not defined and an iterative process tries all the possible combinations of point and cluster. At the end of the iterative process, the clusters are individuated. These are represented by the cluster centre (corresponding to the geometric centre) called “centroid”. The “medoid” is the nearest element to the centroids (Figure 4-6). The sequence is created with selecting the Medoids.

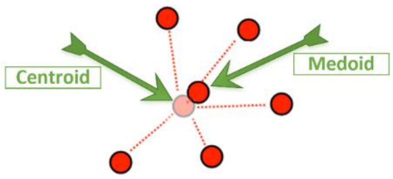

Figure 4-6: Clustering. Identification of Centroid and Medoid.

The Partitioning Around Medoids (PAM) algorithm can be formalizes with these steps:

1. Initialize: randomly select (without replacement) k of the n data points as the medoids;
2. Associate each data point to the closest medoid. "Closest" is defined using any valid distance metric;
3. For each medoid m
    - For each non-medoid data point o
        - Swap m and o and compute the total cost of the configuration
4. Select the configuration with the lowest cost.

Repeat steps 2 to 4 until there is no change in the medoid.

To be classified, the events have to be compared in terms of some characteristics that became the coordinates for the method. The events – considered as days – are characterized by profiles of temperature and irradiance (different component) and other parameters that have smaller influence on the system (such as relative humidity, wind speed and so on). To reduce the number of variables that identify an event, the average ambient temperature and total irradiation on the horizontal surface are considered describing a 2D coordinates. This classification is the simplest possible. Other solutions are given by adding the space load to the classification. It has been proposed with a 3D and 4D clustering where the 3D considers the temperature, irradiance and heating and cooling load (in one vector considering a different sign), while the 4D considers the temperature, the irradiance and the heat and cooling loads separately.

An example of classification of events with the clustering is indicated with the example 1.

Example 1

For example, the 15 events were randomly generated and are indicated in Table 4-4; *from these 15 events, a selection of 3 has to be done. Therefore 3 groups have to be created. The method divides the events into 3 groups by minimizing the distance between each element of the group. From these groups the "Medoids" are identified in the events 6, 9 and 15. The figure shows how the events were grouped.*

Table 4-4: Example of clustering. 15 events with their characteristics and group identity.

Day	Temperature [°C]	Irradiation [Wh/m^2]		Group
1	1.91	2376.85		0
2	9.90	2694.12		1
3	5.98	751.26	Clustering	1
4	8.86	5.65	------------>	1
5	0.14	1048.74		0
6	2.57	1929.99		0
7	4.30	210.95		0
8	0.45	161.38		0
9	8.64	1454.36		1
10	0.58	5923.16		2
11	0.69	4057.67		2
12	3.77	6457.90		2
13	3.72	2715.89		0
14	6.00	4473.34		2
15	0.95	4764.96		2

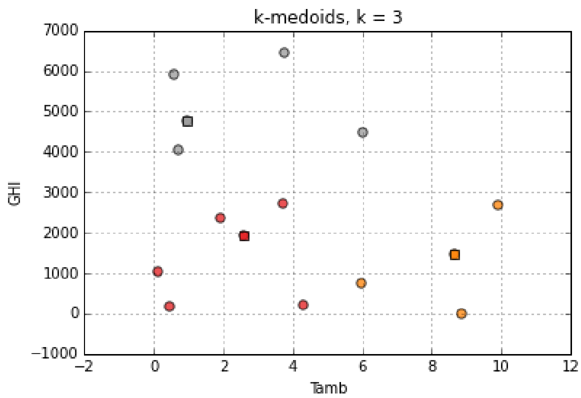

Figure 4-7: Example of clustering.

Classification of Events as a funciton of total irradiation and ambient temperature. The Events are indicated with circles while the Medoids are indicated by squares. The different clours indicates the groups.

Table 4-5: Example of clustering. Number of elements for each group.

Group	N elements
0	6
1	4
2	5
total	15

The aim is to directly extrapolate the annual performance from the sequence. Since the number of element is not the same for the different cluster, the extrapolation of seasonal performance should be done weighing the event performance by the dimension of the clusters. The calculation of seasonal energy from the test results is done with Equation 4-6.

Equation 4-6 $$Q_{seas} = \sum_{i=1}^{n_{cluster}} n_{el,cluster,i} \cdot Q_i$$ [kWh]

Where Q_i is the energy measured during the event corresponding to the "i-th" Medoid and $n_{el,cluster,i}$ is the number of elements of the "i-th" cluster.

The equation is valid for the thermal energies (SH, SC, DHW, collector and so on) and for the electric consumptions.

Another elaboration of the data is needed when a 2D cluster is defined. Since the load is not directly proportional to the coordinates, the medoid load is not equal to the cluster average load. In this way, the single day load energy multiplied with the number of element in the respective cluster does not give exactly the cluster load energy. Therefore, a scaling factor is calculated for each cluster. This factor (once value for each cluster) compensates the deviation between the medoid energy and the cluster average energy.

Equation 4-7 $$L_{sc(i)} = \frac{E_{Simulations.Day(i)}}{E_{Simulations.Cluster(i)}} \cdot N_{Days.In.Cluster(i)}$$ [-]

The scaling factor (L_{sc}) scales the space heating space cooling loads. The scaling factor is lower when a 3D or 4D coordinates are used.

The sequence defined with clustering would be closed to a correct representation of the whole year performances when the performances are linearly dependent from the boundary conditions. This because the days are selected considering the nearest element of geometric centre of each cluster and the consumptions and loads are built through integration (or better through sum of discrete points).

As example, considering one-dimensional case where the consumption (W) is linearly dependent from the temperature, the consumption can be described as:

Equation 4-8 $$W = \alpha \cdot T + \beta$$ [kWh]

Where the parameters α and β are the coefficients of the linear dependence.

The total consumption is a sum of the "i-th" consumptions, and each "i-th" consumptions could be described as a function of the "i-th" temperatures with the Equation 4-8:

Equation 4-9 $$W_{tot} = \sum_{i=1}^{N} W_i = \sum_{i=1}^{N} (\alpha \cdot T + \beta) = \sum_{i=1}^{N} (\alpha \cdot T_i) + \beta \cdot N$$ [kWh]

In this case, the geometric centre corresponds to the average temperature and the last summation could be substituted with the average temperature multiplied by the number of elements:

Equation 4-10 $$W_{tot} = \sum_{i=1}^{N} W_i = (\alpha \cdot \bar{T} + \beta) \cdot N$$ [kWh]

The total consumption could be calculated directly from the geometric centre of the boundary condition (in this case one temperature). The same demonstration could be performed with a multi-dimension problem when the consumptions are linearly dependent from more boundary conditions.

4.3.2 Selection

The clustering has been applied to create sequences for the climate of Bolzano and Zurich to verify the effect of a sequence selection of different duration. Sequences of 6, 8, 10, 12 and 24 days were created with 2D, 3D and 4D coordinates.

Figure 4-8 and Figure 4-9 show the identification of the sequence respectively for Bolzano and Zurich. The green triangular points identify the selection with 2D coordinates (T and GHI), the red diamonds points identify the selection with 3D coordinates (T, GHI and Load) and the blue circle points identify the selection with 4D coordinates (T, GHI, Heating and cooling load). The figure in the left shows the days of the year as function of the average temperature and global horizontal irradiation while the right figure shows the days as a function of the average temperature and the space load distinguished into cooling (blue points) and heating (red points).

The different coordinates of the days (2D, 3D, 4D) modify the geometry of the problem and therefore the selections are different. In the climate of Bolzano, the points identified with a selection of 2D clustering are well distributed in the graph Temperature/Irradiation while in the graphs Temperature/Load do not touch points at high load. At opposite, the selection of 3D and 4D clustering are well distributed in the graph Temperature/Load but not in the other graphs.

In the climate of Zurich, the 2D clustering does not considers days with space cooling load. The 3D clustering selects only one day with very low load (1.6 kWh) while the 4D clustering selects two days with cooling load (one with 1.6 kWh and the other one with 25.5 kWh). The motivation is due for the geometry defined in the clustering since only few events require cooling load. With the 2D clustering, the load is a consequence of the days selected as a function of the temperature and irradiation while the 3D clustering gives importance to the load. The 4D clustering gives equal importance to the cooling and heating load since the coordinates are normalized. This means that in a climate like Zurich where the heating load is about 30 time the cooling load, this selection would give the same number of days to the heating and to the cooling season that corresponds to a not balanced selection.

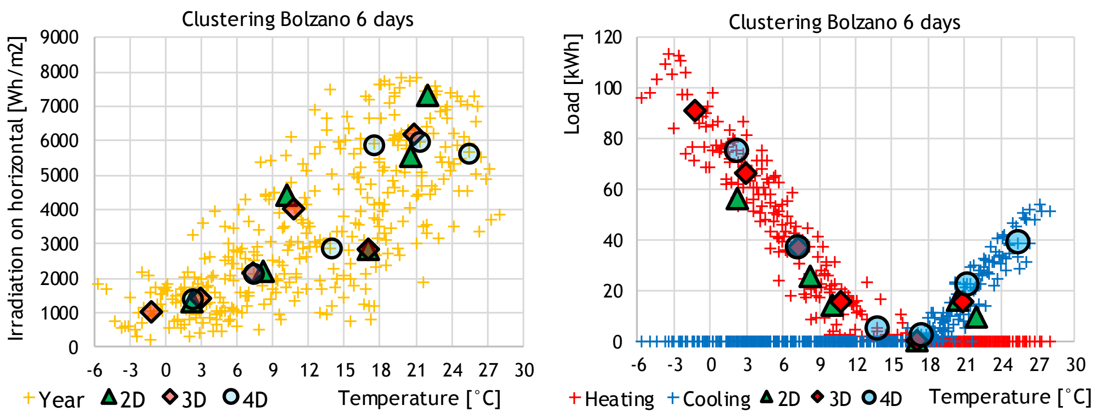

Figure 4-8: Identification of six-days sequences defined with different coordinates. Bolzano climate.

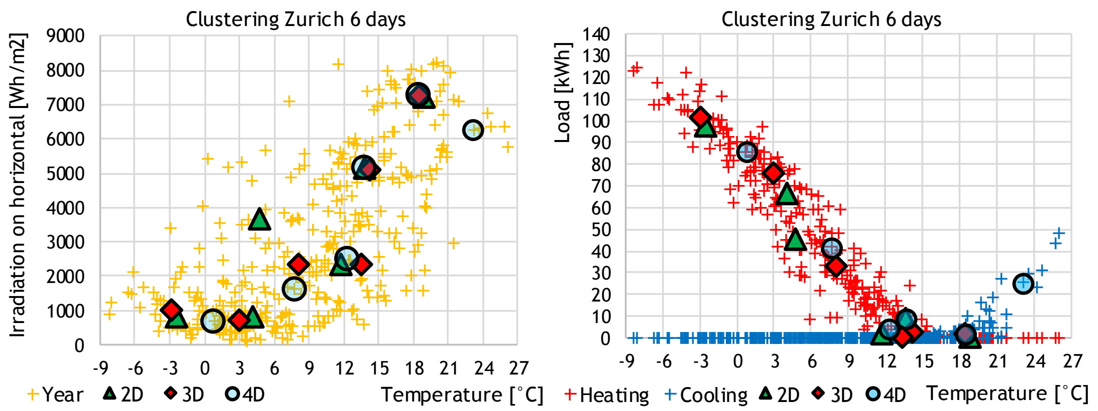

Figure 4-9: Identification of six-days sequences defined with different coordinates. Zurich climate.

The effect of increasing the number of cluster can be seen in the Figure 4-10. The figure shows the selection with six clusters (green triangular points) and with ten clusters (red diamonds points). The ten-days selection covers more extreme days (in terms of temperature, irradiation and load) than the six-days selection. The motivation is that the clustering creates N groups and the selection is made with the Medoids that is the nearest point to the geometric centre of clusters (centroid). As consequence, with only few cluster the extreme conditions could not be reached.

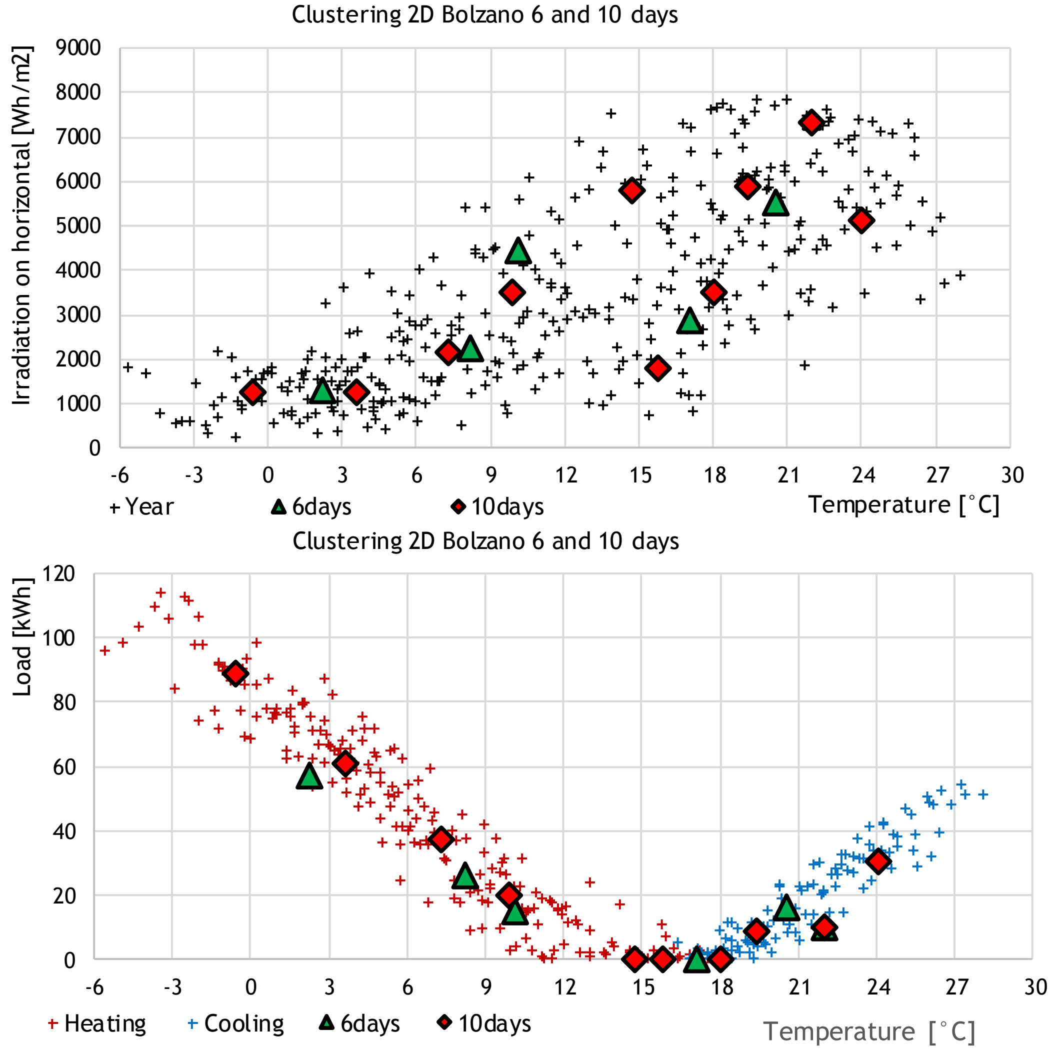

Figure 4-10: Comparison of sequence of six-days and ten-days with 2D clustering. Bolzano climate.

The Appendix D presents the figures of the classification of 8, 10, 12 and 24 days.

4.3.3 Simulation of a sequence

The selections showed in the chapters 4.3.2 were simulated for a solar assisted heat pump (SAHP) system with different configurations of collector area (8 m^2 or 16 m^2) and storages volume (700 l or 1500 l). The volume of 700 l is obtained with a “big storage” of 500 l connected in series with a “small storage” of 200 l and while the 1500 l is obtained with the combination of 1000 l and 500 l. The system model and layout are presented in the Appendix C. The sequences are simulated with the climates of Bolzano and Zurich.

The selection with the clustering method does not give any advice on the order of the sequence. The days are ordered in the same order as they occur in the year starting from the winter and ending the sequence with the autumn conditions. The last day of the sequence is used to precondition the whole sequence. More days were simulated after the end of the core sequence in order to be able to consider different periods of evaluation. In this way, the effect of simulating with a preconditioning with summer days could be evaluated. As example, if the core sequence is defined with six-days 1-2-3-4-5-6, the simulated sequence would be 6-**1-2-3-4-5-6**-1-2-3 where the first day (day 6) is the preconditioning day, the following six-days are the core sequence (**1-2-3-4-5-6**) and the other are used for the different evaluation periods. In this way, the performance evaluation could be done also considering the core sequence starting from day 2 (2-3-4-5-6-1) or day 3 (3-4-5-6-1-2) and so on.

Table 4-6 and Table 4-7 show the results extrapolated from the six-days sequence with the different periods of evaluation for Bolzano and Zurich sequences. The first row indicates the evaluation performed simulating the winter days as first while the second and the third rows starts with one or two summer days. The result is that the solar fraction (and therefore the seasonal performance factor) increase over the annual value if a summer day is simulated before the winter days. The motivation is given by the fact that the average irradiation of the sequence is the same of the average annual irradiation but the stagnation condition of the sequence is different than the annual condition: in a short sequence the storage does not reach storage stagnation instead in the annual simulation the storage reaches the temperature limit during the summer days. The consequence is that all the available irradiation during the year could not be collected. At opposite, in the sequence the available irradiation could be collected since the storage does not reach the stagnation.

This effect has to be added to the fact that the storage temperature is characterized by daily or multi-day frequencies. In the short sequence, a “discharge” of the storage for the different season should be externally forced or avoided. As example, in the sequence a day with heating load could happen after one or two days of a summer day while in the year this is presented after some months. The energy stored before the winter day in the first case is higher than the one of the second case. This energy level influences the possibility to directly heat the house with the solar energy. The effect of the sequence is that the energy stored during the summer is used during the winter that happen after two days while in the year is not possible.

To manage this effect, different solutions could be adopted:

- A forced extraction of energy;
- A reduction of the irradiation during the summer days;
- Simulate the winter days before the summer ones.

The first two solutions require a study for the different systems since the behaviour of the storage depends from the layout and the system’s control strategy. The third solution is easier to be implemented since does not require any prelaminar simulation and the solution could be implemented directly on the file with the sequence boundary conditions. The solution of simulating the winter days before summer days is taken as rule for the method.

Table 4-6: Periods of evaluation of the test sequence. Bolzano climate.

	Q_c [kWh]	Q_h [kWh]	Q_{dhw} [kWh]	Q_{tot} [kWh]	W_c [kWh]	W_{heat} [kWh]	W_{dhw} [kWh]	W_{tot} [kWh]	SPF_c [-]	SPF_h [-]	SPF_d [-]	SPF_t [-]
seq1	1883	9151	2495	13530	438	2079	467	2984	4.30	4.40	5.34	4.53
seq2	1883	9368	2496	13748	438	1736	466	2640	4.30	5.40	5.35	5.21
seq3	1883	9436	2496	13815	438	1520	454	2412	4.30	6.21	5.50	5.73

Seq1: sequence defined with the period of evaluation 1-2-3-4-5-6, seq2: 2-3-4-5-6-1, seq3: 3-4-5-6-1-2.

Table 4-7: Periods of evaluation of the test sequence. Zurich climate.

	Q_{heat} [kWh]	Q_{dhw} [kWh]	Q_{tot} [kWh]	W_{heat} [kWh]	W_{dhw} [kWh]	W_{tot} [kWh]	SPF_h [-]	SPF_d [-]	SPF_t [-]
seq1	12250	2565	14815	3241	343	3584	3.78	7.48	4.13
seq2	12858	2565	15423	2787	601	3388	4.61	4.27	4.55
seq3	12859	2565	15424	2793	711	3503	4.60	3.61	4.40

Seq1: sequence defined with the period of evaluation 1-2-3-4-5-6, seq2: 2-3-4-5-6-1, seq3: 3-4-5-6-1-2.

From those considerations, the sequences were simulated considering before the winter days and then the summer days. Figure 4-10 and Figure 4-11 show the total seasonal performance factor trend as a function of the number of clusters for the climates of Bolzano and Zurich for the different plant configurations. In general, the deviation of SPF decreases as the number of clusters increase. The deviation increases with increasing the storage volume and increasing the collector area; in fact, the simulation set with 16 m^2 and 1500 l is the one with the higher deviation. The sequence obtained with a 2D clustering presents the best agreement with the annual simulation. The motivation is that performance are strongly depending from the profiles of temperature, irradiance and load. The modification of load profile with the scaling factor of Equation 4-7 allows that all the sequences (2D, 3D and 4D) represents well the cluster load and consequently the annual load. However, the 3D and 4D clustering, represents worse the condition of temperature and irradiation as indicated in the previous paragraph.

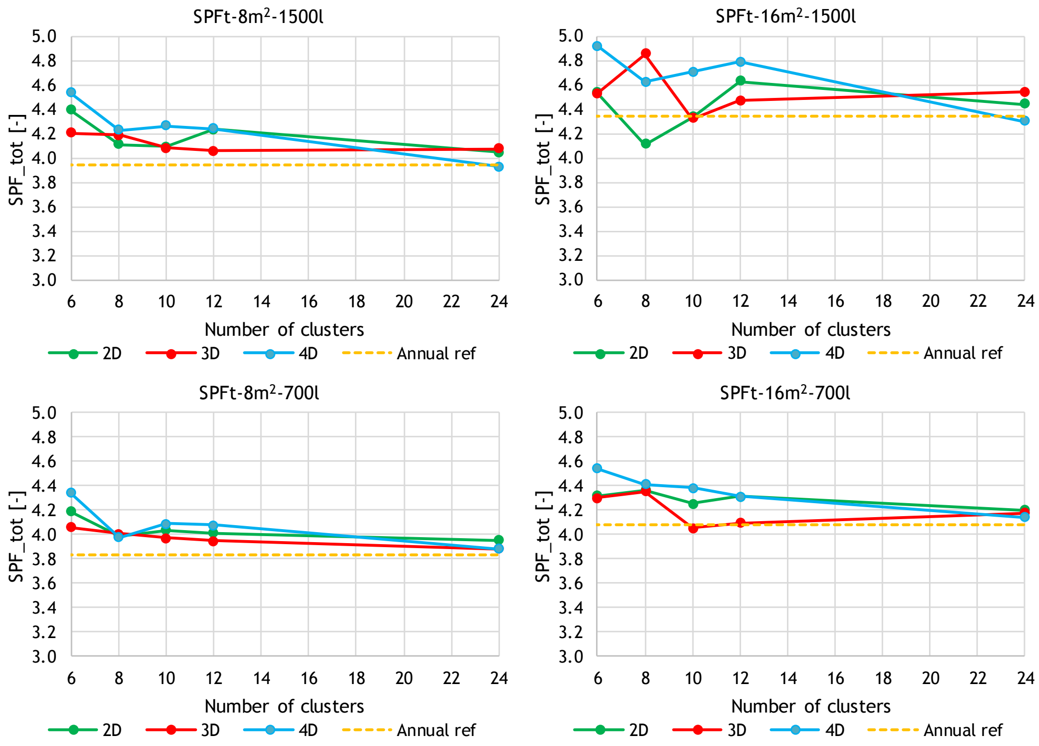

Figure 4-11: Total seasonal performance factor as a function of number of clusters. Bolzano climate.

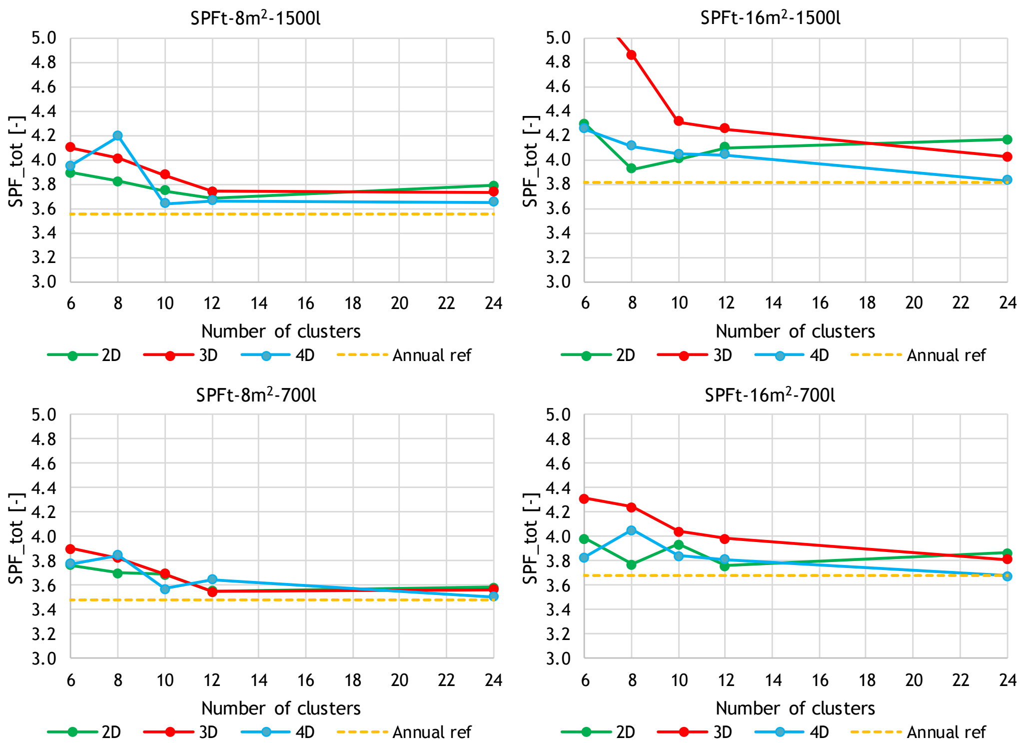

Figure 4-12: Total seasonal performance factor as a function of number of clusters. Zurich climate.

Regarding the solar fraction, Figure 4-13 and Figure 4-14 present the result of Bolzano and Zurich. As the seasonal performance factor, the solar fraction is well reproduced for lower storage volume or collector area. The clustering with a 2D selection represents better the solar fraction. The only exception is represented by the climate of Zurich with 16 m² and 1500 l where the sequence deviates from the annual simulation about 10 %. The cooling solar fraction is 0 since the plant uses only a compression chiller and not thermally driven chillers.

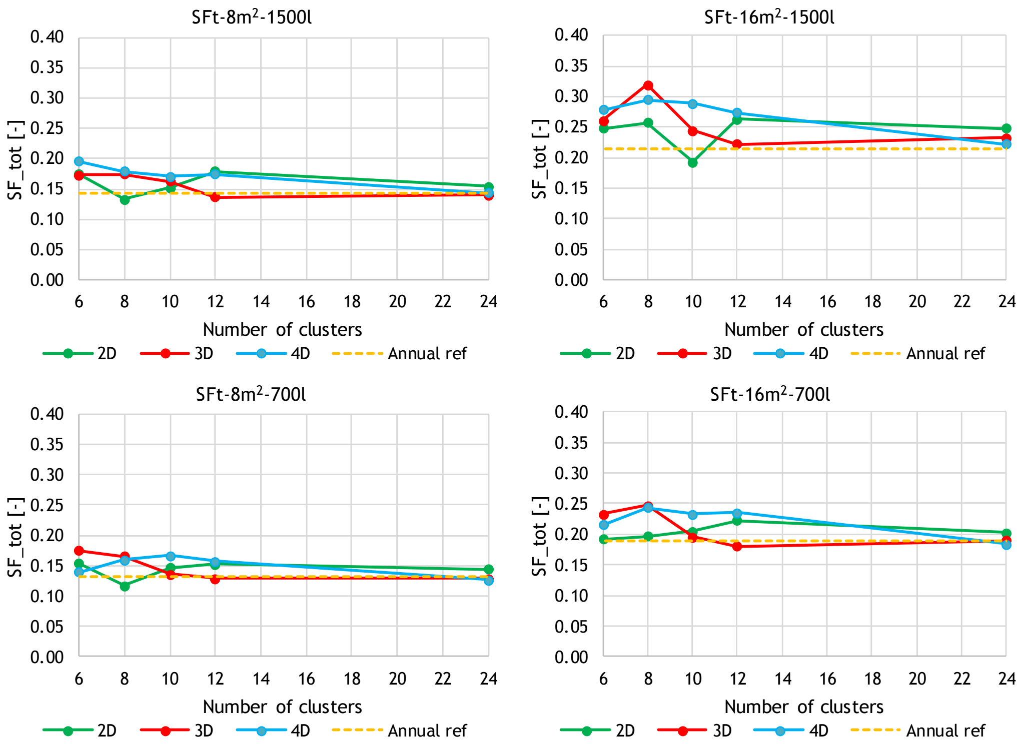

Figure 4-13: Total solar fraction as a function of number of clusters. Bolzano climate.

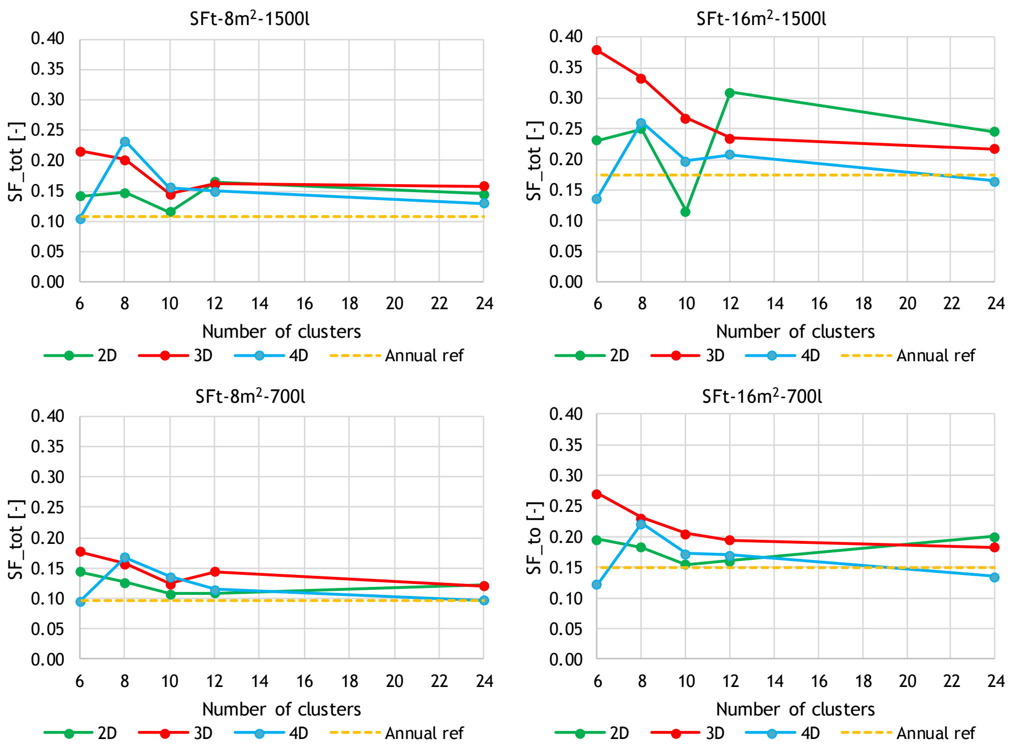

Figure 4-14: Total solar fraction as a function of number of clusters. Zurich climate.

The performance of the heat pump is closed to a linear dependence of the air temperature. In cooling the heat pump is the only one device that satisfies the cooling load. The Figure D-10 and Figure D-12 show that the cooling seasonal performance factors of different sequences are closed to the one calculated with the annual simulation. The deviation is not dependent from the number of clusters.

4.4 Conclusions

This chapter has analysed the procedure to create a short test sequence starting from the annual weather data. The aim was to define an objective procedure applicable to different climates and that allows to directly extrapolate the seasonal results from the short test.

The first method considered is the classification of boundary conditions as performed in the procedure at component level. However, the good results obtained in the chapter 2 are not replicated in the case of the whole system since the data reduction has required an application of a high value of threshold. The consequence is a selection of few peaks that are not representative of the entire year. Different classification parameters are considered and all of these have given an overestimation of performances.

From this method, the decision has been to move toward a clustering approach. The days are grouped into clusters wherein each element is more similar to each other than to those in other groups. To build the sequence, for each cluster, the closest element to the geometric centre is selected. The days are described with different coordinates and the optimal solution is to consider the daily average temperature and the daily irradiation on horizontal surface. The order of days in the sequences has been evaluated; the outcome is that the days within sequence have to be ordered with the same order they occur in the year starting from the winter days and concluding with the summer days.

The sequence defined with clustering represents correctly the seasonal performances when those are linearly dependent from the boundary conditions; this could be a good approximation of heat pump system while for solar system the performances are not linearly dependent from boundary conditions.

Different system configurations have been simulated. The deviation between the short sequence performance and the annual performance increases with increasing the collector area and the volume of storage. Moreover, the deviation decreases with the number of clusters. With a six-days sequence, the expected deviation is lower than 8%.

5 Application of procedure

The procedure developed and presented in chapter 3 has been implemented in the laboratory and the solar assisted heat pump system presented in Appendix C has been set-up in the laboratory. Test sequences of six-days and ten-days were created with the clustering approach presented in the chapter 4.3.

The system was studied under different configuration and different climates as follows:

- Six-days sequence for the climate of Bolzano with 16 m^2 of collector (5.1);
- Ten-days sequence for the climate of Bolzano with 16 m^2 of collector (5.2);
- Six-days sequence for the climate of Bolzano with 8 m^2 of collector (5.3);
- Six-days sequence for the climate of Zurich with 16 m^2 of collector (5.4);
- Six-days sequence for the climate of Gdansk with 16 m^2 of collector (5.5);
- Six-days sequence for the climate of Rome with 8 m^2 of collector (5.6).

The usual outcome of the test is the system's total consumption needed to satisfy a fixed load. From this, the performance factor is easily defined and presented to the end consumer. For example, for the heat pump, the performance is represented by the seasonal coefficient of performance (SCOP) or for a solar and heat pump system is represented by the seasonal performance factor (SPF). In the present study, the system performance is analyzed considering different aspects: the consumption of each load (not only the total), the collector yield and the efficiency, the heat pump efficiency, the storages temperatures and so on.

Each section is divided into two parts: a "sequence result" which presents the performance of the system studied with the test sequence and presents a comparison of the performances assessed with laboratory measurement and with a sequence simulation. The second part "annual extrapolation" presents the extrapolation of seasonal performance from the sequence; this part compares the extrapolation from the test measurement, the extrapolation from a sequence simulation and the result obtained from an annual simulation. The first part allows to show the differences between the experimental observation and the simulation of the sequence. The second part allows to evaluate the representativeness of the sequence compared to the entire year.

5.1 Six-days sequence of Bolzano - collector area of 16 m^2

The first sequence is defined with a 2D clustering approach selecting six-days in the climate of Bolzano. The outcome days are respectively the days N° 87, 163, 250, 253, 316 and 327 of the TRY. The system has 16 m^2 of solar collectors and the load is defined with the building described previously.

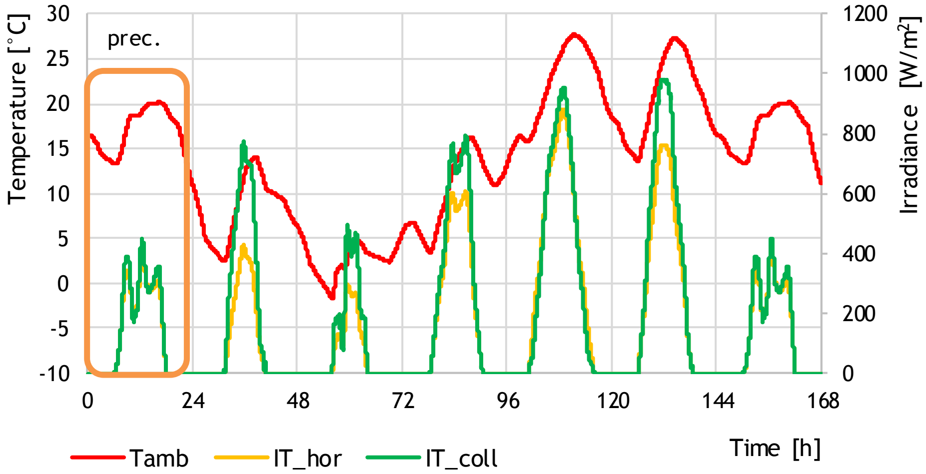

Figure 5-1: Profiles of the ambient temperature and irradiances on horizontal and collector surface during the six-days sequence of Bolzano.

Figure 5-1 shows the profiles of the ambient temperature (primary vertical axis), global horizontal irradiance and total irradiance on the collector surface (secondary vertical axis) during the short test sequence. The sequence starts after a preconditioning day which aim is to reach reasonable temperature levels in the storage; the last day of the sequence is used as a preconditioning day (as indicated with the orange box). Figure 5-2 shows the instantaneous space heating $(\dot{Q}_{SH})$ and cooling $(\dot{Q}_{SC})$ loads adopted during the short test sequence. The loads consider the two floors of the building (ground floor "gf" and first floor "1f"). The first three days have a heating load, day 4 and day 5 require a cooling load while the last day (that is also the preconditioning day) does not present any load.

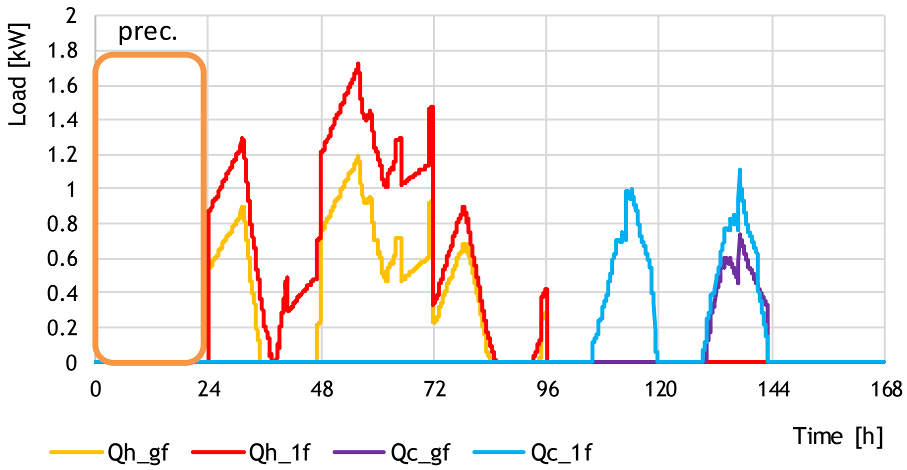

Figure 5-2: Building load profiles during the six-days sequence of Bolzano.

For each test sequence, the same DHW draw off profile is adopted for each day. This is showed in Figure 5-3. The correspondent amount of energy that must be provided is about 11 kWh for each day (where 7 kWh are considered as useful energy - delivered at 40 °C as defined from the test method).

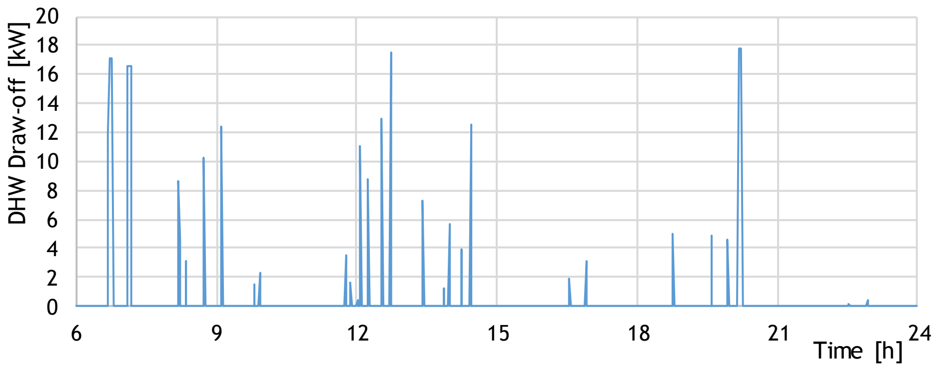

Figure 5-3: DHW draw off profile adopted for each test day of the sequence.

5.1.1 Sequence results

The test results are compared to those obtained with a numerical simulation of the system. These results are presented in the following section. Then, an annual simulation is compared with the direct extrapolation of energy in the next section.

Figure 5-4 shows the daily electrical consumption of the system evaluated with the test and simulation. The high consumption in the day 2 can be explained by the climatic conditions (Figure 5-1) and the load (Figure 5-2 and Figure 5-5). This is the coldest day with very low irradiation and therefore it is the day with the highest load. The consequence is that the system (mainly the heat pump) has to satisfy a high load with lower coefficient of performance than other days. In the figure, it can be seen that the electrical energy differs at maximum about 2 kWh with the exception of day 4 that presents a higher difference. The reason can be identified because of an inconsistence between test and simulation in the space cooling that can be explained with the Figure 5-5.

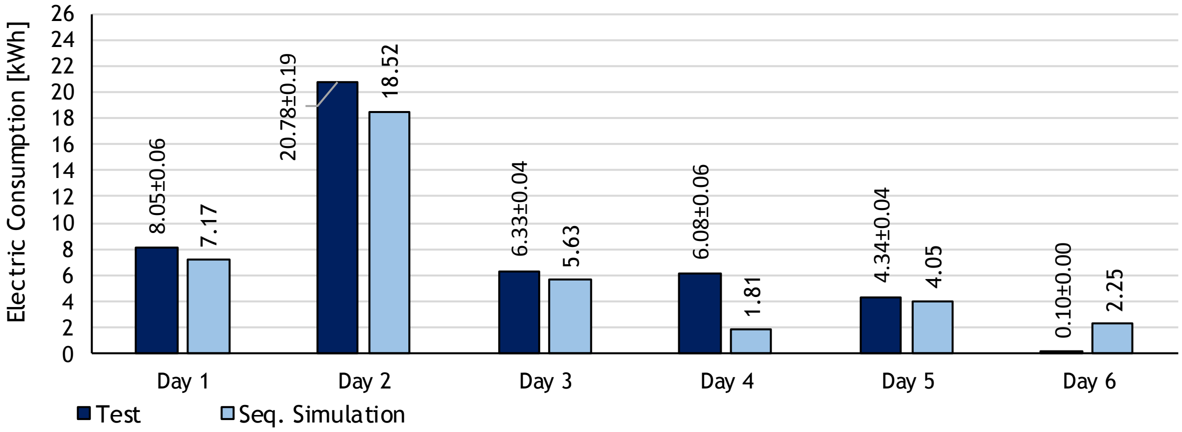

Figure 5-4: Daily total electric consumptions defined with test measurement and sequence simulation. Six-days sequence of Bolzano.

Figure 5-5 presents the space heating and space cooling loads and the consumption divided for the different days of test. In the first three days the load file requires heating load, during day 4 and day 5 it requires cooling load and in the last day it does not require any space load. In the figure, it is possible to see that the cooling load is distributed differently between test and simulation. The inertia of distribution system in the simulation is higher to the one modelled in the emulation: the effect is that during the simulation the load required during the day 4 it is satisfied partially in this day and partially during day 5. At the same time, the load of day 5 in partially satisfied during day 6. Instead, during the test, the load is satisfied during the day which is required: if this does not happen the annual consumption extrapolated from test results through Equation 4-6 will be less accurate.

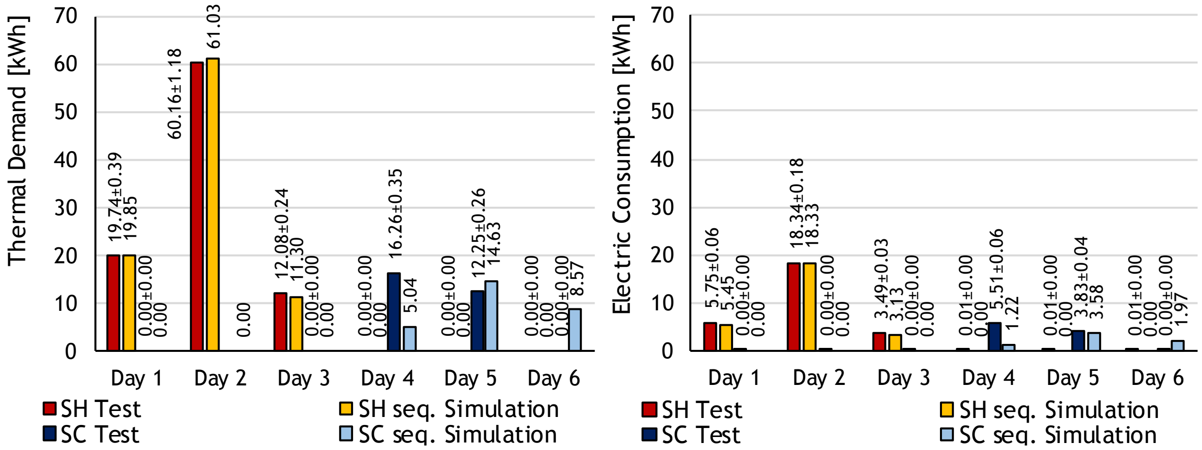

Figure 5-5: Daily SH/SC loads and SH/SC electric consumptions defined with test measurement and sequence simulation. Six-days sequence of Bolzano.

Figure 5-6 shows the domestic hot water load and its electrical consumption. These values are closed to the simulation during all days. The DHW draw-off is controlled differently from the space heating and cooling load as presented in the procedure. The consumption is different between test and simulation since the contribution of solar is different as presented later with Figure 5-10.

Figure 5-7 shows the DHW extraction counting of time and energy extracted, discretized by four temperature ranges. The figure presents a daily average condition. It is possible to see that the delivery temperature is below 40°C for a large time (about 0.81 h compared to the 0.45 h of "useful energy"). In terms of energy extracted, 7 kWh/day is delivered at 40 °C (useful energy) and only 4 kWh/day is delivered at lower temperature as a pre extraction (non-useful energy). The value of 4 kWh of not useful energy is the same values hypothesized with the "constant energy" draw off of paragraph 3.5.2.

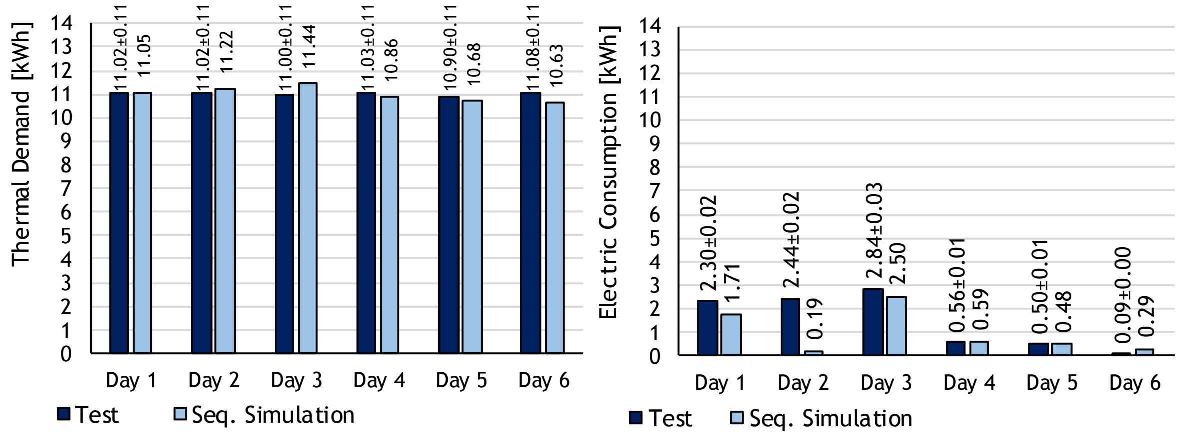

Figure 5-6: Daily DHW loads and DHW electric consumptions defined with test measurement and sequence simulation. Six-days sequence of Bolzano.

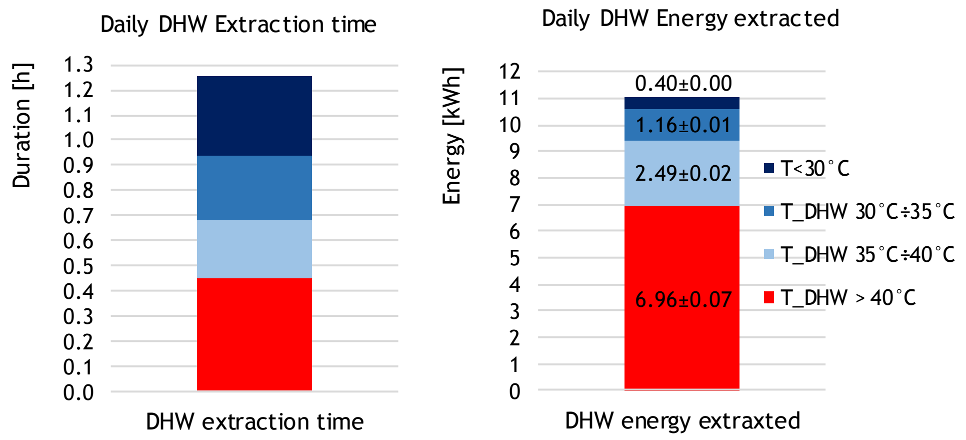

Figure 5-7: Domestic hot water extraction time and energy extracted. Six-days sequence of Bolzano.

From the loads and the electric consumption, the performance factors can be calculated; in the Figure 5-8 the performance factors are distinguished for the different load while Figure 5-9 shows the total SPF. During different days, the performance factors are not defined for the loads which are not covered for that days. In Figure 5-9, the difference between day 4 and day 6 is explained by the redistribution of the space cooling load shown above. The sequence SPF evaluated with the test is 4.1 while with the simulation is 4.5. The SPF is higher when the contribution of the solar source to the load is higher. The daily SPF depends from the fraction of SH, SC and DHW loads respect the total load and from which sources satisfy these loads. The DHW load is satisfied mainly from solar and therefore during the day 6, the SPF reach the maximum value (in the test).

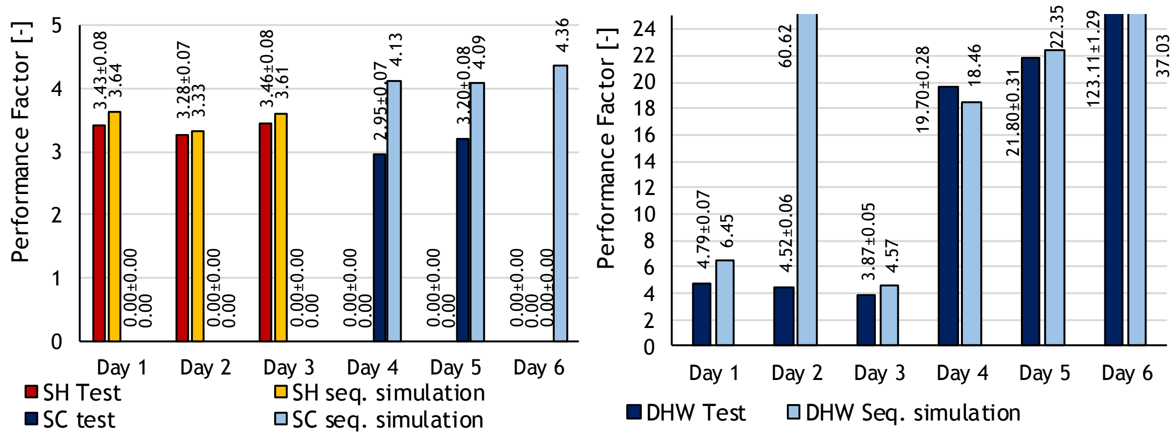

Figure 5-8: Daily performance factors defined with test measurement and sequence simulation. Six-days sequence of Bolzano.

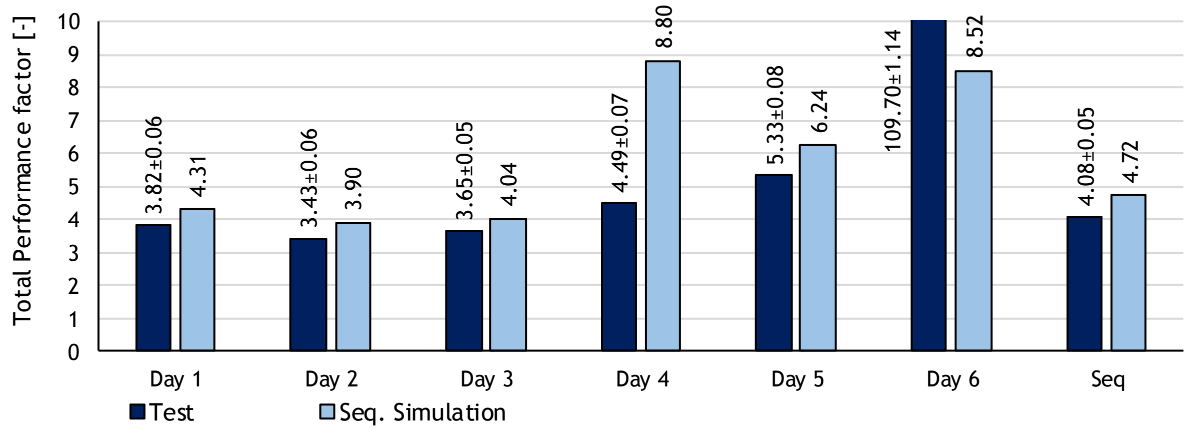

Figure 5-9: Daily total performance factors defined with test measurement and sequence simulation. Six-days sequence of Bolzano.

Regarding the solar collector energy, it is possible to see in Figure 5-10 that the simulation collects more energy compared to the emulated during the test. The difference is about 49 kWh for the whole sequence (simulation 239.5 and emulated 190.5). This difference is mainly due to the day 2 and day 6 of the sequence. During these two days, the different behaviour can be analysed considering the activation of the scheme of the collector; in the simulation the collector is activated more often since the temperature at the inlet is higher than the one measured. The simulation does not consider well the transient of temperature obtained during the activation of the collector scheme.

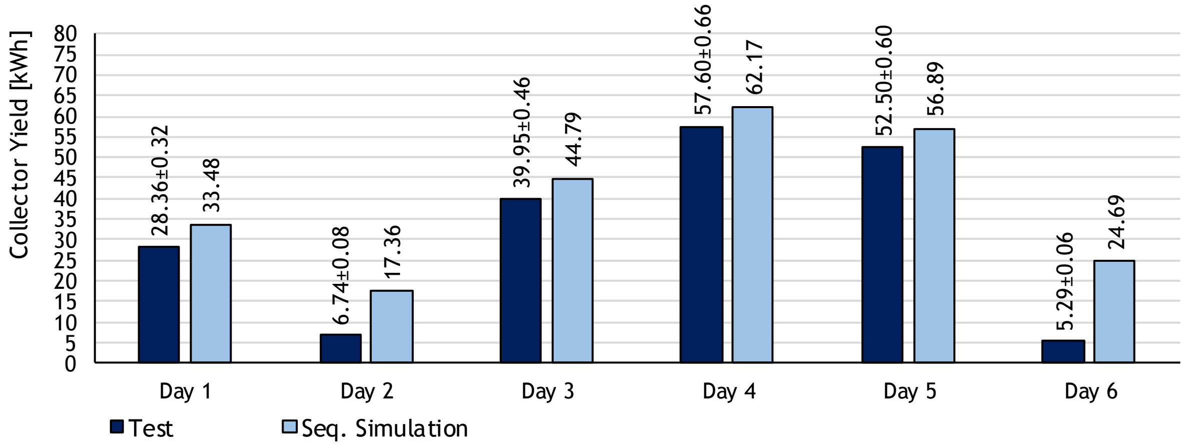

Figure 5-10: Daily collector yield defined with test measurement and sequence simulation. Six-days sequence of Bolzano.

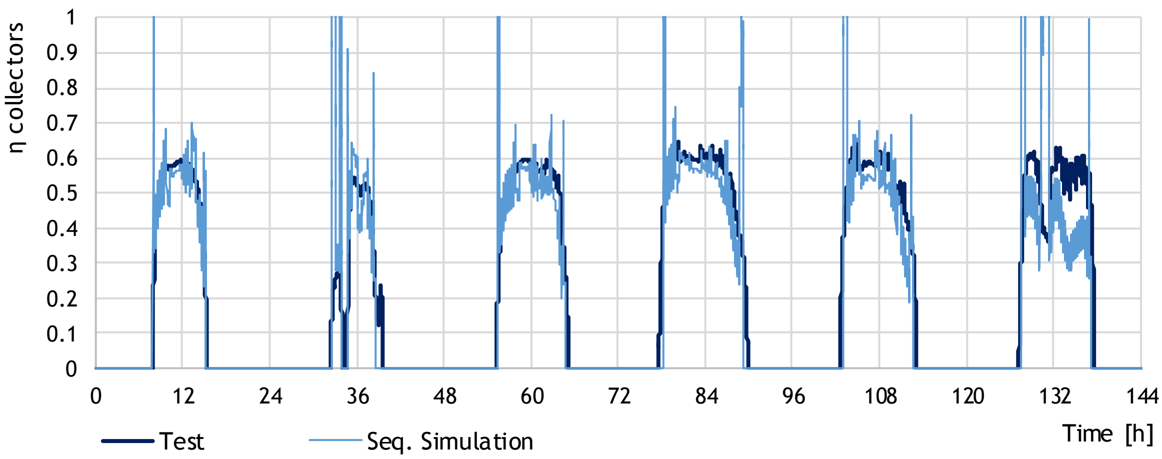

Figure 5-11: Solar collector efficiency emulated during the test and defined with the sequence simulation. Six-days sequence of Bolzano.

Figure 5-11 shows the collector efficiency during the whole sequence. The test and simulations have almost the same efficiency. More in detail, in Figure 5-12 there are the frequency distribution and cumulated distribution of solar collector efficiency. The graph considers the six-days sequence. In the test there is a peak of efficiency at the point $\eta = 0.6$. The simulation has similar behaviour compared to test.

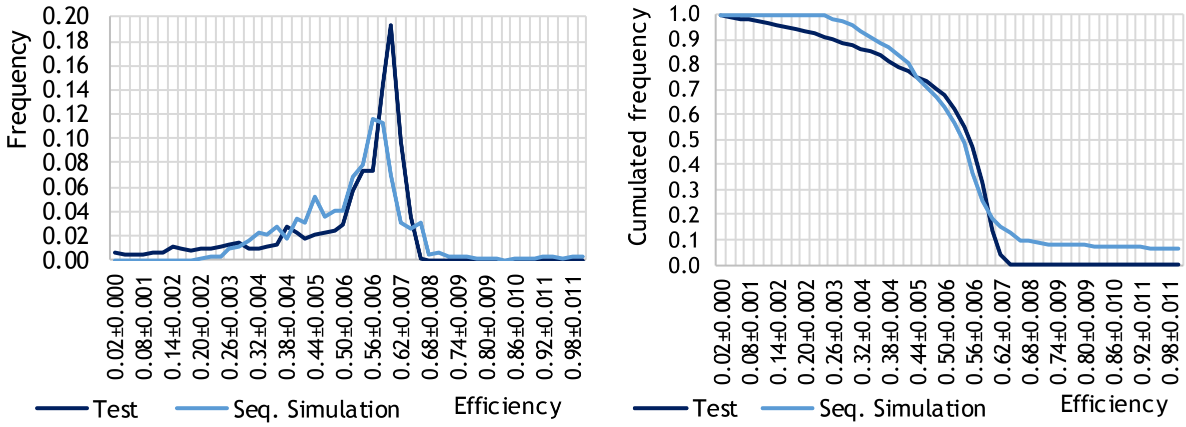

Figure 5-12: Solar collector efficiency distribution defined with test measurement and sequence simulation. Six-days sequence of Bolzano.

Figure 5-13 shows the energy exchanged with the dry cooler distinguishing between the working mode (as air source or air sink). The total amount of energy exchanged by dry cooler during the test is almost the same of the simulated one. The differences during the distribution during the days visible in the second graph are explained by the redistribution of space cooling loads as explained above.

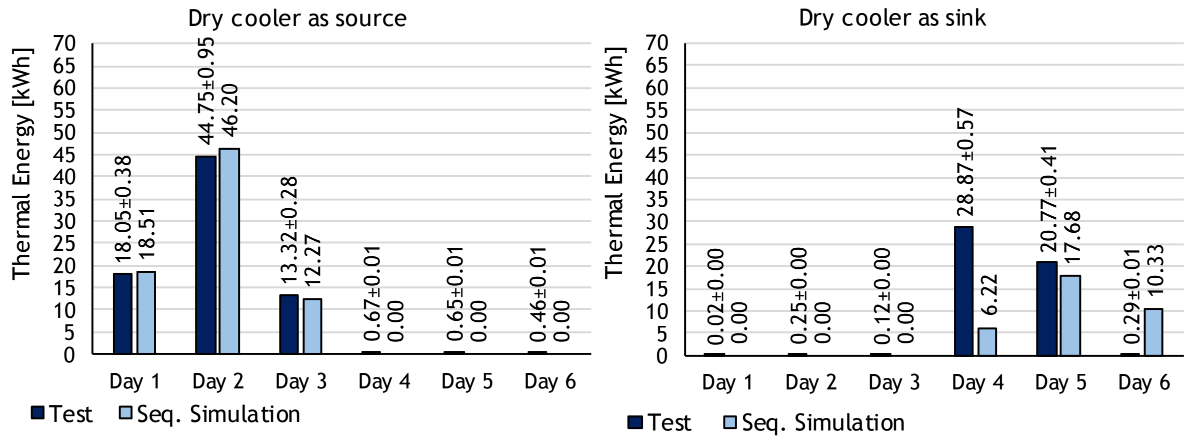

Figure 5-13: Daily dry-cooler energies defined with test measurement and sequence simulation. Six-days sequence of Bolzano.

Figure 5-14 shows the heat pump efficiency for the space cooling (EER), space heating and for domestic hot water (COP) for both simulation and test. It is possible to see that there is not simultaneity activation of the heat pump between test and simulation. The duration of each activation of heat pump during space cooling is also different. This effect can be seen in Figure 5-15 that shows a zoom of Figure 5-14 during the fourth day. In the test, the heat pump is activated 30 times for the space cooling scheme while in the simulation only five times. This behaviour is explained for the lower inertia of the distribution system and the heat pump size (that is oversized). The first cause (low inertia of distribution system) is a lack of the test method while the second one (size of heat pump) is a lack of the tested system. With those two conditions, the inlet temperature of distribution system decrease over the limit of minimum temperature foreseen for the radiant panels (14°C) requiring the deactivation of the system. In the emulation, the distribution system continues to work if there is load request and therefore the temperature increases. When it reaches 21°C, the control system reactivates the system in order to continue providing cooling. This cycling activation continues until the load request is satisfied.

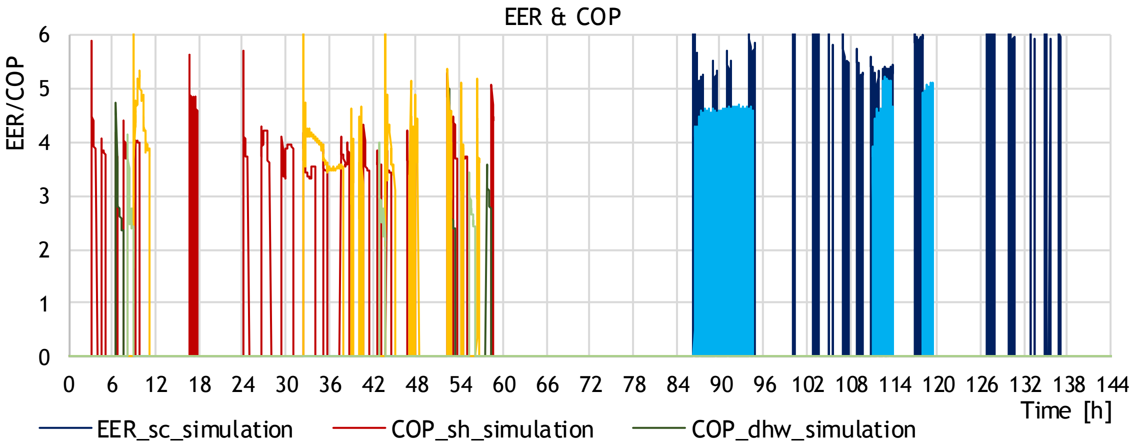

Figure 5-14: COP/EER measured during the test and defined with the sequence simulation. Six-days sequence of Bolzano.

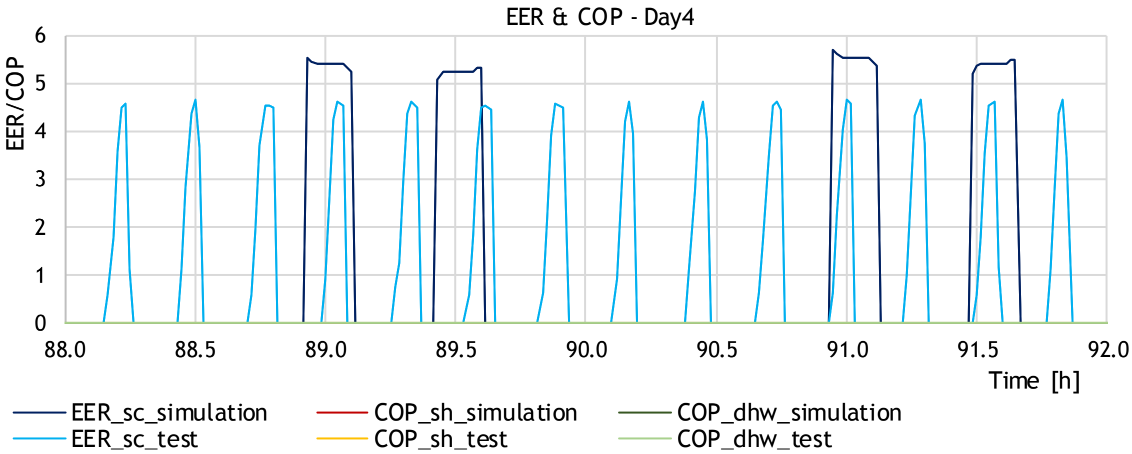

Figure 5-15: COP/EER during four hours in the fourth day measured during the test and defined with the sequence simulation. Six-days sequence of Bolzano.

The consequence of this iterative steps is visible in the distribution of the EER in Figure 5-16. The test has a lower peak of efficiency in space cooling. There is a second peak in the point $EER = 0.5$ this is caused by the transients. The simulation does not present this effect for two reasons: the transients are not considered in the model and there are less and longer activations allowing to get near to stationary working conditions.

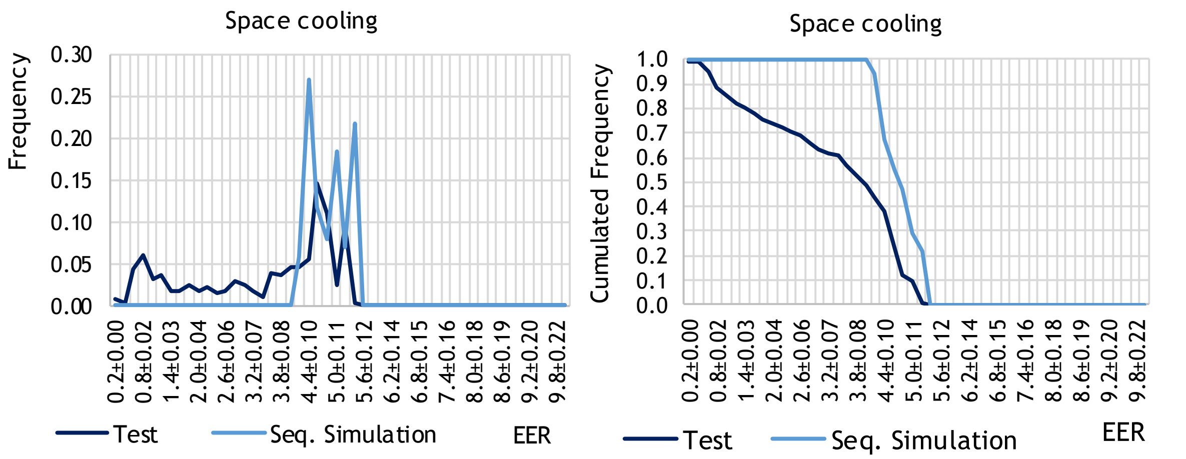

Figure 5-16: EER distribution defined with test measurement and sequence simulation. Six-days sequence of Bolzano.

Looking the other loads Space Heating and Domestic hot water (Figure 5-17), the frequency analysis shows a good correlation between test and simulation.

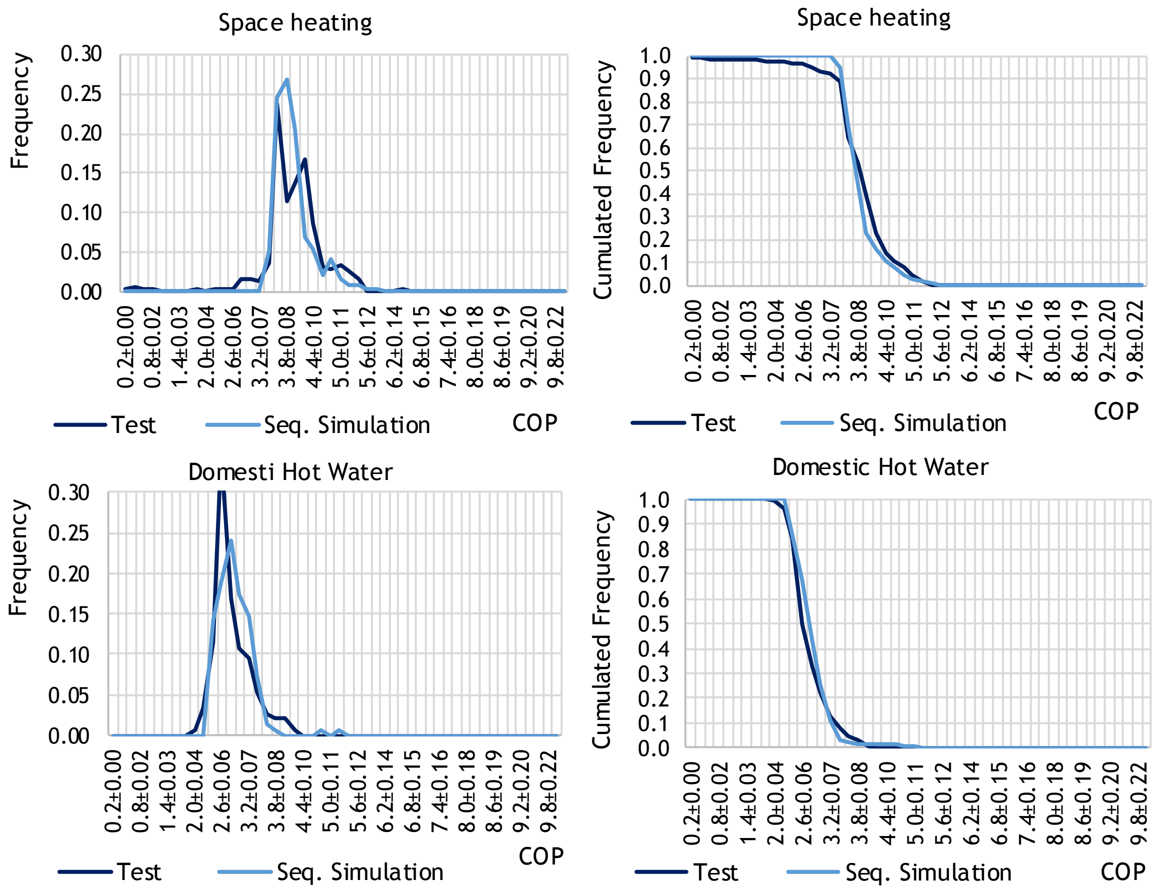

Figure 5-17: COP distribution defined with test measurement and sequence simulation. Six-days sequence of Bolzano.

Continuing the analysis of the system, the following two figures compare the storages temperatures measured in the test and simulated. This comparison is useful to validate the simulation model and explain some unexpected behaviours. Looking the big storage (Figure 5-18), it is possible to see that the temperature development is divergent during the different days. This difference is given by the different energy collected by the solar collector. The stratification trend is quite similar ad exception of the temperature at the top of the storage when the collector is activated. The same effect is visible also in the small storage (Figure 5-19) when the heat pump is activated.

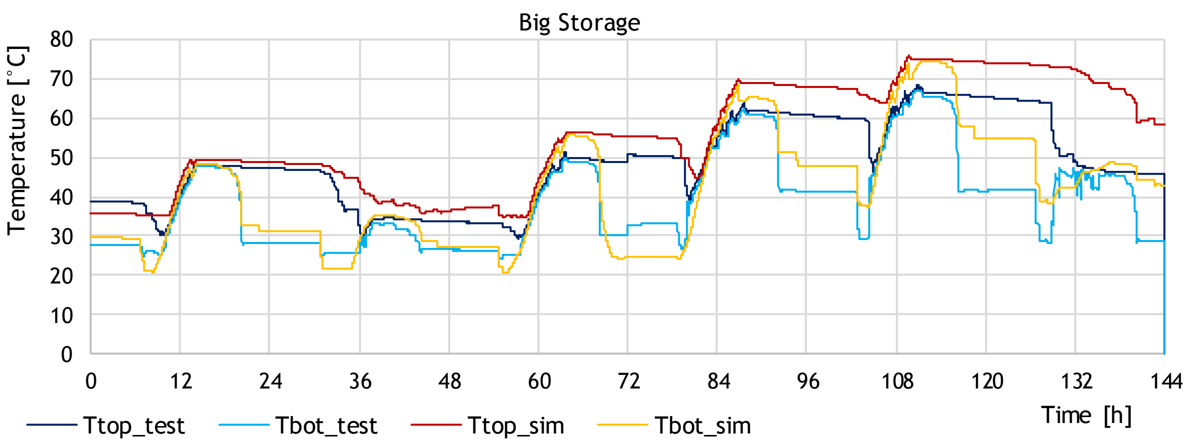

Figure 5-18: Big storage temperatures measured during the test and defined with the sequence simulation. Six-days sequence of Bolzano.

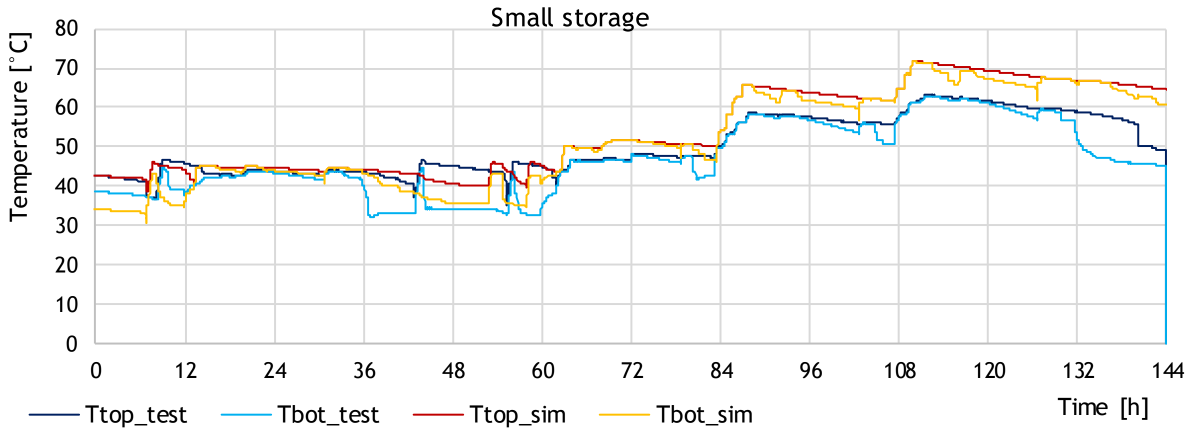

Figure 5-19: Small storage temperatures measured during the test and defined with the sequence simulation. Six-days sequence of Bolzano.

Looking in detail the Figure 5-20, it is possible to see an inefficient behaviour during the storage charge: there is a consistent storage destratification (green arrows) caused by the in the initial phase of the storage charge with the heat pump. When this scheme is activated, before the reaching the heat pump steady state conditions, a mass flow colder than the water at the top is recirculated inside the small storage. This mixing causes the top storage temperature falls. This inefficient behaviour suggests to include a stratification separator in the small storage for improve the system performance.

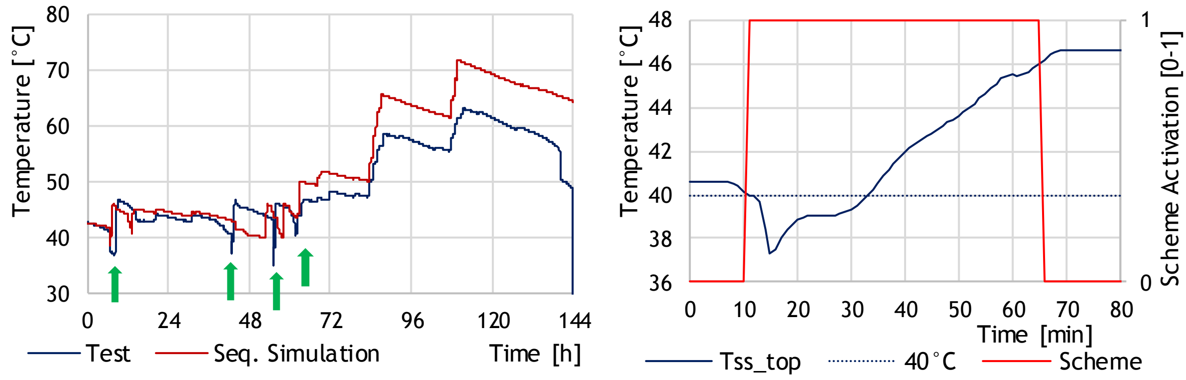

Figure 5-20: Destratification in the small storage. Six-days sequence of Bolzano.

Figure 5-21 presents the activation time of each scheme, measured in the test and in simulation.

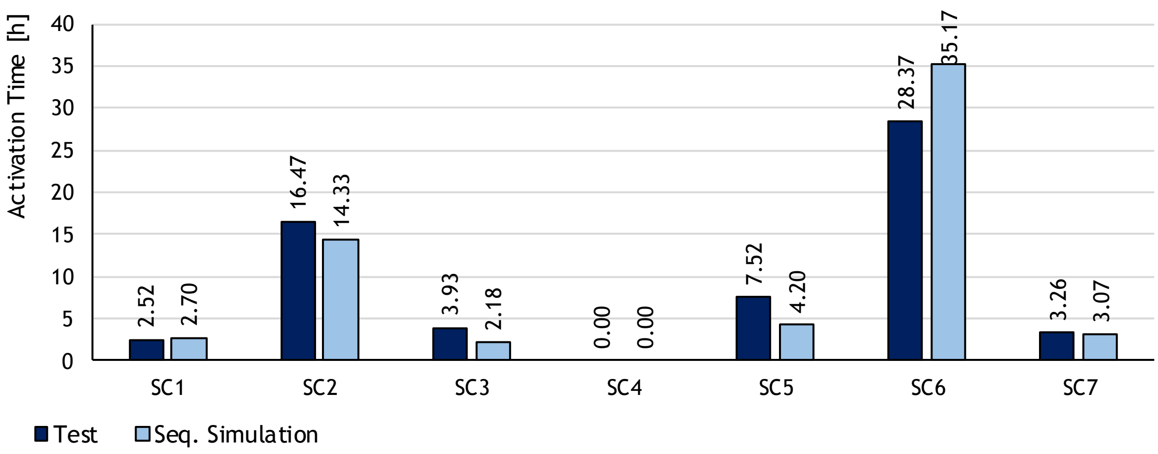

Figure 5-21: Duration of scheme activation defined with test measurement and sequence simulation. Six-days sequence of Bolzano.

The schemes are shown in the Appendix C in the chapter "Solar Assisted Heat Pump System". "SC1" scheme of space cooling, "SC2" scheme of space heating with heat pump, "SC3" scheme of small storage charge with heat *pump, "SC4" scheme of space heating with solar energy, "SC5" scheme of DHW extraction, "SC6" scheme for the activation of the solar collector, "SC7" scheme for the heat transfer from big storage to small storage.*

The little differences between test and simulation in the schemes of space cooling with heat pump is caused by the latency of heat pump. The heat pump in the test reach the stationary condition after a small time lapse. In this period, the scheme is active but there is a lower heat transfer. The difference of activation of solar collector is due to the different behaviour highlighted during the days 2 and 6 as previously described. The difference of activation' duration of DHW extraction is due to the control of laboratory. In the circuit of the laboratory there is a counter of energy. If the return temperature is higher or lower to the set point the scheme is deactivated later or before the foreseen to obtain the fixed energy extraction.

5.1.2 Annual extrapolation

The goal of the procedure is not only to find the performance of the sequence, but also evaluate the performance of the year. This is done weighing the daily energy with the cluster size as indicated in the chapter 4.3.

In this case the sizes of clusters are show in Table 5-1. For find the annual energy balances, just multiply the daily loads and consumptions with the respective cluster size. Subsequently the performance figures are calculated trough the ratio between the total load and the total electrical consumption. In Table 5-1, there are shown the annual thermal and electrical energies of DHW, SH and SC. The table contains also the annual collector yield. Figure 5-22 and Figure 5-23 show graphically the table results, it is possible to see that the simulation and the test are similar, with differences on the collector yield and on the loads.

Table 5-1: Cluster energies evaluation. Six-days sequence of Bolzano.

	Cluster 1	Cluster 2	Cluster 3	Cluster 4	Cluster 5	Cluster 6	Test	Annual Simulation
Size	65	93	36	35	75	61	-	-
Q_{DHW} [kWh]	716.3	1024.9	396.0	386.1	817.5	675.9	4017±40	3754
W_{DHW} [kWh]	149.5	226.9	102.2	19.6	37.5	5.5	541±5	598
Q_{SH} [kWh]	1283.1	5594.9	434.9	0.0	0.0	0.0	7313±143	8363
W_{SH} [kWh]	373.8	1705.6	125.6	0.0	0.0	0.0	2207±22	2272
Q_{SC} [kWh]	0.0	0.0	0.0	569.1	918.8	0.0	1488±32	1865
W_{SC} [kWh]	0.0	0.0	0.0	192.9	287.3	0.0	480±5	450
Q_{coll} [kWh]	1843.4	626.8	1438.2	2016.0	3937.5	322.7	10185±116	11849

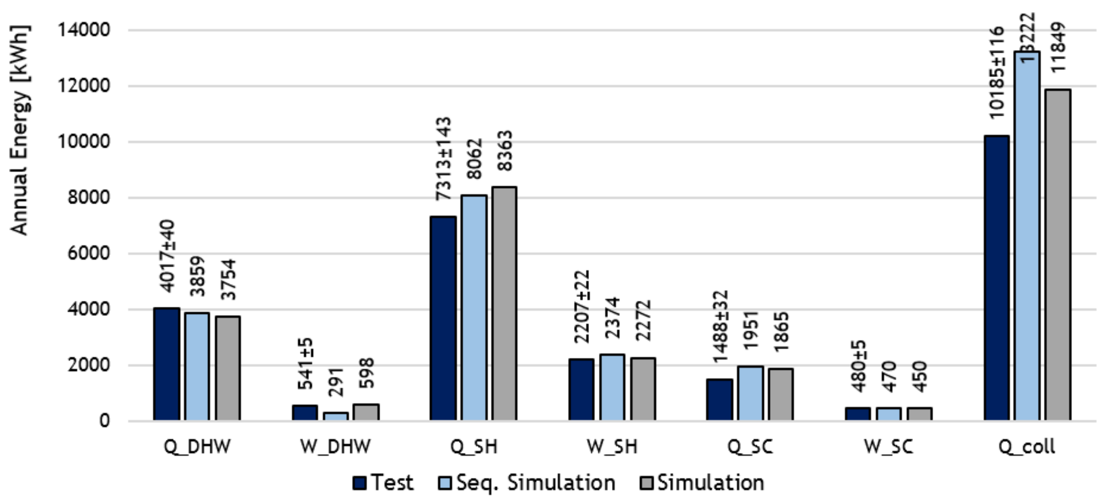

Figure 5-22: Seasonal energies extrapolated from test measurement, extrapolated from sequence simulation and defined with annual simulation. Six-days sequence of Bolzano.

Figure 5-23 shows the seasonal performance factors and the solar fractions obtained with the extrapolation of test results, with the extrapolation from the sequence simulated and with the annual simulation. The largest difference is visible for the DHW, where the SPF and the SF of the sequence simulation is higher than the annual simulation and the test. For the other performance figures, the two simulations agree while the test presents lower performances. The correspondence between the sequence simulation and the annual simulation confirms the validity of the clustering approach to create the test sequence.

The total SPF obtained with the test is 3.97 while with sequence simulation is 4.43 and annual simulation is 4.21. About the solar fraction, the sequence does not presents heating solar fraction in both test and simulation while in the annual simulation is the 5 %. The sequence simulation and the annual simulation find the same total solar fraction that is 0.27. This result is similar to the one calculated from the test (0.26).

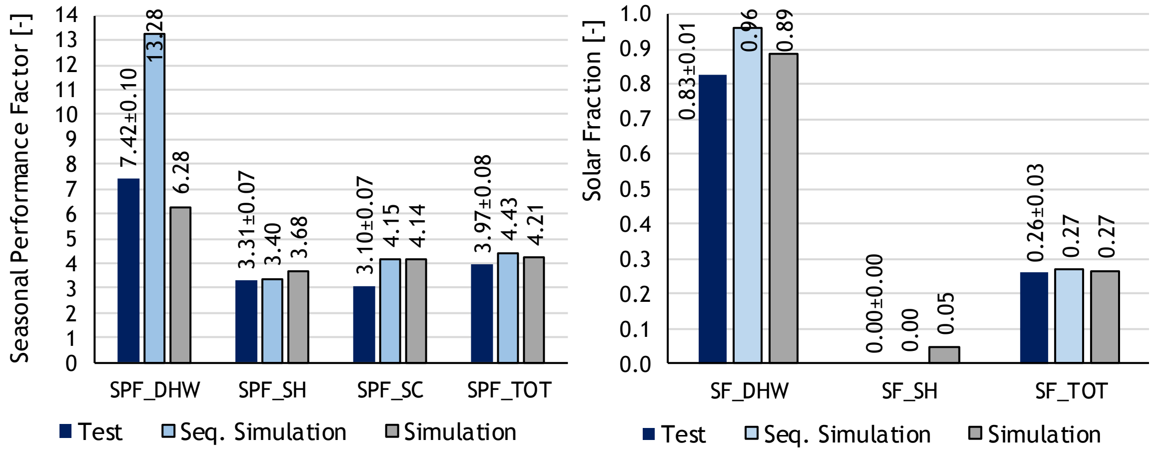

Figure 5-23: Seasonal performance factors and solar fractions extrapolated from test measurement, extrapolated from sequence simulation and defined with annual simulation. Six-days sequence of Bolzano.

More in detail, the distribution figures presented in the "sequence results" section is completed with the comparison of distribution obtained in the annual simulation.

Figure 5-24 includes the distribution of collector efficiency through the whole year. The distribution of the annual simulation is closed to the distribution of the sequence simulation, confirming again the correct representation of the sequence.

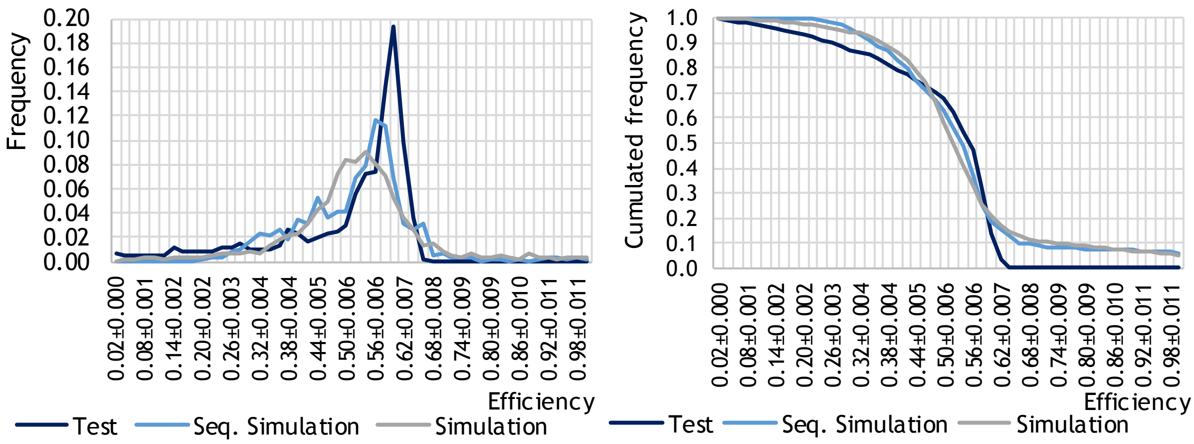

Figure 5-24: Solar collector efficiency distributions defined with test measurement, sequence simulation and annual simulation. Six-days sequence of Bolzano.

Figure 5-25 presents the comparison of EER and COP distributions obtained from the test, the sequence simulation and the annual simulation. The EER' distributions of the two simulations are more closed to each other than the distribution obtained from the test measurements. Both simulation disregard the EER due to the transients while the test considers their effect.

Also for the COP during the space heating and the domestic hot water preparation, the test identifies a distribution at low values for the transients but their influence is lower since the heat pump is activated for longer time.

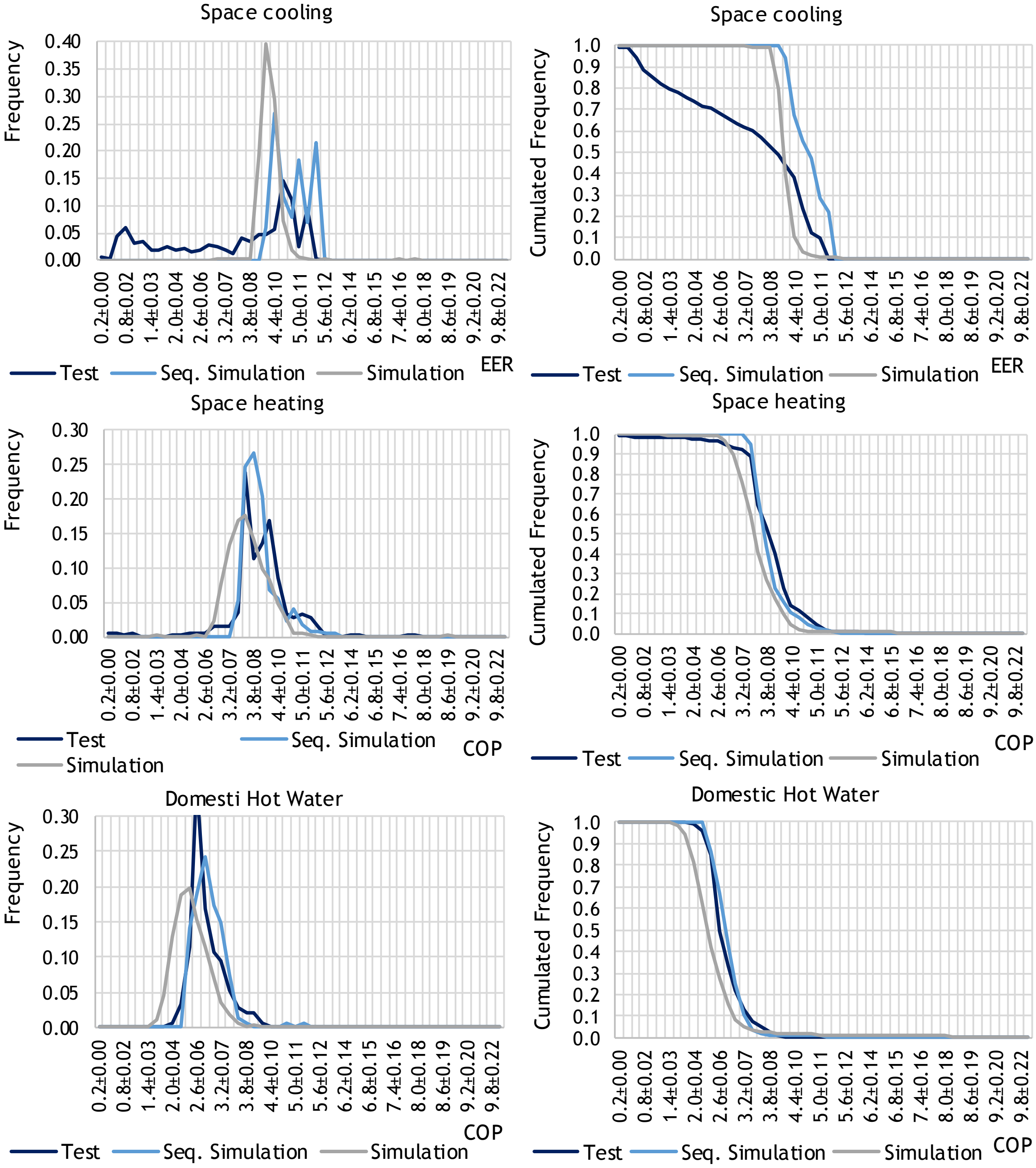

Figure 5-25: EER and COP distributions defined with test measurement, sequence simulation and annual simulation. Six-days sequence of Bolzano.

5.2 Ten-days sequence of Bolzano - collector area of 16m^2

The results presented in this chapter consider a sequence of ten-days instead of six-days as the previous one. The control parameters, the system layout, load and so on do not change. The expectation is a higher accuracy of results since the cluster are more distributed in the annual values.

Figure 5-26 and Figure 5-27 show the test boundary conditions; the first four days regard the heating season, then, one day do not present any heating or cooling load, the next three days present a cooling load while the two day are positioned in the mid-season without space load. Both Figure 5-26 and Figure 5-27 display that all days are different among themselves.

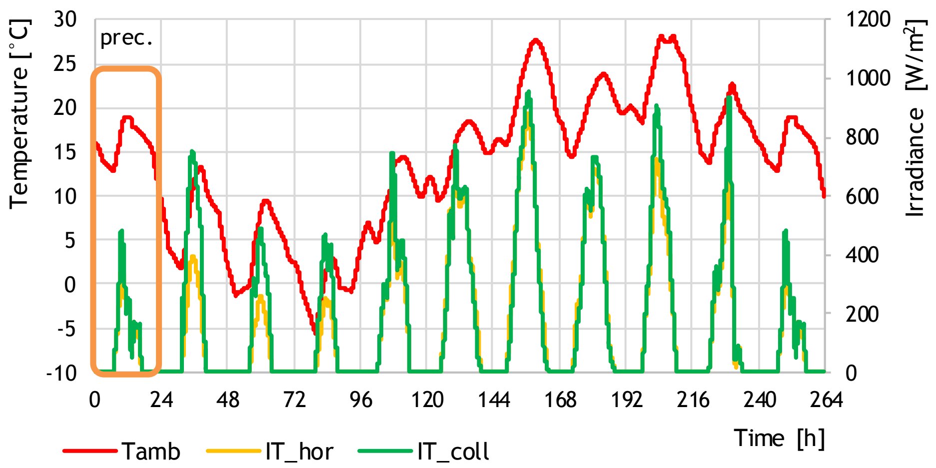

Figure 5-26: Profiles of the ambient temperature and irradiances on horizontal and collector surface during the ten-days sequence of Bolzano.

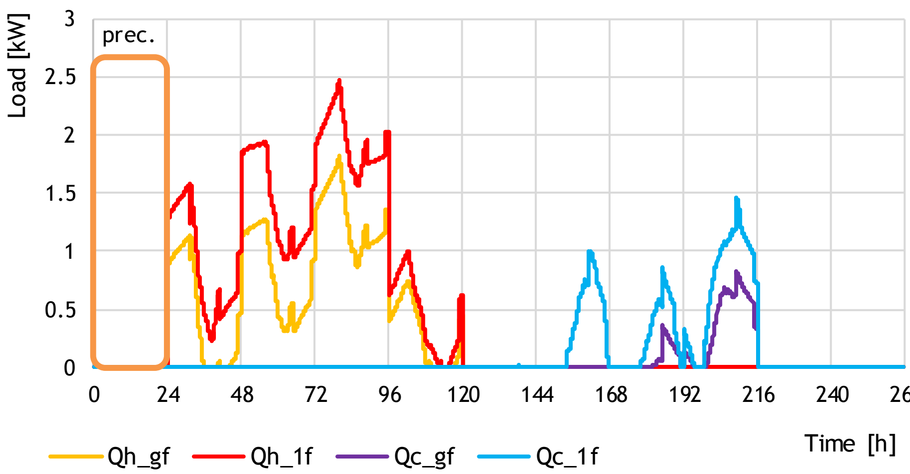

Figure 5-27: Building load profiles during the ten-days sequence of Bolzano.

5.2.1 Sequence results

Regarding the electric consumption in Figure 5-28, the test and the simulation get a deviation similar to the previous case. The simulation considers a lower energy consumption during the different days about 2 kWh/day. As it was seen in the other test, there is a redistribution of space cooling delivered energy.

Figure 5-29 shows the daily domestic hot water loads and consumptions. The loads extracted are similar since the load file is fixed for both; the consumption is different during the different days. The highest deviation is during the day 2: the simulation calculates a low consumption of 0.24 kWh while the electric consumption measured in the test is about 4 kWh. This difference is due to the different solar contribution as it can be seen in the next figures. Again, this behaviour was already identified in the previous test.

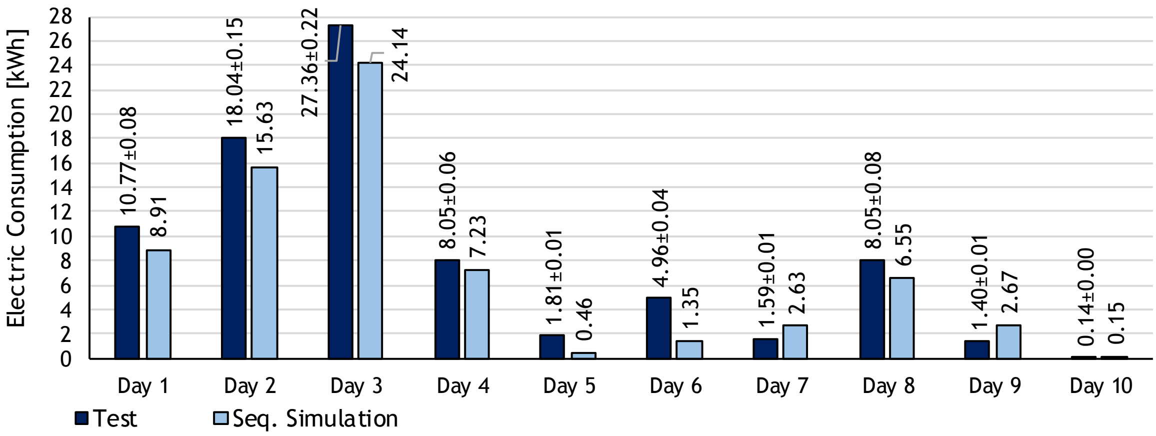

Figure 5-28: Daily total electric consumptions defined with test measurement and sequence simulation. Ten-days sequence of Bolzano.

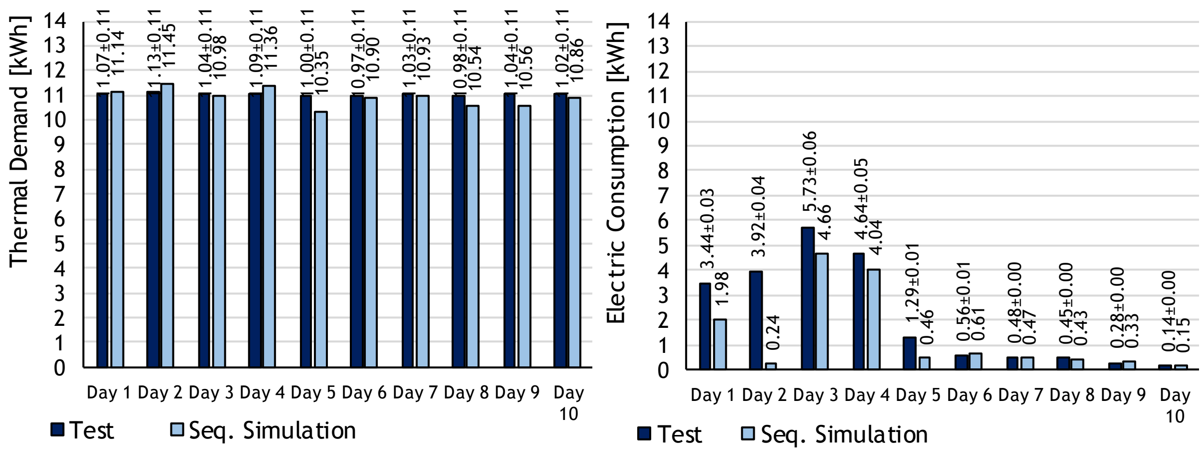

Figure 5-29: Daily DHW loads and DHW electric consumptions defined with test measurement and sequence simulation. Ten-days sequence of Bolzano.

Moving to the space loads, Figure 5-30 shows the load and electric consumption for the heating and cooling loads; again the cooling load is redistributed as motivated in the previous chapter.

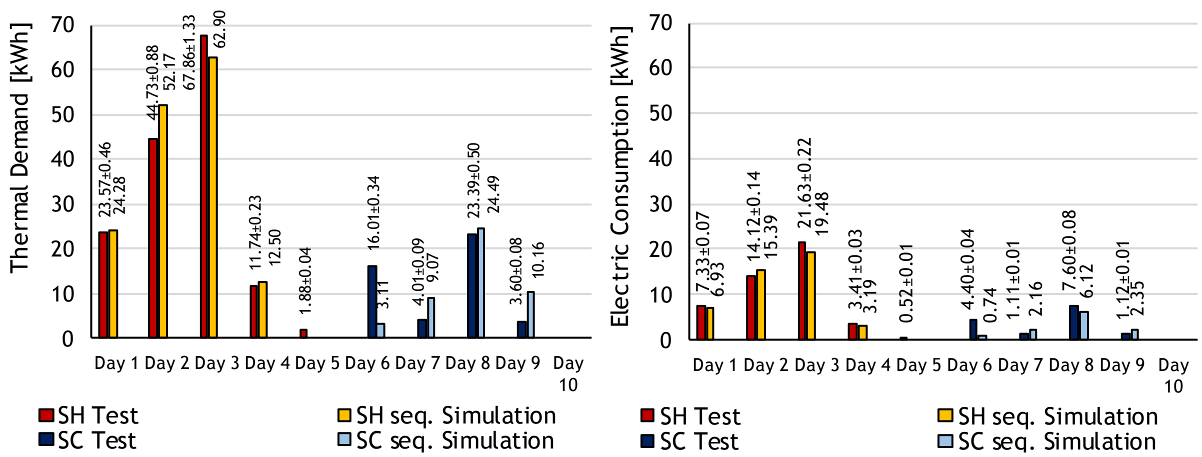

Figure 5-30: Daily SH/SC loads and SH/SC electric consumptions defined with test measurement and sequence simulation. Ten-days sequence of Bolzano.

Figure 5-31 mirrors the figures just explained; the highest deviation are presented in the days where the space cooling load is redistributed. The simulation identifies high values of performance factor also in the days where the domestic hot water is the major load and it is satisfied mainly from the solar source; these days are day 5, day 6 and day 10.

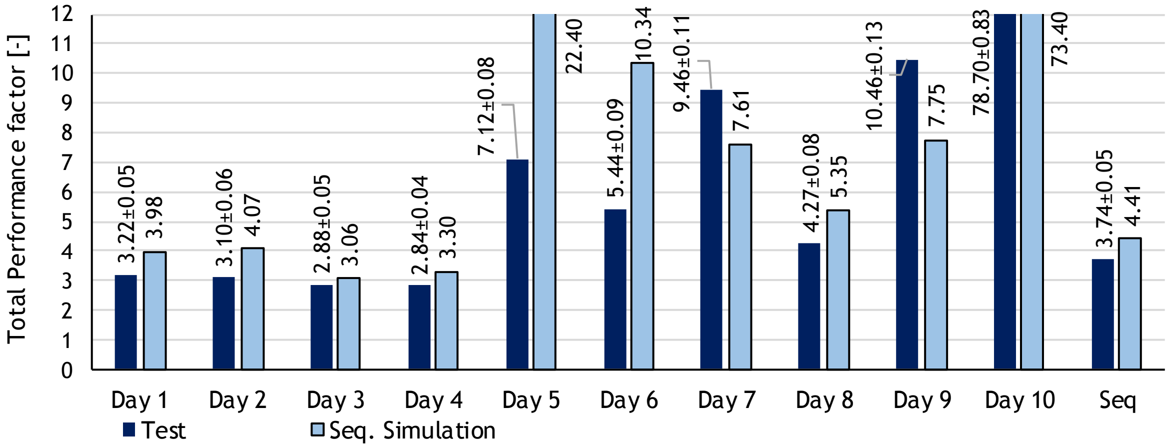

Figure 5-31: Daily total performance factors defined with test measurement and sequence simulation. Ten-days sequence of Bolzano.

The Figure 5-32 compares the collector yield of the test and the simulated one. During the test, the energy collected is about 292 kWh while in the simulation is about 357 kWh. The higher differences are visible during days with low irradiation as resulted in the previous test.

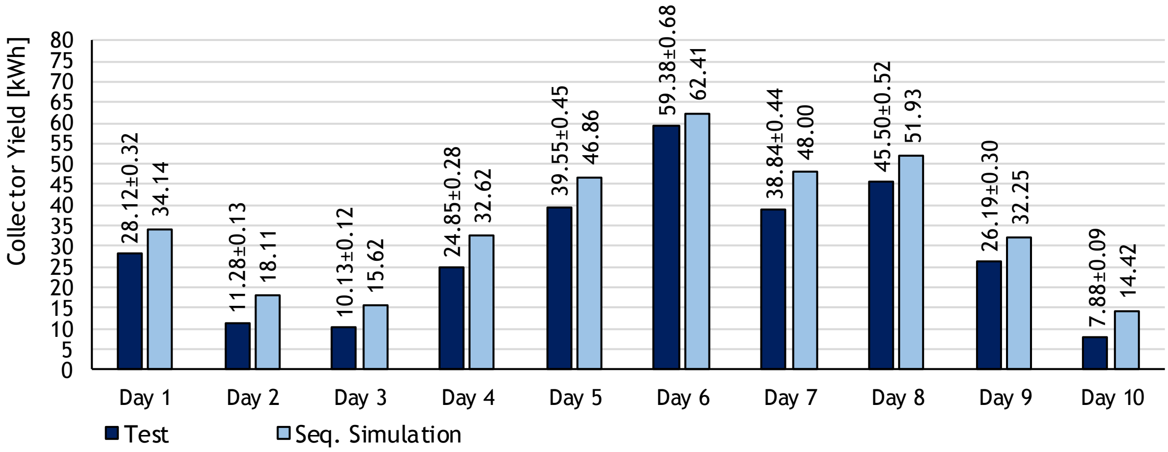

Figure 5-32: Daily collector yield defined with test measurement and sequence simulation. Ten-days sequence of Bolzano.

The outcome from the analysis of the ten-days sequence gives the same considerations of the six-days sequence. The same differences between test and sequence simulation are present in the redistribution of cooling load and the collector yield.

5.2.2 Annual extrapolation

Table 5-2 shows the cluster's sizes and the energies associated to each cluster in terms of loads, consumptions and collector yield. The table is completed by the Figure 5-33 that shows the comparison of the annual energies calculated from test, sequence simulation and annual simulation. During the test, the heating and cooling loads are lower than the simulated one due to a problem in the energy counter of space heating/cooling emulation.

Figure 5-34 shows the seasonal performance factor and the solar fraction for different load calculated with the ten-days test, the sequence simulation and the annual simulation. Again, the sequence simulation and the annual simulation have similar results while the test measures lower seasonal performance factors. The total solar fraction is the performance figure that mostly agrees among the three different calculations.

Table 5-2: Cluster energies evaluation. Ten-days sequence of Bolzano.

	Cl. 1	Cl. 2	Cl. 3	Cl. 4	Cl. 5	Cl. 6	Cl. 7	Cl. 8	Cl. 9	Cl. 10	Test	Annual Simulation
Size	46	54	39	45	26	31	29	30	41	24	-	-
Q_{DHW} [kWh]	509	601	431	499	286	340	320	329	453	264	4032±40	3754
W_{DHW} [kWh]	158	212	223	209	34	17	14	14	11	3	895±9	598
Q_{SH} [kWh]	1084	2415	2647	528	49	0	0	0	0	0	6723±132	8363
W_{SH} [kWh]	337	762	844	153	14	0	0	0	0	0	2110±21	2272
Q_{SC} [kWh]	0	0	0	0	0	496	116	702	148	0	1462±31	1865
W_{SC} [kWh]	0	0	0	0	0	136	32	228	46	0	443±4	450
Q_{coll} [kWh]	1294	609	395	1118	1028	1841	1126	1365	1074	189	10039±114	11849

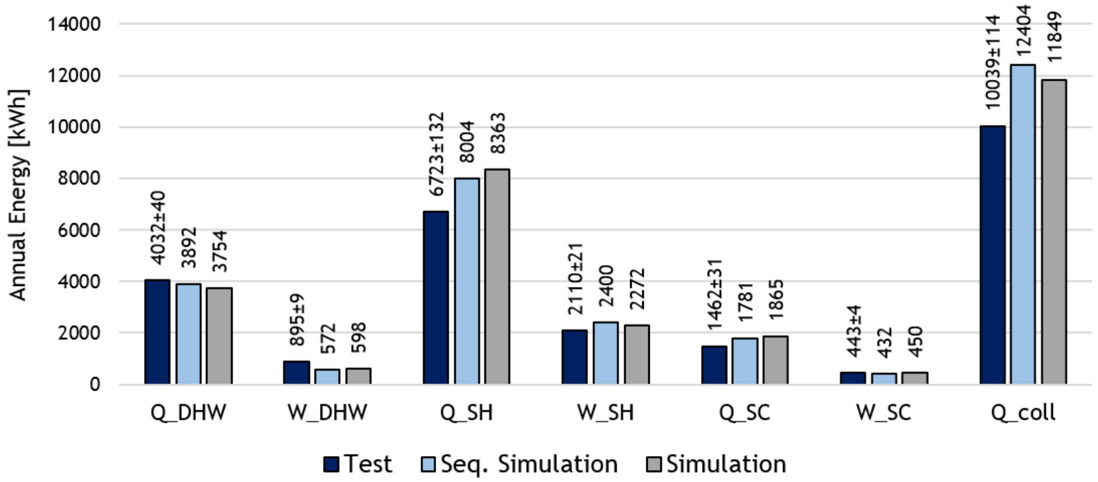

Figure 5-33: Seasonal energies extrapolated from test measurement, extrapolated from sequence simulation and defined with annual simulation. Ten-days sequence of Bolzano.

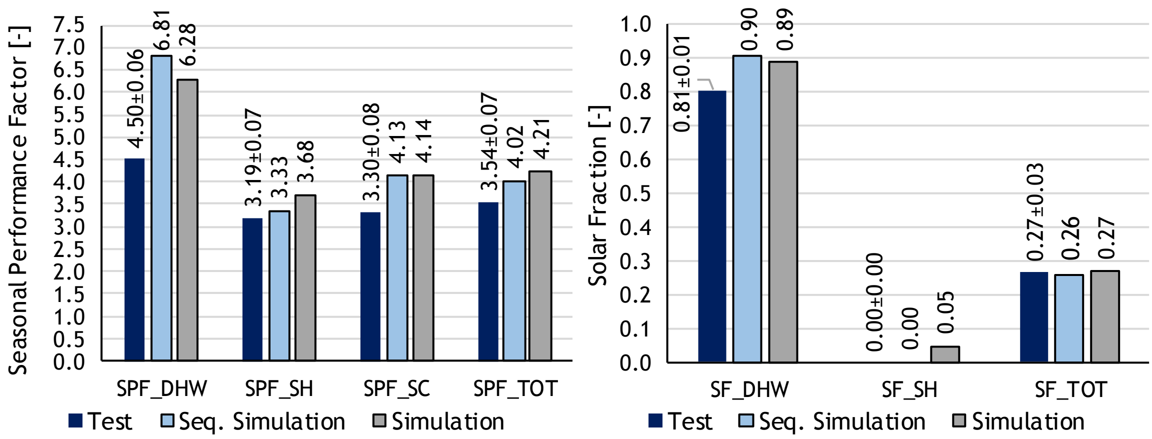

Figure 5-34: Seasonal performance factors and solar fractions extrapolated from test measurement, extrapolated from sequence simulation and defined with annual simulation. Ten-days sequence of Bolzano.

Figure 5-35 presents the comparison of EER and COP distributions obtained from the test, the sequence simulation and the annual simulation. As the previous test, the simulations disregard the lowest EER and COP values due to the transients. The biggest difference in the distributions is obtained again in the cooling mode since the heat pump is activated for short periods not allowing in most cases to reach the stationary working conditions. Instead, the distribution of space heating and domestic hot water preparation are more closed between the different calculations. In heating mode, it can be noticed that the distribution of COP during the DHW preparation is shifted to lower values then the points obtained during the space heating.

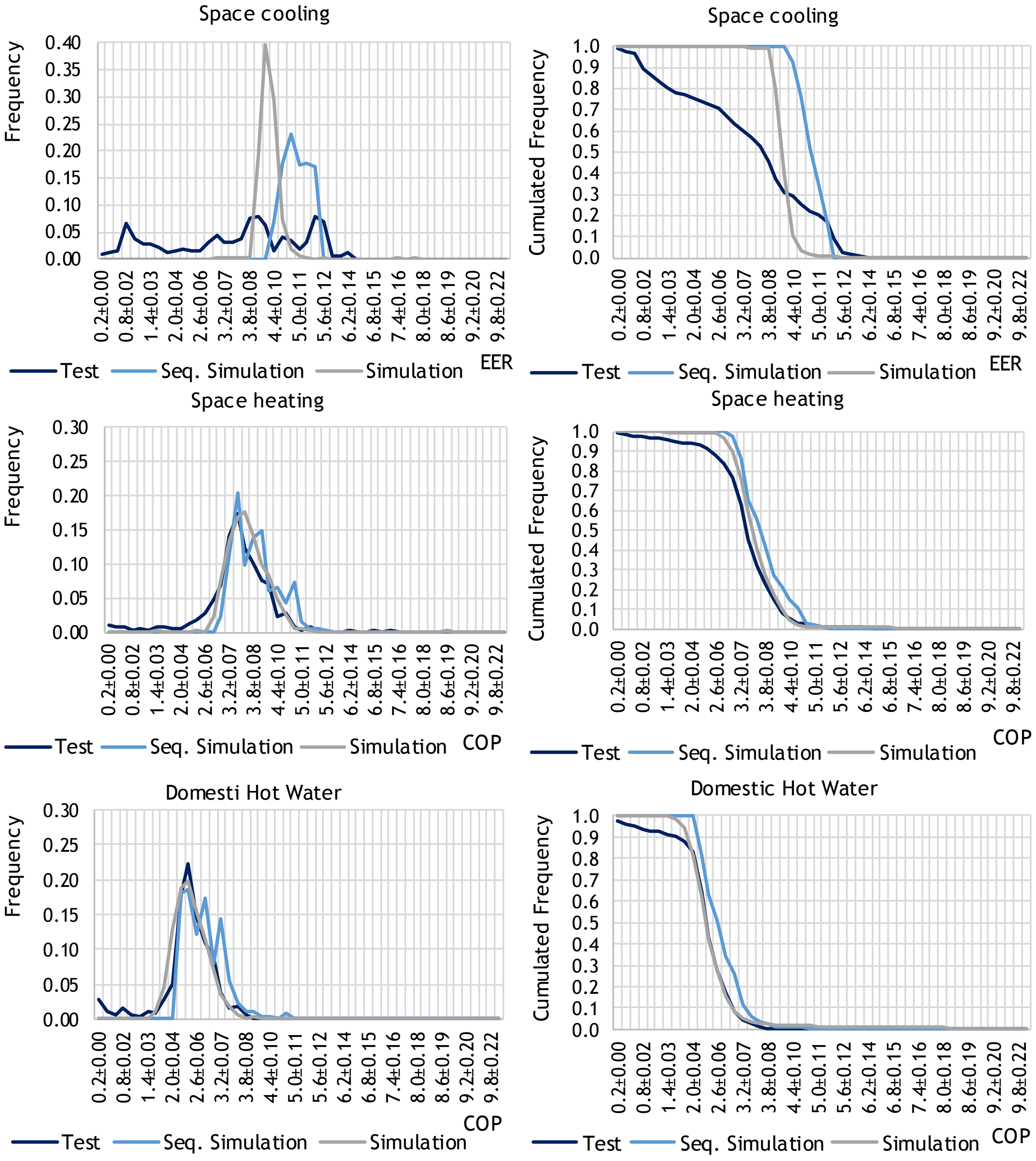

Figure 5-35: EER and COP distributions defined with test measurement, sequence simulation and annual simulation. Ten-days sequence of Bolzano.

Figure 5-36 presents the distribution of collector efficiency calculated with test, sequence simulation and annual simulation. As the previous case, the distribution of the annual simulation is closed to the distribution of the sequence simulation, confirming again the correct representation of the sequence.

The distribution of the test is closed to the ones simulated but it is moved to a slightly higher values. The motivation is that during the test the collector reaches lower temperatures and therefore the thermal losses are lower and consequently the efficiency is higher. It is remembered that during the test, the collector is activated for shorter time and the collector yield is lower (Figure 5-33).

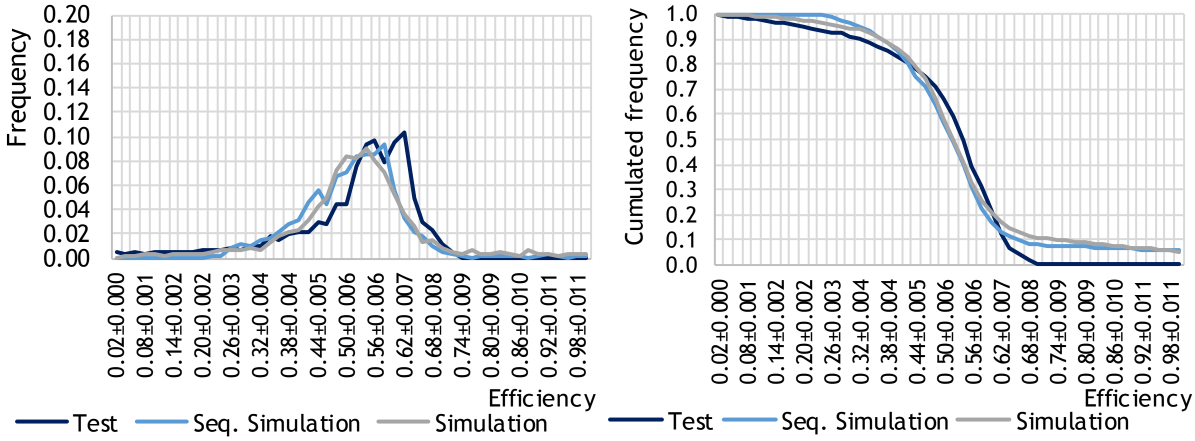

Figure 5-36: Solar collector efficiency distributions defined with test measurement, sequence simulation and annual simulation. Ten-days sequence of Bolzano.

The results of the six-days sequence and the ten-days sequence could be compared in the Table 5-3. The performances comparison shows a difference between the two sequences in both test and simulation. The ten-days sequence presents a lower heating and total seasonal performance factor than the six-days sequence. The motivation can be found in the test boundary conditions: as shown in Figure 5-37, the ten-days sequence considers a wider range of temperatures. The day with the lowest temperature, in the ten-days sequence has average temperature of -0.5 (and it reaches -5°C) while in the six-days sequence has average temperature of 2°C (and it reaches -2°C). Also the day with highest temperature the ten-days sequence has average temperature of 24°C while the six-days sequence has average temperature of 22°C.

Table 5-3: Comparison of SPF and SF extrapolated from six-days and ten-days sequences. Sequences of Bolzano (16 m²).

	Six-days test	Six-days Simulation	Ten-days test	Ten-days simulation	Annual simulation
SPF_{DHW}	7.42±0.10	13.28	4.50±0.06	6.81	6.28
SPF_{SH}	3.31±0.07	3.40	3.19±0.07	3.33	3.68
SPF_{SC}	3.10±0.07	4.15	3.30±0.08	4.13	4.14
SPF_{tot}	3.97±0.08	4.43	3.54±0.07	4.02	4.21
SF_{DHW}	0.83±0.01	0.96	0.81±0.01	0.9	0.89
SF_{SH}	0.00±0.00	0.00	0.00±0.00	0.00	0.05
SF_{tot}	0.26±0.03	0.27	0.27±0.03	0.26	0.27

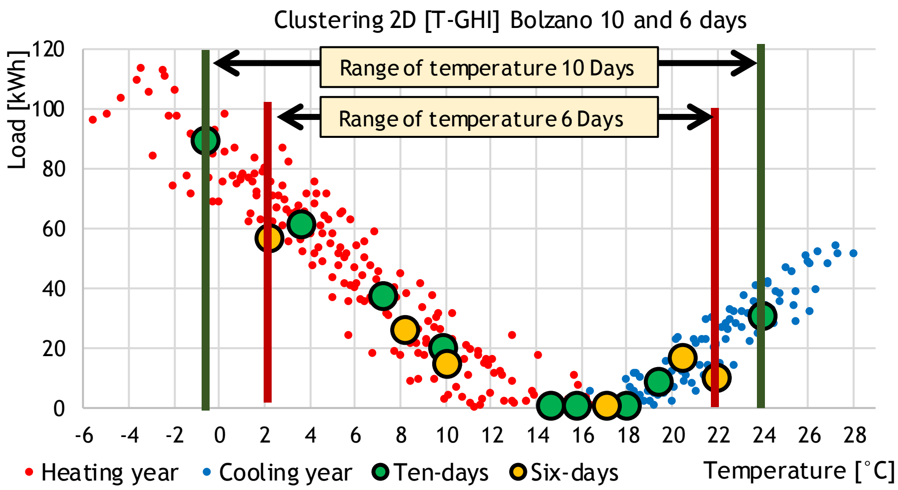

Figure 5-37: 2D Clustering comparison of six-days and ten-days sequences.

5.3 Six-days sequence of Bolzano - collector area of 8m²

This test considers the same boundary conditions to that described in paragraph 5.1 with the reduction of the collector area to 8 m². The expectation is to have a lower solar fraction and therefore a lower seasonal performance factor (since it increases the contribution of air source - i.e. heat pump).

5.3.1 Sequence results

Figure 5-38 shows the electrical consumption in both test and sequence simulation; the values are comparable trough them. As already mentioned in the previous tests, day 4, day 5 and day 6 are still characterised by a redistribution of electrical consumption for space cooling. As expected, the overall consumption is slightly greater than the one presented in the paragraph 5.1 since the contribution of solar energy is reduced for the lower collector area.

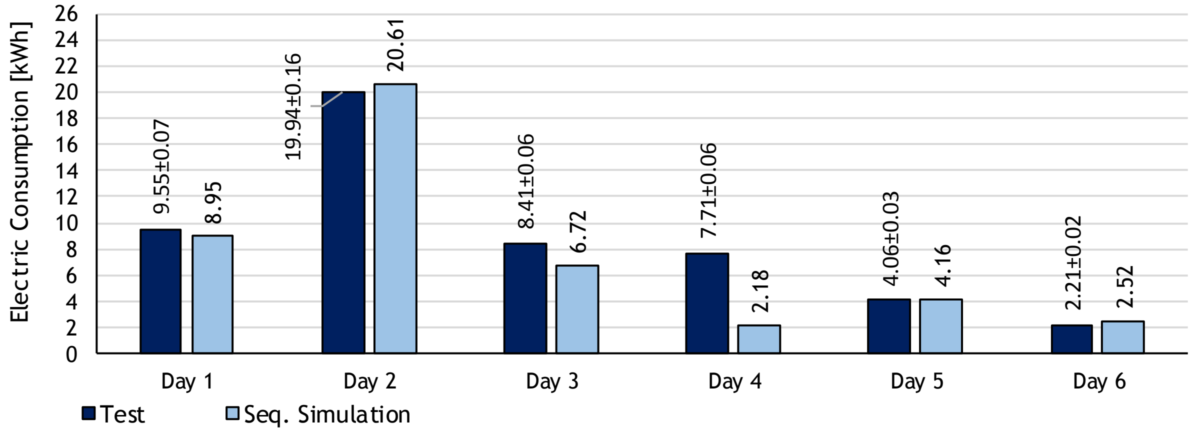

Figure 5-38: Daily total electric consumptions defined with test measurement and sequence simulation. Six-days sequence of Bolzano (8m²).

Figure 5-39 shows the daily space heating and cooling loads and the connected electric consumptions. As previous tests, the space cooling is redistributed during the days while the space heating load is similar.

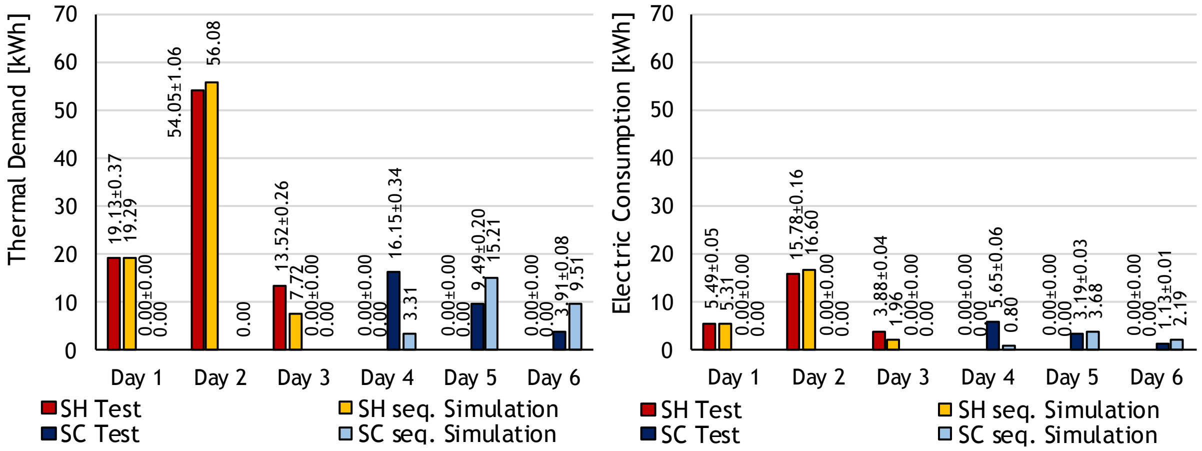

Figure 5-39: Daily SH/SC loads and SH/SC electric consumptions defined with test measurement and sequence simulation. Six-days sequence of Bolzano (8m²).

Figure 5-40 presents the daily DHW energy extraction and the electric consumption. The energy extracted is constant during different days and the electric consumption is slightly higher during the test. Figure 5-41 compares the electric consumption measured during the test and calculated with the sequence simulation for the configuration of the plant with a collector area of 16 m² and 8 m². The electric consumption is respectively 8.7 kWh and 16.8 kWh.

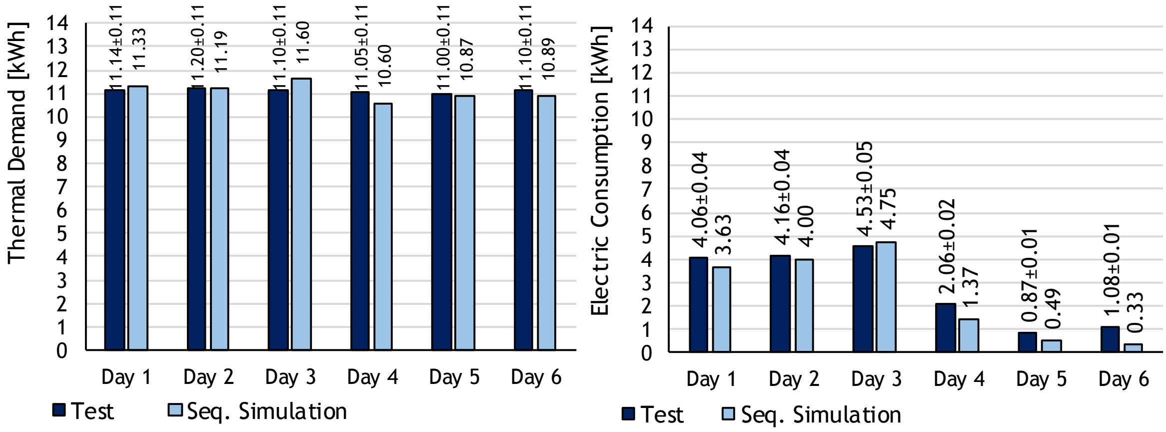

Figure 5-40: Daily DHW loads and DHW electric consumptions defined with test measurement and sequence simulation. Six-days sequence of Bolzano (8m²).

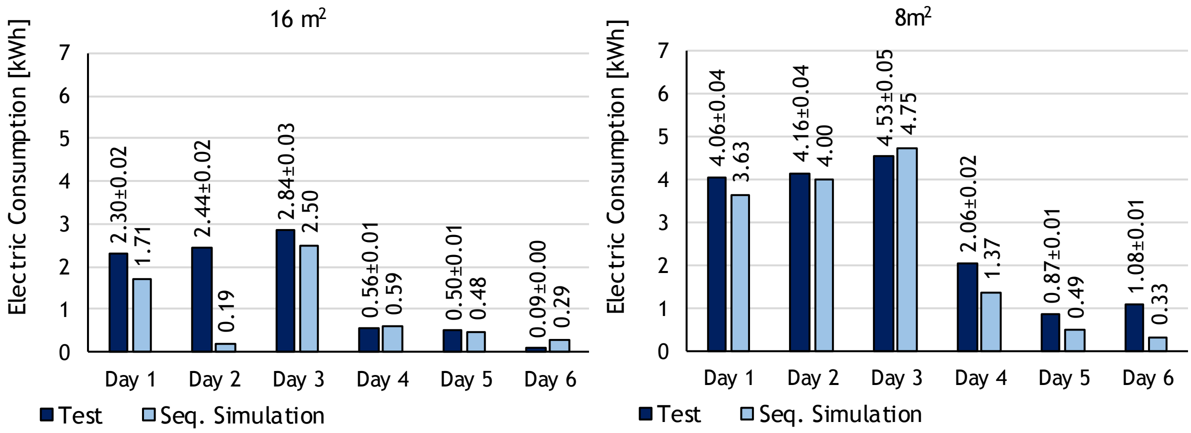

Figure 5-41: Comparison of DHW electric consumption between the configuration with 16 m² and 8 m² of collector area. Six-days sequence of Bolzano.

Figure 5-42 presents the total performance factor. From day 4 to day 6 the test measures a lower performance factor. Comparing again with the solution with a collector area of 16 m², its reduction (from 16 m² to 8 m²) gives a reduction of total performance factor from 4.1 to 3.5.

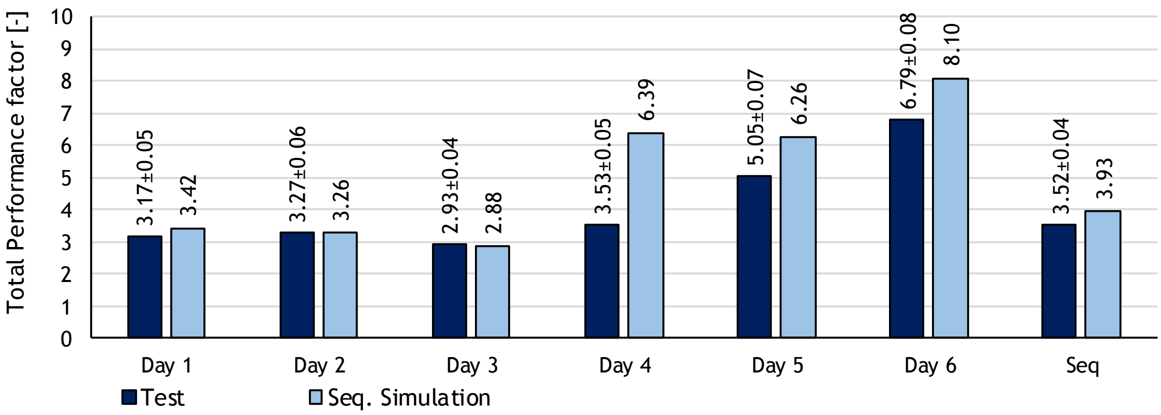

Figure 5-42: Daily total performance factors defined with test measurement and sequence simulation. Six-days sequence of Bolzano (8m²).

Figure 5-43 presents the solar collector yield. As previous tests, the energy collected during the test is lower to the one simulated (respectively 119 kWh and 139 kWh). The test with 8 m² of collector area has a solar yield of 119 kWh while with a collector area of 16 m² is 191 kWh. The collector yield decreased about 38% while the electric consumption for the DHW preparation increased about 93%.

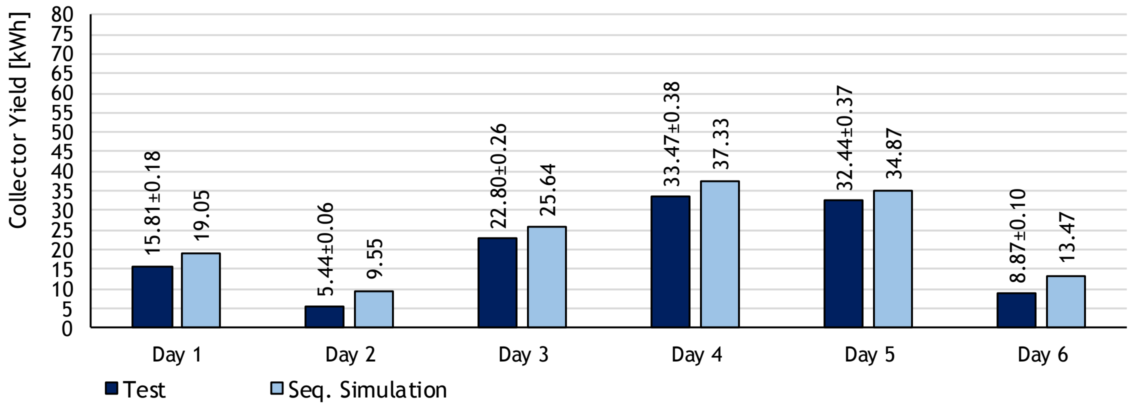

Figure 5-43: Daily collector yield defined with test measurement and sequence simulation. Six-days sequence of Bolzano (8m²).

5.3.2 Annual extrapolation

As shown in Table 5-4 and Figure 5-44, the system has delivered lower space heating and cooling energies. However, the correspondent consumptions are not proportionally lower, at opposite, the consumption for space cooling is higher in the test. It should be noted that the thermal energy collected by solar panels is lower than the one of test with 16 m² of collectors: the area reduction of 50 % has led to a reduction of 36 % of collected energy (from 10100 kWh/year to 6500 kWh/year).

Table 5-4: Cluster energies evaluation. Six-days sequence of Bolzano (8m²).

	Cluster 1	Cluster 2	Cluster 3	Cluster 4	Cluster 5	Cluster 6	Test	Annual Simulation
Size	65	93	36	35	75	61	-	-
Q_{DHW} [kWh]	724	1042	400	387	825	677	4054±40	3592
W_{DHW} [kWh]	264	387	163	72	65	66	1017±10	945
Q_{SH} [kWh]	1243	5027	487	0	0	0	6757±132	8347
W_{SH} [kWh]	357	1468	140	0	0	0	1964±20	2356
Q_{SC} [kWh]	0	0	0	565	712	239	1516±32	1865
W_{SC} [kWh]	0	0	0	198	239	69	506±5	449
Q_{coll} [kWh]	1028	506	821	1171	2433	541	6500±74	7077

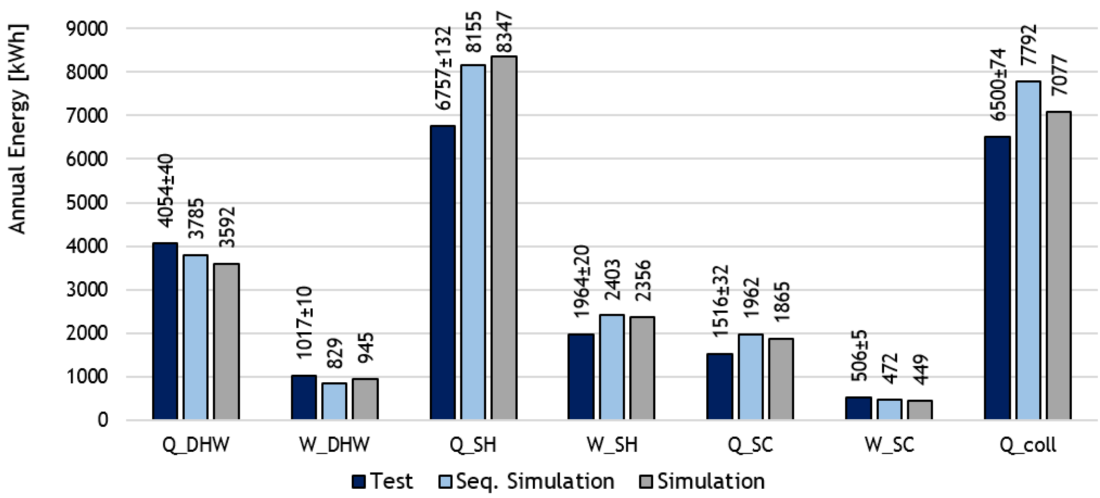

Figure 5-44: Seasonal energies extrapolated from test measurement, extrapolated from sequence simulation and defined with annual simulation. Six-days sequence of Bolzano (8m²).

Note: the reduction of collector area to the 50 % leads to a reduction of the collector yield in the sequence of the 38% while in the annual extrapolation of the 36%. This difference is due to the different weight that days have, since the clusters have a different population.

The performances of test and simulation are very close. As shown in Figure 5-52, only the space cooling test efficiency has large performance reduction caused by the heat pump discontinuous operation. The performance factors of space heating and space cooling are slightly smaller than the performance obtained through the 16 m^2 test for the lower contribution of solar energy.

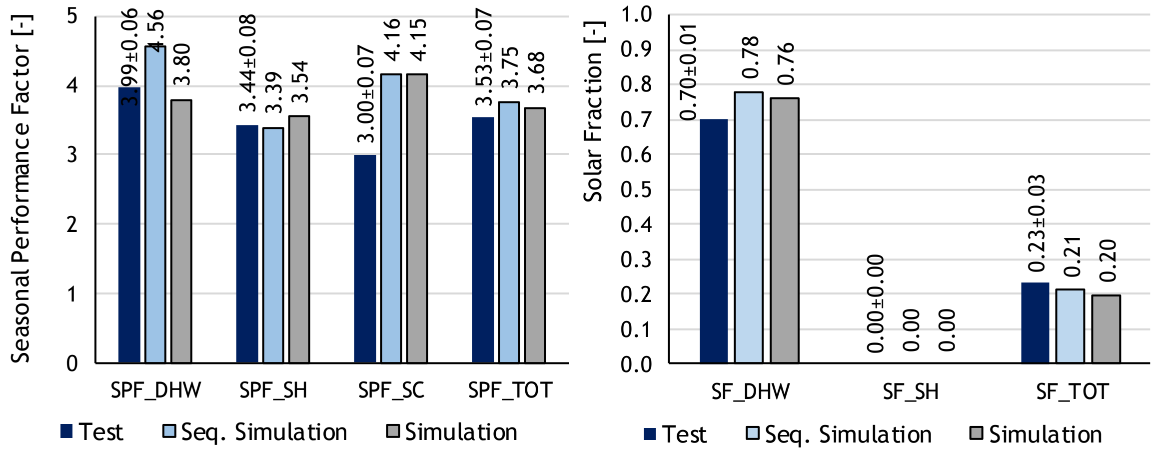

Figure 5-45: Seasonal performance factors and solar fractions extrapolated from test measurement, extrapolated from sequence simulation and defined with annual simulation. Six-days sequence of Bolzano (8m^2).

5.4 Six-days sequence of Zurich - collector area of 16m^2

The second clime considered is Zurich. This climate is currently adopted from the other test methods. Figure 5-46 shows the boundary conditions of the sequence in Zurich climate while Figure 5-47 shows the loads profiles. Zurich is a colder climate than Bolzano and the space cooling request is very low: the total cooling demand is about 400 kWh/year while the heating demand is about 12000 kWh/year. The selection performed with clustering does not considers days with cooling demand.

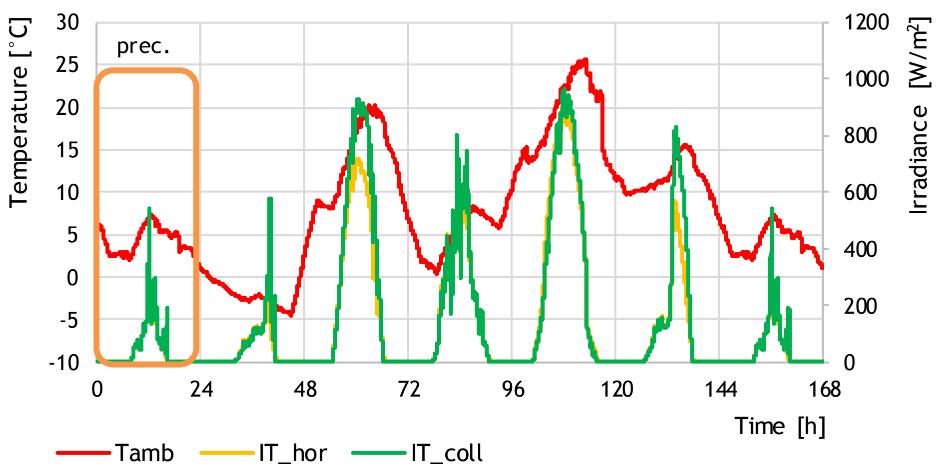

Figure 5-46: Profiles of the ambient temperature and irradiances on horizontal and collector surface during the six-days sequence of Zurich.

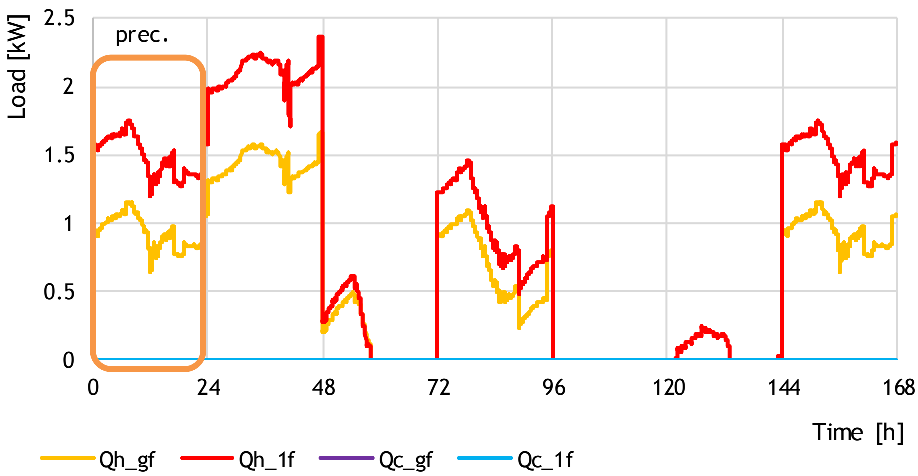

Figure 5-47: Building load profiles during the six-days sequence of Zurich.

5.4.1 Sequence results

Figure 5-48 shows the electric consumptions defined with test measurement and sequence simulation. The total test consumption is about 76 kWh a few higher than the simulated that is 73.1 kWh. During the sequence, the test measures a higher consumption than the simulation ad exception of the day 2 that also presents the highest difference between the two calculations (about 5 kWh).

The motivation can be found in the space heating load: the Figure 5-49 presents the comparison of heating load between the test and the simulation. Part of the space heating in day 2 is satisfied in during day 3 and a small part of day 4 heating load is satisfied in day 5 that does not have load request. This behaviour was already highlighted in the previous tests.

The other load that contribute to the total consumption is the domestic hot water. Figure 5-50 shows the thermal and electrical consumption for the domestic hot water preparation. During the test, the electric consumption is higher than the simulated one. In particular, in first two days the electrical consumption measured with test is higher than the one simulated since during the first and second days of the test the collector yield is almost zero. During the first day of simulation, the consumption is 0.09 kWh since the storage is filled during the preconditioning day.

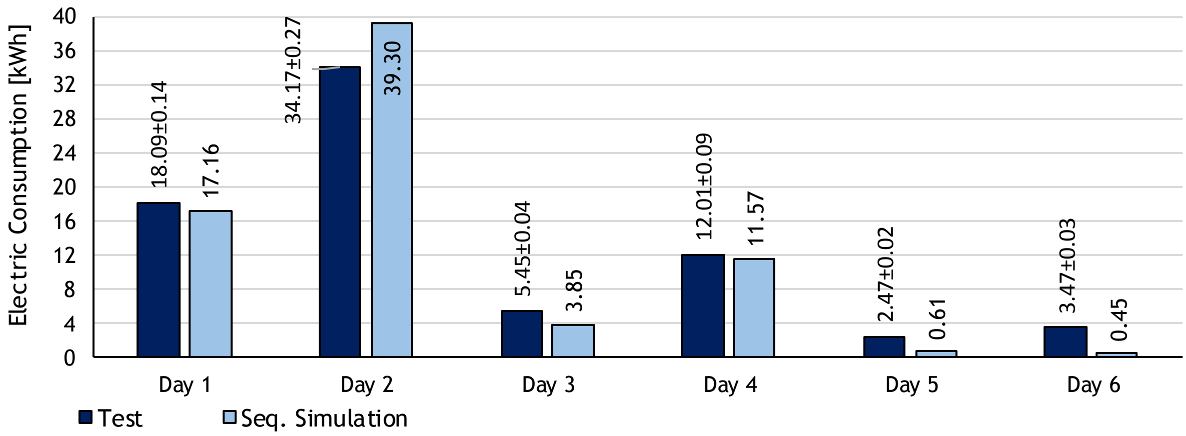

Figure 5-48: Daily total electric consumptions defined with test measurement and sequence simulation. Six-days sequence of Zurich.

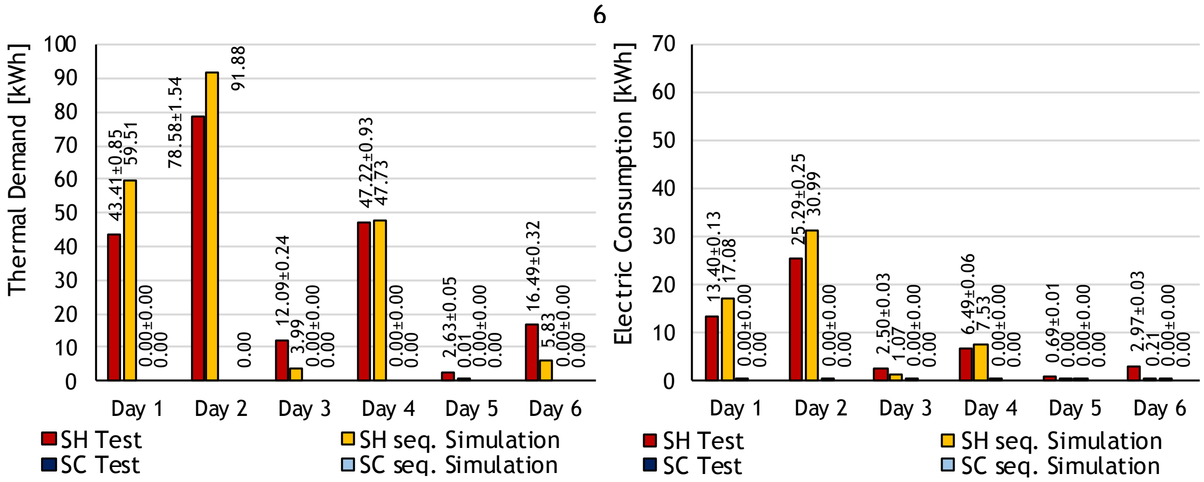

Figure 5-49: Daily SH/SC loads and SH/SC electric consumptions defined with test measurement and sequence simulation. Six-days sequence of Zurich.

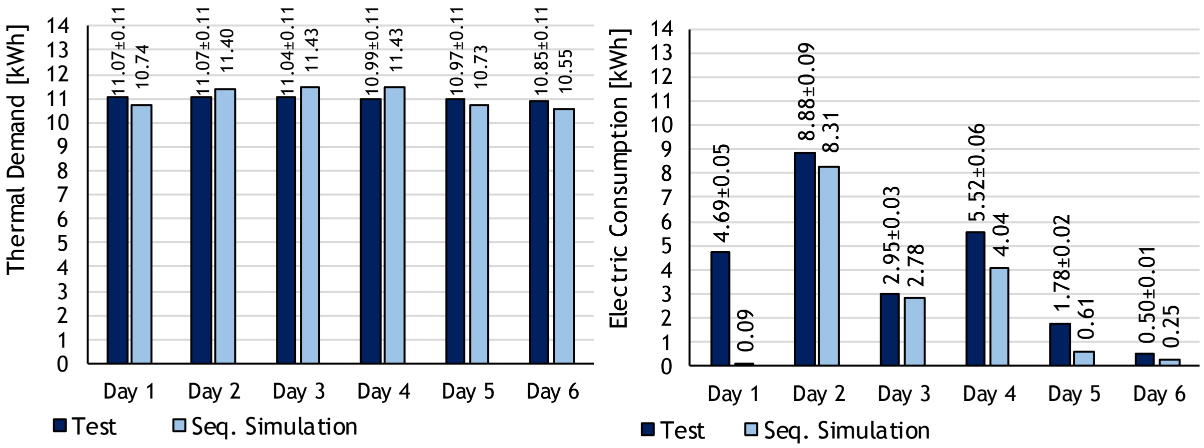

Figure 5-50: Daily DHW loads and DHW electric consumptions defined with test measurement and sequence simulation. Six-days sequence of Zurich.

Figure 5-51 shows the collector yield. The test has measured a collector yield of 151 kWh while the simulation of 182 kWh. During day 1 and day 2, the tested system has activated the solar panels to collect only 0.4 kWh while the simulation collected 9.9 kWh. The first two days have low irradiance and the transients have a predominant effect in the test when the irradiance is low as already indicated in the sequence of Bolzano.

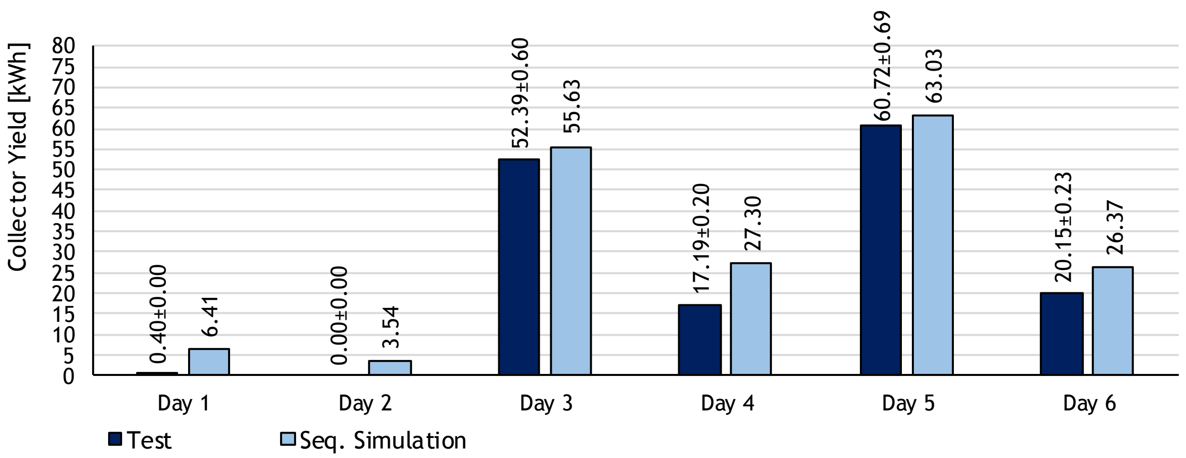

Figure 5-51: Daily collector yield defined with test measurement and sequence simulation. Six-days sequence of Zurich.

In the Figure 5-52 the performance factor is distinguished into DHW performance factor and SH performance factor while the Figure 5-53 presents the total performance factor . As indicated in previous figure, the DHW performance factor during the first two days of test is lower than the simulated ones since the solar contribution is lower.

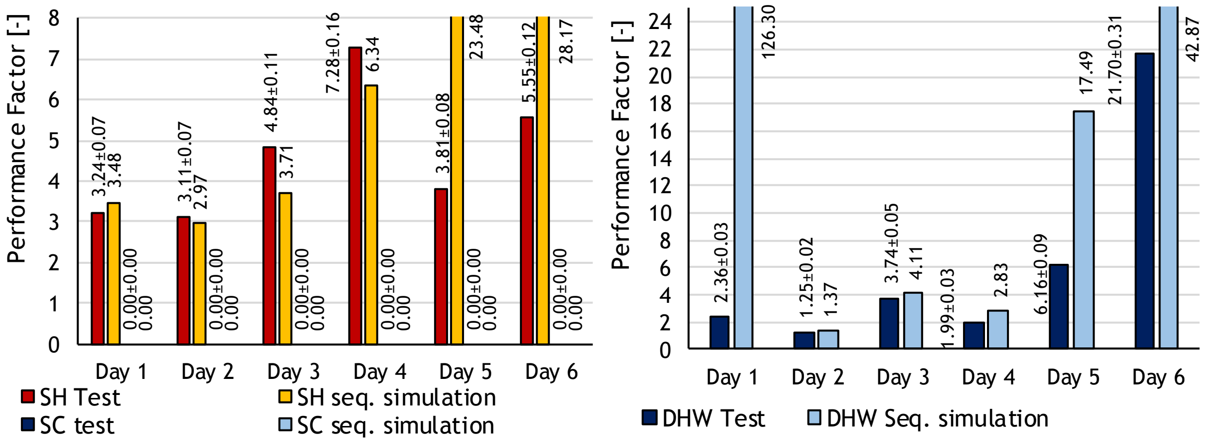

Figure 5-52: Daily performance factors defined with test measurement and sequence simulation. Six-days sequence of Zurich.

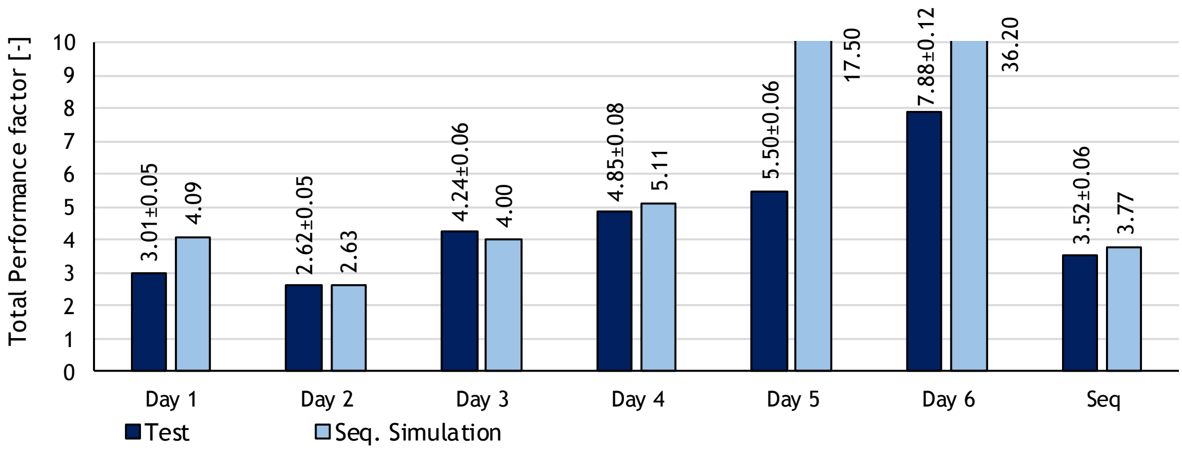

Figure 5-53: Daily total performance factors defined with test measurement and sequence simulation. Six-days sequence of Zurich.

For the simulation, the heating performance factor of day 5 and day 6 is a high value since a small amount of load is required and it is satisfied by the solar energy. In this case the consumption for the space heating is only due to the circulation pumps. The contribution of solar during these two days is important also for the domestic hot water. The consequent total performance factor calculated from the simulation is high too.

The same behaviour is obtained during the test with days 4 and 6 where the heating performance factors of these two days is quite high for the contribution of the solar. However, during the day 4, the DHW performance factor decrease for a consequence of the heating scheme with the solar energy: Figure 5-54 shows the temperature in the storage when the space heating with solar energy works. During this phase, also the scheme of DHW extraction started. The control strategy foresees to start heating with solar energy when the storage temperature is higher than 46°C and is deactivated when it reaches 41°C in order to keep a buffer of energy for the DHW. The test showed that the temperature decrease to 40°C for the system inertia. After, a DHW extraction reduced the temperature below 40°C. In this way the storage has to be charged again with the heat pump. That means the electric energy has to be used to return at a temperature of the storage higher than 40°C for the activation of the charge scheme. The energy extracted for the space heating after the 7 A.M. is about 6.1 kWh while the energy extracted by the DHW is about 2.6 kWh. Than the activation of the scheme of charge of the storage gives 7.56 kWh. The advantage of using solar energy for space heating is loosed by the necessity of feed again the storage. The consequence of this effect is that the extraction of DHW between the 8 A.M. and the 8.7 A.M could not be performed at 40°C since the storage temperature is lower.

A solution could be increasing the lower limit of the hysteresis cycle that controls the space heating with solar energy. In this way a higher COP of the heat pump is obtained since the working condition is moved to the one at higher temperature (storage charge) to one lower (space heating).

This result is important since it indicates that the behaviour of the storage is not well represented with simulation motivating the necessity of experimental observation of the dynamic effect of the system.

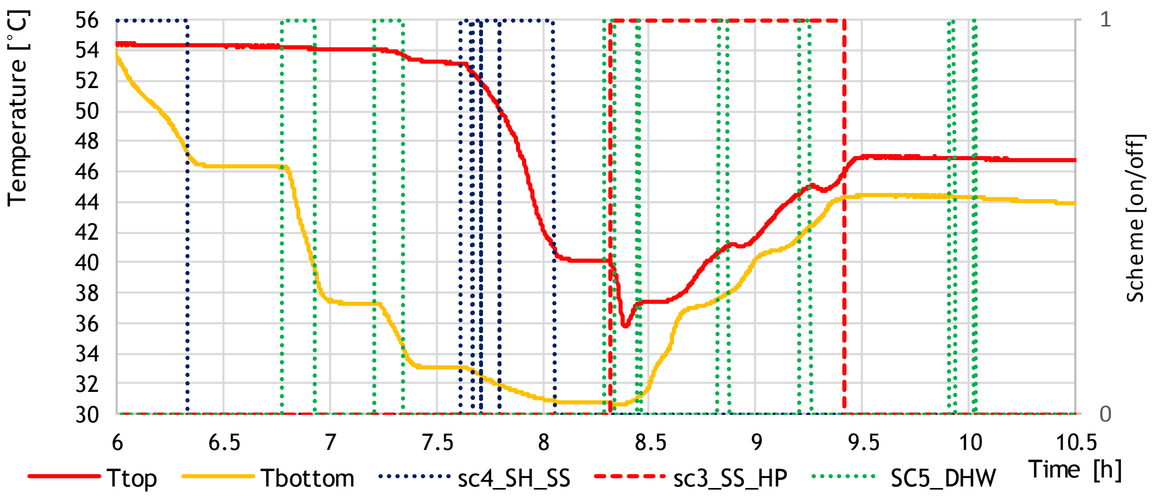

Figure 5-54: Temperature of storage during the heating, DHW and charge schemes.

Figure 5-55 shows the scheme activation time. The scheme of charge small storage with heat pump (scheme 3) has higher activation time in the test compared to simulation. This is caused by the redistribution of solar energy used just explained above.

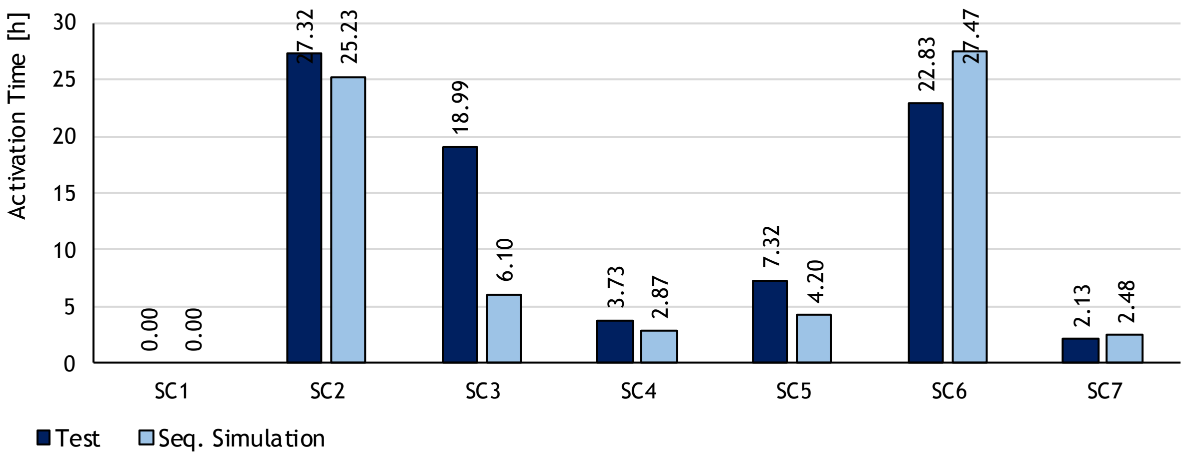

Figure 5-55: Duration of scheme activation defined with test measurement and sequence simulation. Six-days sequence of Zurich.

The schemes are shown in the Appendix C in the chapter "Solar Assisted Heat Pump System". "SC1" scheme of space cooling, "SC2" scheme of space heating with heat pump, "SC3" scheme of small storage charge with heat pump, "SC4" scheme of space heating with solar energy, "SC5" scheme of DHW extraction, "SC6" scheme for the activation of the solar collector, "SC7" scheme for the heat transfer from big storage to small storage.

5.4.2 Annual extrapolation

Table 5-5 shows the annual energies calculated from the sequence days weighed with the cluster size while Figure 5-56 shows graphically the results presented in the previous table. In this case the annual simulation has a space cooling which is absent in the test since the clustering does not select any day with space cooling. Anyway this cooling load is very small and negligible.

Table 5-5: Cluster energies evaluation. Six-days sequence of Zurich.

	Cluster 1	Cluster 2	Cluster 3	Cluster 4	Cluster 5	Cluster 6	Test	Annual Simulation
Size	83	47	68	31	50	86	-	-
Q_{DHW} [kWh]	919	520	751	341	549	933	4012±40	3875
W_{DHW} [kWh]	389	417	201	171	89	43	1310±13	633
Q_{SH} [kWh]	3603	3693	962	1727	132	1878	11995±218	11463
W_{SH} [kWh]	1112	1189	170	201	35	255	2962±30	3085
Q_{SC} [kWh]	0	0	0	0	0	0	0±0	333
W_{SC} [kWh]	0	0	0	0	0	0	0±0	80
Q_{coll} [kWh]	33	0	3563	533	3036	1733	8898±101	7583

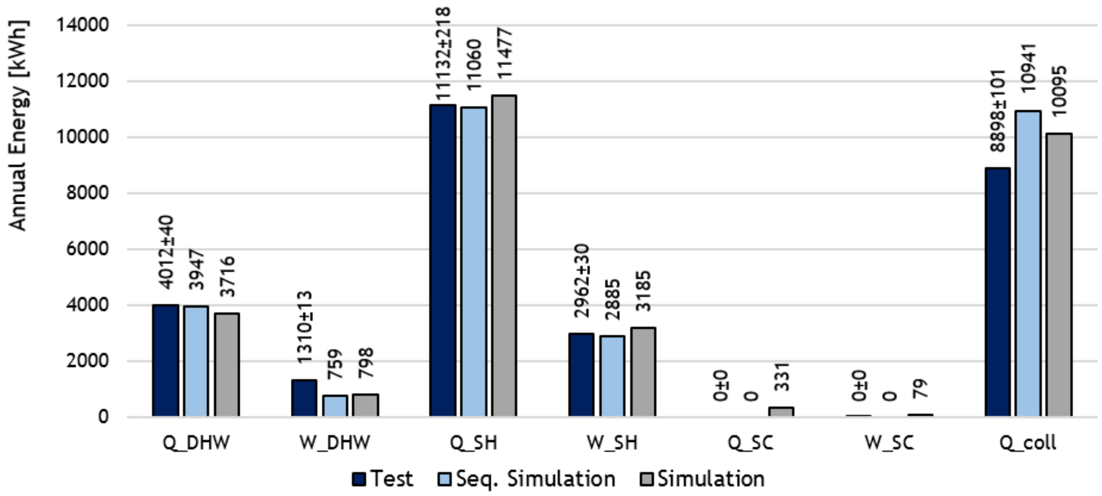

Figure 5-56: Seasonal energies extrapolated from test measurement, extrapolated from sequence simulation and defined with annual simulation. Six-days sequence of Zurich.

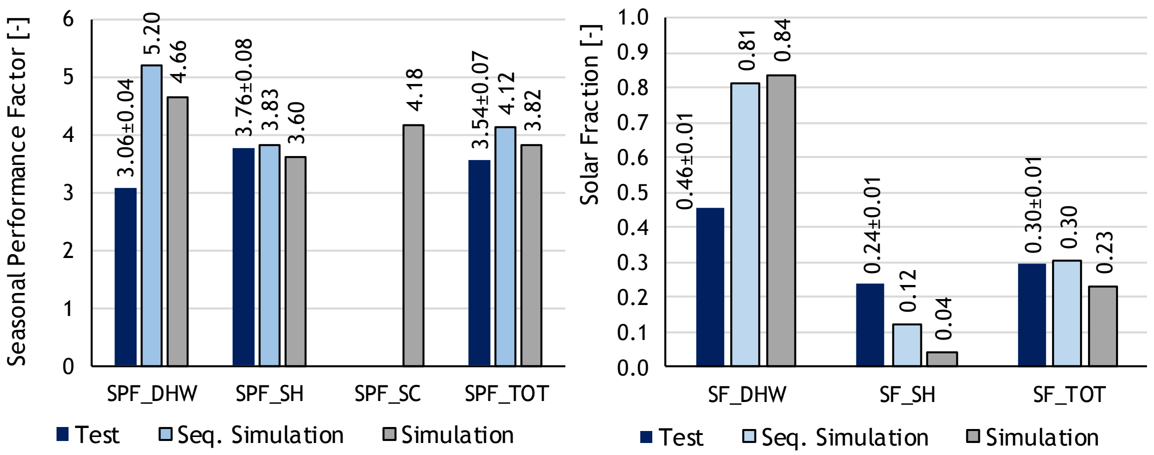

Figure 5-57: Seasonal performance factors and solar fractions extrapolated from test measurement, extrapolated from sequence simulation and defined with annual simulation. Six-days sequence of Zurich.

Figure 5-57 shows the seasonal performance factors and the solar fractions. The test identifies a lower DHW SPF for the effect explained above. The DHW solar fraction is reduced to 0.46 while in the sequence simulation is 0.81 and in the annual simulation it is 0.84. However, the test considers a higher contribution of solar energy to the space heating increasing the heating solar fraction. The difference with the simulations is high since the test has the double solar fraction than the sequence simulation and six times the solar fraction of the annual simulation.

As the other tests, the distributions of instantaneous performance are evaluated with the Figure 5-58 that presents the distribution of collector efficiency calculated with the test, the sequence simulation and the annual simulation. These distributions show a qualitative agreement between test and simulations in terms of collector efficiency but as indicated previously the simulation disregards the conditions of activation of the solar panels when the irradiance is low.

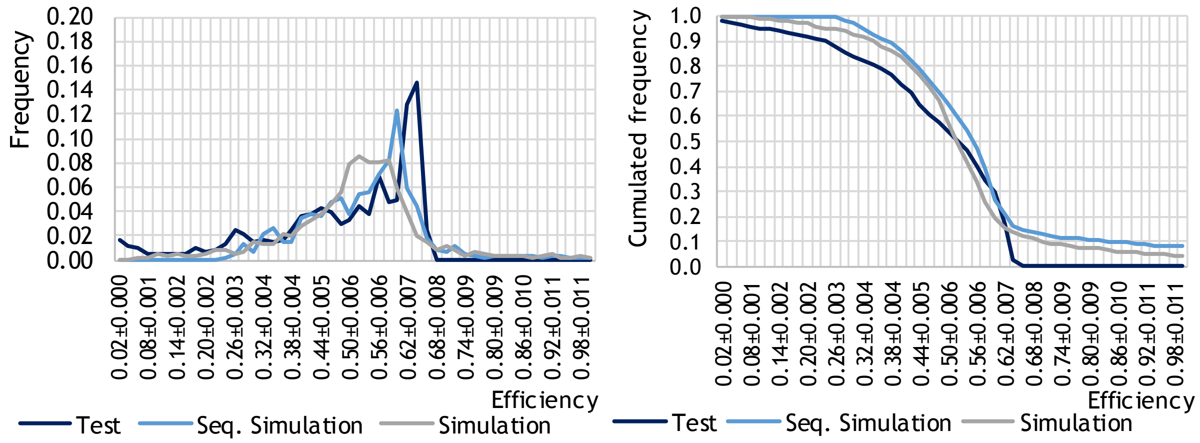

Figure 5-58: Solar collector efficiency distributions defined with test measurement, sequence simulation and annual simulation. Six-days sequence of Zurich.

5.5 Six-days sequence of Gdansk – collector area of 16m²

The third climate considered is Gdansk. This climate is colder than the previous two and as the case of Zurich the cooling load is negligible. The boundary conditions are shown in Figure 5-59 for the temperature and irradiance, and in Figure 5-60 for the heating load. The last two days of the sequence are summer days without any space load.

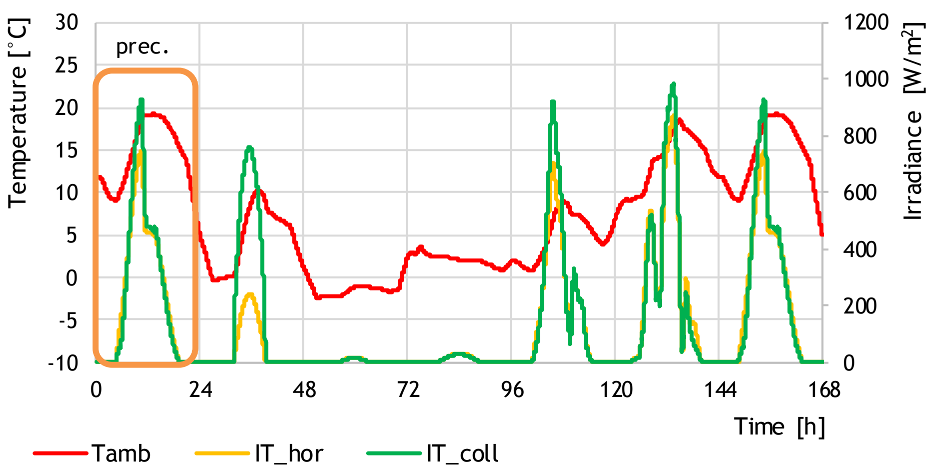

Figure 5-59: Profiles of the ambient temperature and irradiances on horizontal and collector surface during the six-days sequence of Gdansk.

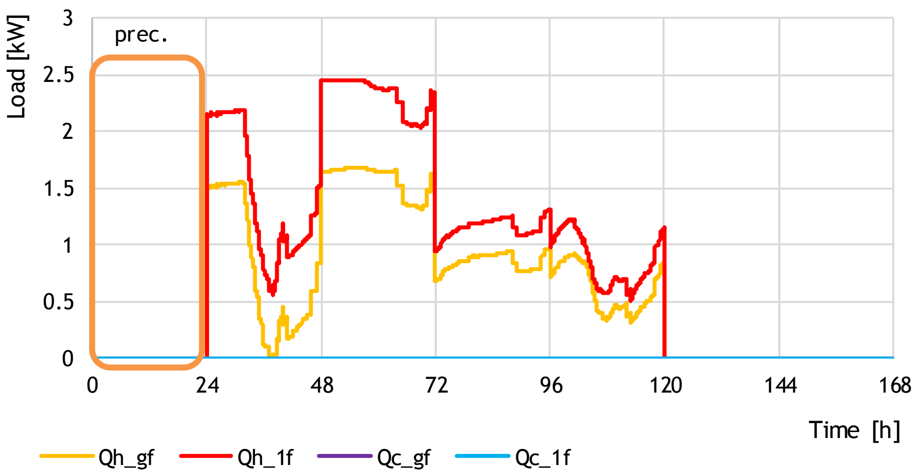

Figure 5-60: Building load profiles during the six-days sequence. Gdansk climate.

5.5.1 Sequence results

Figure 5-61 presents the total electric consumption during the different days. During the different days, the test measures higher consumptions than the simulation. The difference ranges between 1 to 3 kWh. The consumption presented in Figure 5-61 can be divided into the contribution of space heating with Figure 5-62 and domestic hot water in Figure 5-63. These two figures present also the respective loads.

The electric consumption for the space heating is satisfied entirely by the heat pump and the test and simulations consider similar consumptions. The day 2 presents the highest consumption since it has the highest heat demand (about 90 kWh).

Regarding the consumption for the domestic hot water, the test and simulation present different consumption for the first two days: in the test the electric consumption for the first day is 0.36 kWh while the second day is 3.58 kWh. This means that the solar energy collected during the preconditioning day and the first day is enough for the first day but not for the second day. Instead the opposite is verified in the simulation since the first day requires 3.68 kWh while the second day requires only 0.02 kWh (mainly the circulation pump for the water extraction). This difference between the test and simulation again is explained by the not correct representation of the dynamic of the system with the simulation.

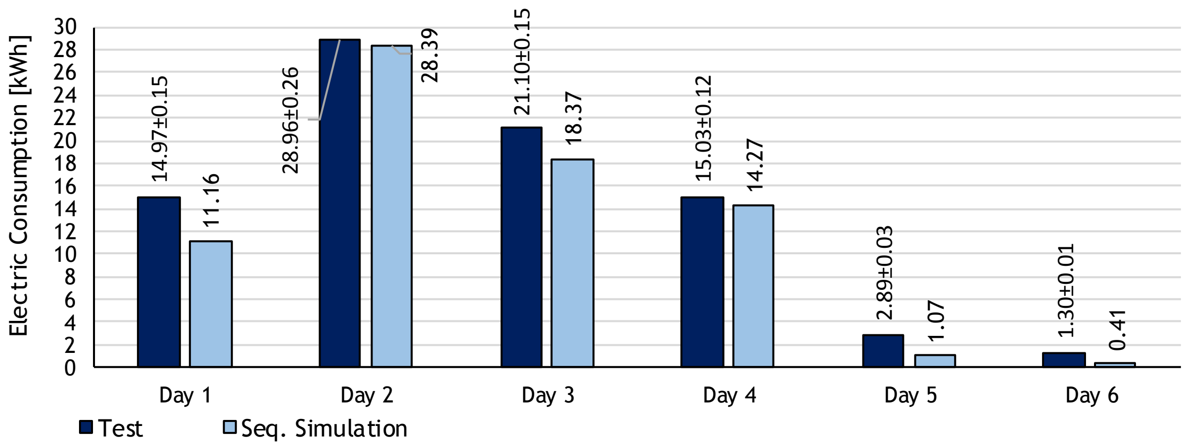

Figure 5-61: Daily total electric consumptions defined with test measurement and sequence simulation. Six-days sequence of Gdansk.

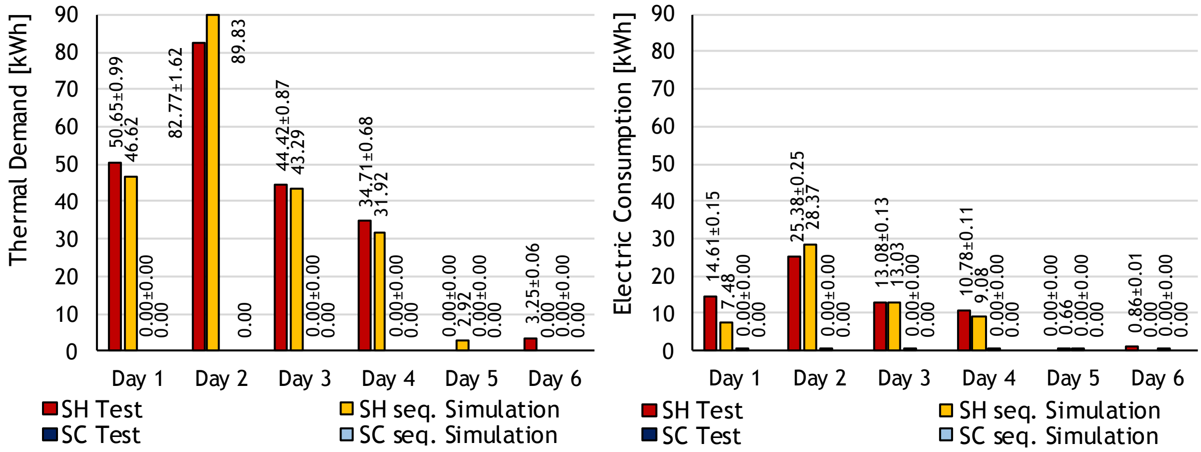

Figure 5-62: Daily SH/SC loads and SH/SC electric consumptions defined with test measurement and sequence simulation. Six-days sequence of Gdansk.

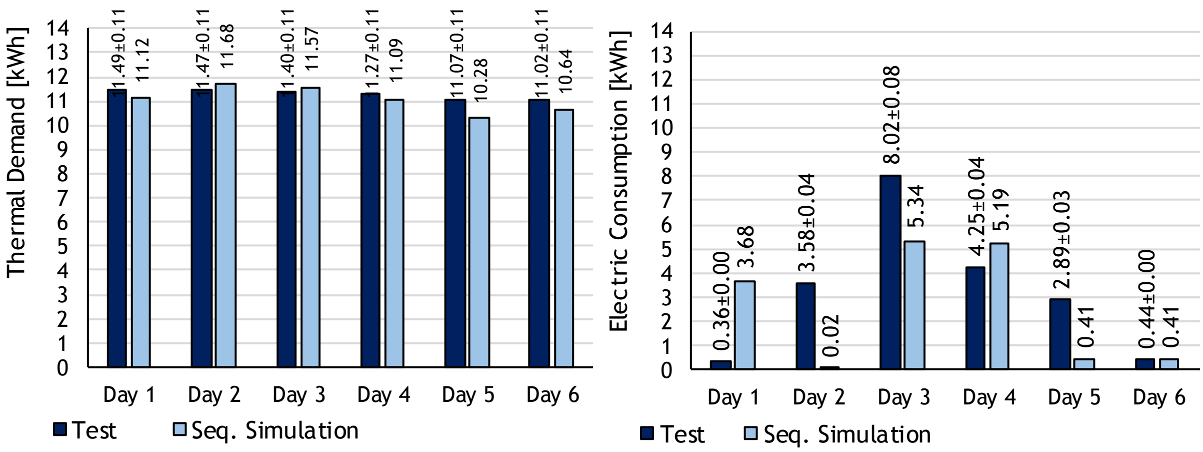

Figure 5-63: Daily DHW loads and DHW electric consumptions defined with test measurement and sequence simulation. Six-days sequence of Gdansk.

From the combination of the previous figures, the total performance factor is shown in the Figure 5-64. The last two days present the highest performance factors since there is a large contribution of solar and the only load is the domestic hot water. The day 2 and day 3 do not have any contribution from solar source as indicated in the Figure 5-65 and the consequence is a very low value of performance factor.

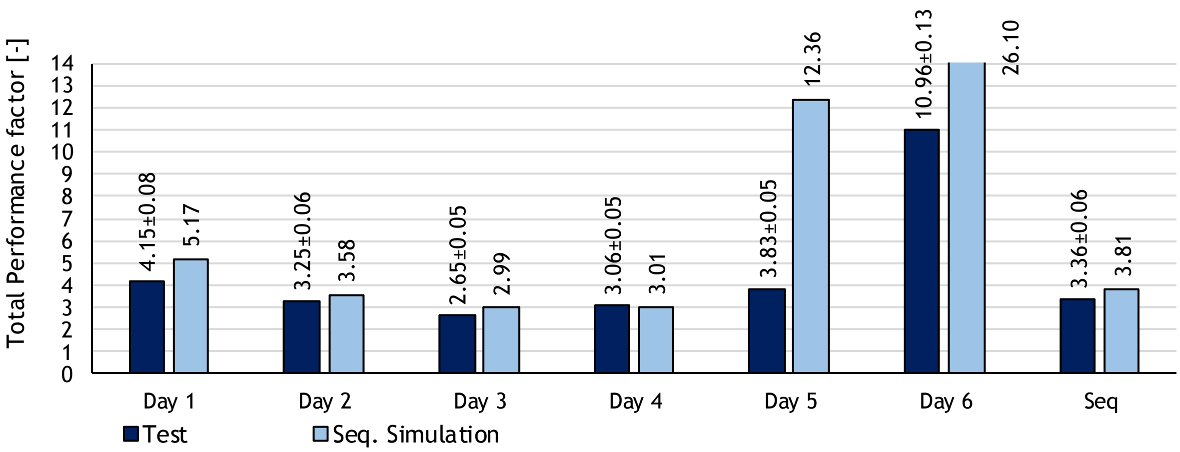

Figure 5-64: Daily total performance factors defined with test measurement and sequence simulation. Six-days sequence of Gdansk.

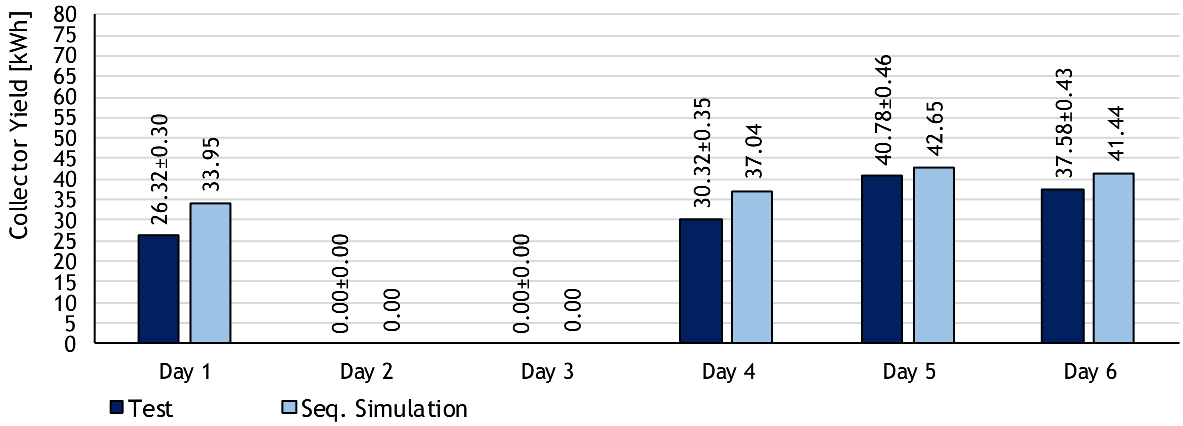

Figure 5-65: Daily collector yield defined with test measurement and sequence simulation. Six-days sequence of Gdansk.

The effect of absence of solar irradiation during day 2 and day 3 can be visible in the storages temperatures. The Figure 5-66 presents the big storage temperatures while the Figure 5-67 presents the small storage temperatures. The temperature level of the small storage is kept between 40°C to 46°C with the heat pump while the temperature of the big storage could increase only with the solar collector contribution. In fact, with absence of this contribution, the average temperature in the storage drops to 20°C in the test and 25°C in the simulation.

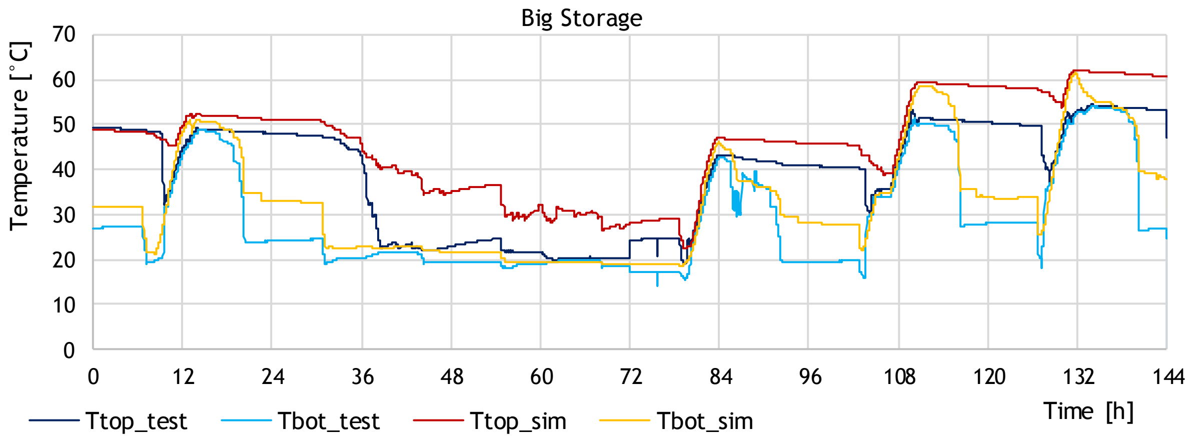

Figure 5-66: Big storage temperatures measured during the test and defined with the sequence simulation. Six-days sequence of Gdansk.

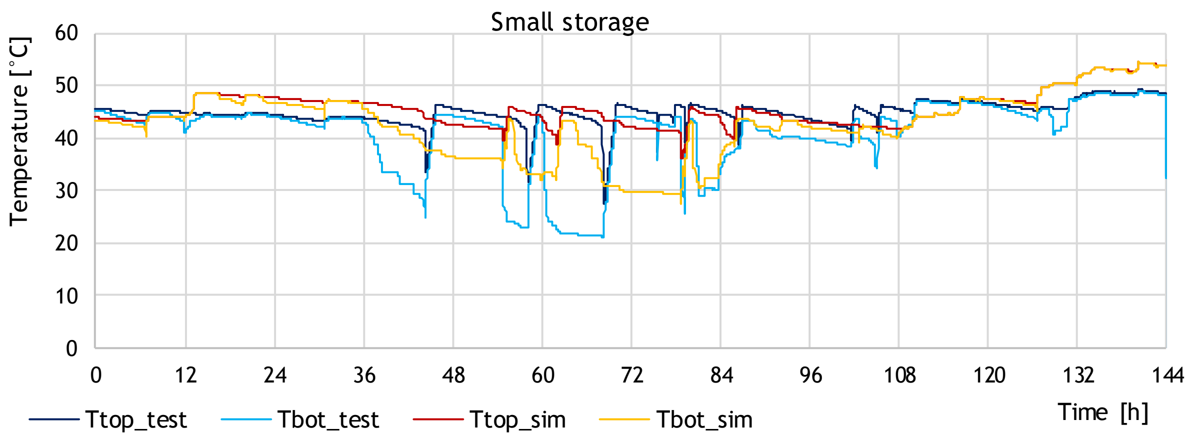

Figure 5-67: Small storage temperatures measured during the test and defined with the sequence simulation. Six-days sequence of Gdansk.

5.5.2 Annual extrapolation

Table 5-6 present the clusters sizes for the six-days sequence of Gdansk. The table presents also the loads and consumptions associated to each cluster. To complete the table, the Figure 5-68 presents the comparison of these energies calculated from the test, the sequence simulation and the annual simulation.

As the case of Zurich climate, the cooling load is visible only with the annual simulation but this load is negligible since is 98 kWh if compared to the 12893 kWh of the heating load (0.76%).

Table 5-6: Cluster energies evaluation. Six-days sequence of Gdansk.

	Cluster 1	Cluster 2	Cluster 3	Cluster 4	Cluster 5	Cluster 6	Test	Annual Simulation
Size	72	44	58	55	68	68	-	-
Q_{DHW} [kWh]	827	505	661	620	753	749	4115±41	3689
W_{DHW} [kWh]	26	158	465	234	197	30	1109±11	941
Q_{SH} [kWh]	3647	3642	2576	1909	0	221	11995±235	12893
W_{SH} [kWh]	1052	1117	759	593	0	58	3579±36	3638
Q_{SC} [kWh]	0	0	0	0	0	0	0±0	98
W_{SC} [kWh]	0	0	0	0	0	0	0±0	23
Q_{coll} [kWh]	1895	0	0	1668	2773	2555	8891±101	9707

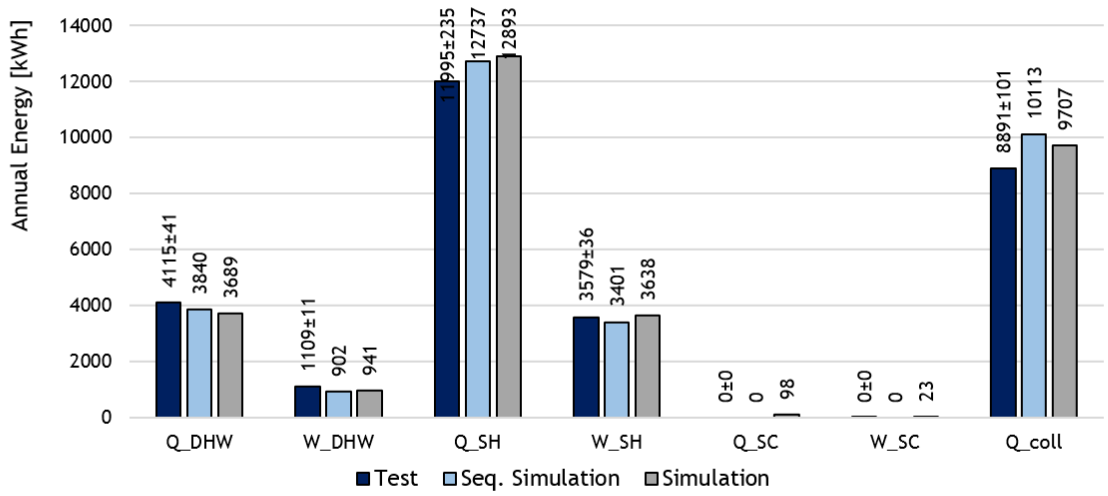

Figure 5-68: Seasonal energies extrapolated from test measurement, extrapolated from sequence simulation and defined with annual simulation. Six-days sequence of Gdansk.

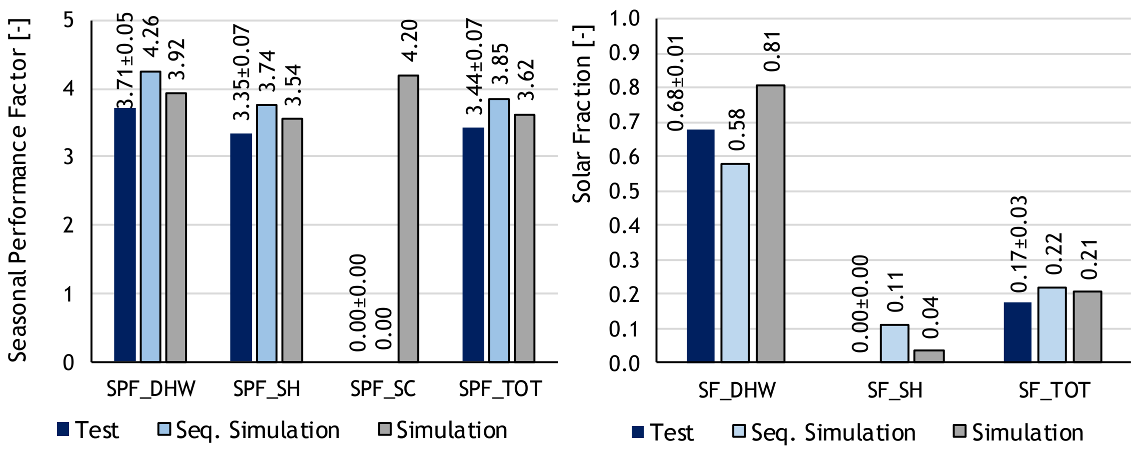

Figure 5-69: Seasonal performance factors and solar fractions extrapolated from test measurement, extrapolated from sequence simulation and defined with annual simulation. Six-days sequence of Gdansk.

Figure 5-69 presents the seasonal performance factors and the solar fraction calculated for different loads with the test, the sequence simulation and the annual simulation. Again, the SPF of cooling could be defined only with the annual simulation. Considering the other climates studied, the total seasonal performance factor of the climate of Gdansk is the lowest value since it is the climate with the worst boundary conditions.

5.6 Six-days sequence of Rome - collector area of 8 m^2

The last climate considered for the characterization of the sequence is the climate of Rome. Oppositely to Gdansk, Rome is the warmest climate considered.

The solar assisted heat pump system does not justify a collector area of 16 m^2 for the climate of Rome since the irradiation available is high. During the summer, the system uses solar energy only for the domestic hot water and the collector yield would be exaggerated for the use. A high collector area would produce stagnation conditions. For this motivation, this system considers a collector area of 8 m^2.

Figure 5-70 presents the temperature and irradiation profiles of the six-days sequence defined for Rome while the Figure 5-71 presents the load conditions. For this climate, the order of magnitude of heating load is similar to the cooling load and the domestic hot water is the dominant load.

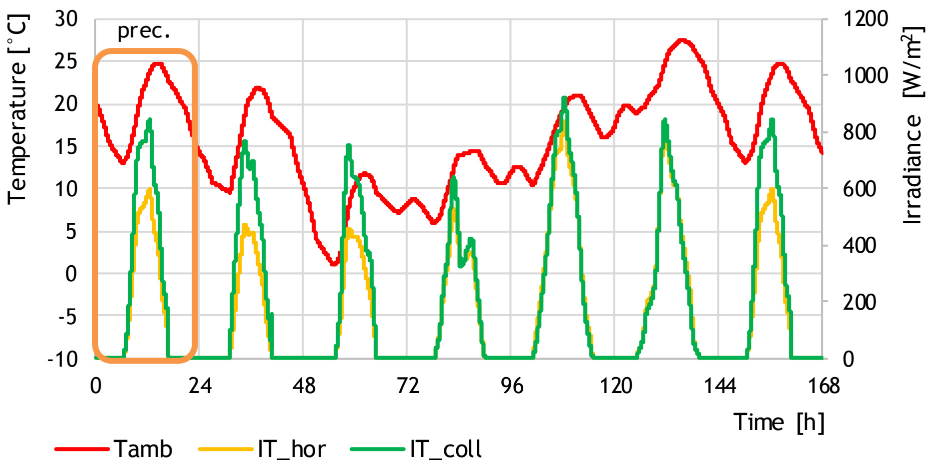

Figure 5-70: Profiles of the ambient temperature and irradiances on horizontal and collector surface during the six-days sequence of Rome.

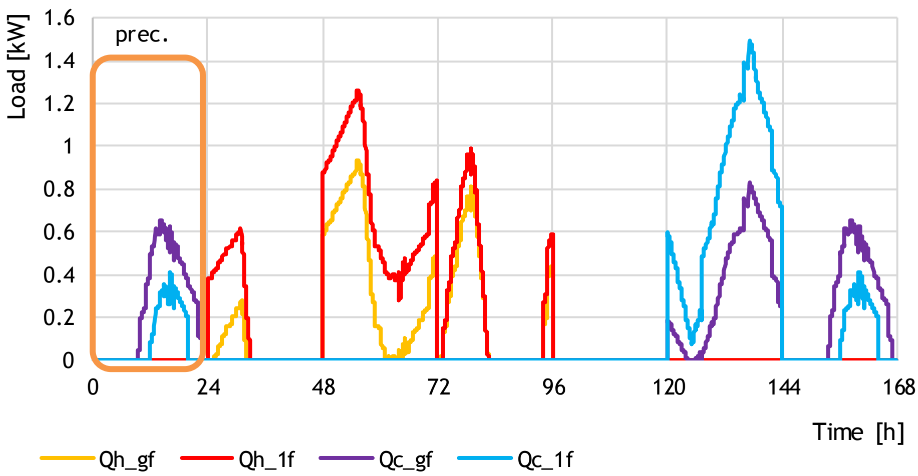

Figure 5-71: Building load profiles during the six-days sequence. Rome climate.

5.6.1 Sequence results

Figure 5-72 presents the electric consumption calculated with the test and with the sequence simulation. It can be noticed that the electric consumption is the lowest of the different tests since this climate requires a lower amount of heating and cooling demand. The electric consumption calculated with the test is 38.4 kWh while with the simulation is 29.6 kWh. At opposite the climate of Gdansk has required 84.3 kWh during the test (and 73.7 in the simulation) despite the double collector area at disposition of the system. However, it has to be considered that the load is different. In total, the test of Rome requires 141 kWh for the total load (space heating, space cooling and domestic hot water) while Gdansk requires 283 kWh for the total load. The comparison of the two climates shows that the SPF in the case of Gdansk is lower since the working condition are worse than Rome. Note that the domestic hot water is the same for the different sequence while the heating and cooling loads depend from the climate.

The test considers a higher consumption than the simulation ad exception of the Day 5. The motivation can be found in Figure 5-73 since the simulation satisfies a higher cooling demand; during the test, part of the cooling demand of day 5 has been satisfied during the last day since the heat pump started with a delay due to a technical problem. Again, these typologies of inconvenience could not be identified with a simulation but only observed experimentally.

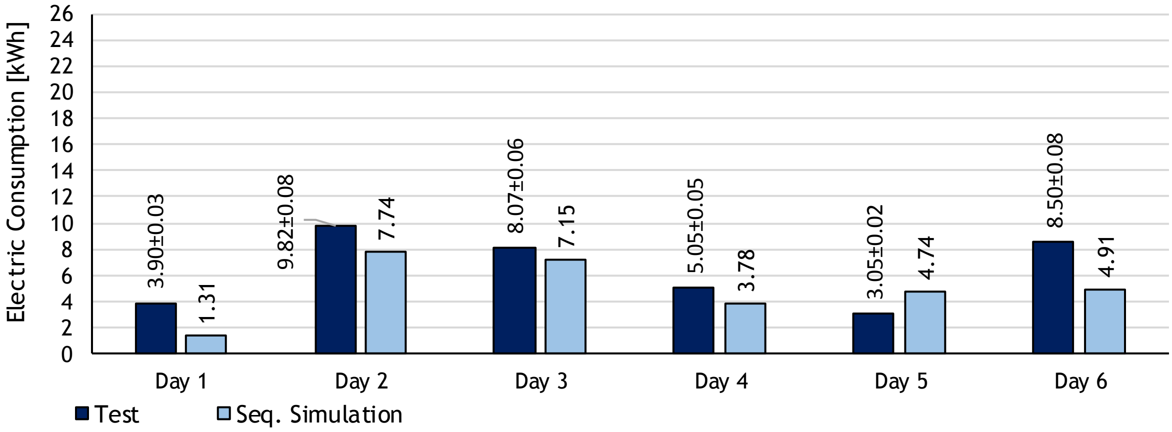

Figure 5-72: Daily total electric consumptions defined with test measurement and sequence simulation. Six-days sequence of Rome.

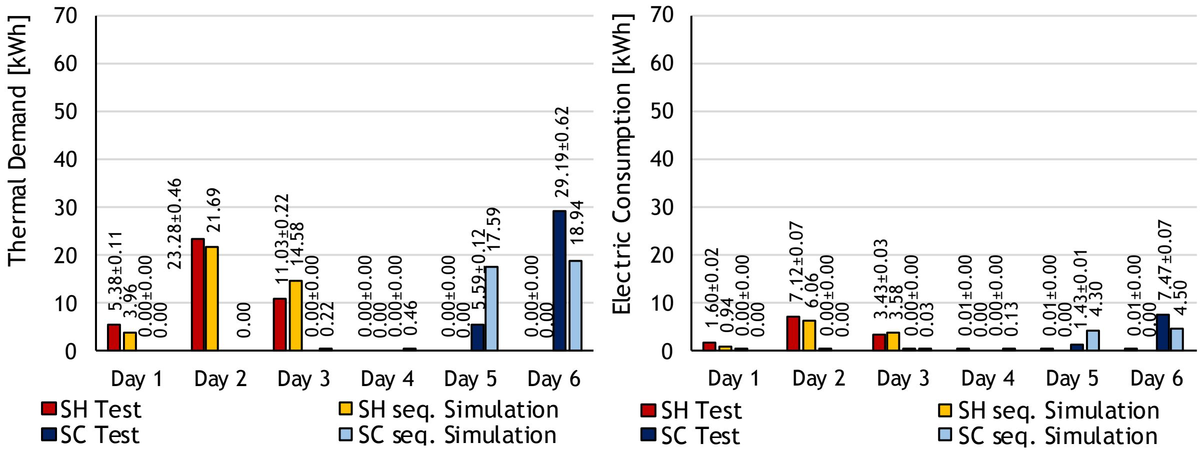

Figure 5-73: Daily SH/SC loads and SH/SC electric consumptions defined with test measurement and sequence simulation. Six-days sequence of Rome.

Moving to the domestic hot water load and its consumption, Figure 5-74 compares the test with the simulation. Also in this case, the test measures a higher consumption during the different days. The difference on the evaluation of electric consumption for the preparation of DHW between the test and simulation is ranged in the interval of 1 kWh/day and 2 kWh/day.

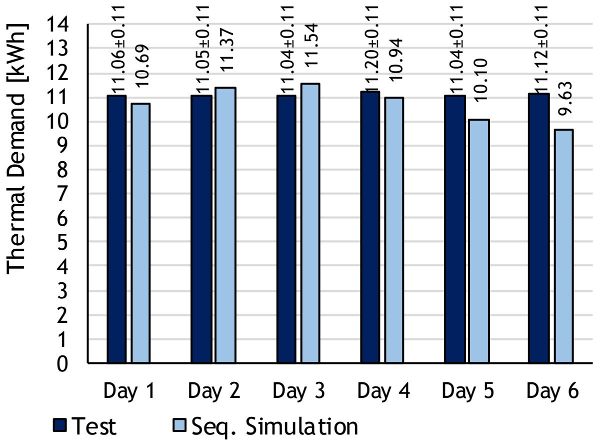

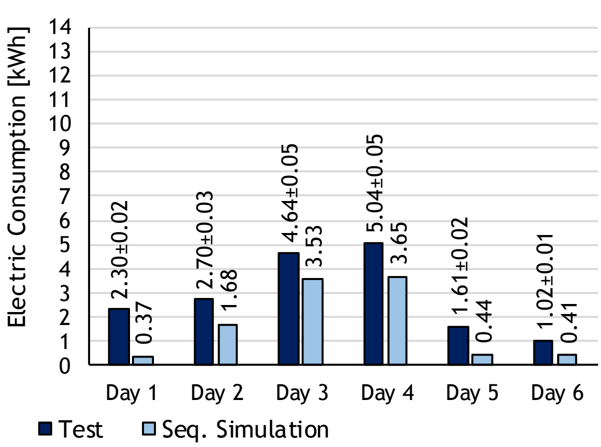

Figure 5-74: Daily DHW loads and DHW electric consumptions defined with test measurement and sequence simulation. Six-days sequence of Rome.

Figure 5-75 presents the total performance factor. In this case, the trend is driven by the domestic hot water since it is the load with the highest demand. The differences presented with Figure 5-74 on the electric consumption cause the difference on the total performance factor of each day. This affect also the seasonal performance factor as indicated in the next section.

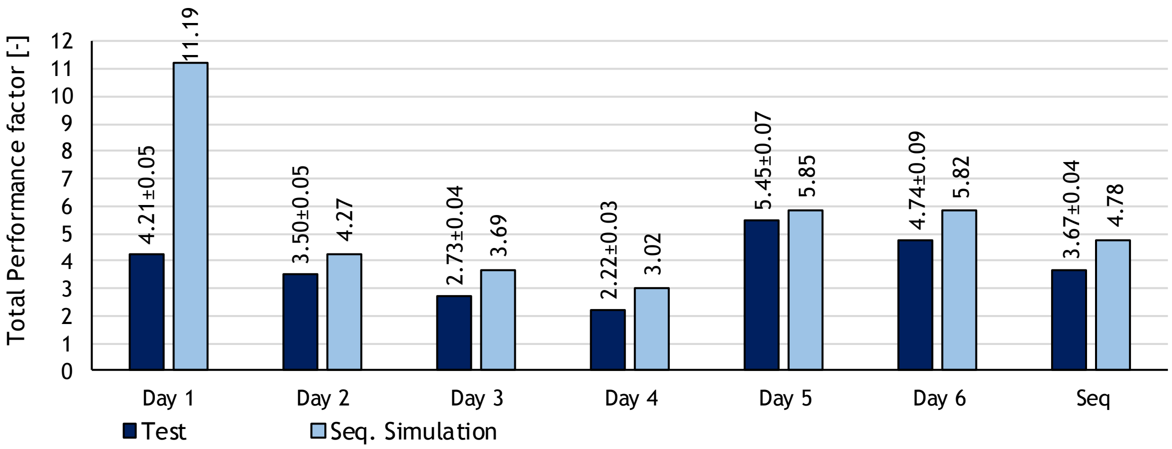

Figure 5-75: Daily total performance factors defined with test measurement and sequence simulation. Six-days sequence of Rome.

Figure 5-76 presents the collector yield calculated with the sequence simulation and with the test. The collector energy during the different days is almost the same.

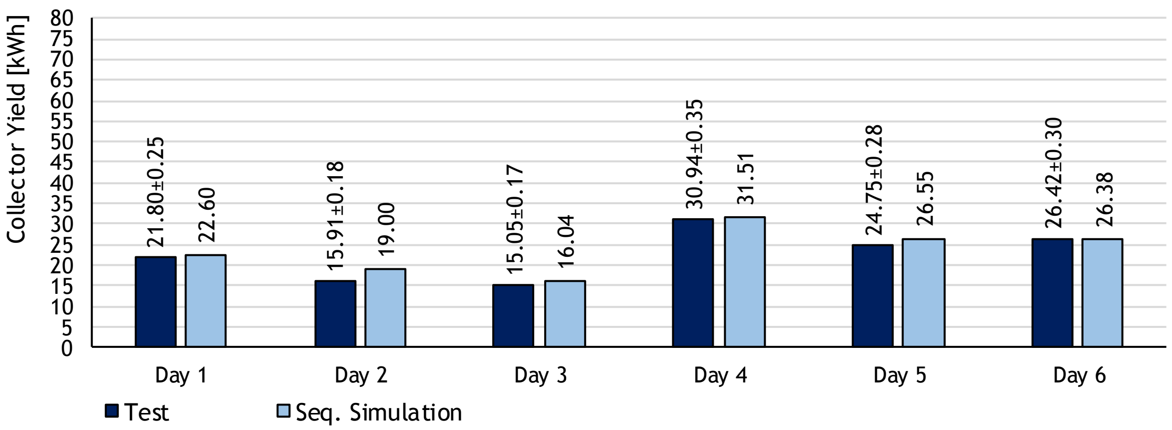

Figure 5-76: Daily collector yield defined with test measurement and sequence simulation. Six-days sequence of Rome.

5.6.2 Annual extrapolation

Table 5-7 present the clusters sizes and the connected loads and consumptions. In the Figure 5-77, the loads and consumptions are compared between the test, sequence simulation and annual simulation. It can be notices that the consumption for the domestic hot water calculated with test is the double to the ones simulated.

Table 5-7: Cluster energies evaluation. Six-days sequence of Rome.

	Cluster 1	Cluster 2	Cluster 3	Cluster 4	Cluster 5	Cluster 6	Test	Annual Simulation
Size	71	65	49	53	74	53	-	-
Q_{DHW} [kWh]	785	718	541	594	817	589	4044±40	3653
W_{DHW} [kWh]	163	176	227	267	119	54	1006±10	522
Q_{SH} [kWh]	382	1513	540	0	0	0	2436±48	3112
W_{SH} [kWh]	114	463	168	0	0	0	746±7	776
Q_{SC} [kWh]	0	0	0	0	414	1547	1961±42	3049
W_{SC} [kWh]	0	0	0	0	106	396	502±5	737
$Q_{col}l$ [kWh]	1548	1034	737	1640	1832	1400	8191±93	8992

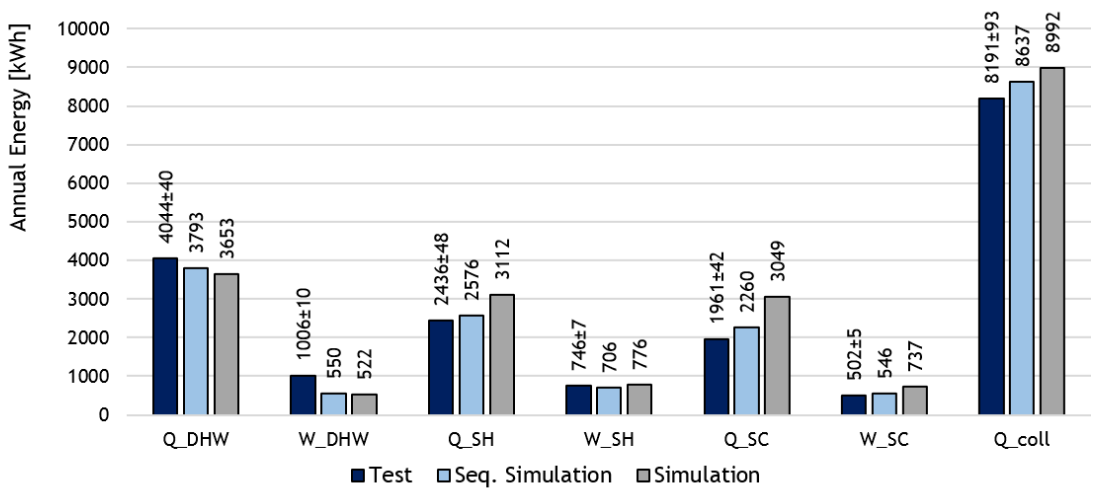

Figure 5-77: Seasonal energies extrapolated from test measurement, extrapolated from sequence simulation and defined with annual simulation. Six-days sequence of Rome.

Figure 5-78 presents the seasonal performance factors and the solar fractions for the different load calculated with the test, sequence simulation and annual simulation. As pointed previously, in this test the total SPF is mainly influenced by the DHW load. This test presents the highest deviation between test and simulation and in this case is due to the DHW. The DHW SPF calculated from test is 4.02 while the one calculated with the sequence simulation is 6.89 and with annual simulation is 6.99. The two simulations have a good correspondence to each other while the deviation with test is huge. As consequence, also the total SPF calculated with test is 3.74 compared to the 4.79 and 4.82 simulated with respectively sequence and annual boundary conditions.

The comparison of two simulations confirm the validity of clustering classification to create a short test sequence while the comparison with test confirms the necessity of performing a dynamic test to perform a reliable evaluation of performances.

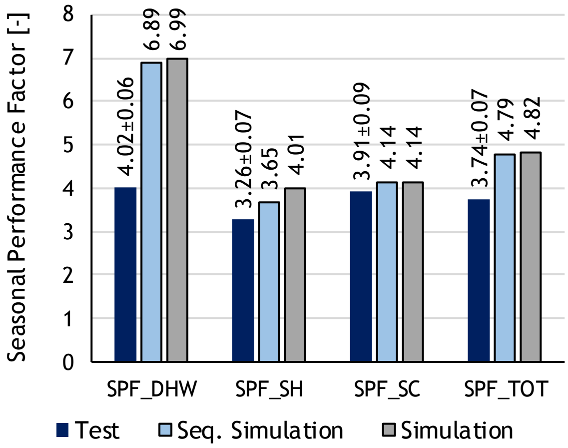

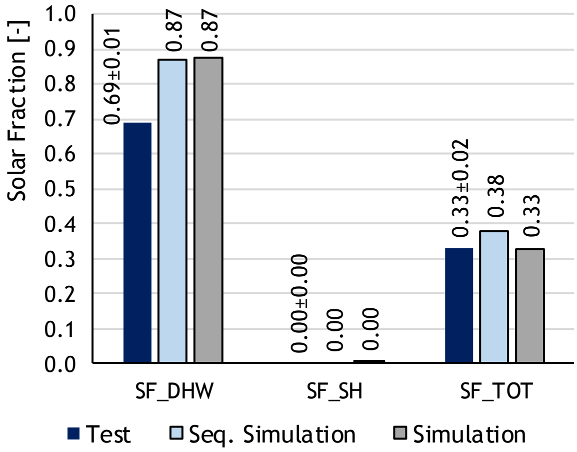

Figure 5-78: Seasonal performance factors and solar fractions extrapolated from test measurement, extrapolated from sequence simulation and defined with annual simulation. Six-days sequence of Rome.

5.7 Conclusions

This chapter has presented the procedure application to the whole system test. Different climates, plant configurations and sequence durations have been executed in laboratory and simulated numerically to verify the representativeness of the sequence with the procedure developed.

For each case, two simulations have been carried out: the first one is the simulation of the sequence and the second one is the simulation of the entire year. With the sequence simulation, the laboratory measurement could be compared directly to the simulation while the representativeness of the sequence is evaluated with the comparison of the sequence simulation and the annual simulation.

As general outcome, the tests highlight some limitations of the tested system while in the simulation these limits are not identified. Again, as the dynamic test performed at component level, the dynamic test is necessary to perform a reliable characterization of the system performance. In this way, the test performed in laboratory gives output that could be used to improve the system performance before its commercialization.

The evaluation of seasonal performance directly extrapolated from the test results are compared with the extrapolation from the sequence simulation and with the annual simulation. A summary of the results is reported in the Table 5-8 which contains the total seasonal performance factors and the solar fractions. The Table 5-9 presents the deviations of SPF between the test and the sequence simulation and the deviation between the sequence simulation and the annual simulation. The deviation between the sequence simulation and the annual simulation is lower than 8 % in both seasonal performance factor and solar fraction; instead, the results extrapolated from test deviates differently in the various conditions. The performance assessed with dynamic test is lower to the one simulated for all the cases considered.

The test performed with a larger number of days has evaluated the performance with more extreme boundary conditions and the performance obtained are lower. The aim of the test is to verify the working condition of the system under realistic conditions: a longer sequence allows to evaluate the performance with more stressing condition; however, this would involve in a more expensive experimentation phase.

Table 5-8: Summary of test results. Total SPF and total SF.

Test	SPF_{tot} test	SPF_{tot} seq. simulation	SPF_{tot} annual simulation	SF_{tot} test	SPF_{tot} seq. simulated	SF_{tot} annual simulated
BZ-6d-16m²	3.97±0.08	4.15	4.21	0.26±0.03	0.27	0.27
BZ-10d-16m²	3.54±0.07	4.02	4.21	0.27±0.03	0.26	0.27
BZ-6d-8m²	3.53±0.07	3.75	3.68	0.23±0.03	0.21	0.20
ZU-6d-16m²	3.75±0.07	4.12	3.82	0.30±0.03	0.30	0.23
GD-6d-16m²	3.44±0.07	3.85	3.62	0.17±0.03	0.22	0.21
RM-6d-8m²	3.74±0.07	4.79	4.82	0.33±0.03	0.38	0.33

Table 5-9: Summary of test results. SPF Deviations between test and sequence simulation and SPF deviations between sequence simulation and annual simulation.

Test	Test-Seq. Simulation	Seq. Simulation - annual simulation
BZ-6d-16m^2	-4.34%	-1.43%
BZ-10d-16m^2	-11.94%	-4.51%
BZ-6d-8m^2	-5.87%	1.90%
ZU-6d-16m^2	-8.98%	7.85%
GD-6d-16m^2	-10.65%	6.35%
RM-6d-8m^2	-21.92%	-0.62%

The results obtained presented some important outcomes for improving the control strategy of the system in particular in the management of:

- Collector activation: the transient phases are not well caught by the simulation.
- Storage charging phase: a delay on the activation of heat pump causes a reduction of temperature. The secondary pump should be activated only in the contemporaneity of the activation of heat pump that starts after some minutes than the primary pump.
- Utilization of solar heating scheme: the control hysteresis should be modified in order to avoid an undesired discharge of storage for the inertia of the system.
- Control of heat pump in cooling mode.

The results of this chapter, as the one of the second chapter, have confirmed the necessity of the adoption of dynamic test to characterize the system’s performance. If the dynamic tests are applied before the commercialization of new systems, the test results allow to optimize the systems and they would resolve problems that could occur in the real application.

6 Experience at SPF-HSR - Development of a six-days test sequence for the CCT method

This chapter presents the development of a six-days test sequence for the CCT method applied at the institute for solar energy SPF-HSR (Switzerland). The new sequence is needed after the harmonization work performed by SPF, SERC and CEA INES. The chapter 6.1 presents the method for the development of the test sequence. The sequence was optimized for one reference system and the effect of the sequence on about 100 different system was investigated and the results are presented in the chapter 6.2. Correction factors are defined and applied for the systems 6.3. The sequences defined during the internship at SPF-HSR and the one defined with the clustering is compared in the chapter 6.4.

6.1 Method

6.1.1 Boundary conditions and simulation set-up

Weather data

The weather data considered in this study is used in the Concise Cycle Test (CCT) method of the Institute for Solar Energy SPF-HSR [16,17]. This weather data set corresponds to a test reference year (TRY) that was resampled with a 1/32 h time step from measured data with a 10 min resolution measured by MeteoSwiss for Zürich - Fluntern from 1994-1998. The reason for using a time step of 1/32 h is technical of nature and had to do with the time step of test bench control and with restrictions of TRNSYS simulation time steps at the time the test is conceived.

Reference system and loads

The solar and heat pump (SHP) system shown in Figure 6-1 is used as reference system. The parameters that characterize the system are shown in Table 6-1. The collector field is made of flat plate collectors with an aperture area of 9.28 m^2, south oriented with a slope of 45°. The auxiliary heater is an air source heat pump with a heating power of 5 kW at design conditions (8.5 kW @A2W35). The solar collector field and the heat pump charge a 0.725 m^3 storage that delivers heat to DHW and space heating.

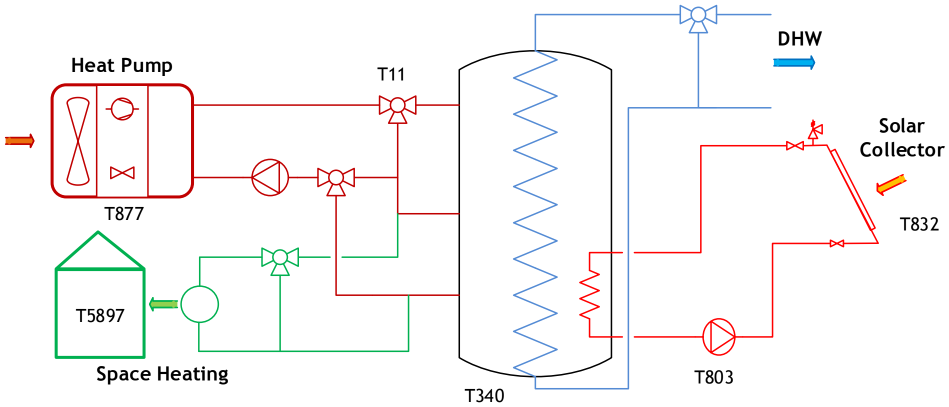

Figure 6-1: Simplified hydraulic scheme of reference air source SAHP system.

The heating load is given by the building (SFH045) defined in the IEA SHC Task 44/ HPP Annex 38. This building has a SH load of 60 kWh/m^2 (heated floor area of 140 m^2) for the climate of Zurich.

The DHW profile is defined by statistical distribution with the method defined in IEA SHC Task 26 [53]. For the six-days deck, the DHW load profile includes the cold water temperature, the mass-flow required at a 45°C set-point temperature (and consequently the energy required). The six-days DHW profile requires a total energy of 50 kWh. That is directly proportional to the DHW load used in the annual simulations (3042 kWh).

Table 6-1: System parameters.

Collector	Thermal Cap. [kJ/K]	Sens. rel. pos. [-]	Pipe conf. [-]	BU unit Tact. [°C]	Heat vert. tr. [W/mK]	U Piping [W/m²K]	UA Storage [W/K]	Stor. Vol. [m³]	Coll. Area [m²]	HP power [kW]
η_0: 0.793 a_1: 3.95 a_2: 0.0122	40000	0.7	4	-7	0.6	2.58	Side:2.81 Top: 0.67 Bottom: 0.3	0.76	9.28	5

Collector parameters: η0 [-], a1 [W/m²K], a2 [W/m²K²]. Thermal Cap.: distribution system thermal capacitance. Sens. rel. pos.: relative position of the sensor for the DHW and SH activation. Pipe conf.: configuration of the pipe connection to the storage. BU unit Tact: activation temperature of the back-up unit. Heat vert. tr.: heat vertical transfer of the storage. U Piping: heat loss coefficient of the pipes. UA storage: overall heat loss coefficients for the side, top and bottom of the store respectively. Storage volume. Collector aperture area. HP power: capacity of the heat pump at design conditions.

Simulation

The reference system is modelled in TRNSYS [46]. The building model is a non-standard TRNSYS component programmed by Leconte et al. [57] based on ISO 13790 [41]. The collector model was developed by SPF-HSR, type 832 [42], while the heat pump model was developed in the IEA SHC Task 44, type 877 [58]. The storage tank model is type 340 [59].

The same system model was simulated once with six-days weather data and once with annual weather data in order to be able to compare the two results. The TRY weather data from Zurich that was described previously is used for the annual simulation and a subset of it is used for the six-days sequence simulation as described in the next chapter. Both simulations are preconditioned with the last days of the weather data input file. For the annual simulation the preconditioning is done with the days of December and for the six-days simulations with the last two days of the respective six-days sequence.

6.1.2 Six-days sequence

Requirements

The aim was to find a test sequence of six-days that is representative for the annual conditions. To reach this objective some requirements are defined:

- The energy content of the system is the same at the end as it was at the start of the test sequence;
- The order of the days in the sequence is according to the order of the days in the annual weather data;
- The energy used and energy supplied (electric consumption, building load, DHW and solar yield) during the six-days sequence shall be directly proportional to the respective values of the annual simulation.

The procedure used to determine if the energy content of the system at the end of the test sequence differs from the energy content at the beginning of the test sequence is as follows: the core test sequence that comprises days **1-2-3-4-5-6** is preceded by two pre-conditioning days that correspond to day 5 and **day 6**, and at the end of the core test sequence **day 1** and **day 2** are repeated. Thus, the simulated sequence is **5-6-1-2-3-4-5-6-1-2**. If the energy content of the system at the beginning of **day 1** would differ from the energy content after **day 6**, then one would expect that the energy balance of the second **day 1** in the series would not be the same as for the first day 1 of the series. If the deviation between the two days 1 is negligible, then also the difference in energy content of the system at the beginning and at the end of the test sequence may with good reasoning be assumed to be negligible.

Another requirement for the selection of the days for the test sequence is that the order of the days of the sequence should correspond to the order of these days in the course of the TRY data. The reason for this is that this would allow to perform an annual simulation during the six-days test where days in between the test days are simulated at a “normal” speed, and a change to a time synchronous simulation speed is done for the six-days that are selected for the test sequence.

To simplify the elaboration of the results, it should be possible to calculate the annual energetic performance figures with a direct factor (365/6). Therefore, the annual values for electricity demand, fuel consumption, the heating demand and the collector gains are evaluated directly by multiplying the six-day sequence results with the factor 365/6:

Equation 6-1

$$E_{6d,a} = \frac{365}{6} \cdot E_{6d} \quad \text{[kWh]}$$

where E_{6d} is the total electricity demand, or the heating demand or the collector gains of the six-days sequence and $E_{6d,a}$ is the extrapolated annual energy.

The annual energy quantities derived using this multiplication factor based on the simulation of six-days are compared with the results from simulations of the entire year. The annual result is used as reference in the calculation of the deviation of the direct evaluation:

Equation 6-2

$$\delta_E = \frac{E_{6d,a} - E_{annual}}{E_{annual}} \quad \text{[-]}$$

where E_{annual} is the energy output of annual simulation; again, the equation is valid for total electricity demand, the heating demand, and the collector gains.

Since the sequence has to represent the electricity demand, the heating demand, and the collector yield, the seasonal performance factor is also reproduced correctly as a consequence when the electricity and building energies are correctly represented.

Sequence development

Considering the requirements previously described, Figure 6-2 shows a block diagram of the method used for the development of the six-days sequence. The definition of the sequence can be divided into main activities:

- Selection of an initial test sequence of six-days from the TRY-SPF data, matching closely the properties of the low-resolution six-days sequence of Solar Energy Research Center SERC/SP.
- Application of scaling factors for temperature and irradiance on single days for better correlation between six-days and annual results.
- Parametric study for determination of the universal applicability of the extrapolation factor of correction factors.

SERC defined a six-days sequence that allows for a direct evaluation of performance with a constant correction factor as indicated in Equation 6-1. Within the MacSheep project, the sequence was adapted with the aim to test solar assisted heat pump systems. In the new six-days sequence defined by SERC, the DHW profile was changed from the previously utilised in the Combitest method as presented in the MacSheep report [45]. This new DHW profile is used in the definition of the high resolution test sequence. The profile includes a large discharge at the end of the summer period (day 4) in order to reduce the solar energy content of the store before day 5, i.e. before the days that represent autumn and winter. There is also a large discharge at the end of day 6 in order to force a DHW charge of the store at the end of the day, so that the core sequence starts and ends just after a DHW charge of the store. This minimizes differences in system internal energy content at start and end of the core sequence.

Comparison of Meteo files

Figure 6-3 shows a comparison between two pairs of days taken from the two data sets. Since 100% equal days could not be found within the TRY data, Figure 6-3a considers two days with 13°C average temperature and 3460 Wh/m^2 solar irradiation on the horizontal, while Figure 6-3b considers two days with 7°C average temperature and 3860 Wh/m^2 solar irradiation on the horizontal. The consequence is that the hourly values of Meteonorm are similar, but not identical, to the TRY hourly values.

These figures show that fluctuations with a period lower than 60 minutes are not present in the Meteonorm data. With 10 min data, the temperature shows a small fluctuation while a large fluctuation is visible for the irradiance.

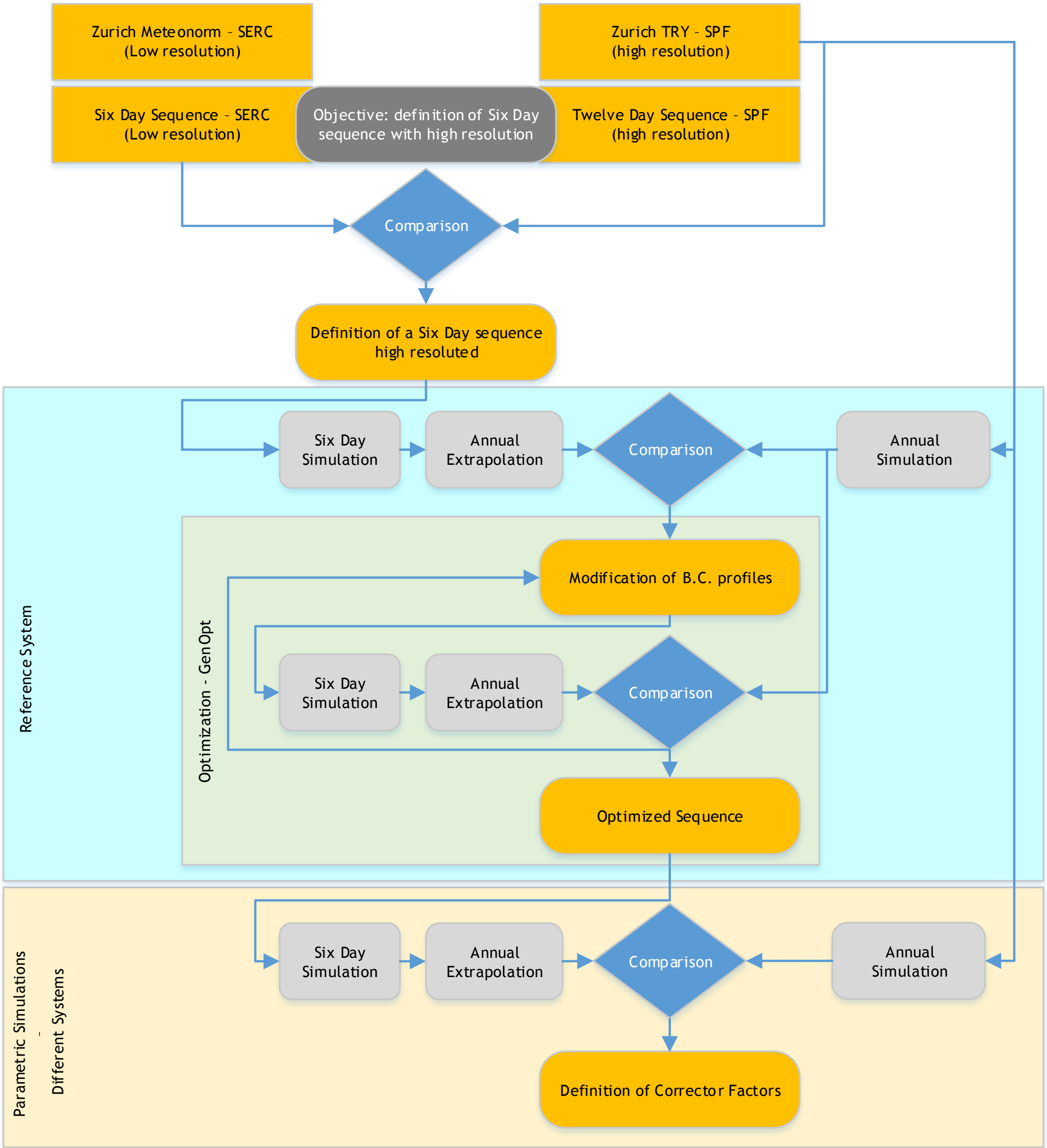

Figure 6-2: Block diagram of the method for the definition of the six-days sequence.

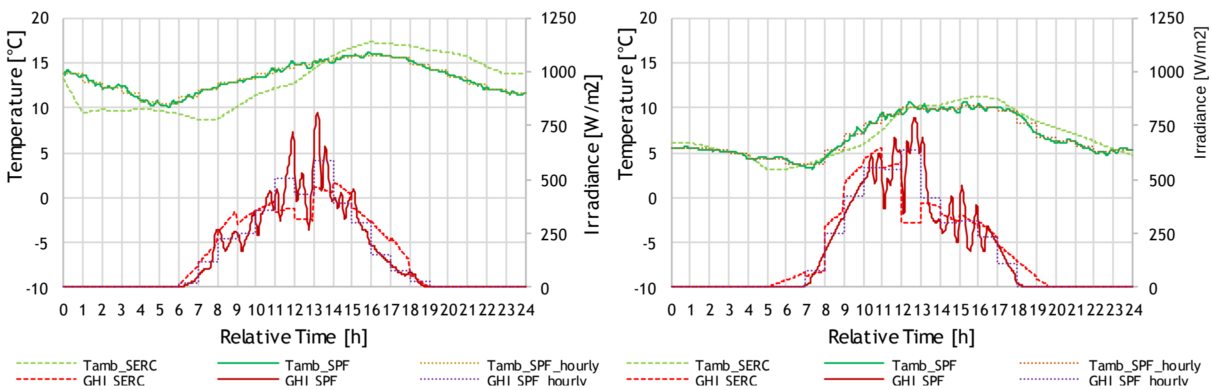

Figure 6-3: Comparison of days within the weather data with different resolution.

a) Comparison of day 96 of SPF-TRY and day 244 of Meteonorm. Days with average temperature of 13 °C and GHI of 3460 Wh/m². b) Comparison of day 77 and day 133. Days with average temperature of 7 °C and GHI of 3860 Wh/m².

Table 6-2 shows the comparison between the two data sets. The difference of annual average temperature (T_{amb} = 9.04°C) is small (about 0.02 K) while for the irradiation the difference is significant. The table shows the annual irradiation on global horizontal (GHI) and the total (ITC), beam (IBC) and diffuse (IDC) on collector surface. The Meteonorm' global horizontal irradiation is 2.1 % lower than the TRY value while the total collector irradiation is 6.6 % lower. A large difference is shown in the components of irradiation because the Meteonorm data present a large diffuse irradiation (46.2 % higher than the TRY). The origin of this difference has not been investigated further.

Table 6-2: Comparison of weather data files. Reference years of SPF and Meteonorm.

	Simulation resolution	Original resolution	T_{amb} [°C]	GHI [kWh/m²]	ITC [kWh/m²]	IBC [kWh/m²]	IDC [kWh/m²]
TRY	1/32h	10 min	9.04	1111	1262.6	793.6	469.0
Meteonorm	1/30h	60 min	9.06 (0.3%)	1088 (-2.1%)	1179.2 (-6.6%)	493.7 (-37.8%)	685.5 (46.2%)

Ambient average temperature (T_{amb}), global horizontal irradiation (GHI), total collector irradiation (ITC), beam irradiation on collector (IBC) and diffuse irradiation on collector (IDC).

<u>*Definition of sequence*</u>

To define the six-days sequence, days similar to the SERC test sequence were identified. Table 3 presents the characteristics of the days of the SERC sequence. The parameters considered are the ambient temperature (average, maximum and minimum values), total daily irradiation on horizontal surface and irradiation on collector surface.

Table 6-3: Characteristic of sequence defined by SERC.

Day	Annual Index	$T_{amb\ avg}$ [°C]	$T_{amb\ max}$ [°C]	$T_{amb\ min}$ [°C]	GHI [kWh/m²]	ITC [kWh/m²]
Day 1	32	3.25	6.27	1.27	1.660	2.208
Day 2	280	9.27	13.37	3.23	3.132	3.911
Day 3	168	12.78	18.96	6.66	6.465	7.440
Day 4	154	15.02	18.67	11.87	3.224	3.246
Day 5	281	5.71	9.97	2.37	2.435	2.809
Day 6	7	-4.24	-2.94	-5.63	0.443	0.450

Ambient average, maximum and minimum temperature (T_{amb}), global horizontal irradiation (GHI), total collector irradiation (ITC).

Six-days were identified in the SPF-TRY dataset with similar characteristics as those shown in Table 6-3. The resulting SPF-TRY days are listed in Table 6-4.

Table 6-4: Corresponding days. Index of days considering the annual order.

Sequence	Day 1	Day 2	Day 3	Day 4	Day 5	Day 6
SERC	32	280	168	154	281	7
SPF-HSR	281	109	122	169	78	7

A requirement is to have the day in the same order as they appear in the annual data. In order to fulfil this requirement, the Day 1 and Day 5 in the SPF-HSR sequence were exchanged. This change is justifiable because both are winter days. The sequence so-defined is shown in Table 6-5.

Table 6-5: Characteristic of first version of new sequence.

Day	Annual Index	$T_{amb\ avg}$ [°C]	$T_{amb\ max}$ [°C]	$T_{amb\ min}$ [°C]	GHI [kWh/m²]	ITC [kWh/m²]
Day 1	78	5.86	8.74	2.72	2.289	3.586
Day 2	109	9.21	15.07	4.32	4.075	4.326
Day 3	122	12.87	18.08	8.91	6.010	6.396
Day 4	169	15.82	19.88	12.42	3.266	3.555
Day 5	281	4.04	7.28	1.03	1.605	1.596
Day 6	7	-4.02	-1.90	-7.78	0.412	0.383

Ambient average, maximum and minimum temperature (T_{amb}), global horizontal irradiation (GHI), total collector irradiation (ITC).

To avoid unrealistic step variation between two consecutive days, for a period of three hours at the beginning and the ending of each day the temperature profiles are smoothed linearly.

GenOpt optimization

The sequence defined in Table 6-5 has been used for simulations of the reference system and the extrapolated annual performance based on the six-days sequence is determined with Equation 6-1. These results are compared to the annual simulation results of the same system and the deviation in total electricity demand is calculated with Equation 6-2. Optimization algorithms have been used in order to find scaling factors for irradiance and ambient temperature of each day that would minimize the objective function given in Equation 6-3.

Equation 6-3 $$ob.func. = |\delta_{W_{el}}| + |\delta_{Q_{buil}}| + |\delta_{Q_{coll}}| \quad [-]$$

The optimization is performed with GenOpt [60]. The aim of the optimization is to minimize the deviation between the annual results based on six-days simulation and extrapolation, and the annual results based on annual simulation, for a number of values: electric demand, heating demand and collector yield, thus an objective function is defined as the sum of the absolute values of the deviations of these three values.

The algorithm "Generalized Pattern Search Particle Swarm Optimization with Constriction Coefficient Hooke Jeves" (GPSPGOCCHJ) is used for the optimization. This is a hybrid GPS algorithm where first a "Particle Swam optimization" is run and then a "Hooke Jeves" algorithm is used to refine the results. With this kind of algorithm the probability to find a global minimum instead of only a local one is higher [61,62]. Further information can be found in the GenOpt manual [60].

Within the optimization process, the weather data profiles were modified by shifting the outdoor temperature of the single days (Equation 6-4) within a range of maximum ± 2K and by scaling the solar irradiance of single days (Equation 6-5) in a range of maximum ±15 %. These limits for shifting or scaling are introduced in order to stay within realistic values for the corresponding variables.

Equation 6-4 $$T_{day\_i}(\tau) = T_{day\_i}(\tau) + T_{cd,i} \cdot FF(\tau) \quad [°C]$$

Equation 6-5 $$I_{day\_i}(\tau) = I_{day\_i}(\tau) \cdot I_{cd} \quad [W/m^2]$$

Where "i" indicates the daily corrections (from 1 to 6).

In Equation 6-4 a forcing function was used to reduce the effect of the $T_{cd,i}$ coefficients in order to avoid a sudden change in temperature between two days that would result when two different shifting factors are applied to the two consecutive days. The forcing function FF(τ) is shown in Figure 6-4.

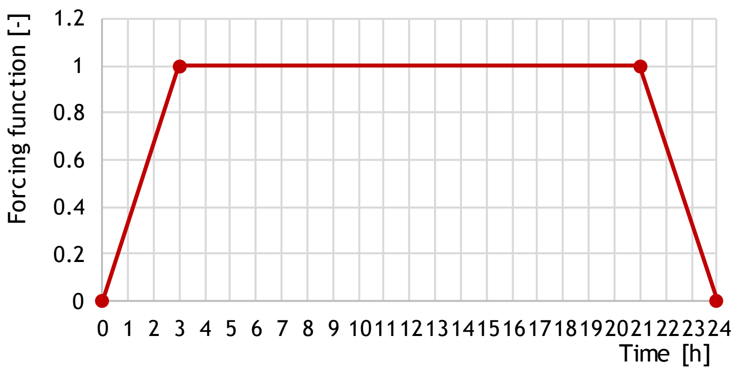

Figure 6-4: Forcing function.

The output of the optimization are the coefficients (T_{cd} and I_{dc}) needed to modify the six-days sequence in order to achieve a small deviation between the extrapolation of six-days results to annual values and the annual results that are based on annual simulations.

6.1.3 Parametric simulation

The influence of changes in system parameters on the deviation between the six-days extrapolated results and the annual simulations has been investigated by changing different parameters of the reference system (size of heat pump, size or efficiency of collector field, thermal losses etc.). Thus, about 100 different systems with air to water heat pump are considered varying the parameters described in Table 6-6. In addition, 7 collectors (flat plate or evacuated tube collector) with different efficiencies are considered. The collector efficiency parameters were taken from online fact sheets of the Institute for Solar Energy SPF-HSR [63] and are shown in Table 6-7.

Table 6-6: Range of variation of parameters for parametric simulations of different systems simulation.

	Thermal Cap. [kJ/K]	Sens. rel. pos. [-]	Pipe conf. [-]	BU unit Tact. [°C]	Heat vert. tr. [W/mK]	U Piping [W/m²K]	UA Storage [W/K]	Storage Volume [m³]	Coll. Area [m²]	HP power [kW]
Min	1150	0.5	3	-7	0.6	1.31	Side: 1.41 Top: 0.34 Bottom: 0.15	0.763	9.28	3.75
Max	40000	0.7	4	100	12.0	7.75	Side: 8.43 Top: 2.01 Bottom: 0.9	1.335	16.24	6.25

Thermal Cap.: heat distribution system thermal capacitance. Sens. rel. pos.: relative position of the sensor for the DHW and SH activation. Pipe conf.: configuration of the pipe connection to the storage. BU unit Tact: activation outdoor temperature of the back-up unit. Heat vert. tr.: vertical heat transfer of the storage. U Piping: thermal transmittance of the pipes. UA storage: storage thermal conductance; the UA values of the storage are respectively the side, top and bottom values. Storage volume. Collector aperture area. HP Power: design power of the heat pump.

Table 6-7: Collectors.

Collector	Reference	Coll_1	Coll_2	Coll_3	Coll_4	Coll_5	Coll_6
Type	FP	FP	FP	FP	ET	ET	ET
η0 [-]	0.793	0.793	0.857	0.728	0.833	0.661	0.525
a1 [W/m²K]	3.95	1.95	4.16	3.94	1.85	2.43	1.05
a2 [W/m²K²]	0.0122	0.0122	0.0089	0.007	0.0007	0.0078	0.002
C_col [J/ m²K]	7000	7000	6800	6600	9000	23000	13000

FP: indicates flat plate collector. ET: evacuated tubes collectors. η0, a0, a1: efficiency coefficients. C_col: Collector' specific thermal capacity.

6.2 Results

6.2.1 Reference system results

Table 6-8 show the correction applied with Equation 6-4 and Equation 6-5 after the optimization. The Figure 6-5 presents the initial test sequence with dotted lines (selected days, without smoothing) and the profiles after the optimization with the continuous lines. The irradiance of the days with maximum and minimum irradiance are not changed during the optimization process in order not to lose the extreme irradiance conditions.

Table 6-8: Shifting and multiplication factors for temperatures and irradiance on the six chosen days, determined by optimization algorithms.

	Temperature [K]	Radiation [-]
D1	1.84	0.92
D2	1.6975	1.00
D3	1.86	1.00
D4	0.4	0.92
D5	1.44	1.00
D6	-1.68	1.00

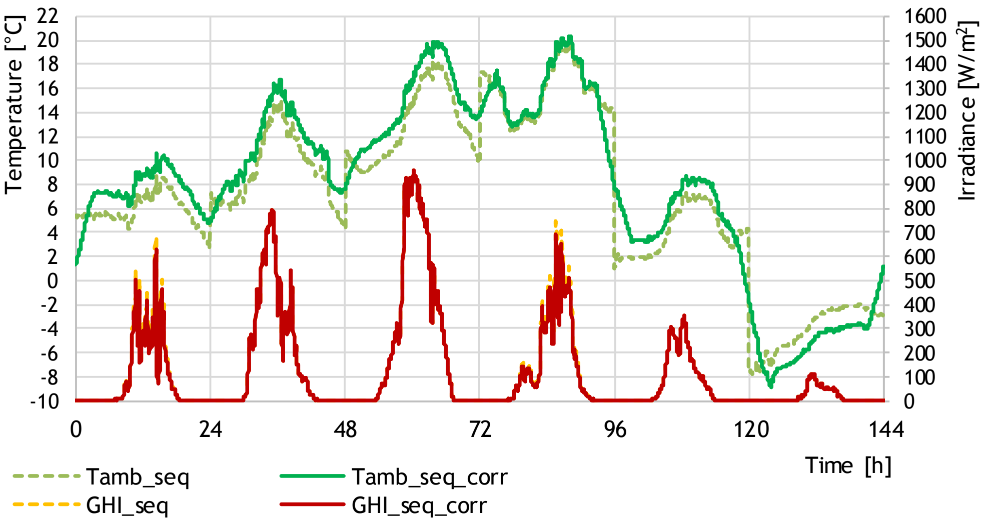

Figure 6-5: Ambient temperature and solar irradiance on collector plane of the six-days sequence before and after the optimization.

If one would replace the original days in the annual sequence with the optimized daily profiles, the annual average temperature would change about 0.02 K, while total annual irradiation changes about 0.44 kWh/m^2 (of 1111 kWh/m^2).

Figure 6-6 shows the frequency of combined daily values for GHI and temperature within the whole year. The non-optimized and optimized test sequence days are indicated in the annual distribution. The square points (blue) indicate the sequence before the optimization while the round points (red) indicate the number after the optimization. Day 6 represents an extreme winter condition with low temperature and nearly no solar irradiation. The extreme summer conditions are not present but the summer is represented by day 4 while day 3 is "late spring".

T [°C] \ GHI [Wh/m²]	0	500	1000	1500	2000	2500	3000	3500	4000	4500	5000	5500	6000	6500	7000	7500	8000
-8	0	0	2	0	0	0	0	0	0	0	0	0	0	0	0	0	0
-7	0	0	0	1	0	0	0	0	0	0	0	0	0	0	0	0	0
-6	0	6 0	1	1	1	0	0	0	0	0	0	0	0	0	0	0	0
-5	0	0	0	1	0	0	0	0	0	0	0	0	0	0	0	0	0
-4	0	6 2	2	4	0	0	0	0	0	0	0	0	0	0	0	0	0
-3	0	3	2	1	1	0	0	1	0	0	0	0	0	0	0	0	0
-2	0	4	0	0	1	1	0	0	0	0	0	0	0	0	0	0	0
-1	1	7	0	4	0	0	1	0	0	0	0	0	0	0	0	0	0
0	0	0	3	1	0	1	0	0	1	0	0	1	0	0	0	0	0
1	0	6	4	1	1	1	1	1	0	0	0	0	0	0	0	0	0
2	2	5	6	1	2	0	0	0	0	0	1	0	0	0	0	0	0
3	1	6	4	2	2	0	0	1	0	0	0	1	0	0	0	0	0
4	3	2	2	1 5	0	1	1	1	0	0	1	0	0	0	0	0	0
5	1	1	6	2	1	0	1	2	1	0	0	1	0	0	0	0	0
6	0	5	1	2 5	0	1 1	2	0	0	0	0	0	0	0	0	0	0
7	2	3	3	1	2	2	0	2	1	0	1	0	0	0	1	0	0
8	1	1	0	2	2	3 1	0	2	0	0	1	1	0	0	0	0	0
9	0	2	0	0	3	1	0	1	1 2	1	1	0	0	0	0	0	0
10	0	3	1	4	3	4	1	2	0	0	1	0	0	0	0	0	0
11	0	0	3	1	1	1	6	0	2 2	3	1	3	0	0	0	0	1
12	0	0	2	0	0	4	1	2	1	3	1	4	1	0	0	0	0
13	0	1	2	0	2	3	0	4	1	2	0	1	3 3	0	0	0	0
14	0	1	0	2	0	0	0	1	2	0	4	3	2	0	0	1	0
15	0	0	0	3	1	1	0	1	1	0	2	3	1 3	0	3	1	0
16	0	0	0	1	0	0	2	1 4	0	0	2	1	2	0	1	4	1
17	0	0	0	1	0	0	1 4	1	0	1	3	0	0	0	0	1	0
18	0	0	0	0	1	1	1	1	0	0	1	0	0	1	3	3	1
19	0	0	0	1	1	0	1	0	2	1	3	0	0	0	2	1	1
20	0	0	0	0	0	0	0	0	0	0	1	3	0	1	1	2	2
21	0	0	0	0	0	0	1	0	0	0	0	2	1	1	1	0	2
22	0	0	0	0	0	0	0	0	0	0	0	0	0	0	2	0	0
23	0	0	0	0	0	0	0	0	0	0	0	0	1	0	0	0	0
24	0	0	0	0	0	0	0	0	0	0	0	0	0	1	1	0	0
25	0	0	0	0	0	0	0	0	0	0	0	0	0	1	0	0	0
26	0	0	0	0	0	0	0	0	0	0	0	1	0	1	0	0	0

Figure 6-6: Frequency of combinations of daily average temperature and irradiation of the whole year and location of the selected test days within the frequency plot.

Table 6-9 presents the deviation in the annual evaluation of energy with the six-days sequence before and after the optimization. Equation 6-2 is used to calculate the electric, building, collector and seasonal performance factor (SPF) deviations, while Equation 6-3 is used to calculate the objective function. The non-optimized days achieve an objective function value of 20.0% (2.5% from electric energy, 11.4% from building heating demand and 6.1% from solar yield), and a deviation of the seasonal performance factor of 5.3%. The optimization reduced the objective function to 2.69 % with respectively 0.12 %, 1.58 % and 0.99 % of deviations from electric energy consumption, heating demand and collector energy.

Table 6-9: Deviation of annual extrapolated results from simulated results based on the original and optimized test sequence. Simulation of the reference system described in the section 2.1.

	W_{el} [%]	Q_{bui} [%]	Q_{coll} [%]	SPF [%]	Obj. func. [%]
Original sequence	2.5	11.38	6.06	5.33	20.0
Optimized sequence	0.12	1.58	0.99	1.00	2.69

Table 6-10 shows the daily performance of the optimized sequence. The “sequence” rows consider the sum of energies calculated in the core sequence (following different periods of evaluation) and from those, the “annual extrapolated” rows are calculated with the direct extrapolation (Equation 6-1). The deviations (“deviation” rows - Equation 6-2) are defined from the comparison with the annual simulation data (“annual” row).

Day 1 and Day 6 have high space heat demand, while day 4 does not have a space heat demand at all. The daily performance factor depends on the contribution from solar. The highest performance factor is reached during the day 4 which load is satisfied by solar energy collected in the previous day and during the same day. At opposite, the lowest performance factor is obtained in the day 6 which has the highest heat demand and does not have solar contribution. The DHW load on the different days is different because it is defined with a statistical distribution.

One requirement is to have the same energy content of the system at the start and at the end of the sequence. This is checked by simulating twice the day 1 and the day 2 at the end of the sequence. The difference of energy consumption between the first simulation of the day 1 and the second simulation (after 8 days) is about 10%. Instead, the difference between the first simulation of day 2 and the second simulation is about 2%. The annual extrapolation with the sequence 1-2-3-4-5-6 (indicated in the table with “sequence 1-6”) has a lower deviation with the annual simulation than the sequence 2-3-4-5-6-1 (indicated in the table with “sequence 2-1”) since the sequence 1-2-3-4-5-6 is considered in the GenOpt optimization. However, the sequence defined as days 1-2-3-4-5-6 is not satisfying the requirement. In this case, the sequence to consider for the extrapolation of annual result is 2-3-4-5-6-1.

Table 6-10: Daily performance.

	W_{el} [kWh]	Q_{dhw} [kWh]	Q_{bui} [kWh]	Q_{coll} [kWh]	PF [-]
Day 5	16.76	11.35	21.89	4.42	1.98
Day 6	33.06	9.07	63.97	0.00	2.21
Day 1	14.36	8.29	41.96	9.67	3.50
Day 2	5.02	4.31	15.27	16.88	3.90
Day 3	2.52	9.28	5.07	27.58	5.69
Day 4	0.57	7.71	0.00	6.66	13.45
Day 5	3.62	11.35	6.28	2.07	4.87
Day 6	29.36	9.07	57.01	0.00	2.25
Day 1	12.81	8.29	39.19	9.46	3.71
Day 2	4.90	4.31	14.97	17.20	3.94
Sequence 1-6	55.5	50.0	126	63	3.17
Sequence 2-1	53.9	50.0	122.8	62.7	3.21
Annual Extrapolated 1-6	3374	3042	7640	3824	3.17
Annual Extrapolated 2-1	3279	3042	7471	3812	3.21
Annual	3380	3042	7519	3777	3.12
Deviation 1-6	-0.12%	0.0%	1.58%	0.99%	1.00%
Deviation 2-1	-2.58%	0.0%	-1.37%	-1.26%	2.88%

6.2.2 Parametric results

The test sequence has been optimized only for the reference system. It is desired that the relative change of energy (electric, building or collector) introduced by a system change would be the same for the test sequence as for the annual simulation. This would mean that the test sequence can be used for the determination of the annual performance independently from the system parameters.

Equation 6-6 represents the percent change of energy from the annual simulation of the "i-th" system compared to the reference system, while Equation 6-7 represents the percent change of energy in the six-days simulation. The deviation between the six-days sequence and the annual sequence in the "i-th" system can be calculated with Equation 6-2. These equations are calculated for the electric, building and collector energies.

Equation 6-6 $$\Delta E_{annual(i-ref)} = \frac{E_{a,sys,i} - E_{a,sys,ref}}{E_{a,sys,ref}} \qquad [-]$$

Equation 6-7 $$\Delta E_{6d(i-ref)} = \frac{E_{6d,sys,i} - E_{6d,sys,ref}}{E_{6d,sys,ref}} \qquad [-]$$

The first point analysed is the requirement of having the same energy in the system at the start and the end of the sequence. Figure 6-7 shows the box plot for the electric consumption and the building demand for the entire set of simulation and for the differences between the first and second simulations of day 6, day 1 and day 2. From the figure, it can be seen that the biggest difference is obtained during the preconditioning (day 6) while it is reduced in the day 1 and day 2. The difference between the two simulations of day 1 in the reference system (highlighted in the discussion of Table 6-10) is near to the maximum point of the entire set.

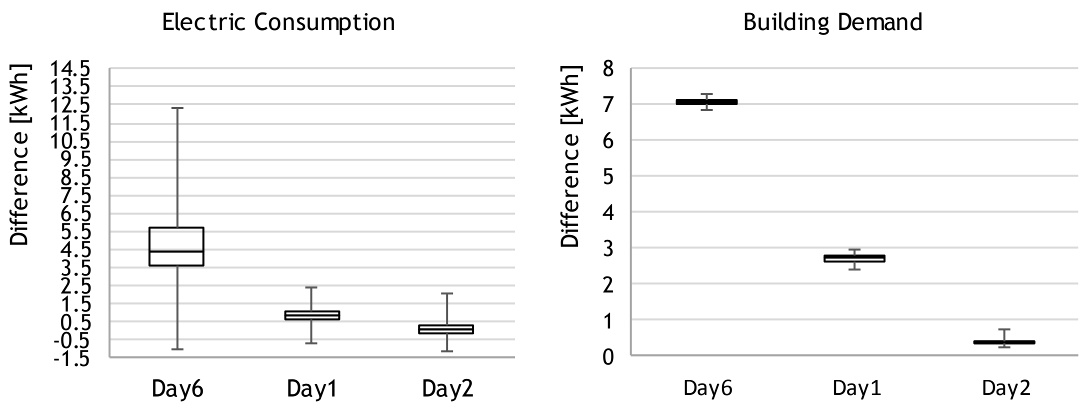

Figure 6-7: Box plot of differences between first simulation and second simulation of day 6, day 1 and day 2 for the parametric simulations. Electric consumption and building demand.

For the whole set of simulations, the annual energies are evaluated from different periods of evaluation that are 1-2-3-4-5-6, 2-3-4-5-6-1 and 3-4-5-6-1-2.

Figure 6-8 shows the deviations of electric energy, collector yield, building demand and SPF obtained for those periods of evaluation for the different systems considered in the parametric analysis. The change of system parameters does not affect the total load because the change on building heating demand is negligible (lower than 0.5%) and the DHW profile is fixed. However, a change of the system parameters may affect the electric consumption and the collector yield. Since the load is constant, the seasonal performance factor changes solely as a consequence of the electric energy change.

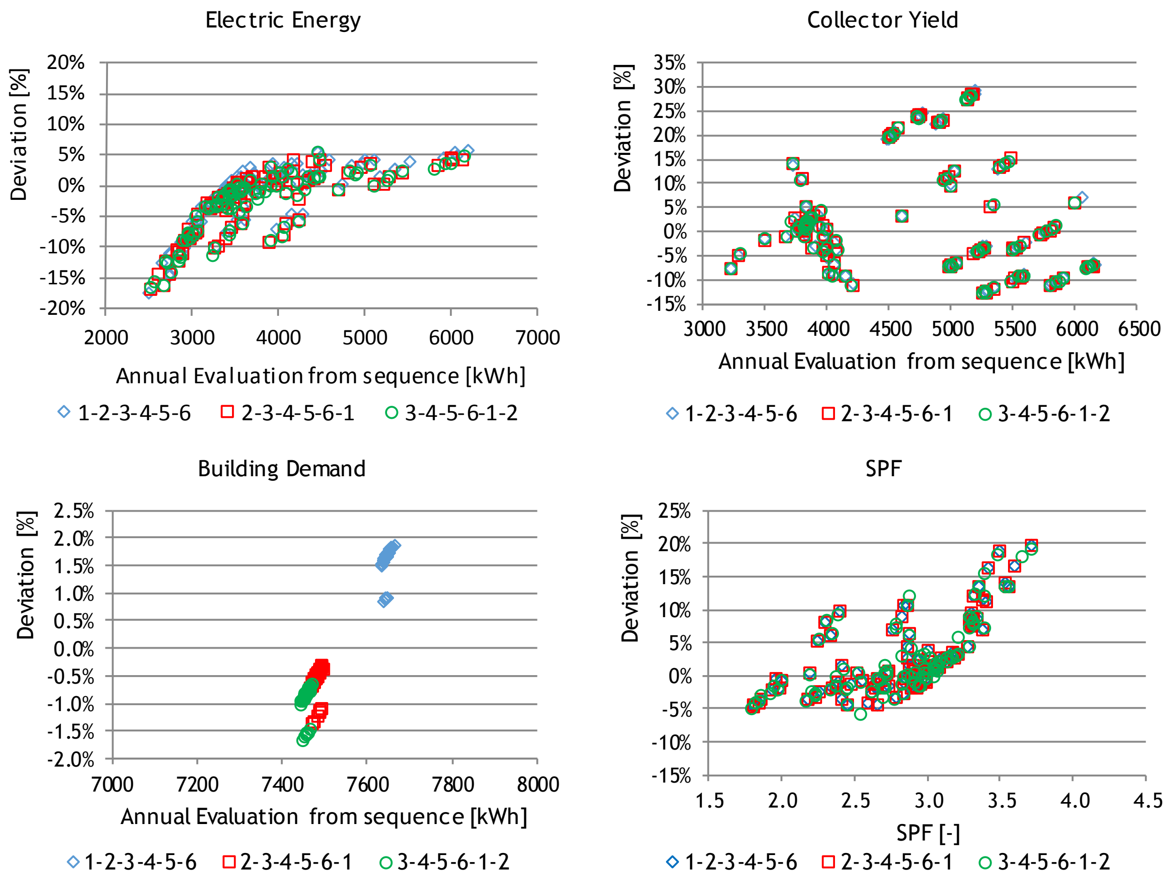

Figure 6-8: Deviation of annual extrapolation from the sequences with the annual simulation. Electric consumption and building demand, collector yield and SPF.

Figure 6-9 shows the electric energy changes and the collector energy changes of the test sequence, i.e. the difference between the reference system and "i-th" system, as a function of the change in the annual simulation, in percent of the reference system's value (square symbols, see also Equation 6-6 and Equation 6-7). At the same time, the deviation between the annual extrapolated result and the annual simulated result is shown with round symbols. The lines presented in the figures indicate the best case when the energy change in the six-days sequence is equal to the one obtained in the annual simulation and therefore the deviation between annual extrapolated and annual simulation is zero. Most test sequence simulations agree with the annual simulations also in case of high change of electric consumption compared to the reference, while a few simulations also show a significant deviation if the relative change is not large.

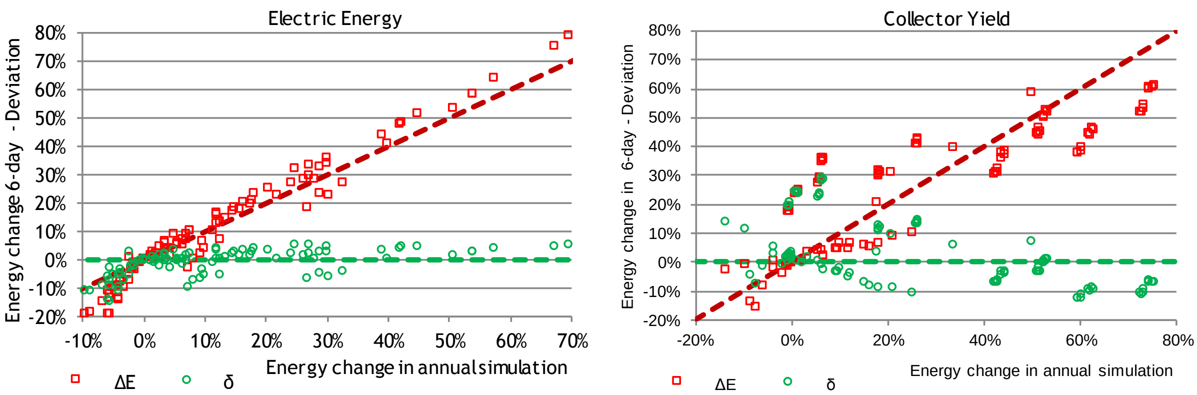

Figure 6-9: Electric energy consumption changes and collector yield changes in the annual and six-days simulation, resulting from change of different system parameters.

Figure 6-9 considers simulations obtained by changing different system parameters simultaneously. To analyse these parameters independently, they are divided in different groups. In Figure 6-10 and Figure 6-11, the following parameter groups are considered: system size, collector efficiency, thermal losses and layout. The induced change of energy that can be seen in these figures is lower than the induced changes of Figure 6-9, because the following pictures consider only one independent variable modification while the previous figures superimpose effects from different parameters.

The group “size” considers the change of HP size and the change of the collector area with either constant store volume or with constant specific store volume (78 l/m^2). The second group considers the different collectors of Table 6-7. The group “losses” considers the change of UA-values of pipes and storage; these changes are considered with different combinations; the legend indicates which parameter is varied. The last group “layout” considers all other parameters of the system.

The correspondence between the extrapolation from the six-days sequence and the annual deviation is good for the group “layout” while the other groups have a deviation between extrapolated and annual simulation results that increases with the increasing effect on the energetic performance induced by the variable’s change.

The effect of collector efficiency and area is similar and can be explained together, although the importance of the effect on the deviation is slightly different. Increasing the nominal power of collector array means that the collector gains increase while the electric consumption decreases. The six-days sequence, compared to the annual simulation, overestimates the changes in electric consumption and collector gains induced by larger or more efficient collector fields. Our hypothesis is that in the annual sequence, stagnation occurs on summer days and on these days a better collector efficiency or larger collector field does not increase the collector yield, whereas in the six-days sequence, no stagnation occurs and better efficiency or larger collector field will lead to additional yield on all days.

Higher thermal losses lead to fewer days with collector stagnation. This increases the amount of heat delivered by the collectors in the annual simulation, where days with stagnation are present, but it does not equally increase the yield in the six-days sequence, where collector stagnation does not occur.

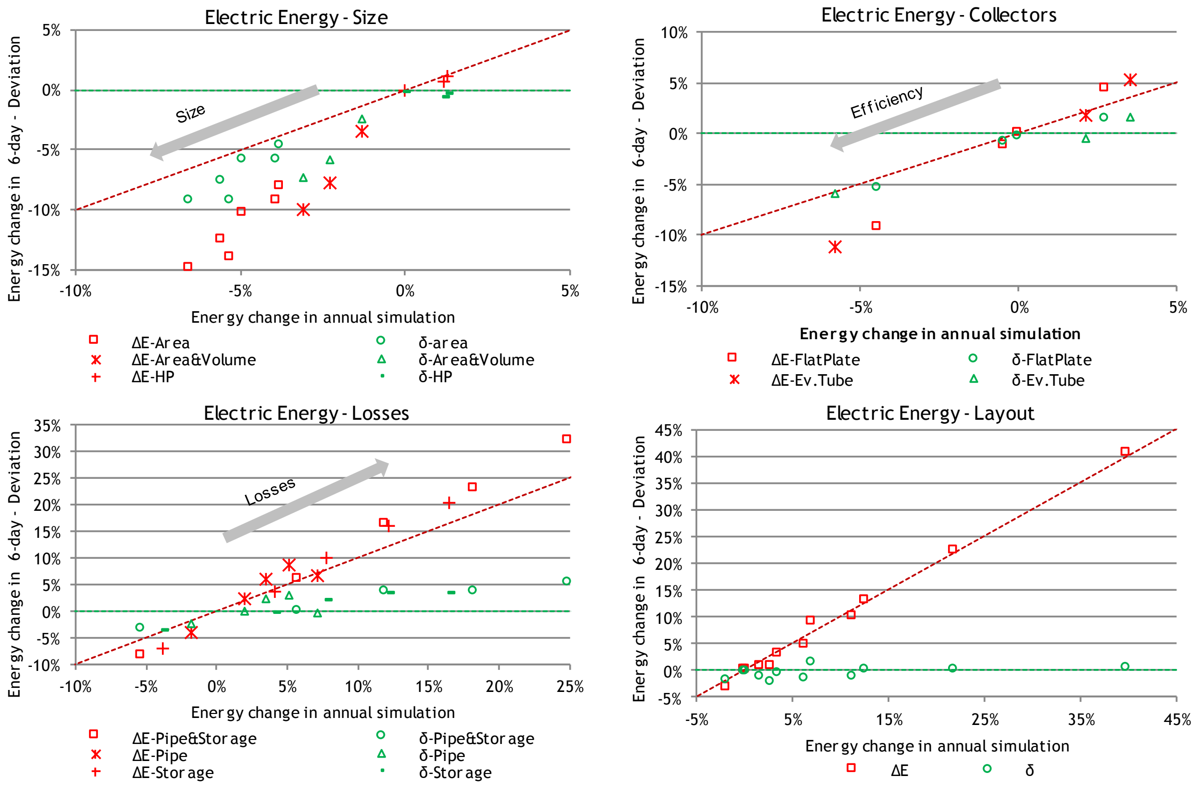

Figure 6-10: Electric energy consumption change in the annual and six-days simulations and deviation between annual extrapolated and annual simulated, induced by change of different system parameters.

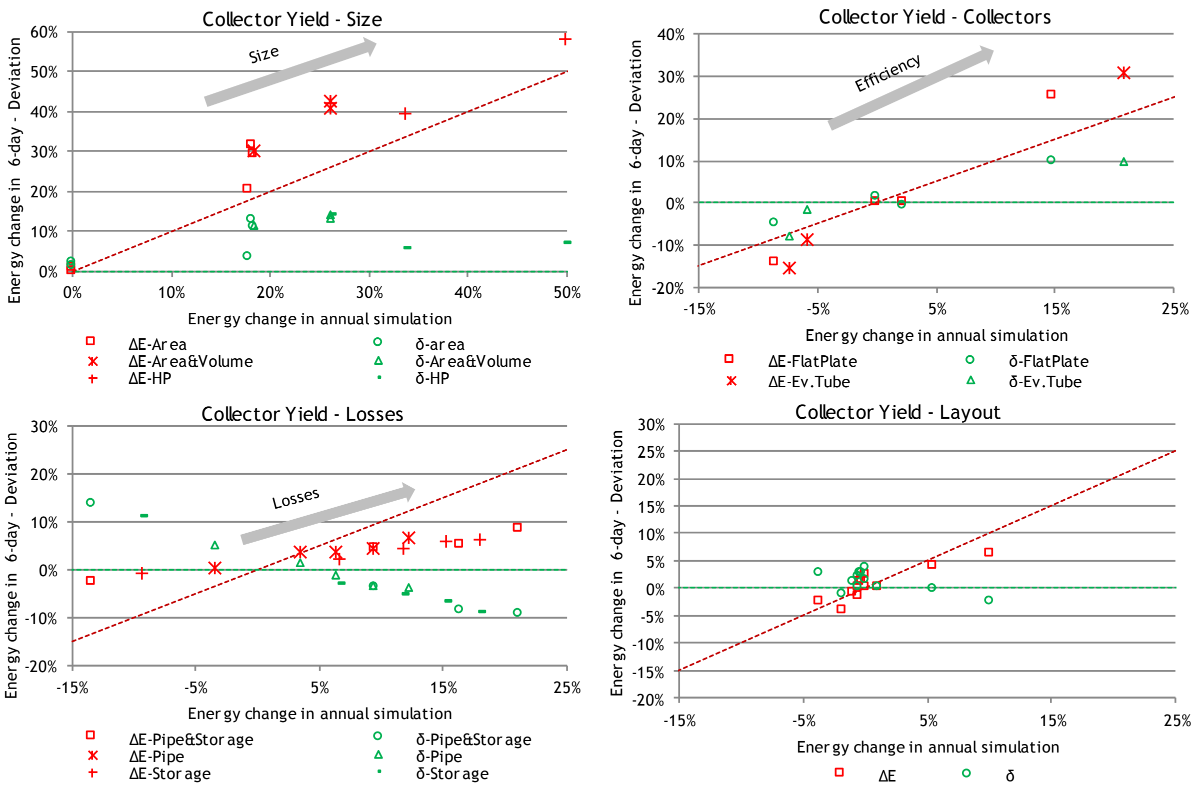

Figure 6-11: Collector yield change in the annual and six-days simulations and deviation between annual extrapolated and annual simulated, induced by change of different system parameters.

6.3 Correction factors

6.3.1 Formulation of correction factors

The previous chapter showed that the influences of thermal losses and solar collector field power lead to systematic deviations between the extrapolated and the simulated annual results. The deviation shown in (Equation 6-2), can be reduced by the application of correction factors as indicated by Equation 6-8 and Equation 6-9:

Equation 6-8 $$E_{6d,corr} = E_{6d,a} \cdot CF \qquad \text{[kWh]}$$

Equation 6-9 $$CF = \left(cc_0 + cc_{1,c} \cdot \left(\frac{P_{col}}{P_{col,ref}} - 1\right) + cc_{1,l} \cdot \left(\frac{Q_{los}}{Q_{los,ref}} - 1\right)\right) \qquad \text{[-]}$$

Where cc_0, cc_1 are constants (correction coefficients of zero and first order); “c” and “i” are the subscripts for the effects of collector and losses changes; P_{col} is the power of the collector field and Q_{los} are the storage thermal losses.

The reference thermal loss is 934 kWh/year calculated from the extrapolation of test result. The power of the collector field is defined at the condition of 40 K temperature difference (collector/ambient) and 700 W/m^2 irradiance. For the reference collector with 9.28 m^2, the reference power is 3.82 kW. This parameter considers both the effect of collector area and the effect of collector efficiency, and is calculated with the equation of the quadratic efficiency as defined in EN 12975-2:2006 [64].

Equation 6-10 $$\delta_{corr} = \frac{E_{6d,corr} - E_a}{E_a} \qquad \text{[-]}$$

The correction factors are defined by a linear regression between the annual energy extrapolated from the six-days sequence and the annual energy evaluated with the annual simulation. This relation is defined for the simulation where only the independent variables are varied. These independent variables correspond to the power of the collector and storage losses – i.e. to the same groups shown in Figure 6-10 and Figure 6-11.

Table 6-11 shows the correction factors identified for the electric energy, building demand and the collector energy. The correction factors are calculated for the different periods of evaluation of the sequence. The effect of these correction factors on results where different system parameters are changed simultaneously is shown in section 6.1.3.

Table 6-11: Correction factors for the different periods of evaluation of the sequence.

		Electric consumption	Building demand	Collector yield
Period of Evaluation: 1-2-3-4-5-6				
Base correction	CC_0	1.0081	0.984	0.9835
Collector field power correction	$CC_{1,c}$	0.1049	0.000	-0.1849
System loss correction	$CC_{1,l}$	-0.0550	0.000	0.1203
Period of Evaluation: 2-3-4-5-6-1				
Base correction	CC_0	1.0276	1.0056	0.9838
Collector field power correction	$CC_{1,c}$	0.1101	0.0000	-0.1846
System loss correction	$CC_{1,l}$	-0.0616	0.0000	0.1208
Period of Evaluation: 3-4-5-6-1-2				
Base correction	CC_0	1.0285	1.0088	0.9837
Collector field power correction	$CC_{1,c}$	0.1110	0.0000	-0.1843
System loss correction	$CC_{1,l}$	-0.0603	0.0000	0.1204

For example, considering the period of evaluation 1-2-3-4-5-6 and considering an area of the collector field that is 1.75 times the one of the reference system, the correction factor for electric energy consumption is 1.0868 on electric consumption evaluation and the correction factor for collector yield is 0.8448. Similarly, for the same period of evaluation, a decrease by 50% of the thermal losses would require a correction factor of 1.0356 on electric consumption and of 0.9233 on collector yield.

6.3.2 Effect of correction factors

Figure 6-12 and Figure 6-13 show the effect of the application of the correction factor for the extrapolated annual electric energy consumption for the different simulations obtained changing the parameter indicated with the Table 6-6 and Table 6-7. Figure 6-12 compares the box plots before and after the application of the correction factors for the three different periods of evaluation and for the electric consumption, collector yield, building demand and SPF. The effect of application correction factor implies to reach a similar quality of matching the annual demand for all three periods of evaluation.

Figure 6-13 shows the deviations of the corrected annual extrapolation as a function of the annual energy extrapolated. The different series of the figure shows the periods of evaluation. In the figure, the points are distributed mainly horizontally and this means that the deviations has a small dependency from the system performance after the application of the correction factor. As example, a system that has an electric demand of 3000 kWh has similar deviation of another system that has an electric demand of 6000 kWh (considering that both systems are satisfying the same load).

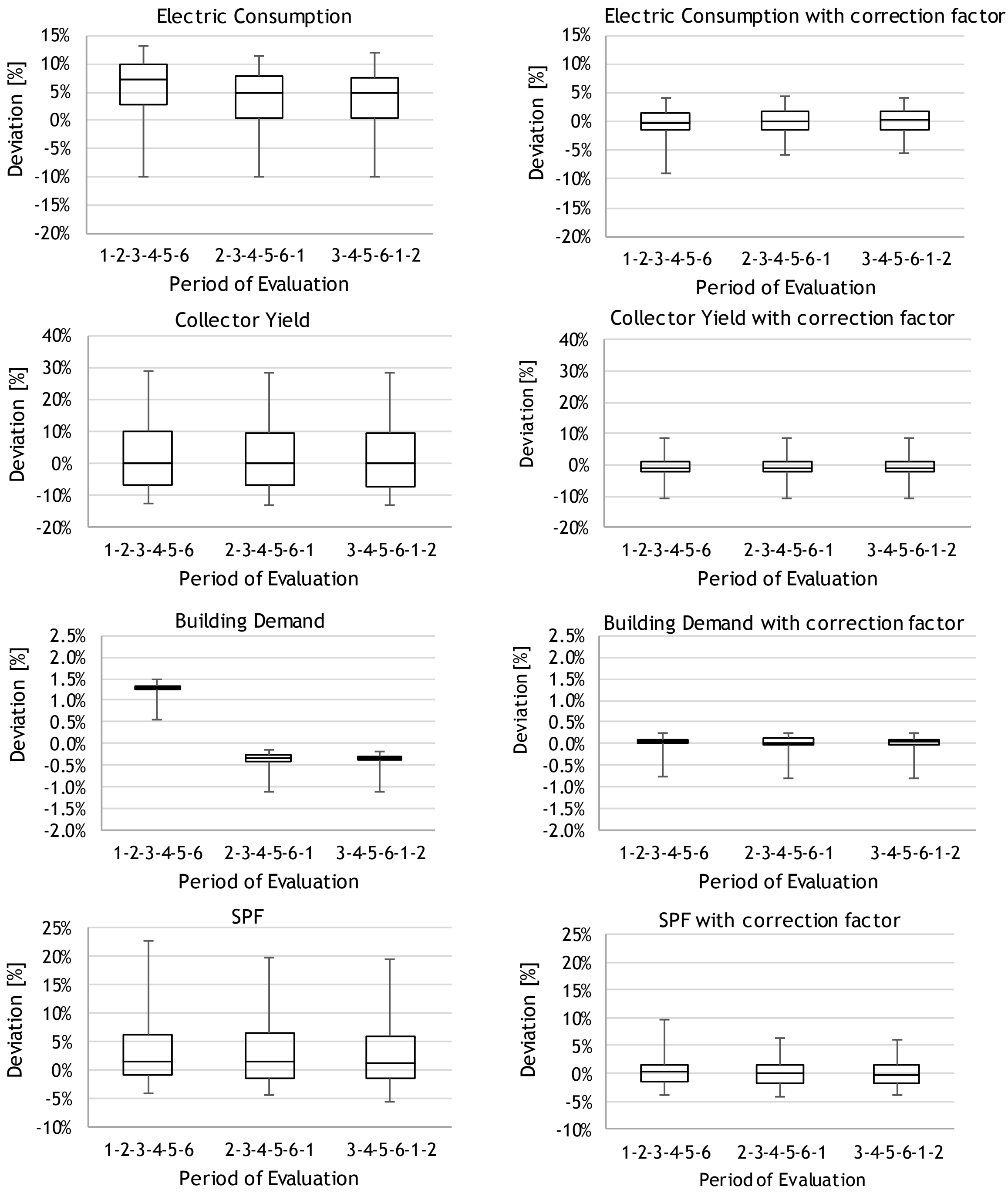

Figure 6-12: Box plot of deviation evaluated with different selection before and after the correction.

Table 6-12 shows the statistics of the correction of electric energy demand and collector yield for the different periods of evaluation. The correction factors reduce the deviation (RMSD) for the electric energy consumption from about 5 % to 2.2 %. The maximum deviation obtained before and after the correction was -17.6 %, and reduces this -8.9 % respectively; the points with highest deviations (between - 8.9 % and -5.9 %) are obtained in extreme cases, where the collector area was 1.75 times the reference and thermal losses are 0.5 times the reference. For the collector, the RMSD is reduced from about 11.5 % to 2.7 %. The range of deviations is largely reduced from a range of -12.7 % to 29.08 % to a range of -7.76 % to 8.08 %, and only few points have a deviation higher than 5 %. However, the main goal is to evaluate the auxiliary energy consumption; therefore, the deviation of the collector yield is less important.

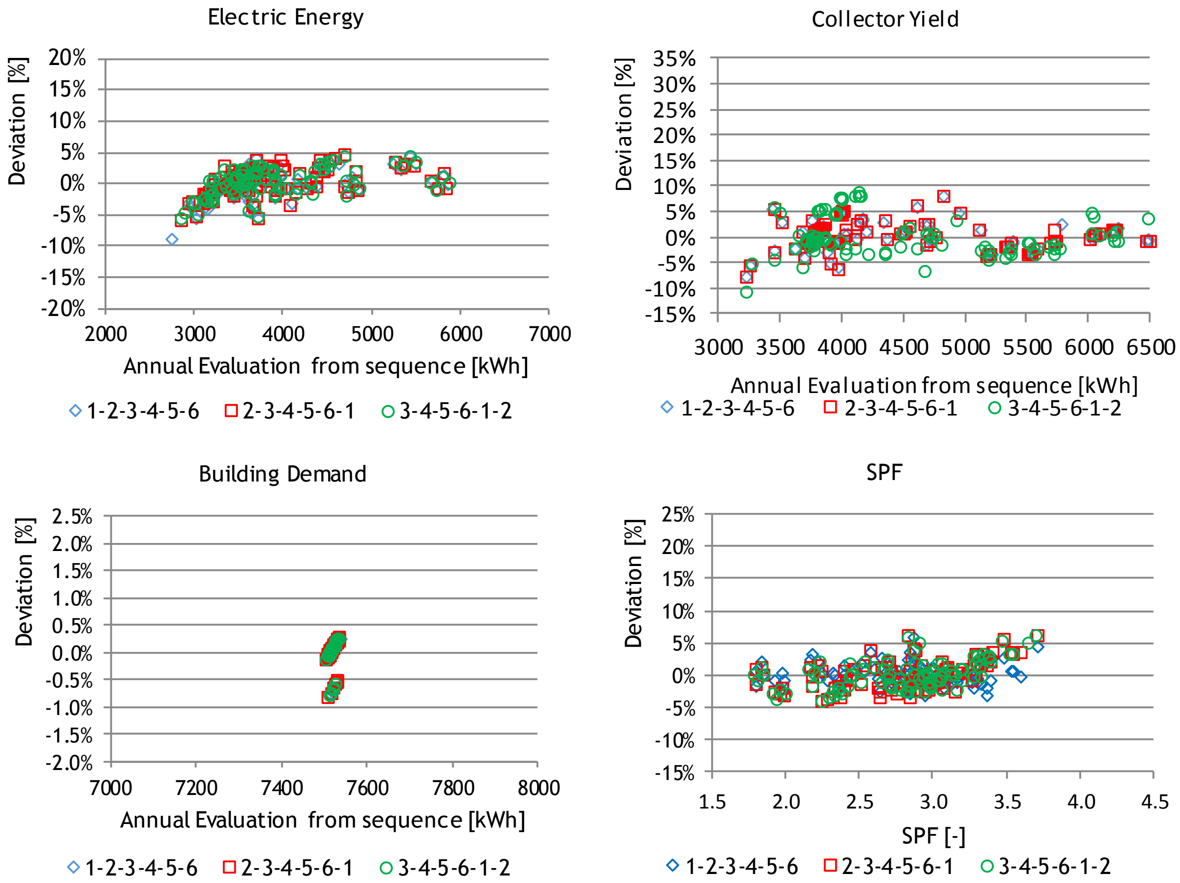

Figure 6-13: Electric energy demand, collector yield, building demand and SPF deviations after the correction for the different periods of evaluation.

Table 6-12: Electric and collector energies corrected extrapolation statistics. Comparison of different periods of evaluation.

	Electric energy			Collector Energy		
	RMSD [%]	Max [%]	Min [%]	RMSD [%]	Max [%]	Min [%]
Period of evaluation 1-2-3-4-5-6						
Not corrected	5.06	5.65	-17.6	11.48	29.08	-12.68
Corrected	2.38	4.14	-8.87	2.67	8.08	-7.76
Period of evaluation 2-3-4-5-6-1						
Not corrected	5.11	4.49	-16.79	11.49	28.54	-12.86
Corrected	2.23	4.41	-5.83	2.67	8.12	-7.75
Period of evaluation 3-4-5-6-1-2						
Not corrected	5.01	5.41	-16.64	28.10	-12.76	28.10
Corrected	2.17	4.21	-5.58	7.77	-7.77	7.77

6.4 Comparison with methodology developed

The test methods applied at the SPF-HSR and the one developed at EURAC have different approaches. The main differences can be identified in the definition of the test sequence and in the definition of load. This section presents the comparison of the two test methods in terms of:

- Sequences defined for the climate of Zurich (6.4.1);
- Definition of load: from annual profile or from a six-days simulation (6.4.2);
- Simulation of two methods (6.4.3).

In this section, the method presented in the chapter 3 and chapter 4 is called "EURAC" while the method of the Institute for Solar Energy is called "SPF-HSR". For the test sequences, it is referred to "EURAC sequence" and "SPF-HSR sequence" respectively.

6.4.1 Comparison of sequences

Figure 6-14 shows the comparison of temperature and irradiance profiles between the six-days sequence defined with the clustering of the Zurich climate (EURAC sequence) and the sequence developed through the optimization performed at the SPF-HSR (SPF-HSR sequence). The temperature profile of the SPF-HSR sequence reaches the minimum point during the last day while it is less variable during the other days. The maximum temperature is reached in the EURAC sequence. In both sequences, the coldest day presents the lower irradiation while the hottest day presents the highest irradiation.

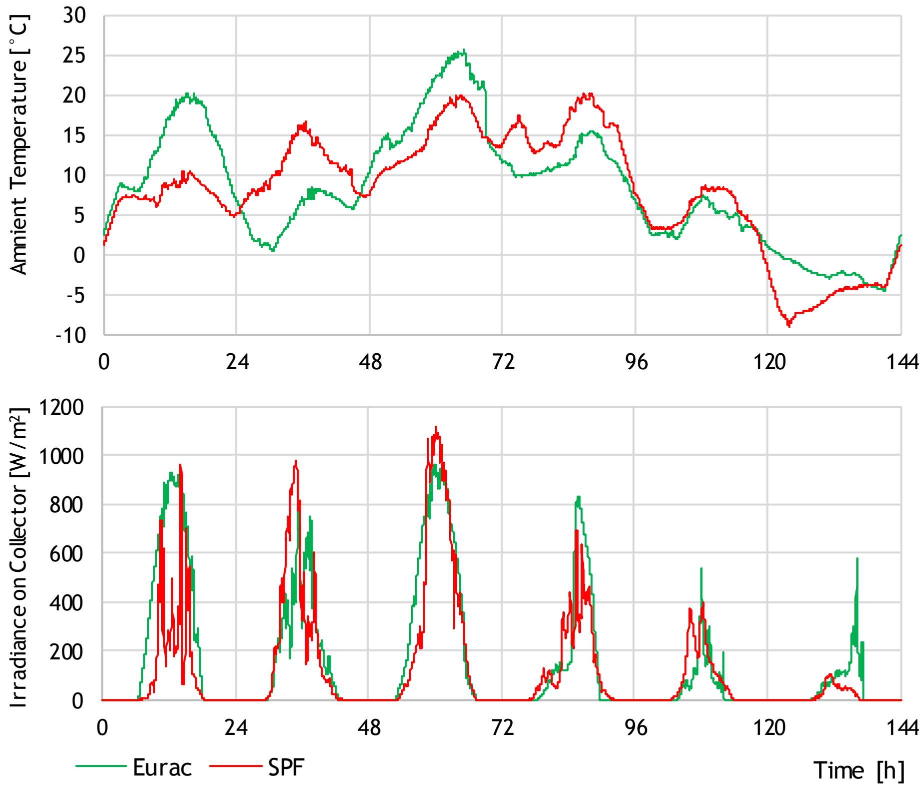

Figure 6-14: Comparison of Eurac and SPF-HSR profiles of the ambient temperature and irradiation on the collector surface during the short test sequence.

The profiles presented in the previous figure can be shown as average daily values in the Table 6-13, Figure 6-15. The Table 6-13 is completed with the information of the heating and cooling load[4] (also

[4] NOTE: Since the two methods adopt different buildings, the load presented in this section is defined with the simulation of the building used by Eurac.

shown in the Figure 6-16). The table presents the average, minimum and maximum values of sequence and the ones of the annual profile. The average values of the EURAC sequence is weighted with the clusters' size. The comparison of the temperature shows that the EURAC sequence is closer to the annual average and maximum values while the SPF-HSR sequence is closer to the minimum value.

The same trend is verified for the irradiation where the EURAC sequence is closer to the annual average and maximum values while the SPF-HSR sequence is closer to the minimum value. Again, also the heating load, the EURAC sequence is closer to the annual average value.

The two sequences do not identify days with space cooling load (Qc – last column of table) while during the year there are few days with cooling load.

Table 6-13: Comparison of EURAC and SPF-HSR sequences.

	Temperature [°C]		GHI [Wh/m^2]		Q_h [kWh]		Q_c [kWh]	
	EURAC	SPF-HSR	EURAC	SPF-HSR	EURAC	SPF-HSR	EURAC	SPF-HSR
Day 1	12.91	7.31	5134.5	2105.5	8.6	42.9	0.0	0.0
Day 2	5.37	10.75	3662.1	4074.7	45.5	24.8	0.0	0.0
Day 3	18.39	14.54	7204.7	6010.2	0.0	4.5	0.0	0.0
Day 4	11.58	15.60	2327.3	3004.6	2.0	0.0	0.0	0.0
Day 5	4.22	5.34	823.9	1608.5	66.7	48.6	0.0	0.0
Day 6	-1.92	-4.88	842.0	412.0	97.4	122.2	0.0	0.0
Seq_{avg}	8.82	8.11	3098.7	2869.3	33.7	43.8	0.0	0.0
Seq_{min}	-1.92	-4.88	823.9	412.0	0.0	0.0	0.0	0.0
Seq_{max}	18.39	15.60	7204.7	6010.2	97.4	122.3	0.0	0.0
$Year_{avg}$	9.04	9.04	3044.3	3044.3	35.6	35.6	1.1	1.1
$Year_{min}$	-8.28	-8.28	122.7	122.7	0.0	0.0	0.0	0.0
$Year_{max}$	26.04	26.04	8244.8	8244.8	124.7	124.7	48.4	48.4
ΔAvg	-0.2	-0.9	54.3	-175.1	-1.9	8.2	-1.1	-1.1
ΔMin	6.4	3.4	701.3	289.3	0.0	0.0	0.0	0.0
ΔMax	-7.7	-10.4	-1040	-2235	-27.2	-2.4	-48.4	-48.4

Avg: average, min: minimum, max: maximum, seq: sequence. ΔAvg= Seq_{avg} - $Year_{avg}$, ΔMin = Seq_{min} - $Year_{min}$, ΔMax = Seq_{max} - $Year_{max}$

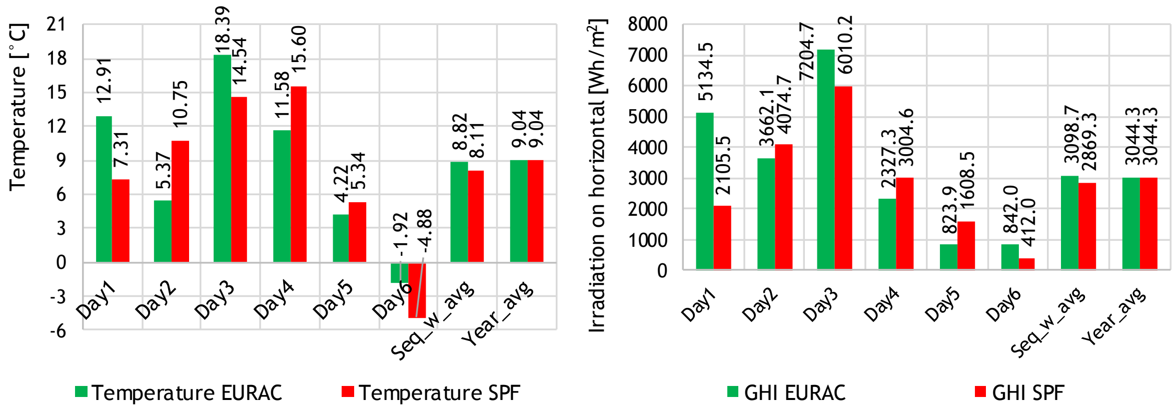

Figure 6-15: Daily average temperatures and total irradiation on horizontal surface. Comparison of EURAC and SPF-HSR sequences.

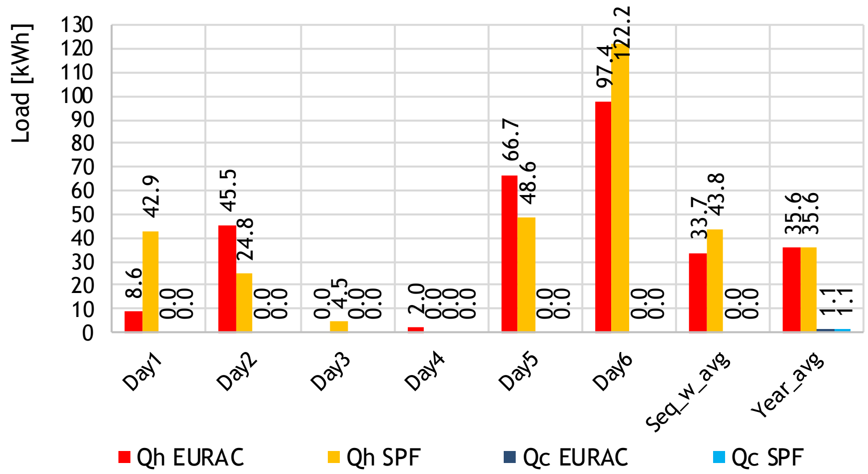

Figure 6-16: Daily heating and cooling loads, average of sequence and annual loads. Comparison of EURAC and SPF-HSR sequences.

The points presented in previous table and figures are presented in the Figure 6-17 compared to the 365 days of the year. This figure helps to understand how the days are distributed within the year. The points of the EURAC sequence are equally-distributed in the graphs.

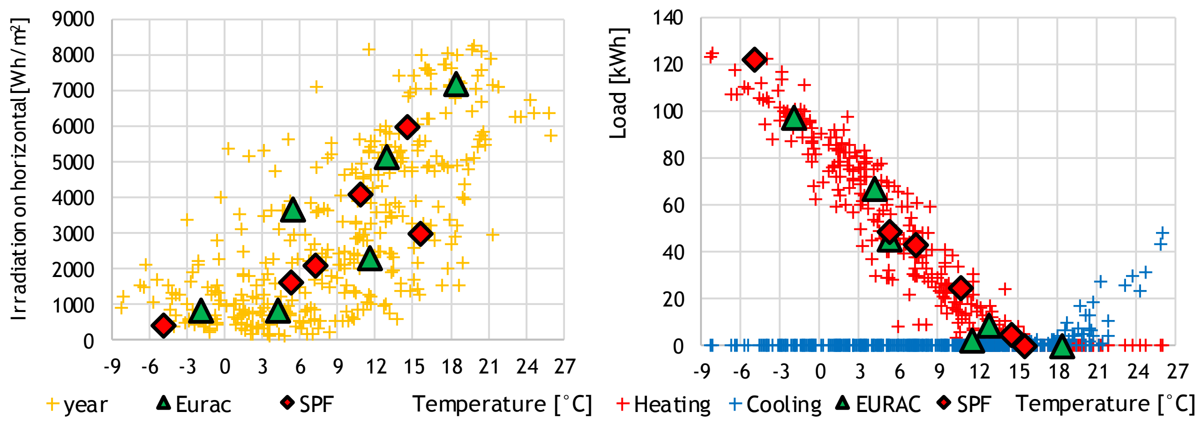

Figure 6-17: Identification of six-days sequences of EURAC and SPF-HSR. Zurich Climate.

In general, the sequence of EURAC has temperature, irradiation and load parameters more closed to the annual average conditions. This outcome is consequence of the clustering since the year data is divided into groups which the nearest elements of groups' geometric centres are considered for the selection.

6.4.2Comparison of methods for the definition of the load file

The two procedures differ for the definition of the load. The EURAC procedure defines a load file that considers the load during the sequence days that is the one that the days have in the year. In this sections, the label "load file from annual" is used to refer to this method. Instead, the SPF-HSR procedure considers the simulation of load during the sequence: the six-days sequence is simulated is order to get a load file, then during the test the load file is applied to get an equal amount of heating by all systems for the same day of the profile, while the building is simulated in parallel in order to get the correct return temperature and the building temperature during the test. The label "six-days simulated load" is used to refer to the approach of the SPF-HSR.

The load resulting with the two procedures is different since the dynamic effects of previous days are affecting the load because of the inertia of the building. The loads defined with a load file from the simulation of the whole year and the load defined with the simulation of the sequence are compared in the Figure 6-18. The figure considers the two buildings that are used as reference by the two institutes. Since the two six-days sequences are different, in this figure the sequence considered is the one of SPF-HSR.

As result, the daily loads are different and the maximum load can be reach only with the days taken from the annual load file, testing therefore the worst load condition. The total loads of the two approaches are different and the "load file from annual" is higher than the "six-days simulated load". The load defined with both methods does not present any day with cooling load.

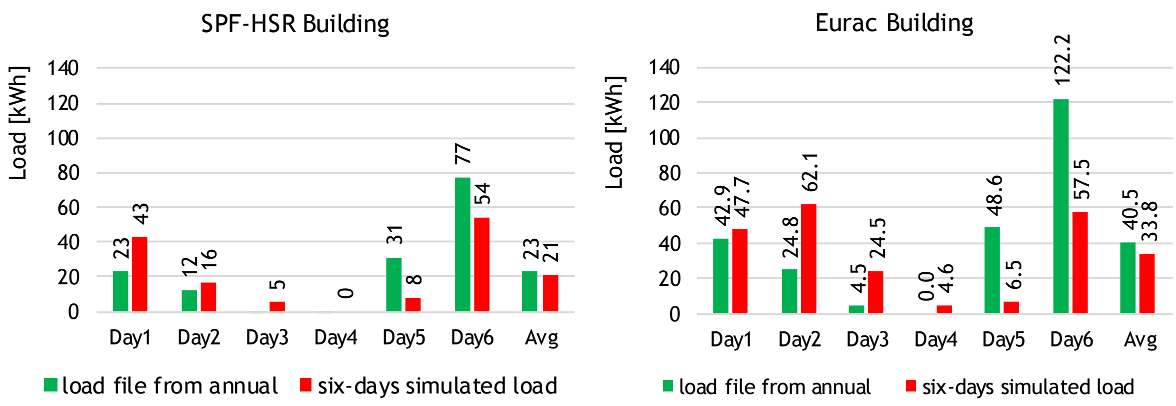

Figure 6-18: Comparison of daily loads defined in the SPF-HSR and Eurac methods.

Note: the figure shows the average load instead of the sequence total load since it would have a different order of magnitude and the scale of graph would not be readable.

6.4.3 Comparison of sequences' simulations

The sequences compared in the section 6.4.1 and the loads compared in the section 6.4.2 were used to simulate the system. The system considered in this section is the one used for the test with the EURAC procedure (layout and simulation set-up in the Appendix C). The Table 6-14 presents the results of the simulations performed with the EURAC and SPF-HSR approaches. The simulation of EURAC approach considers the sequence defined with the clustering and the imposition of the "load file from annual" as described in the section 3.3. Instead the simulation of the SPF-HSR approach considers the sequence defined with the optimization procedure (section 6.1 and 6.2) and the "six-days simulated load". Only in this section, the building is simulated with type 56 instead of the method described in the section 6.1 that considers the type 5897 [57]. The simulation of SPF-HSR is corrected with the correction factors defined in the section 6.3.

The results show similar deviation with the annual simulation. Between the two sequences, the total SPF deviates about 1 % while the two sequences deviate from the annual simulation about 7%. The largest deviation is obtained in the calculation of the SPF of domestic hot water.

Table 6-14: Comparison of simulations of EURAC and SPF-HSR methods.

	Q_{heat} [kWh]	Q_{dhw} [kWh]	Q_{tot} [kWh]	W_{heat} [kWh]	W_{dhw} [kWh]	W_{tot} [kWh]	Q_{coll} [kWh]	SPF_h [-]	SPF_d [-]	SPF_t [-]
Eurac	12250	2565	14815	3241	343	3584	7722	3.78	7.48	4.13
SPF-HSR	13595	2435	16029	3376	546	3922	7252	4.03	4.46	4.09
Annual	12996	2546	15542	3646	428	4074	10095	3.56	5.95	3.82

A detailed comparison could be performed distinguishing the simulation of the two sequences with the adoption of a "load file from annual" (EURAC approach) or the "six-days simulated load" (SPF-HSR approach).

In Table 6-15 and in Table 6-16, the two sequences were simulated considering the procedure of EURAC: the load is fixed for each day considering the load that the days have during the year - "load file from annual". The results obtained with the SPF-HSR sequence are corrected with the correction factors defined in the chapter 6.3. For the simulation of the SPF-HSR sequence, the DHW profile defined by SPF-HSR is used but it is scaled to have the same energy extraction of the EURAC's DHW profile.

The tables show also the sequence evaluated with different periods of evaluation (1-2-3-4-5-6, 2-3-4-5-6-1, 3-4-5-6-1-2). In the Table 6-15 the energies and the seasonal performance factor are indicated for those periods of evaluation while in the Table 6-16, the deviation between the periods of evaluation is shown. In the previous chapter, it was indicated that the SPF-HSR sequence was developed with the requirement of having the same energy content at the beginning and at the end of the test. Instead, this requirement is not asked in the EURAC sequence. In the SPF-HSR procedure, to help to satisfy this requirement, the DHW profile was increased between a summer and autumn day to represent the reduction of energy stored due to the different season. The EURAC draw-off instead, at this stage, considers the same daily profile repeated for the different days and simulate the winter days before the summer days.

The EURAC sequence evaluated in the period of evaluation 1-2-3-4-5-6 as foreseen by the method has a low deviation with the annual simulation while the difference increase by considering the other two sequences. In these two cases, the evaluation is made considering a period that is not suggested by the test method. The SPF-HSR sequences instead obtain similar performance with the different periods of evaluation. With the SPF-HSR sequence, the load is overestimated but it should be considered that the method considers the simulation of the building instead of the imposition of the load file.

Table 6-15: Comparison of simulation of sequences defined at EURAC and at SPF-HSR. "Load file from annual".

	Q_{heat} [kWh]	Q_{dhw} [kWh]	Q_{tot} [kWh]	W_{heat} [kWh]	W_{dhw} [kWh]	W_{tot} [kWh]	Q_{coll} [kWh]	SPF_h [-]	SPF_d [-]	SPF_t [-]
seq1_Eurac	12250	2565	14815	3241	343	3584	7722	3.78	7.48	4.13
seq2_Eurac	12858	2565	15423	2787	601	3388	7765	4.61	4.27	4.55
seq3_Eurac	12859	2565	15424	2793	711	3503	7791	4.60	3.61	4.40
seq1_SPF-HSR	15733	2456	18188	4167	773	4940	7710	3.78	3.18	3.68
seq2_SPF-HSR	16292	2675	18967	4312	737	5049	7995	3.78	3.63	3.76
seq3_SPF-HSR	16444	2919	19362	4350	830	5179	7948	3.78	3.52	3.74
Annual	12996	2546	15542	3646	428	4074	10095	3.56	5.95	3.82

Seq1: sequence defined with the period of evaluation 1-2-3-4-5-6, seq2: 2-3-4-5-6-1, seq3: 3-4-5-6-1-2.

Table 6-16: Deviation between period of evaluation of sequences defined at EURAC and at SPF-HSR. "Load file from annual".

	Q_{heat}	Q_{dhw}	Q_{tot}	W_{heat}	W_{dhw}	W_{tot}	Q_{coll}
				Eurac			
Seq1-Seq2	-4.96%	-0.02%	-4.11%	14.01%	-75.29%	5.47%	-0.55%
Seq2-Seq3	-0.01%	0.00%	-0.01%	-0.22%	-18.18%	-3.41%	-0.34%
				SPF-HSR			
Seq1-Seq2	-3.55%	-8.93%	-4.28%	-3.48%	4.71%	-2.20%	-3.69%
Seq2-Seq3	-0.93%	-9.09%	-2.08%	-0.88%	-12.56%	-2.59%	0.58%

Seq1-Seq2: deviation between the sequence 1 and sequence 2. Seq2-Seq3: deviation between the sequence 2 and sequence 3. Seq1: sequence defined with the period of evaluation 1-2-3-4-5-6, seq2: 2-3-4-5-6-1, seq3: 3-4-5-6-1-2.

Table 6-17 and Table 6-18 show the comparison of the EURAC sequence and the SPF-HSR sequence simulated with the "six-days simulated load". The consequence is that the heating load is different from the previous table and is not anymore closed to the annual load (for the case of EURAC sequence). The tables show also the sequences evaluated with different periods of evaluation (1-2-3-4-5-6, 2-3-4-5-6-1, 3-4-5-6-1-2). In the Table 6-17 the energies and the seasonal performance factor are indicated for those periods of evaluation while in the Table 6-18, the deviation between the periods of evaluation is shown.

Again, the performance of the EURAC sequence (seq1) is closed to the one calculated with the annual simulation while the other periods of evaluation have and higher deviation (but these do not represent the method). The SPF-HSR sequences are more closed each other and the deviation decrease when the correction factors are applied. The deviation of heating load with the SPF-HSR sequence decrease form the results presented in the Table 6-15.

Table 6-17: Comparison of simulation of sequences defined at EURAC and at SPF-HSR. "Six-days simulated load".

	Q_{heat} [kWh]	Q_{dhw} [kWh]	Q_{tot} [kWh]	W_{heat} [kWh]	W_{dhw} [kWh]	W_{tot} [kWh]	Q_{coll} [kWh]	SPF_h [-]	SPF_d [-]	SPF_t [-]
seq1_Eurac	11450	2565	14014	3015	399	3414	7570	3.80	6.42	4.11
seq2_Eurac	12128	2565	14693	2416	665	3082	7575	5.02	3.86	4.77
seq3_Eurac	12311	2565	14876	2516	697	3213	7583	4.89	3.68	4.63
seq1_SPF-HSR	13595	2435	16029	3376	546	3922	7252	4.03	4.46	4.09
seq2_SPF-HSR	13506	2657	16164	3243	502	3745	7527	4.17	5.29	4.32
seq3_SPF-HSR	13375	2901	16275	3217	646	3862	7493	4.16	4.49	4.21
Annual	12996	2546	15542	3646	428	4074	10095	3.56	5.95	3.82

Seq1: sequence defined with the period of evaluation 1-2-3-4-5-6, seq2: 2-3-4-5-6-1, seq3: 3-4-5-6-1-2.

Table 6-18: Deviation between period of evaluation of sequences defined at EURAC and at SPF-HSR. "Six-days simulated load".

	Q_{heat}	Q_{dhw}	Q_{tot}	W_{heat}	W_{dhw}	W_{tot}	Q_{coll}
				Eurac			
Seq1-Seq2	-5.93%	0.01%	-4.84%	19.84%	-66.61%	9.73%	-0.07%
Seq2-Seq3	-1.51%	0.00%	-1.25%	-4.11%	-4.75%	-4.25%	-0.10%
				SPF-HSR			
Seq1-Seq2	0.65%	-9.16%	-0.84%	3.96%	7.95%	4.52%	-3.80%
Seq2-Seq3	0.98%	-9.15%	-0.69%	0.79%	-28.52%	-3.14%	0.46%

Seq1-Seq2: deviation between the sequence 1 and sequence 2. Seq2-Seq3: deviation between the sequence 2 and sequence 3. Seq1: sequence defined with the period of evaluation 1-2-3-4-5-6, seq2: 2-3-4-5-6-1, seq3: 3-4-5-6-1-2.

6.5 Conclusions

This chapter has presented the development of a six-days sequence for the CCT method. The sequence was developed with the aim of performing a direct extrapolation of the results (with a multiplication of a factor 365/6) to evaluate the building demand, electrical consumption and the collector yield.

The sequence has been optimized for a reference system and the effect on about 100 different system configurations has been evaluated. In the reference system, the deviation between the direct extrapolation and the annual simulation is about 1 % while the parametric simulation showed a dependency of the deviation with some independent parameters that can be reduced to the collector nominal power and the storage losses. The change of these parameters gives a deviation between 5 % and 15% in the electric consumption and -15 % and 30 % in the collector yield evaluations. Correction factors are defined considering these two parameters and the RMSD between the extrapolated and simulated annual results is reduced to about 2.2 % for the electric energy demand, and for 2.6% for the collector yield.

The work done at the SPF-HSR is useful to compare the procedure developed in this thesis with the one applied at the SPF-HSR. The comparisons are performed in terms of boundary conditions (profiles of temperature and irradiance), methods of application of load and simulations of those two approaches with the same case study. In the SPF-HSR sequence, the boundary conditions reach the lowest temperature condition while the EURAC sequence reaches the highest temperature condition and the average values are more closed to the seasonal values. Regarding the definition of the load the adoption of a "load file from annual" (EURAC procedure) has a different load distribution during the days than the "six-days simulated load". A "load file from annual" allows to test the system with the maximum load condition. The simulation of the two methods on a solar assisted heat pump system shows that the SPF between the two sequence deviates about 1 %.

As conclusion, the procedure developed in the thesis performs test with more extreme load condition and obtains a similar accuracy with a procedure that is simpler in terms of application.

Conclusions

The topic of the dynamic characterization of heating and cooling systems’ performance is analysed. The activity is divided in two mains groups that concern the procedure applied at component and at system level.

The first part regards the development of the procedure at component level. That has been applied to characterize an adsorption chiller and an electric heat pump. The procedure foresees the definition of the boundary conditions of the machine and the selection of a representative part in order to perform a short dynamic test. The results are used to analyse the capability of the short sequence to represent the whole seasonal operation and to analyse the components’ performances.

To evaluate the selection procedure, the whole boundary conditions have been tested and the results are compared with the different short sequence tests. The selection procedure allows to represent the seasonal performance in terms of energy and performance factors and also in terms of distribution of instantaneous performance figures. With a short sequence the deviation with the seasonal test is about 2%.

The results show that the dynamics of boundary conditions affect the performance of those components. For the adsorption chiller, an initial transient phase of about 30 min has been measured which the machine works with about half efficiency. For the heat pump, the initial transient is long about few minutes; moreover, the study of the heat pump showed other transients during the switching of the working schemes. When the machine changes the load, the useful effect could decrease or increase due to an “energy storage effect”. The main effect is present when the working conditions are changed from the space heating to the DHW production: the output thermal power decrease to 0 to increase again to the stationary conditions while the electric consumption is kept constant.

The performance obtained with the dynamic test of the two components are compared with two other methodologies that are the CTSS and Bin methods. The comparison highlights the necessity of adoption of dynamic test method since the deviation is high. For the adsorption chiller, the deviation of both the procedures is an overestimation of SEER of about 15%. For the heat pump the deviation is lower: in the case heating operation and is about 3% for the bin method and 6% for the simulation while the deviation become high in the cooling operation since it is about 30%. This high deviation is explained with the not optimized control strategy that controls the heat pump: the heat pump is activated a large time but with real short periods. The initial transients assume high importance since the duration of activation are short.

Regarding the whole system procedure, the systems are tested with a load file in order to be able to perform a comparison of system performance. The advantages of the method for the application of the load file is that the system can control the distribution actuators and a reference system is not required to define the load.

Other advantages of the procedure are that the method could be easily applied to different climates and the method does not require the coupling of Trnsys and laboratory control since simplified emulations are used. The consequence is that the procedure could be more cost attractive for the industries.

Different sequences durations have been evaluated with the method adopted in the component level procedure but the selections have given high deviations since a high number of events are disregarded to reach a short test duration. A new approach is adopted that is a clustering method. The clustering allows to classify the events to a number of groups decided previously and for each group give one element that is representative of the other in the same group. Different sequence of 6, 8, 10, 12 and 24 days have been simulated for the climates of Bolzano and Zurich and with different plant configuration. The outcome is that the deviation with the annual simulation is decreasing with increasing the sequence duration. A shorter test sequence is more cost attractive for the industries than a longer one. The deviation is higher when the collector field or the storage volume are higher. The simulation of a plant with 8 m^2 of collector show that a six-days sequence is giving a deviation on evaluation of performance similar to the one with more days while the simulation of the plant with a storage volume of 1500 l and 16 m^2 of collector have a different trend.

From the sequences defined with clustering, different tests have been carried out considering the climates of Bolzano, Zurich, Gdansk and Rome. Six-days sequences were defined for those climates and for the climate of Bolzano the performances were investigated for also a ten-days sequence.

The test results are compared with simulation in terms of short sequence and annual extrapolation of result. The comparison of test measurement with the sequence simulation shows that not all transients of the system are caught with the simulation:

- The first example is the dynamic behaviour of the heat pump as highlighted with the results obtained at component level.
- Another effect is the storage destratification during the initial charge phase with the heat pump or the solar collector (respectively the small and the big storages). Considering the example of the small storage, the heat pump and the two circulation pumps are activated when the temperature reaches 40°C; however, before having an outlet temperature higher than 40°C cold water circulates in the storage. Different solutions could be adopted as a delayed activation of secondary pump or the installation of a stratification device.
- The behaviour of the collector yield is different during the days with low irradiation. The energy collected during the test is lower than the one simulated.
- The effect of the space heating with the solar energy stored observed from test is different from the simulated one. The control strategy foresees to start heating with solar energy when the storage temperature is higher than 46°C and is deactivated when it reaches 41°C in order to keep a buffer of energy for the DHW. The test showed that the temperature decrease over 40°C for the delay due to the plant inertia. In this way electric energy has to be used to return at a temperature of the storage higher than 40°C. The advantage of using solar energy for space heating is loosed by the necessity of feed again the storage. A solution could be the increasing of the lower limit of the hysteresis cycle that controls the space heating with solar energy.
- Control of heat pump in cooling mode: the heat pump works discontinuously during the cooling mode.

The comparison of the sequence simulation with the annual simulation shows a small deviation of performance evaluation with a direct extrapolation of the six-days sequence. The total seasonal performance factor obtained with the sequence simulation differs from the annual simulation about 0.2 (up to 8 %).

The sequence of ten days shows a worse performance of the system compared to the six-days sequence since it considers more extreme conditions. The aim of the test is to verify the working condition of the system under realistic conditions: a longer sequence allows to evaluate the performance with more stressing condition; however, this would involve in a more expensive experimentation phase.

The selection procedure could be further developed by defining a clustering that classify elements in to groups with the same population in order to do not have different weighing factor of the cluster simplifying the extrapolation of results. Moreover, a method for the extension of results to different load condition (different climates or building) should be defined.

The procedure foresees the emulation of a distribution system at low temperature (radiant system); however, a higher temperature application requires a different model. Moreover, other emulations models should be developed to extend the possibility of testing other systems like heat pumps connected to a PV field, heat pumps connected to ground probes, system with a biomass back-up unit and so on.

As following step, the procedure will be applied to characterize a solar combi plus system, where the solar energy drives an adsorption chiller.

In the last chapter it is analysed the development of a six-days sequence for the CCT method. This work has been done during the internship at the Institute for Solar Energy (SPF) of the University of Applied Science of Rapperswil (HSR) in Switzerland. The aim is the definition of a six-days test sequence that allows for direct extrapolation is defined with a weather data resolution of 10 min.

The motivation of adopting a 10 min resolution weather file is to perform a reliable characterization of heating systems, including also systems that are influenced by short term fluctuations of solar irradiance (i.e. PV+HP).

The sequence is defined with an optimization carried out considering a solar thermal and heat pump reference system. The deviation obtained for this system is really low (about 1% in different performance figures). The sequence has been simulated for about one hundred different system configuration by changing some parameters as the heat pump size, collector efficiency or collector area, storage volume, storage and pipe losses and so on. The results show an influence of some independent parameters on the deviation between a direct extrapolation of the results and the annual simulations. These independent parameters could be reduced to the nominal power of collector field and to the storage thermal losses. For example, doubling the collector area leads to an underestimation of electric energy consumption by about 10 % while the collector yield is overestimated by about 15 %, if the annual result is taken as a direct extrapolation from the six-days test without any correction factors. For a system with increased thermal losses the test sequence overestimates the electrical consumption and underestimates the collector yield. For example, for heat losses that are four times those of the reference system, the direct extrapolation from six-days test sequence results to annual values overestimates the electric consumption by 5 % while it underestimates the collector yield by 10 %. When these independent variables are combined, the deviation between extrapolated and simulated annual results may deviate by up to 15 % for electric energy consumption, and by up to 30 % for the collector yield, if no correction factors are applied.

Therefore, a correction factors are defined based on the nominal power of the collector field and based on the storage losses. The nominal power of the collector field is defined as the heat output with 40 K temperature difference to the ambient and 700 W/m^2 solar irradiance on the field. The correction factors are defined for the different periods of evaluation considered. In these three cases, the RMSD between the extrapolated and simulated annual results thus reduced to about 2.2 % for the electric energy demand, and for 2.6 % for the collector yield.

Further work would include the simulation of other types of systems like heat pumps driven by PV, or solar thermal with other back-up units (biomass, gas boilers). Moreover, the application of a multi-objective optimization to the methodology for the determination of the sequence could reduce the deviation from the direct extrapolation and the annual simulation for different systems reducing the need for correction factors.

The sequence so defined is compared with the one defined with the EURAC procedure. The two procedures are compared in the method which the load comes out since the CCT method foresees a building emulation and the EURAC method foresees the definition of a load file. The results show a closed deviation (about 1 %) between the EURAC sequence and the SPF sequence after the application of correction factors. The low deviation justifies the application of the method presented in this thesis since it simplifies the application of a dynamic procedure without losing in reliability.

Bibliography

[1] European Commission, Joint Research Centre, European Technology Platform on Renewable Heating and Cooling (RHC-Platform), 2020-2030-2050, common vision for the renewable heating and cooling sector in Europe: European technology platform on renewable heating and cooling, EUR-OP, Luxembourg, 2011.

[2] European Commission, European energy security strategy.pdf, (2014).

[3] European Commission, A Roadmap for moving to a competitive low carbon economy in 2050, (2011).

[4] EC, Indication by labelling and standard product information of the consumption of energy and other resources by energy-related products, (2010) L153/1.

[5] EC, Commission Delegated Regulation (EU) No 626/2011, (2011).

[6] EC, Commission delegated Regulation (EU) No 811/2013, (2013).

[7] EN 14825:2012, Air conditioners, liquid chilling packages and heat pumps, with electrically driven compressors, for space heating and cooling — Testing and rating at part load conditions and calculation of seasonal performance, European Committee for Standardization, Brussels, Belgium, 2012.

[8] EN 15316-4-2:2008, Heating systems in buildings - Method for calculation of system energy requirements and system efficiencies. Part 4-2: Space heating generation systems, heat pump systems, European Committee for Standardization, Brussels, Belgium, 2008.

[9] C. Wemhoener, T. Afjei, R. Dott, IEA HPP Annex 28 – standardised testing and seasonal performance calculation for multifunctional heat pump systems, Appl. Therm. Eng. 28 (2008) 2062–2069. doi:10.1016/j.applthermaleng.2007.12.003.

[10] H. Kerskes, Validation of the CTSS Test Procedure bu In-situ Measurements, Institut für Thermodynamik und Wärmetechnik (ITW), Stuttgart, Germany, 2002.

[11] UNI CEN/TS 12977-2:2012, Thermal solar systems and components - Custom built systems. Part 2: Test methods for solar water heaters and combisystems, European Committee for Standardization, Brussels, Belgium, 2012.

[12] AS 4234:2008, Heated water systems - Calculation of energy consumption, Standard Australian Committee, 2008.

[13] AS 5389:2013, Solar heating and cooling systems - Calculation of energy consumption, Standard Australian Committee, 2013.

[14] M. Goldsworthy, S. White, Overview of a desiccant based air-conditioner component for a Solar Cooling Australian Standard, CSIRO, 2012.

[15] M.Y. Haller, R. Haberl, T. Persson, C. Bales, P. Kovacs, D. Chèze, et al., Dynamic whole system testing of combined renewable heating systems – The current state of the art, Energy Build. 66 (2013) 667–677. doi:10.1016/j.enbuild.2013.07.052.

[16] P. Vogelsanger, The concise cycle test method - a twelve day system test, 2002.

[17] R. Haberl, E. Frank, P. Vogelsanger, Holistic System Testing-10 Years of Concise Cycle Testing, in: ISES 2009, 2009: pp. 351–360. http://www.solarenergy.ch/fileadmin/daten/publ/202_Haberl_Frank_Holistic_System_Testing_FullPaper.pdf (accessed June 19, 2013).

[18] B. Mette, J. Ullmann, H. Druck, M. Albaric, A. Leconte, P. Papillon, Comparison of Test Methods, 2010.

[19] A. Leconte, G. Achard, P. Papillon, Global approach test improvement using a neural network model identification to characterise solar combisystem performances, Sol. Energy. 86 (2012) 2001–2016. doi:10.1016/j.solener.2012.04.003.

[20] F. Boudéhenn, M. Albaric, N. Chatagnon, J. Heintz, N. Benabdelmoumene, P. Papillon, Dynamical studies with a semi-virtual testing approach for characterization of small scale asorption chiller, in: EUROSUN 2010, Graz, Austria, 2010.

[21] M. Albaric, J. Nowag, P. Papillon, Thermal performance evaluation of solar combisystems using a global approach, in: EUROSUN 2008, Lisbon, Portugal, 2008.

[22] A. Leconte, G. Achard, P. Papillon, Solar Combisystem Characterization with a Global Approach Test and a Neural Network Based Model Identification, Energy Procedia. 30 (2012) 1322–1330. doi:10.1016/j.egypro.2012.11.145.

[23] A. Lazrak, A. Leconte, D. Chèze, G. Fraisse, P. Papillon, B. Souyri, Numerical and experimental results of a novel and generic methodology for energy performance evaluation of thermal systems using renewable energies, Appl. Energy. 158 (2015) 142–156. doi:10.1016/j.apenergy.2015.08.049.

[24] C. Bales, Combitest - A new test method for thermal stores used in Solar Combisystems., Doctoral Thesis, Department of Building Technology, Chalmers university of Technology, 2004.

[25] C. Bales, Combitest-Initial development of the acdc test method.pdf, Solar Energy Research Center SERC, Borlänge, Sweden, 2002.

[26] H. Drück, S. Bachmann, Performance Testing of Solar Combisystems, Institut für Thermodynamik und Wärmetechnik (ITW), Stuttgart, Germany, 2002.

[27] T. Persson, U. Pettersson, K.M. Win, M. Johansson, H. Persson, M. Rönnbäck, et al., Provningsmetod för sol-och biovärmesystem: Systemprestanda och emissionsdata, (2012). http://du.diva-portal.org/smash/record.jsf?pid=diva2:523282 (accessed December 13, 2013).

[28] U. Pettersson, M. Johansson, H. Persson, M. Rönnbäck, T. Persson, J.-O. Dalenbäck, Provningsmetod för integrerade sol-biosystem: \AArsverkningsgrad genom korttidsmätning, (2011). http://du.diva-portal.org/smash/record.jsf?pid=diva2:523264 (accessed December 13, 2013).

[29] D.J. Naron, Using the DST test method for testing'solar-only'and'preheat'solar domestic hot water systems, (2000). http://ptp.irb.hr/upload/mape/solari/22_Daniel_Naron_Using_the_DST_test_method_for_testing_solar-o.pdf (accessed June 19, 2013).

[30] G. Panaras, E. Mathioulakis, V. Belessiotis, A method for the dynamic testing and evaluation of the performance of combined solar thermal heat pump hot water systems, Appl. Energy. 114 (2014) 124–134. doi:10.1016/j.apenergy.2013.09.039.

[31] M.D. Schicktanz, C. Schmidt, R. Fedrizzi, Classification of Rating Methods for Solar Heating and Cooling Systems, Energy Procedia. 48 (2014) 1676–1687. doi:10.1016/j.egypro.2014.02.189.

[32] EN 12039, Gas-fired absorption and adsorption air-conditioning and/or heat pump appliances with a net heat input not exceeding 70 kW - Rational use of energy, European Committee for Standardization, Brussels, Belgium, 2014.

[33] F.A. Peuser, K.-H. Remmers, M. Schnauss, Solar Thermal Systems, Solarpraxis, 2002.

[34] M.D. Schicktanz, J. Döll, H. Fugmann, Calculation of Solar Gains for Solar Heating and Cooling Using the Bin-method, Energy Procedia. 48 (2014) 1665–1675. doi:10.1016/j.egypro.2014.02.188.

[35] A. Loose, B. Mette, S. Bonk, H. Druck, Development of performance test merhods for combined solar thermal and heat pump systems, in: ESTEC 2011, Marseille, France, 2011.

[36] P. Frey, S. Fischer, H. Drück, Artificial Neural Network modelling of sorption chillers, Sol. Energy. 108 (2014) 525–537. doi:10.1016/j.solener.2014.08.006.

[37] M. Uhlmann, S. Bertsch, Dynamischer Wärmepumpentest, Interstaatliche Hochschule für Technik Buchs NTB, Buchs, Switzerland, 2010. http://www.bfe.admin.ch/forschungwkk/02425/02724/02727/index.html?lang=de&dossier_id=03610.

[38] P. Papillon, M. Albaric, M. Haller, R. Haberl, T. Persson, U. Pettersson, et al., Whole system testing: the efficient way to test and improve solar combisystems performance and quality, in: ESTEC 2011, Marseille, France, 2011.

[39] P. Riederer, V. Partenay, O. Raguideau, Dynamic test method for the determination of the global seasonal performance factor of heat pumps used for heating, cooling and domestic hot water preparation, in: IBPSA, Glasgow, Scotland, 2009. http://www.ibpsa.org/proceedings/BS2009/BS09_0752_759.pdf (accessed June 19, 2013).

[40] U. Jordan, K. Vajen, Influence Of The DHW Load Profile On The Fractional Energy Savings: A Case Study Of A Solar Combi-System With TRNSYS Simulations, Sol. Energy. 69 (2001) 197–208.

[41] ISO 13790: 2008, Energy performance of buildings - Calculation of energy use for space heating and cooling, International Organization for Standardization, Geneva, Switzerland, 2008.

[42] M. Haller, B. Perers, C. Bales, J. Paavilainen, A. Dalibard, S. Fischer, et al., TRNSYS Type 832 v5. 00 „Dynamic Collector Model by Bengt Perers ": Updated Input-Output Reference, 2012. http://orbit.dtu.dk/fedora/objects/orbit:118161/datastreams/file_9f7ef35f-ad1c-478a-86f8-3fde87fc0696/content (accessed May 13, 2015).

[43] B. Mette, J. Ullmann, H. Druck, M. Albaric, P. Papillon, Standards "Solar combisystem test methods," 2011.

[44] D. Chèze, P. Papillon, A. Leconte, M.Y. Haller, R. Haberl, T. Perrson, et al., Towards an Harmonized Whole System Test Method for Combined Renewable Heating Systems for Houses, in: International Solar Energy Society, 2015: pp. 1–10. doi:10.18086/eurosun.2014.03.06.

[45] R. Haberl, M.Y. Haller, P. Papillon, D. Chèze, T. Persson, C. Bales, Testing of combined heating systems for small houses: Improved procedures for whole system test methods, 2015. http://www.macsheep.spf.ch/fileadmin/user_upload/macsheep/dokumente/MacSheep_D2_3_Improved_Procedures_for_whole_system_testing_150211_final.pdf (accessed March 19, 2015).

[46] SEL, TRANSSOLAR, CSTB, TESS, TRNSYS 17 A Transient System Simulation Programme Volume 4 Mathematical Reference, SEL (Solar Energy Laboratory, Univ. of Wisconsin-Madison), TRANSSOLAR (TRANSSOLAR Energietechnik GmbH), CSTB (Centre Scientifique et Technique du Bâtiment), TESS (Thermal Energy Systems Specialists), 2012.

[47] P. Johannesson, Rainflow analysis of switching Markov loads, 1999.

[48] T. Endō, Y. Murakami, The rainflow method in fatigue, Butterworth-Heinemann, 1992.

[49] J.J. Xiong, R.A. Shenoi, A load history generation approach for full-scale accelerated fatigue tests, Eng. Fract. Mech. 75 (2008) 3226–3243. doi:10.1016/j.engfracmech.2007.12.004.

[50] R.J. Barlow, Statistics, 1st ed., John Wiley & Sons, Chichester, 1989.

[51] W. Sparber, P. Melograno, A. Costa, J.R. Santiago, Test facility for solar-assisted heating and cooling systems, in: Sol. Air-Cond. 2007, Tarragona, Spain, 2007.

[52] M. D'Antoni, D. Bettoni, R. Fedrizzi, W. Sparber, Parametric analysis of a novel Solar Combi+ configuration for commercialization.pdf, in: Larnaka, Cyprus, 2011.

[53] U. Jordan, K. Vajen, DHWcalc: Program to generate domestic hot water profiles with statistical means for user defined conditions, in: ISES Sol. World Congr., 2005. http://solar-publikationen.umwelt-uni-kassel.de/uploads/2005%20ISES-SWC%20Jordan%20und%20Vajen%20Program%20to%20Generate%20Domestic%20Hot%20Water%20Profiles%20with%20Statistical%20Means%20for%20User%20Defined%20Conditions.pdf (accessed March 5, 2015).

[54] D. Menegon, Development of a Dynamic Test Procedure for the Laboratory Characterization of Thermally Driven Devices, University of Udine, 2012.

[55] D. Menegon, A. Vittoriosi, R. Fedrizzi, A new test procedure for the dynamic laboratory characterization of thermal systems and their components, Energy Build. 84 (2014) 182–192. doi:10.1016/j.enbuild.2014.07.085.

[56] F. Domínguez-Muñoz, J.M. Cejudo-López, A. Carrillo-Andrés, M. Gallardo-Salazar, Selection of typical demand days for CHP optimization, Energy Build. 43 (2011) 3036–3043. doi:10.1016/j.enbuild.2011.07.024.

[57] A. Leconte, D. Chèze, X. Jobard, Proforma Type 5897 – Iso Building Model, (2014).

[58] M.Y. Haller, R. Dott, J. Ruschenburg, F. Ochs, J. Bony, The Reference Framework for System Simulations of the IEA SHC Task 44/HPP Annex 38 Part A: General Simulation Boundary Conditions, Technical Report IEA-SHC Task44 Subtask C, 2013. https://www.task44.iea-shc.org/data/sites/1/publications/T44A38_Rep_C1_A_BoundaryConditions_Final_Revised.pdf (accessed May 13, 2015).

[59] H. Drück, T. Pauschinger, MULTIPORT Store-Model, Type, 2006. http://www.trnsys.de/download/en/ts_type_340_en.pdf (accessed May 13, 2015).

[60] M. Wetter, Generic optimization program. User manual, Version 3.1.0, Lawrence Berkeley National Laboratory, Berkley, USA, 2011.

[61] Y.H. Kwak, S.H. Cheon, J.M. Park, C.Y. Jang, J.H. Huh, Framework Development and Case Study of a Real-time Weather Forecast Data-based Optimal Operating Strategy, (n.d.). https://www.ibpsa.org/proceedings/asim2012/0078.pdf (accessed May 21, 2015).

[62] R. Bandara, R.A. Attalage, Optimization of Life Cycle Cost of Buildings in terms of Envelope Elements through Combined Performance Modelling and Generic Optimization, (n.d.). http://www.researchgate.net/profile/Priyantha_Bandara4/publication/268578485_Optimization_of_Life_Cycle_Cost_of_Buildings_in_terms_of_Envelope_Elements_through_Combined_Performance_Modelling_and_Generic_Optimization/links/54717a1d0cf216f8cfad1221.pdf (accessed May 21, 2015).

[63] Institute for Solar Energy SPF, SPF Online Collector Catalogue, (2015). http://www.solarenergy.ch/index.php?id=111&L=6.

[64] EN 12975-2:2006, Thermal solar systems and components – Solar collectors – Part 2: Test methods., European Committee for Standardization, Brussels, Belgium, 2006.

[65] EN 13005:1999, Guide to the expression of uncertainty in measurement, European Committee for Standardization, Brussels, Belgium, n.d.

[66] D. Bettoni, Design and assessment of optimised control strategies for solar heating and cooling systems, PhD Thesis, Universitá degli studi di Bergamo, 2013.

[67] F. Besana, Heat rejection problematic in Solar Combi+ system, PhD Thesis, Universitá degli studi di Bergamo, 2009.

[68] iNSPiRE prject, (2013). http://www.inspirefp7.eu/.

Appendix A: Standard

Standards for solar thermal collectors

ISO 9806-1/ ISO 9806-2: the first part describes the outdoor/indoor test procedure to assess the steady-state and quasi-steady-state thermal performance of solar collectors. It is not applicable to tracking concentrating collectors. The second part is applied to all types of solar collectors. It describes the tests method to assess their durability and reliability.

EN 12975-2: it allows to assess the collector performance in steady-state or quasi-dynamic conditions. It is not applicable for tracking concentrating collectors or when the storage unit is integrated with the collector. The testing conditions are different compared to the previously standard. The main features that are assessed are:

- Collector output power;
- Collector instantaneous efficiency: dependence of direct and diffuse radiation, wind speed, sky temperature, incidence angle effects and effective thermal capacitance.

ASHRAE 93: It allows to assess the collector performance under steady state conditions. This standard gives a procedure for determining the collector incident angle modifier for non-concentrating, stationary concentrating and for single-axis tracking collectors.

Standards for solar thermal systems

ISO 9459-2: through the Complete System Testing Group (CSTG), it is applicable to solar system without auxiliary heating. This test method uses a series of one-day outdoor tests and a "black box" procedure that produces a family of "input-output" correlation equations. The system characterization is obtained by the determination of:

- Input-Output diagram;
- Draw-off temperature profile;
- Tank overnight heat losses coefficient.

This information is needed in order to obtain Long Term Performance Prediction (LTPP) of the system for one load pattern.

ISO 9459-5: through the Dynamic System test (DST) some parameters are assessed and are used to predict the annual system performance. This latter passage is obtained with a specific computer program that uses hourly values of local solar irradiation, ambient air temperature and cold-water temperature.

EN 12976-2: It is applied to describe the reliability and performance tests for “factory made” systems. Reliability test consists into verifying the resistance of these systems to mechanical loads, thermal shocks, freezing, etc. For what concerns the performance assessment the two procedure of ISO 9459-2 and ISO 9459-5 can be applied.

EN 12977-2: It describes the procedure to assess the performance of “custom built” systems through the Component Test System Simulation (CTSS) method. According to it, some parameters are determined through tests carried out for each single component. The performance of the whole system is predicted using a simulation program (TRNSYS).

Standards for heat pumps

EN 14511-3: It provides the procedures to assess the performance of electrically driven heat pumps for SH and/or SC at full capacity and under stationary conditions. For this purpose, a tolerance of 2,5% for each temperature from the beginning to the end of “equilibrium” period must be respected.

Rating conditions are given for each kind of unit to assess the Coefficient of Performance (COP, for heating mode) and Energy Efficiency Ratio (EER, for cooling mode). The energy consumptions of integrated or not integrated auxiliaries (such as fans and pumps) are taking into account.

EN 14825: It describes the temperature bin method to calculate the Seasonal Coefficient of Performance (SCOP) for heating and the Seasonal Energy Efficiency Ratio (SEER) for cooling applications. Three ambient temperature frequency distribution are given to evaluate the performance of three reference climates (warm, cold and average climate). For each bin temperature, the performances are extrapolated from the test described by EN 14511.

EN 15316-4-2: It allows to calculate the SPF with the temperature bin method for heat pumps used for SH and/or DHW production that can be driven electrically, with a combustion engine or thermally (absorption only). The nominal COP is evaluated with EN 14511 and EN 16147, while the performance at partial load can be calculate according to EN 14825.

EN 16147: It specifies test conditions and test method for electrically driven heat pumps connected to or including a domestic hot water storage tank. In particular, the Coefficient of Performance for DHW production (COP_{DHW}) is determined for five reference tapping cycles, thus considering non-stationary operating conditions.

ANSI/ASHRAE 37: this standard defines five test method to evaluate the steady state performance of a unit depending on its capacity. A complete cycle for heating units is composed by a heating period and a defrost period. The efficiency of the equipment is not calculated in this standard.

AHRI 320, 325, 330: they provide rating conditions for factory made Water-source/Ground water-source/Ground source closed-loop heat pumps. There are the definitions for the efficiency figures of the unit (COP, EER). The heating and cooling capacities are considering the net values, excluding supplementary resistance heat. The energy consumptions of auxiliaries are taking into account and a pump penalty is defined for ground source HP.

EN 12309-2: it defines test methods for the determination of the Gas Utilization Efficiency (GUE) of gas driven adsorption or absorption heat pumps in heating and cooling mode. This performance figure is assessed at the full capacity and at steady state conditions. Therefore, energy consumption of auxiliaries and the degradation effect due to part load operation are not taking into accounts.

DIN 33830-4: this German standard can be applied to test absorption heat pump units for heating. Different rating conditions are defined according intended place of installation and type of test.

JIS B 8622: this Japanese standard is applied to absorption water/LiBr machines with refrigerating capacities of more than 25 kW_{th}. Tests are performed in stationary conditions but additional tests to assess the performance at partial load are defined. The COP is defined but there are no specifications related to additional energy consumption due to pressure losses, etc.

ANSI/AHRI 560: the test procedure provides a definition of steady state operation with tolerances for water/LiBr chilling machines. Part load performances are assessed at different conditions.

ANSI/ASHRAE 182: It uses test data at steady state conditions for the performance assessment of only absorption water-cooled units. These can use different working fluids (water/LiBr, ammonia/water, etc.) and can be direct-fired by fuels or indirectly fired by other hot heat-transfer fluids. The standard covers both heating and/or cooling applications.

VDI 4650-1: It expresses the efficiency of the heat pump in terms of the seasonal performance factor (SPF) in which the performance in space heating and DHW production are calculated separately (with EN 14511 and EN 16147 respectively) and weighted according to the respective contribution to the annual energy demand.

VDI 4650-2: It defines several performance factors and uses efficiencies to assess the seasonal performance of a gas fired thermally driven heat pump in covering the different demands. This evaluation takes into account partial load test conditions.

Appendix B: Laboratory

The test described in this thesis were performed in the laboratory of the Institute of Renewable Energy of the EURAC [51].

The plant has been developed for testing small size machines with a chilling power[5] lower than 20 kW or heating power lower than 50 kW. The plant is structured to obtain a modular and flexible structure in such a way to have different configurations by adding or removing of some component of the hydraulic system.

The instrumentation is connected to a PXI of National Instrument so the controller software (COSMO) is developed in LabVIEW ambient (Laboratory Virtual Instrumentation Engineering Workbench). This is a graphical language and its application are data acquisition, control of electronic device and analysis and elaboration of data.

Hydraulic configuration

The test facility is presented with a simplified scheme in Figure B-1 where it is showed the configuration for the thermally driven chiller (in the middle) and for a compression heat pump (in the bottom). The different colours represent the sub-systems connected to the components: at the top the heat rejection system (green), on the left the chilling/user system (blue) and on the right the heat production system (brown in the middle).

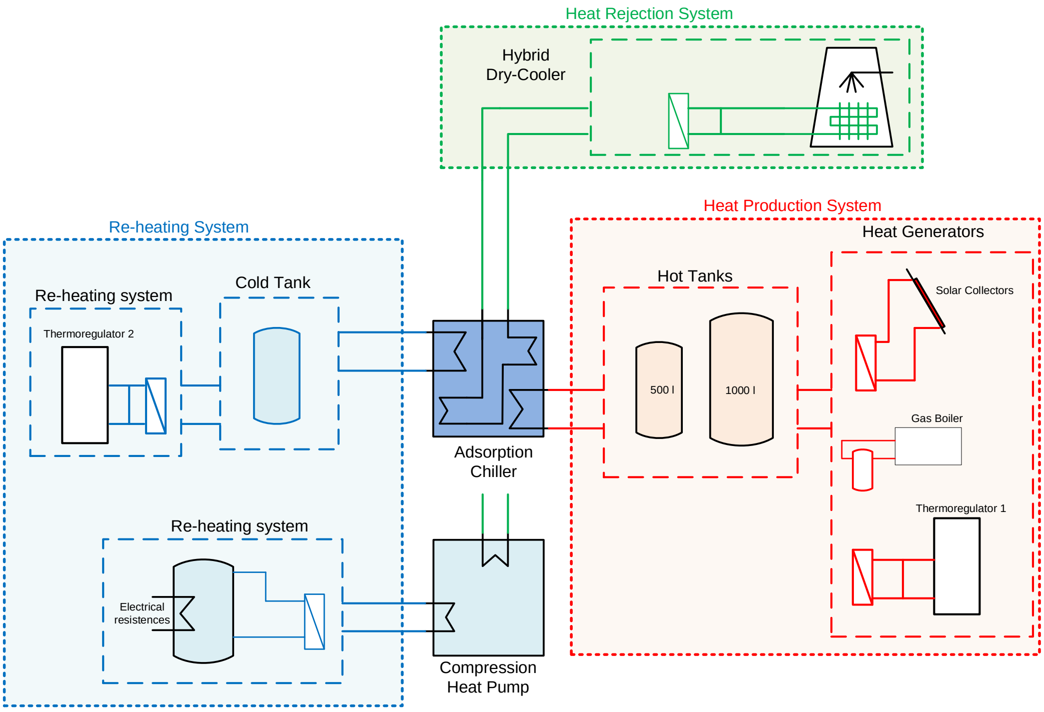

Figure B-1: Hydraulic scheme of the test facility.

<u>Heat rejection circuit</u>

The heat rejection system dissipates the heat at medium temperature in the environment. This system is divided in two circuits connected in series by a heat exchanger. These circuits have different heat transfer fluid. The first one uses water and is directly connected to the chiller, the second one is

[5] This value depends by the EER of thermally driven chiller, because the limit is given by the heat rejection system.

connected to the hybrid cooler and uses glycol/water. This configuration has the advantage of allow to test machines that do not support glycol/water mixture, an easy calculation of the heat capacity and during the replacement of the tested component there is wasted only water saving glycol.

On the roof the hybrid air cooler is installed, which has maximum cooling capacity of 50 kW and maximum electric power consumption of 2.1 kW. The three fans are working in cascade and the hybrid air cooler works as dry cooler or wet cooling tower depending on the target temperature. The speed of the first one is regulated by an inverter through a PID controller, the other two work in ON/OFF mode. When all the fans are running the sprinklers that spray demineralized water according to the settings of the imposed control (e.g. 30 s every 120 s).

To control the condenser inlet temperature (that should be equal to the set value) two variable pumps and one 3-way valve are installed.

The limit of this system is the lack of control of the external temperature: the temperature can be reached in the inlet of condenser is function of the external temperature and the external relative humidity. For example, in the summer it is difficult to reach T_{in_cond} = 28°C or less when the external conditions are 29°C and UR 40%. The worst condition is when the external humidity is very high (80%) because the efficiency of sprinkler is the lowest.

Re-heating circuit

Two different re-heating systems are available in the laboratory. The first one it is used to simulate the behaviour of the user for the chillers while a second one it is used for simulate the behaviour of the air source.

The first re-heating system consists of a thermal regulator with a maximum heating capacity of 20 KW and a cold water storage of 1000 litres. The circuit is connected to the evaporator and heat the cooled water from the chiller until the set entering condition. This system could be divided in two circuit: the first is composed by a thermal regulator connected by a heat exchanger to the other circuit. The cold tank is used to provide temperature that is not fluctuating so the 3-way valve and the pump can provide the set temperature to the inlet of the chiller evaporator.

The second re-heating system is composed by a tank heated by six resistances of 5 kW. The inlet temperature is controlled by pumps and 3-way valves. The thermo-vector fluid of this system is a mixture of water and propylenic glycol.

Heating circuit

The heat production system is composed of one primary circuit and three different heating circuits:

- Gas boiler circuit;
- Thermo regulator circuit (P_{max}= 40 kW, T_{max}=140 °C);
- Solar collector circuit.

The gas boiler circuit is connected to the primary one by a vessel (for legal prescription) and the other two are connected to the primary circuit by a heat exchanger. Mainly is the thermal regulator to produce the heat necessary for reaching the inlet set temperature on the generator of the thermally driven chiller. This temperature can be set to a constant level (for the steady state test) or it is possible to follow a variable temperature profile (for the dynamic test). So this allows, to replicate the heat produced by the solar collector field. As reference, on the roof are installed three flat plate collectors. The gas boiler is used only for back-up and start when is not possible reach the set temperature with others devices.

The primary circuit is connected to the chiller and is equipped with two storages of 1000 and 500 litres. It is possible to use none or only one of them or to use them connected in series, obtaining a tall water column of 1500 litres completely stratified, or in parallel obtaining a storage of 1500 litres. A 3-way valve is installed between the inlet and the outlet of the chiller, for a better control of the inlet temperature. The volume flow is guaranteed by variable pumps. The configuration presented allows to set a large number of configurations depending on the needs.

Monitoring and control

All the meaningful quantities (over 170 values) of the test facility are measured by mean a series of sensors of temperature, pressure, volume, electric consumption. Among these, the data that are needed for the evaluation of the performance of the tested machine are recorded.

LabVIEW is used both as test bench control software and "component emulation" software. The input boundary conditions are given with a resolution of one minute while the acquisition frequency is 5 seconds.

In the table it is present a list of the models and their characteristics of all the typologies of the sensor utilized in the test facility.

Table B-1: Measurement Equipment characteristics.

Instrument	Model	Class	Range	Tolerance
Thermo-resistance	TC Direct PT100 high temperature	A	60 to 100 °C	0.25 °C
	medium temperature	A	10 to 50°C	0.25 °C
	low temperature	A	0 to 30°C	0.25 °C
Pressure probe	Siemens QBE2002-P10	N.A.	0 to 10 Bar	±0.4 % FS
Volume flow meter	Sitrans FM Magflo MAG6000	1	0 to 10 m^3/h	±0.25%
Electric Meter	Vemer Energy-230 D63A	1	0 to 63 A @ 230 V	

The temperature measurements are taken at the inlets and outlets of all the components (evaporator, condenser, generator, storages, mixing points) by the thermo-resistance TC Direct PT100 (4-wires, class A).

Figure B-2: Thermo-resistance Pt100. Source: TC Direct.

In order to evaluate the pressure drop at the internal heat exchangers the pressure is measured only at the inlet and outlet of the chiller evaluate with the piezo-resistive QBE2002-P10 made by Siemens.

Figure B-3: Pressure probe QBE2002-P10. Source: Siemens.

The volumetric flows are measured by electromagnetic flow meters Siemens Sitrans FM Magflo MAG 6000 that permit an accurate measurement. There is installed one flow meter to each branch of the plant.

Figure B-4: Volume flow meter. Source: Siemens.

For the electric consumption of thermos-regulators, chiller, hybrid air-cooler, pumps and actuators of the 3-way valves, have been installed five electric meters Vemer Energy-230 D63A Class 1.

Figure B-5: Electric Meter. Source: Vemer.

The test facility control and the data acquisition is done using the National Instrument PXI NI PXI - 8115. It allows to communicate with different devices (i.e. pumps, valves, etc.) and acquiring data in real time through system controllers and peripheral modules. The PXI require software developed in LabVIEW ambient and the control software is write by EURAC researchers.

Uncertainty

The measurement uncertainties of temperatures and mass flows are calculated according to EN 13005 [65]. From these, the multiplication and divisions uncertainties are computed as:

Equation 0-1 $$u_{Multiplication} = \sqrt{\left(Fact_1 \cdot u_{Fact_2}\right)^2 + \left(Fact_2 \cdot u_{Fact_1}\right)^2}$$ [-]

Equation 0-2 $$u_{Division} = \frac{1}{Den} \cdot \sqrt{(u_{Num})^2 + (Division \cdot u_{Den})^2}$$

Where $Multiplication = Fact_1 \cdot Fact_2$ *and* $Division = \frac{Num}{Den}$

The uncertainty on the quantities elaborated through the integration is calculated as:

Equation 0-3 $$u_Q = \int u_{\dot{Q}} \cdot d\tau = \sum_i \left(u_{\dot{Q}_i} \cdot \tau_i\right)$$ [-]

For the laboratory equipment, the calculation of uncertainty according to EN 13005 [65] is presented in Table B-2.

Note: the uncertainty calculated for the temperature sensors is a function of the temperature; however, for the range of application it could be considered as constant.

Table B-2: Measurement Equipment Uncertainty.

Parameter	Unit	Uncertainty values
Temperature sensor	°C	0.32 °C
temperature difference	°C	0.45 °C
Volumetric flow sensor	l/h	0.25 % of the read value
Electrical Power sensor	kW	1% of the read value
Time	h	True value assumption

Appendix C: Simulations and case studies

The simulations were used for the definition of boundary conditions of the test at component level and for the procedure at system level. In both cases, the simulations are computed with Trnsys software version 17 [46]. Here it is reported a short description of the types used in both cases.

The models of components have been validated during the PhD thesis of Bettoni [66]. In particular, the types have been validated through laboratory test or through monitoring data of a demo case. The main models used are:

- The heat pump model (type 847) is based on a map of the performance: for different combination of inlet temperatures and mass flow on the condenser and evaporator circuits, the map presents the heating (or cooling) power and the electrical consumption. During the simulation, the heat pump model extrapolates from this map its performance and calculates the return temperatures. The outputs of the type are the outlet temperatures, flows, thermal power, electric consumption and the COP (or EER). The model has been adapted to read a four-dimension map. The map was validated with laboratory measurements performed on the heat pump installed in the Eurac laboratory.
- The adsorption chiller model (type 290) is developed by Sortech. As the heat pump, the model works with fixed maps, based on rated manufacturer data including a delay in the starting phase for simulate the machine heating up. The manufacturer provides the DLL of the model therefore the code modification is not possible on this type.
- The collector model (type 1) considers the collectors' parameters calculated in the certification test of one commercial collector. The type 1 is coupled to a moving average to introduce inertia effects.
- The Storages model (type 340) is a commercial type [59]. It considers the stratification with an iterative calculus. This model is largely used by other researchers.
- The building model is type 56. The model is used for the definition of the load file.
- The weather file is read with the type 109 for the simulation of the whole year. The sequence' weather data is read with type 9.
- The dry-cooler model (type 880) was developed by Besana [67] and improved by Bettoni [66]. The calculation is based on the ε/NTU method which includes also capacitance effects.
- Other traditional model are the pipes (type 31), circulation pump (type 110), mixing and tempering valves (type 11) and heat exchanger (type 5b).

Solar Combi Plus system for the test at Component Level

Figure C-1 shows the scheme of the plant. For each component there are indicated the types used to model the system.

The control system has been developed for the manufacturer in the thesis of Bettoni [66]. Beyond the schemes presented in the chapter 2.3, the control strategy of the system foresees a direct space heating with the solar source and the direct feeding of DHW storage from solar source.

The characteristics of the adsorption chiller and the electric heat pump are shown respectively in chapters 2.4 and 2.5.

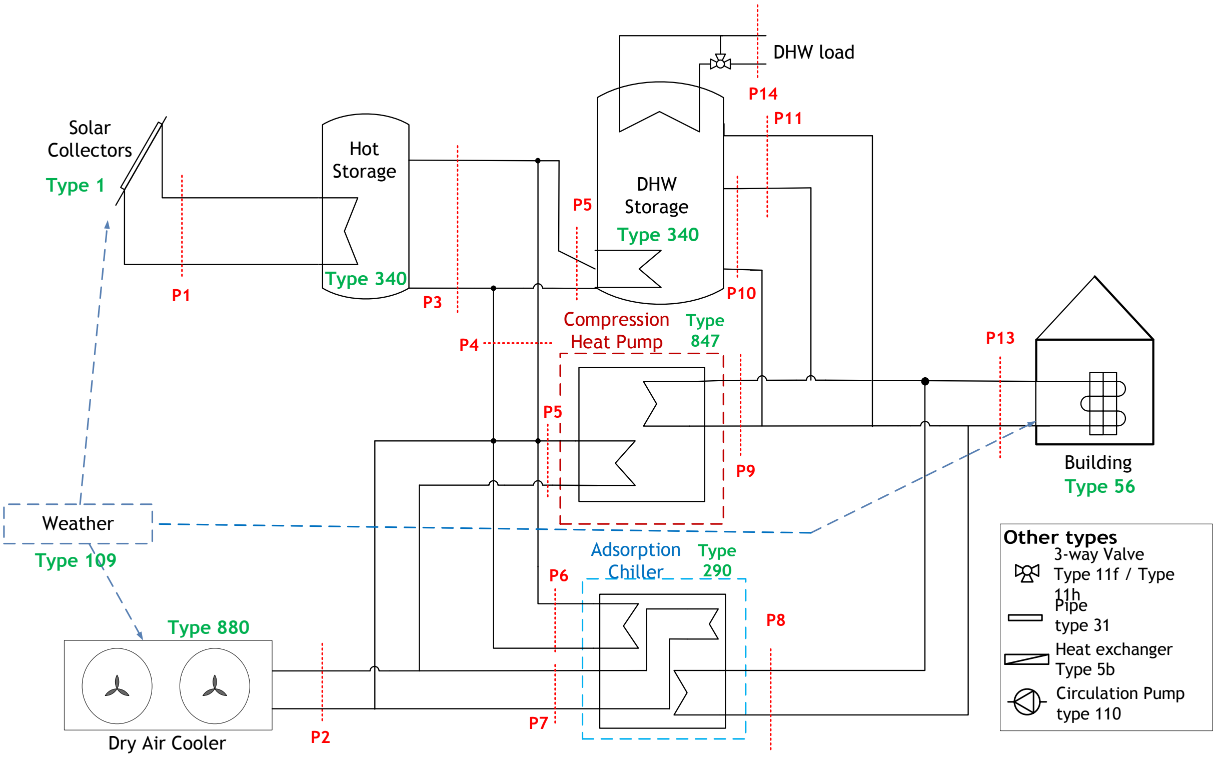

Figure C-1: Layout of Solar Combi Plus system and identification of Types used to modelled the system. Component boundaries definition.

Solar Assisted Heat Pump System

The solar assisted heat pump system was design and build with the equipment present in the laboratory. Therefore, this hybrid system is in a non-industrialized system. A dedicated control strategy was developed and implemented in the laboratory. Figure C-2 shows the layout of the system with the type used for the model. The red ports indicated in the figure are used for the energy balance of the system.

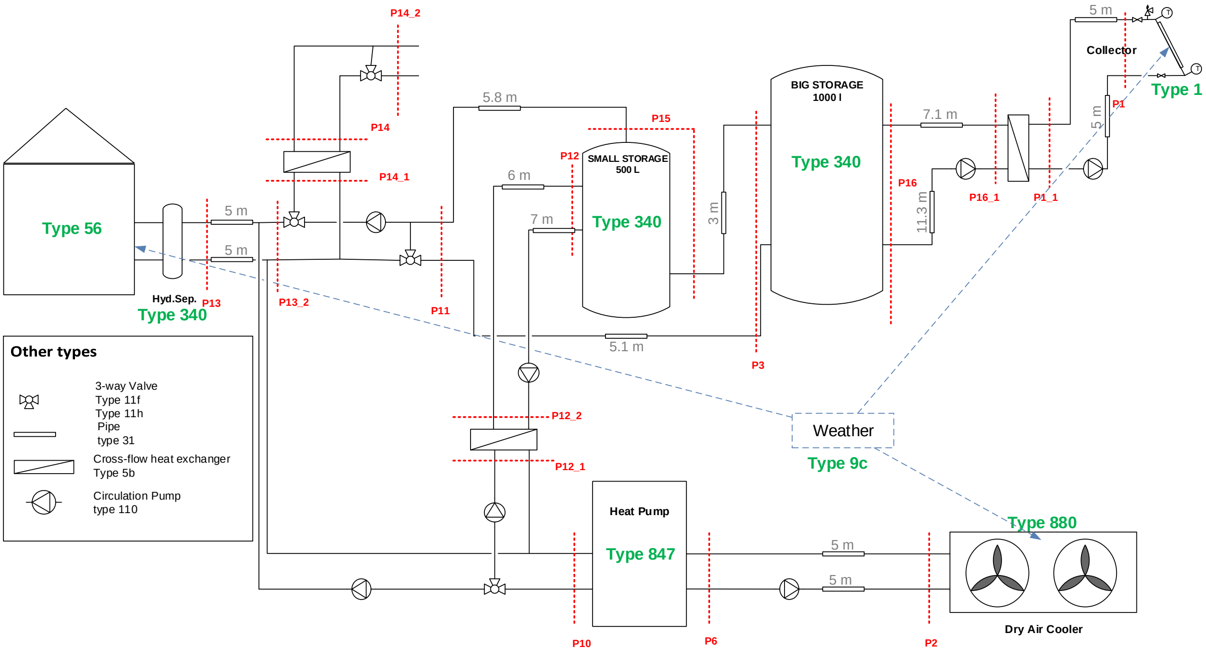

Figure C-2: Layout of SAHP system and identification of Types used to modelled the system. Whole system.

The installed system consists of:

- An electrically driven water to water compression heat pump (Clivet WSHN-EE 31 – shown in chapter 2.5).
- Two storages connected in series with a volume of 500 and 1000 litres.
- One hydraulic module, controlled by an energy.
- The controller.

The heat pump is connected to a two different circuits through a hydraulic module manager developed in the EU FP7 founded project iNSPiRE [68]. The Hydraulic module manages the heat fluxes from the heat pump to the building (heating or cooling) or to the small storage (DHW charge). Figure C-3 shows the heat pump connections. Note that the heat pump is reversible, then it is possible to invert the evaporator and condenser for the cooling operation.

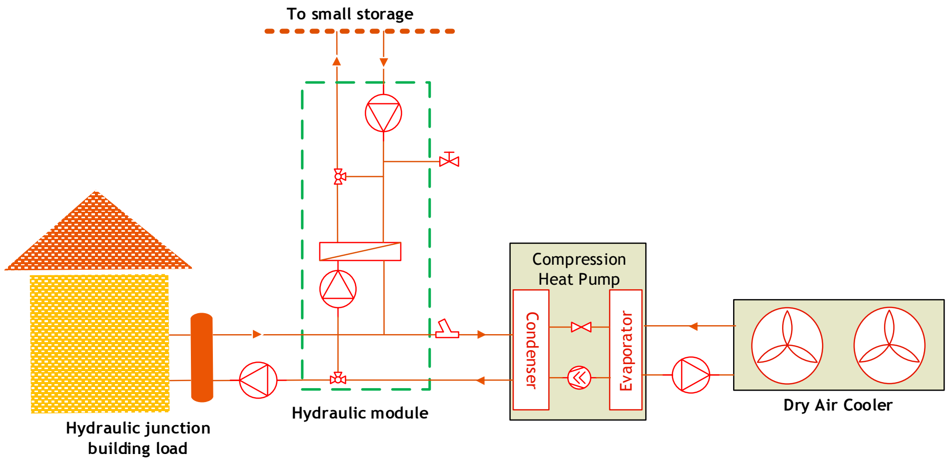

Figure C-3: Heat pump connection with loads through a hydraulic module.

The storage system is composed by two storages; the big storage has a volume of 1000 litres the small storage has a volume of 500 litres. The storages are connected in series. They have an external heat exchanger, 10 cm of insulation and they do not have any stratification separator.

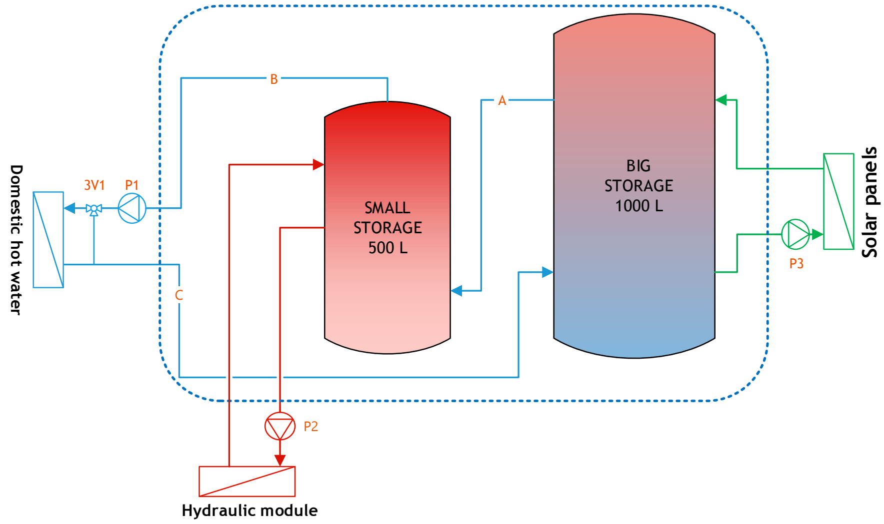

Figure C-4: Storage system.

The system works with the schemes indicated in Figure C-5. The mathematical description of the control scheme is not reported.

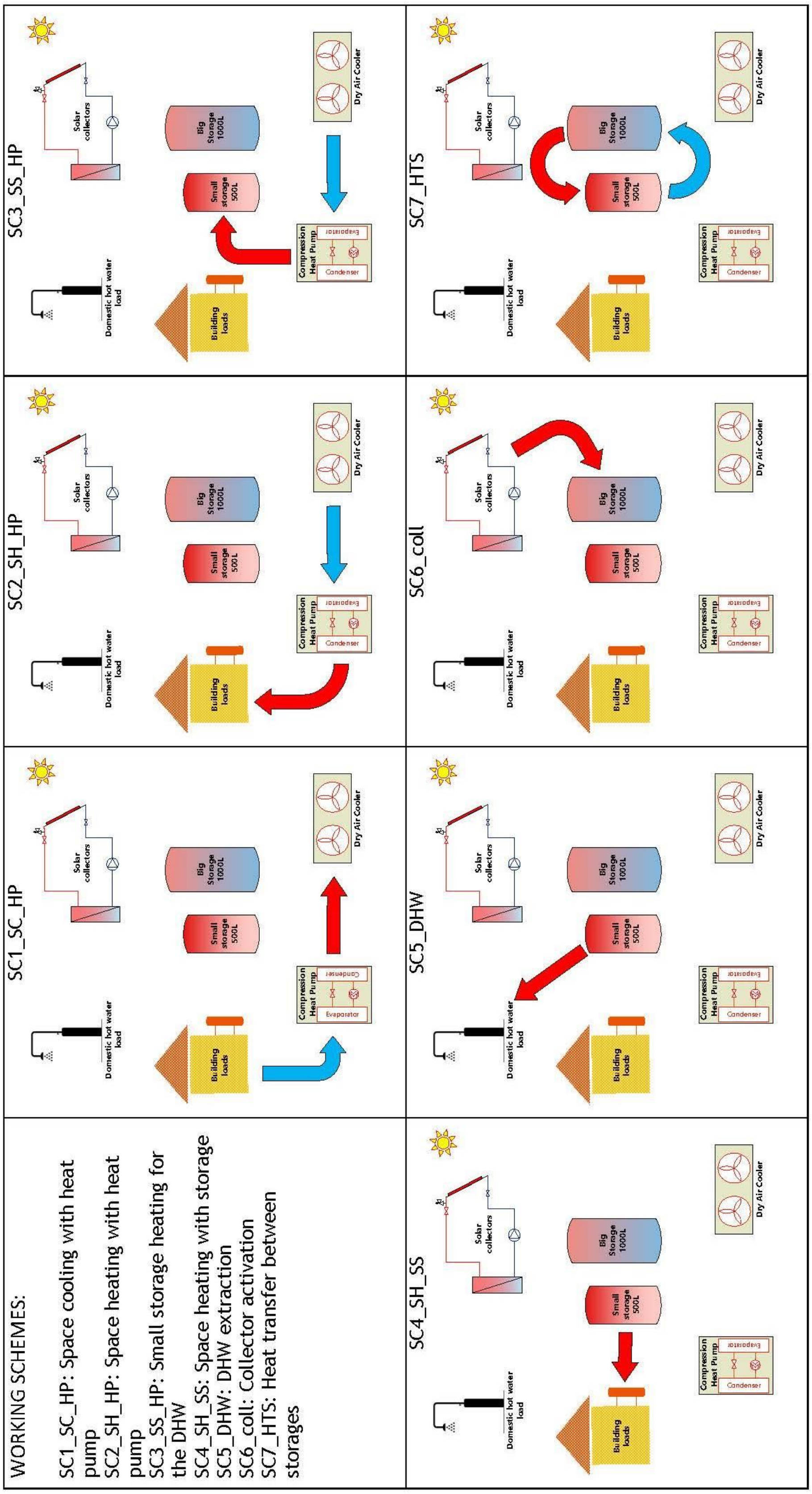

Figure C-5: Working schemes of hybrid system

The model of the system contains the control strategy of the system and prints the energy or power balances. The Figure C-6 shows the model developed in TRNSYS.

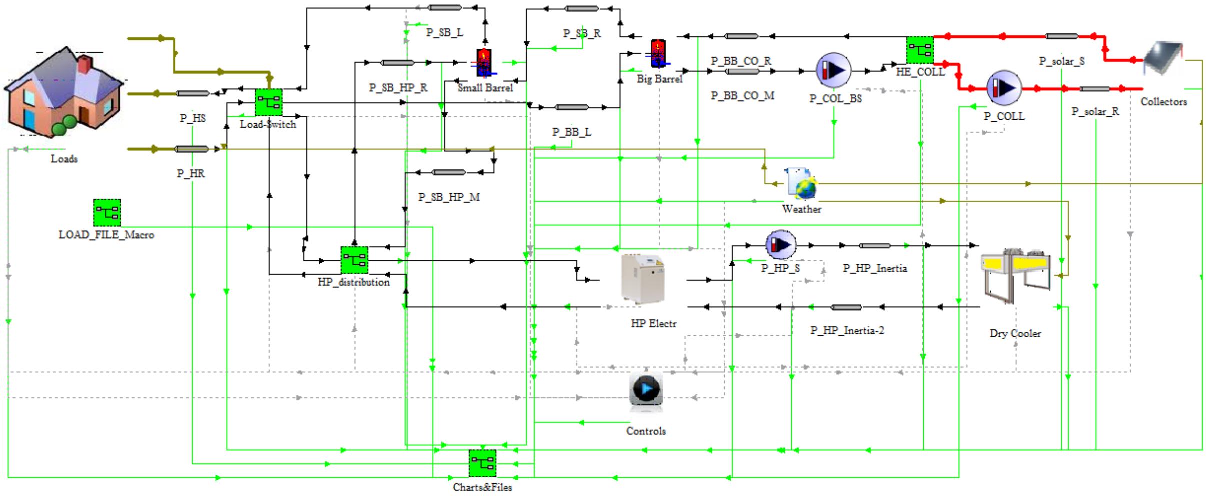

Figure C-6: Image of Trnsys simulation studio used for the simulations.

Appendix D: Clustering

Sequence

The following figures shows the selection for the climates of Bolzano and Zurich for the 8, 10, 12 and 24 clusters created with the 2D, 3D and 4D coordinates.

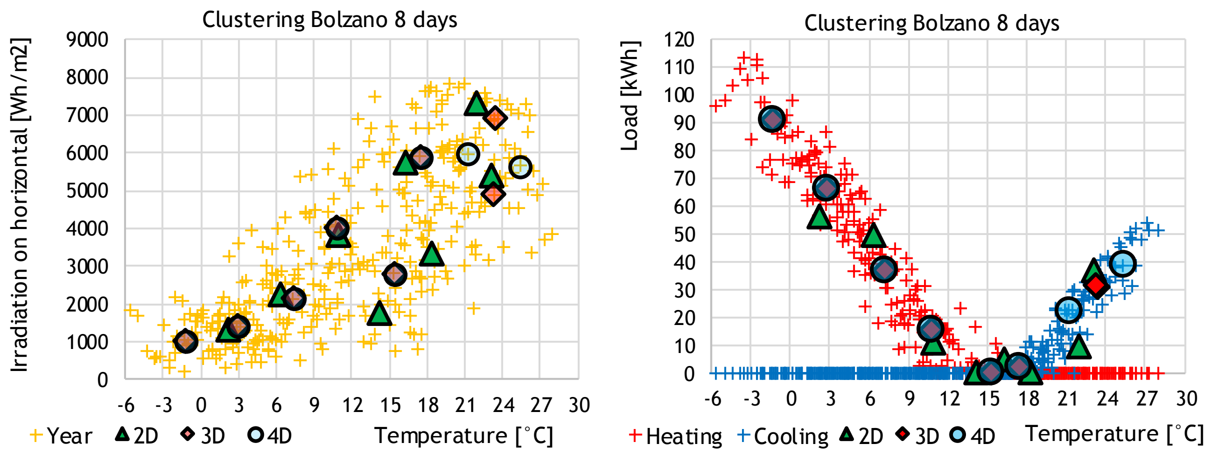

Figure D-1: Identification of eight-days sequences defined with different coordinates. Bolzano climate.

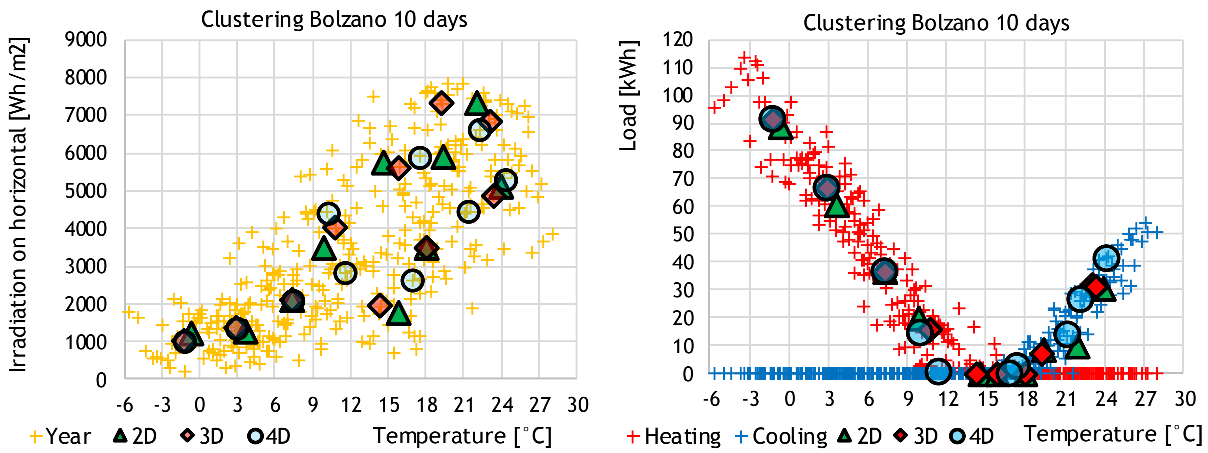

Figure D-2: Identification of ten-days sequences defined with different coordinates. Bolzano climate.

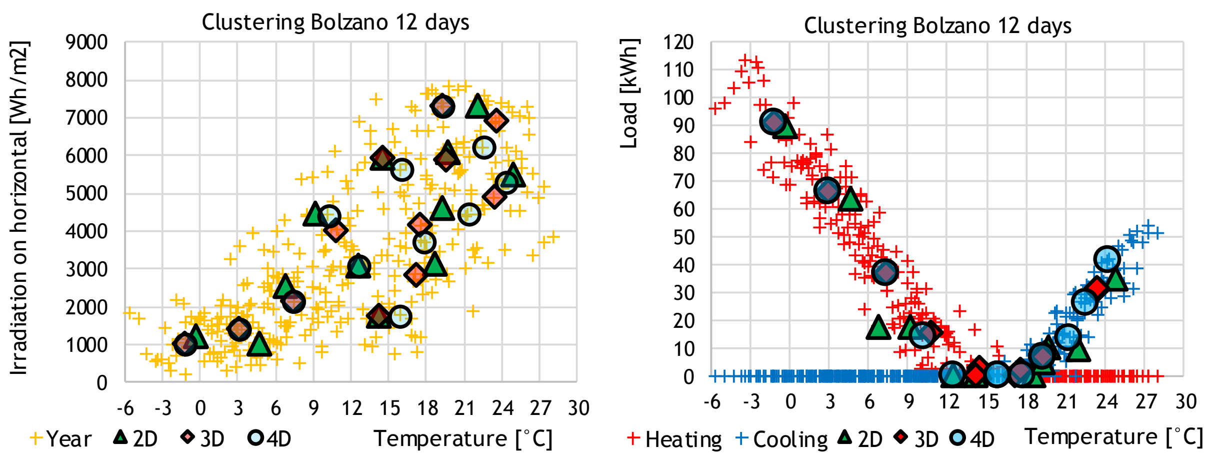

Figure D-3: Identification of twelve-days sequences defined with different coordinates. Bolzano climate.

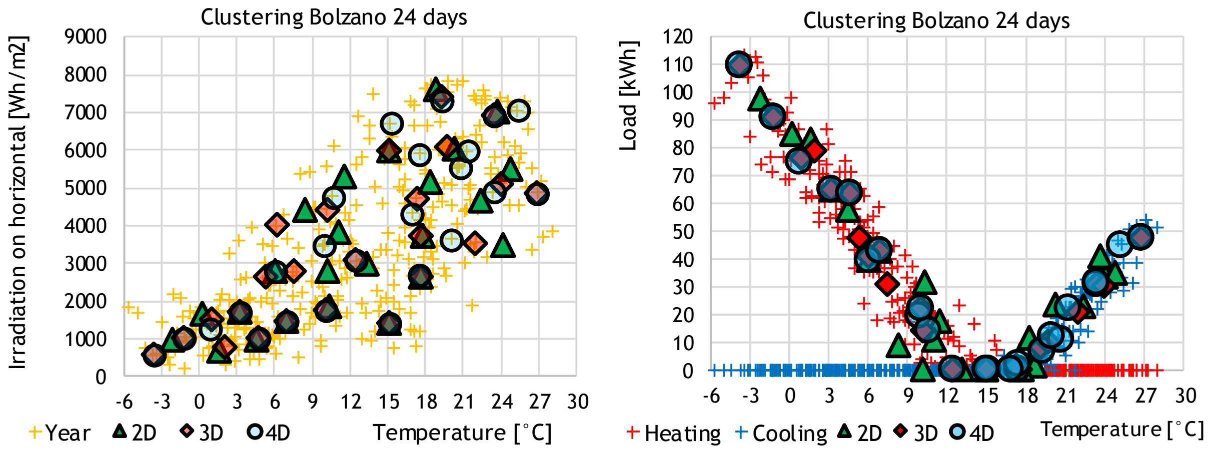

Figure D-4: Identification of 24-days sequences defined with different coordinates. Bolzano climate.

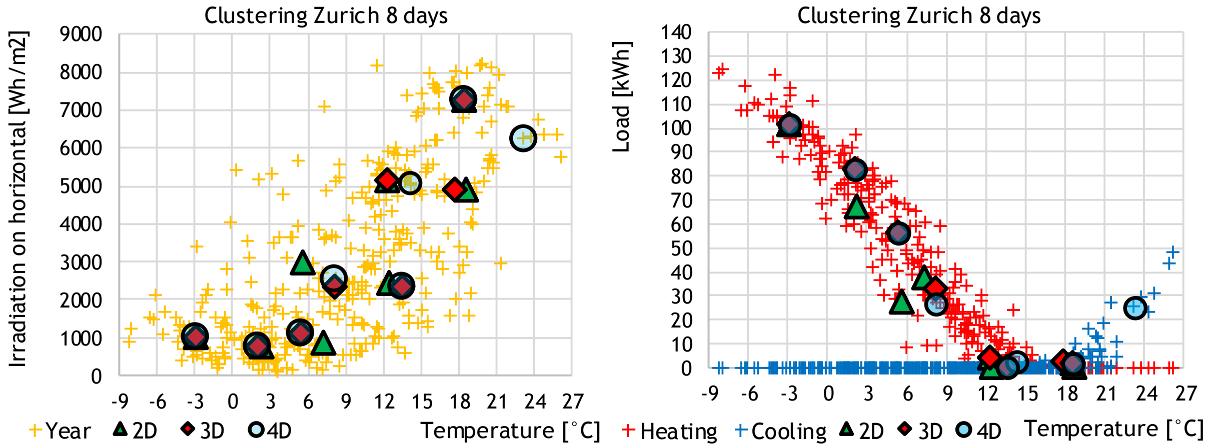

Figure D-5: Identification of eight-days sequences defined with different coordinates. Zurich climate.

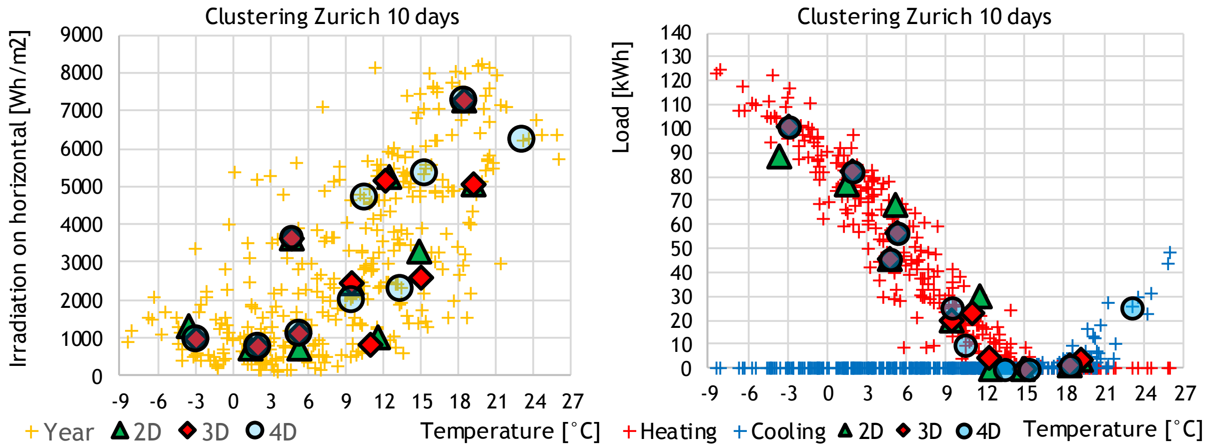

Figure D-6: Identification of ten-days sequences defined with different coordinates. Zurich climate.

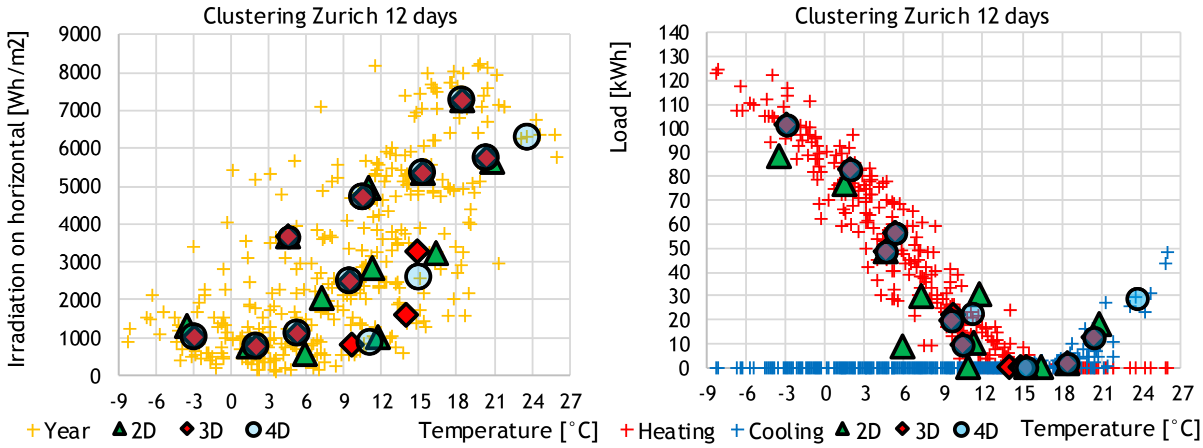

Figure D-7: Identification of twelve-days sequences defined with different coordinates. Zurich climate.

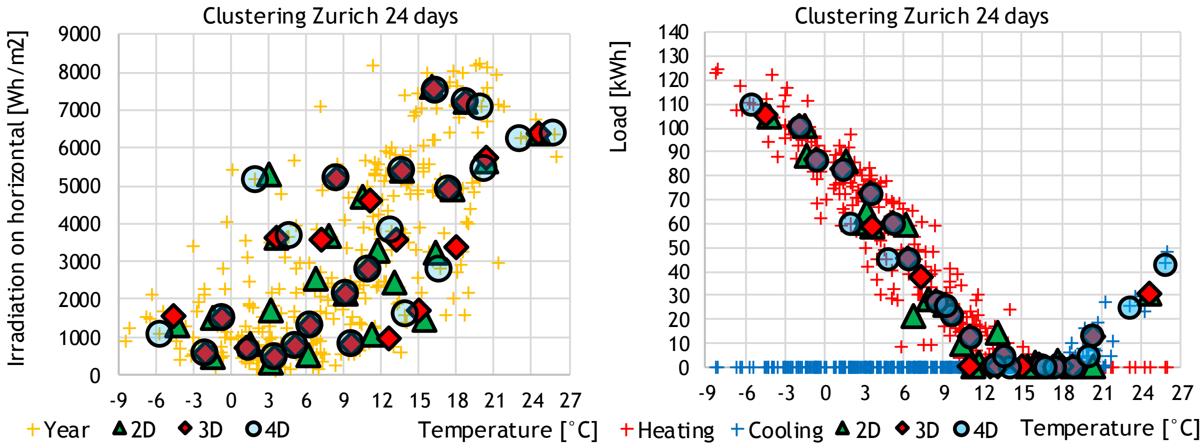

Figure D-8: Identification of 24-days sequences defined with different coordinates. Zurich climate.

BOLZANO 2D	6 Days 2D					
Days	88	164	251	254	317	328
Nelements	36	35	75	61	65	93
Date	29/03	13/06	08/09	11/09	13/11	24/11
Irradiation	4437	7322	5532	2862	2216	1310
Temperature	10.1	22.0	20.5	17.1	8.2	2.3
Qh	14.5	0.0	0.0	0.0	25.6	56.6
Qc	0.0	9.6	16.1	0.0	0.0	0.0
BOLZANO 3D	6 Days 3D					
Days	29	40	78	197	254	321
Nelements	62	31	43	104	72	53
Date	29/01	09/02	19/03	16/07	11/09	17/11
Irradiation	1392	1039	4022	6205	2862	2127
Temperature	2.9	-1.2	10.8	20.9	17.1	7.3
Qh	66.3	91.1	15.8	0.0	0.0	36.8
Qc	0.0	0.0	0.0	15.5	0.0	0.0
BOLZANO 4D	6 Days 4D					
Days	19	152	171	238	279	321
Nelements	87	67	30	33	88	60
Date	19/01	01/06	20/06	26/08	06/10	17/11
Irradiation	1392	5911	5660	5976	2879	2127
Temperature	2.3	17.5	25.4	21.3	13.8	7.3
Qh	75.2	0.0	0.0	0.0	4.9	36.8
Qc	0.0	2.1	38.9	22.5	0.0	0.0
ZURICH 2D	6 Days 2D					
Days	52	89	105	145	269	325
Nelements	47	68	31	50	86	83
Date	21/02	30/03	15/04	25/05	26/09	21/11
Irradiation	842	5134	3662	7205	2327	824
Temperature	-2.5	13.7	4.7	18.8	11.7	4.1
Qh	97.4	8.6	45.5	0.0	2.0	66.7
Qc	0.0	0.0	0.0	0.0	0.0	0.0
ZURICH 3D	6 Days 3D					
Days	3	64	95	150	218	365
Nelements	43	77	66	55	50	74
Date	03/01	05/03	05/04	30/05	06/08	31/12
Irradiation	1000	2320	5100	2331	7264	727
Temperature	-2.9	8.1	14.2	13.5	18.4	3.0
Qh	101.4	33.2	2.5	0.0	0.0	76.0
Qc	0.0	0.0	0.0	0.0	1.6	0.0
ZURICH 4D	6 Days 4D					
Days	89	218	228	270	302	342
Nelements	67	42	9	69	78	100
Date	30/03	06/08	16/08	27/09	29/10	08/12
Irradiation	5134	7264	6249	2479	1612	676
Temperature	13.7	18.4	23.2	12.3	7.7	0.8
Qh	8.6	0.0	0.0	3.8	41.7	85.7
Qc	0.0	1.6	25.5	0.0	0.0	0.0

BOLZANO 2D	8 Days 2D							
Days	65	118	164	174	216	267	294	328
Nelements	46	42	35	41	40	39	32	90
Date	06/03	28/04	13/06	23/06	04/08	24/09	21/10	24/11
Irradiation	2250	3800	7322	5389	5759	3319	1751	1310
Temperature	6.4	11.0	22.0	23.2	16.4	18.4	14.2	2.3
Qh	49.7	10.6	0.0	0.0	0.0	0.0	0.0	56.6
Qc	0.0	0.0	9.6	37.3	5.0	0.3	0.0	0.0
BOLZANO 3D	8 Days 3D							
Days	29	40	78	152	191	248	288	321
Nelements	62	31	34	59	29	33	66	51
Date	29/01	09/02	19/03	01/06	10/07	05/09	15/10	17/11
Irradiation	1392	1039	4022	5911	6913	4894	2797	2127
Temperature	2.9	-1.2	10.8	17.5	23.4	23.3	15.4	7.3
Qh	66.3	91.1	15.8	0.0	0.0	0.0	0.0	36.8
Qc	0.0	0.0	0.0	2.1	31.2	31.4	0.0	0.0
BOLZANO 4D	8 Days 4D							
Days	29	40	78	152	171	238	288	321
Nelements	63	30	34	59	30	32	67	50
Date	29/01	09/02	19/03	01/06	20/06	26/08	15/10	17/11
Irradiation	1392	1039	4022	5911	5660	5976	2797	2127
Temperature	2.9	-1.2	10.8	17.5	25.4	21.3	15.4	7.3
Qh	66.3	91.1	15.8	0.0	0.0	0.0	0.0	36.8
Qc	0.0	0.0	0.0	2.1	38.9	22.5	0.0	0.0
ZURICH 2D	8 Days 2D							
Days	3	60	90	217	218	264	278	299
Nelements	44	54	50	27	44	65	35	46
Date	03/01	01/03	31/03	05/08	06/08	21/09	05/10	26/10
Irradiation	1000	756	5145	4929	7264	2467	2969	878
Temperature	-2.9	2.2	12.3	18.6	18.4	12.4	5.5	7.2
Qh	101.4	67.7	4.2	0.0	0.0	0.0	27.8	37.8
Qc	0.0	0.0	0.0	0.2	1.6	0.0	0.0	0.0
ZURICH 3D	8 Days 3D							
Days	3	28	64	90	150	212	218	332
Nelements	38	37	62	45	53	32	44	54
Date	03/01	28/01	05/03	31/03	30/05	31/07	06/08	28/11
Irradiation	1000	1123	2320	5145	2331	4881	7264	777
Temperature	-2.9	5.3	8.1	12.3	13.5	17.7	18.4	2.0
Qh	101.4	56.5	33.2	4.2	0.0	0.0	0.0	82.8
Qc	0.0	0.0	0.0	0.0	0.0	2.8	1.6	0.0
ZURICH 4D	8 Days 4D							
Days	3	28	95	150	218	228	300	332
Nelements	38	44	65	53	41	9	61	54
Date	03/01	28/01	05/04	30/05	06/08	16/08	27/10	28/11
Irradiation	1000	1123	5100	2331	7264	6249	2557	777
Temperature	-2.9	5.3	14.2	13.5	18.4	23.2	8.2	2.0
Qh	101.4	56.5	2.5	0.0	0.0	0.0	27.1	82.8
Qc	0.0	0.0	0.0	0.0	1.6	25.5	0.0	0.0

BOLZANO 2D	10 Days 2D									
Days	84	155	164	167	247	256	287	321	356	365
Nelements	45	26	31	29	30	41	24	46	54	39
Date	25/03	04/06	13/06	16/06	04/09	13/09	14/10	17/11	22/12	31/12
Irradiation	3495	5774	7322	5883	5111	3493	1772	2127	1268	1240
Temperature	9.9	14.7	22.0	19.4	24.0	18.0	15.8	7.3	3.6	-0.6
Qh	19.5	0.0	0.0	0.0	0.0	0.0	0.0	36.8	60.8	88.8
Qc	0.0	0.0	9.6	8.2	30.4	0.0	0.0	0.0	0.0	0.0
BOLZANO 3D	10 Days 3D									
Days	29	40	78	158	194	218	248	256	272	321
Nelements	62	31	33	38	25	21	33	37	37	48
Date	29/01	09/02	19/03	07/06	13/07	06/08	05/09	13/09	29/09	17/11
Irradiation	1392	1039	4022	5627	6841	7311	4894	3493	1965	2127
Temperature	2.9	-1.2	10.8	15.9	23.1	19.3	23.3	18.0	14.4	7.3
Qh	66.3	91.1	15.8	0.0	0.0	0.0	0.0	0.0	0.0	36.8
Qc	0.0	0.0	0.0	0.0	31.7	7.2	31.4	0.0	0.0	0.0
BOLZANO 4D	10 Days 4D									
Days	29	40	88	152	183	211	225	253	295	321
Nelements	63	30	27	54	19	23	27	45	26	51
Date	29/01	09/02	29/03	01/06	02/07	30/07	13/08	10/09	22/10	17/11
Irradiation	1392	1039	4437	5911	4456	5320	6633	2648	2851	2127
Temperature	2.9	-1.2	10.1	17.5	21.3	24.2	22.2	16.9	11.5	7.3
Qh	66.3	91.1	14.5	0.0	0.0	0.0	0.0	0.0	0.3	36.8
Qc	0.0	0.0	0.0	2.1	13.8	41.4	26.4	0.0	0.0	0.0
ZURICH 2D	10 Days 2D									
Days	32	75	105	147	210	218	242	303	307	326
Nelements	34	38	26	32	25	40	45	29	42	54
Date	01/02	16/03	15/04	27/05	29/07	06/08	30/08	30/10	03/11	22/11
Irradiation	1308	713	3662	3300	5058	7264	5280	1007	2469	751
Temperature	-3.5	5.3	4.7	14.9	19.3	18.4	12.5	11.7	9.5	1.5
Qh	88.4	68.2	45.5	0.0	0.0	0.0	0.0	30.4	20.0	77.0
Qc	0.0	0.0	0.0	0.0	3.9	1.6	0.0	0.0	0.0	0.0
ZURICH 3D	10 Days 3D									
Days	3	28	90	105	210	218	250	296	307	332
Nelements	38	39	45	27	26	40	40	23	34	53
Date	03/01	28/01	31/03	15/04	29/07	06/08	07/09	23/10	03/11	28/11
Irradiation	1000	1123	5145	3662	5058	7264	2584	852	2469	777
Temperature	-2.9	5.3	12.3	4.7	19.3	18.4	15.0	11.1	9.5	2.0
Qh	101.4	56.5	4.2	45.5	0.0	0.0	0.0	23.0	20.0	82.8
Qc	0.0	0.0	0.0	0.0	3.9	1.6	0.0	0.0	0.0	0.0
ZURICH 4D	10 Days 4D									
Days	3	28	105	150	160	218	228	251	298	332
Nelements	38	38	24	49	30	40	9	40	44	53
Date	03/01	28/01	15/04	30/05	09/06	06/08	16/08	08/09	25/10	28/11
Irradiation	1000	1123	3662	2331	4698	7264	6249	5349	2032	777
Temperature	-2.9	5.3	4.7	13.5	10.5	18.4	23.2	15.3	9.5	2.0
Qh	101.4	56.5	45.5	0.0	9.6	0.0	0.0	0.0	25.5	82.8
Qc	0.0	0.0	0.0	0.0	0.0	1.6	25.5	0.0	0.0	0.0

BOLZANO 2D	12 Days 2D											
Days	96	110	145	164	166	217	226	289	294	299	334	349
Nelements	18	21	29	30	30	23	22	26	27	39	51	49
Date	06/04	20/04	25/05	13/06	15/06	05/08	14/08	16/10	21/10	26/10	30/11	15/12
Irradiation	5961	4469	3126	7322	4626	6104	5495	3073	1751	2557	1231	1028
Temperature	14.5	9.1	18.6	22.0	19.2	19.7	24.8	12.5	14.2	6.8	-0.3	4.7
Qh	2.8	17.4	0.0	0.0	0.0	0.0	0.0	0.0	0.0	17.6	90.0	63.8
Qc	0.0	0.0	0.0	9.6	4.7	10.0	34.9	0.0	0.0	0.0	0.0	0.0
BOLZANO 3D	12 Days 3D											
Days	29	40	78	96	167	191	218	248	254	259	294	321
Nelements	62	31	32	19	24	21	19	29	29	23	28	48
Date	29/01	09/02	19/03	06/04	16/06	10/07	06/08	05/09	11/09	16/09	21/10	17/11
Irradiation	1392	1039	4022	5961	5883	6913	7311	4894	2862	4145	1751	2127
Temperature	2.9	-1.2	10.8	14.5	19.4	23.4	19.3	23.3	17.1	17.5	14.2	7.3
Qh	66.3	91.1	15.8	2.8	0.0	0.0	0.0	0.0	0.0	0.0	0.0	36.8
Qc	0.0	0.0	0.0	0.0	8.2	31.2	7.2	31.4	0.0	2.3	0.0	0.0
BOLZANO 4D	12 Days 4D											
Days	29	40	88	158	183	211	218	228	268	287	289	321
Nelements	63	30	25	29	21	22	22	26	25	28	24	50
Date	29/01	09/02	29/03	07/06	02/07	30/07	06/08	16/08	25/09	14/10	16/10	17/11
Irradiation	1392	1039	4437	5627	4456	5320	7311	6220	3721	1772	3073	2127
Temperature	2.9	-1.2	10.1	15.9	21.3	24.2	19.3	22.5	17.8	15.8	12.5	7.3
Qh	66.3	91.1	14.5	0.0	0.0	0.0	0.0	0.0	0.0	0.0	0.0	36.8
Qc	0.0	0.0	0.0	0.0	13.8	41.4	7.2	26.0	0.4	0.0	0.0	0.0
ZURICH 2D	12 Days 2D											
Days	32	58	133	139	149	174	218	227	251	288	303	326
Nelements	34	22	32	27	23	29	36	18	29	33	27	55
Date	01/02	27/02	13/05	19/05	29/05	23/06	06/08	15/08	08/09	15/10	30/10	22/11
Irradiation	1308	3667	571	2071	3250	4960	7264	5629	5349	2813	1007	751
Temperature	-3.5	4.6	5.9	7.3	16.4	10.9	18.4	20.8	15.3	11.3	11.7	1.5
Qh	88.4	48.9	8.5	30.0	0.0	0.0	0.0	0.0	0.0	10.0	30.4	77.0
Qc	0.0	0.0	0.0	0.0	0.0	0.0	1.6	18.4	0.0	0.0	0.0	0.0
ZURICH 3D	12 Days 3D											
Days	3	28	58	115	146	147	160	218	232	251	307	332
Nelements	38	37	21	16	25	26	30	36	17	31	35	53
Date	03/01	28/01	27/02	25/04	26/05	27/05	09/06	06/08	20/08	08/09	03/11	28/11
Irradiation	1000	1123	3667	837	1586	3300	4698	7264	5728	5349	2469	777
Temperature	-2.9	5.3	4.6	9.7	14.0	14.9	10.5	18.4	20.4	15.3	9.5	2.0
Qh	101.4	56.5	48.9	22.2	0.0	0.0	9.6	0.0	0.0	0.0	20.0	82.8
Qc	0.0	0.0	0.0	0.0	0.0	0.0	0.0	1.6	12.7	0.0	0.0	0.0
ZURICH 4D	12 Days 4D											
Days	3	28	58	160	218	229	232	250	251	296	307	332
Nelements	38	38	22	32	36	7	7	37	38	23	34	53
Date	03/01	28/01	27/02	09/06	06/08	17/08	20/08	07/09	08/09	23/10	03/11	28/11
Irradiation	1000	1123	3667	4698	7264	6284	5728	2584	5349	852	2469	777
Temperature	-2.9	5.3	4.6	10.5	18.4	23.6	20.4	15.0	15.3	11.1	9.5	2.0
Qh	101.4	56.5	48.9	9.6	0.0	0.0	0.0	0.0	0.0	23.0	20.0	82.8
Qc	0.0	0.0	0.0	0.0	1.6	29.5	12.7	0.0	0.0	0.0	0.0	0.0

Table D-1: Selection of 6, 8, 10 and 12 days sequences of Bolzano and Zurich.

BOLZANO 2D	24 Days 2D																							
Days	9	46	54	94	102	109	118	162	176	187	206	214	215	226	246	268	275	282	290	308	323	327	329	344
Nelements	17	19	22	11	14	10	12	14	9	16	18	20	15	16	12	16	11	16	12	22	14	13	23	13
Date	09/01	15/02	23/02	04/04	12/04	19/04	28/04	11/06	25/06	06/07	25/07	02/08	03/08	14/08	03/09	25/09	02/10	09/10	17/10	04/11	19/11	23/11	25/11	10/12
Irradiation	968	1655	2765	5311	6013	4390	3800	7621	3482	2666	7003	6018	5144	5495	4674	3721	2814	1433	3001	1730	1864	1481	982	664
Temperature	-2.2	0.2	6.0	11.5	15.1	8.4	11.0	18.7	24.1	17.6	23.7	20.3	18.3	24.8	22.4	17.8	10.2	15.0	13.2	3.2	10.3	6.9	4.6	1.6
Qh	97.7	85.2	39.6	17.4	0.0	8.8	10.6	0.0	0.0	0.0	0.0	0.0	0.0	0.0	0.0	0.0	0.0	0.1	0.0	64.9	31.4	42.9	57.9	83.3
Qc	0.0	0.0	0.0	0.0	0.0	0.0	0.0	1.8	33.6	0.1	40.8	23.4	11.4	34.9	22.7	0.4	0.0	0.0	0.0	0.0	0.0	0.0	0.0	0.0
BOLZANO 3D	24 Days 3D																							
Days	39	40	66	88	93	102	149	187	191	217	230	245	247	255	266	282	289	308	309	313	327	341	349	360
Nelements	16	14	7	21	14	16	16	17	20	19	6	11	17	14	19	17	22	21	10	14	14	13	20	7
Date	08/02	09/02	07/03	29/03	03/04	12/04	29/05	06/07	10/07	05/08	18/08	02/09	04/09	12/09	23/09	09/10	16/10	04/11	05/11	09/11	23/11	07/12	15/12	26/12
Irradiation	1487	1039	3996	4437	2771	6013	7403	2666	6913	6104	4859	3550	5111	3727	4720	1433	3073	1730	2620	1745	1481	777	1028	564
Temperature	0.9	-1.2	6.1	10.1	7.4	15.1	19.2	17.6	23.4	19.7	26.9	21.9	24.0	17.5	17.3	15.0	12.5	3.2	5.3	10.0	6.9	1.9	4.7	-3.7
Qh	76.7	91.1	41.3	14.5	30.8	0.0	0.0	0.0	0.0	0.0	0.0	0.0	0.0	0.0	0.0	0.1	0.0	64.9	47.6	22.3	42.9	78.8	63.8	109.6
Qc	0.0	0.0	0.0	0.0	0.0	0.0	8.6	0.1	31.2	10.0	47.9	21.1	30.4	0.0	1.4	0.0	0.0	0.0	0.0	0.0	0.0	0.0	0.0	0.0
BOLZANO 4D	24 Days 4D																							
Days	40	54	84	89	126	138	152	191	209	218	230	236	238	241	248	262	282	289	308	313	327	332	349	360
Nelements	17	24	14	17	17	13	14	14	6	12	8	12	12	12	12	21	17	18	21	16	15	25	21	7
Date	09/02	23/02	25/03	30/03	06/05	18/05	01/06	10/07	28/07	06/08	18/08	24/08	26/08	29/08	05/09	19/09	09/10	16/10	04/11	09/11	23/11	28/11	15/12	26/12
Irradiation	1039	2765	3495	4765	2692	6709	5911	6913	7054	7311	4859	5553	5976	3647	4894	4326	1433	3073	1730	1745	1481	1269	1028	564
Temperature	-1.2	6.0	9.9	10.6	17.5	15.2	17.5	23.4	25.3	19.3	26.9	20.7	21.3	20.0	23.3	16.9	15.0	12.5	3.2	10.0	6.9	0.8	4.7	-3.7
Qh	91.1	39.6	19.5	14.2	0.0	0.3	0.0	0.0	0.0	0.0	0.0	0.0	0.0	0.0	0.0	0.0	0.1	0.0	64.9	22.3	42.9	74.9	63.8	109.6
Qc	0.0	0.0	0.0	0.0	0.0	0.0	2.1	31.2	45.1	7.2	47.9	10.8	22.5	12.1	31.4	0.1	0.0	0.0	0.0	0.0	0.0	0.0	0.0	0.0
ZURICH 2D	24 Days 2D																							
Days	15	43	57	80	85	97	145	149	151	160	167	203	212	222	234	244	283	294	304	305	319	338	341	346
Nelements	15	23	9	15	6	21	21	13	18	17	30	15	13	6	10	8	7	20	11	11	21	17	14	24
Date	15/01	12/02	26/02	21/03	26/03	07/04	25/05	29/05	31/05	09/06	16/06	22/07	31/07	10/08	22/08	01/09	10/10	21/10	31/10	01/11	15/11	04/12	07/12	12/12
Irradiation	1313	804	3625	1714	5307	3263	7205	3250	1052	4698	5411	7604	4881	6363	1445	5667	3684	2140	2423	2560	327	492	1509	518
Temperature	-4.2	1.6	3.7	3.2	3.1	11.7	18.8	16.4	11.3	10.5	13.7	16.1	17.7	24.7	15.4	20.4	7.9	9.2	13.1	6.8	3.2	-1.4	-1.3	6.3
Qh	105.0	86.2	58.4	61.6	60.3	2.0	0.0	0.0	0.0	9.6	4.7	0.0	0.0	0.0	0.0	0.0	28.7	26.3	14.5	21.4	64.8	100.8	88.6	59.5
Qc	0.0	0.0	0.0	0.0	0.0	0.0	0.0	0.0	0.0	0.0	0.0	1.8	2.8	31.1	0.0	0.0	0.0	0.0	0.0	0.0	0.0	0.0	0.0	0.0
ZURICH 3D	24 Days 3D																							
Days	30	34	36	57	65	115	125	141	145	167	192	213	214	216	222	232	240	266	282	287	294	322	339	351
Nelements	19	25	15	13	21	13	15	10	21	27	8	13	14	13	6	7	11	13	10	22	16	20	15	18
Date	30/01	03/02	05/02	26/02	06/03	25/04	05/05	21/05	25/05	16/06	11/07	01/08	02/08	04/08	10/08	20/08	28/08	23/09	09/10	14/10	21/10	18/11	05/12	17/12
Irradiation	769	707	1548	3625	1327	837	7579	5211	7205	5411	967	4906	1725	3401	6363	5728	4587	3591	3583	2797	2140	451	1524	578
Temperature	5.2	1.3	-4.5	3.7	6.4	9.7	16.3	8.5	18.8	13.7	12.6	17.4	15.1	18.0	24.7	20.4	11.1	13.2	7.3	11.1	9.2	3.5	-0.6	-1.9
Qh	60.2	83.0	105.6	58.4	45.5	22.2	1.0	27.2	0.0	4.7	0.0	0.0	0.0	0.0	0.0	0.0	0.0	0.0	37.8	12.8	26.3	72.5	86.9	101.2
Qc	0.0	0.0	0.0	0.0	0.0	0.0	0.0	0.0	0.0	0.0	0.0	0.4	0.0	0.0	31.1	12.7	0.0	0.0	0.0	0.0	0.0	0.0	0.0	0.0
ZURICH 4D	24 Days 4D																							
Days	4	30	34	65	81	105	115	141	145	146	155	167	201	213	219	223	228	231	275	287	294	322	339	351
Nelements	12	19	25	21	5	16	14	11	13	18	18	32	15	16	9	2	5	6	13	22	16	20	19	18
Date	04/01	30/01	03/02	06/03	22/03	15/04	25/04	21/05	25/05	26/05	04/06	16/06	20/07	01/08	07/08	11/08	16/08	19/08	02/10	14/10	21/10	18/11	05/12	17/12
Irradiation	1079	769	707	1327	5166	3662	837	5211	7205	1586	3799	5411	7490	4906	7077	6373	6249	5449	2806	2797	2140	451	1524	578
Temperature	-5.6	5.2	1.3	6.4	2.0	4.7	9.7	8.5	18.8	14.0	12.9	13.7	16.4	17.4	20.0	25.8	23.2	20.2	16.8	11.1	9.2	3.5	-0.6	-1.9
Qh	110.6	60.2	83.0	45.5	60.0	45.5	22.2	27.2	0.0	0.0	1.1	4.7	0.0	0.0	0.0	0.0	0.0	0.0	0.0	12.8	26.3	72.5	86.9	101.2
Qc	0.0	0.0	0.0	0.0	0.0	0.0	0.0	0.0	0.0	0.0	0.0	0.0	1.3	0.4	4.7	43.5	25.5	13.2	0.0	0.0	0.0	0.0	0.0	0.0

Table D-2: Selection of 24-days sequences of Bolzano and Zurich.

Simulation

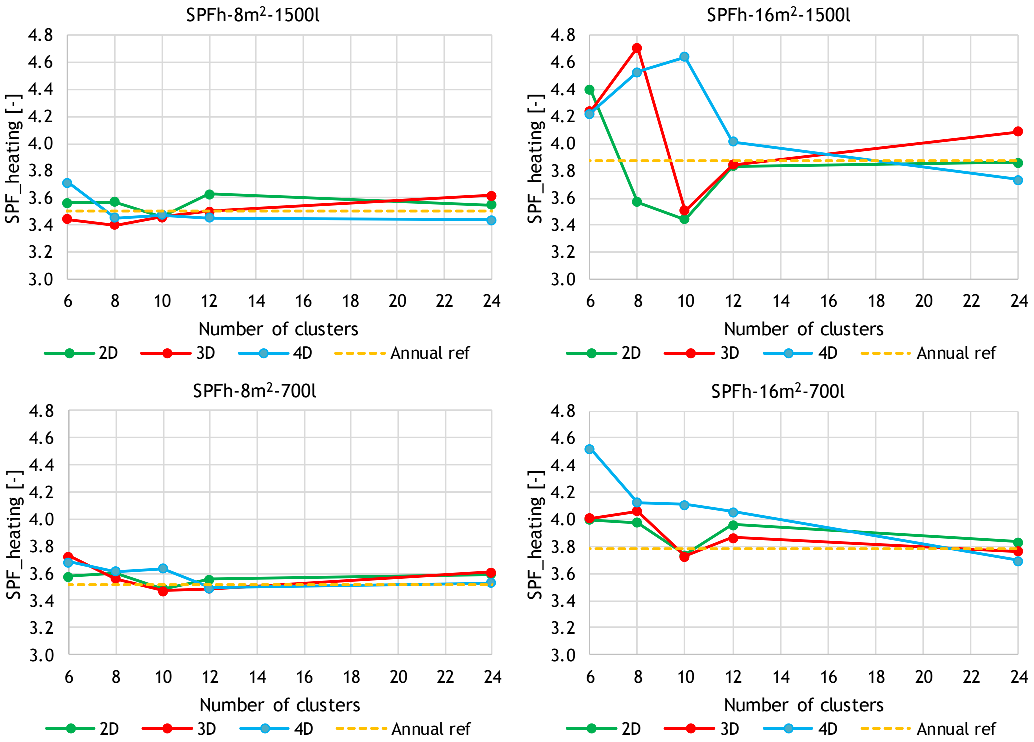

Figure D-9: Heating seasonal performance factor as a function of number of clusters. Bolzano climate.

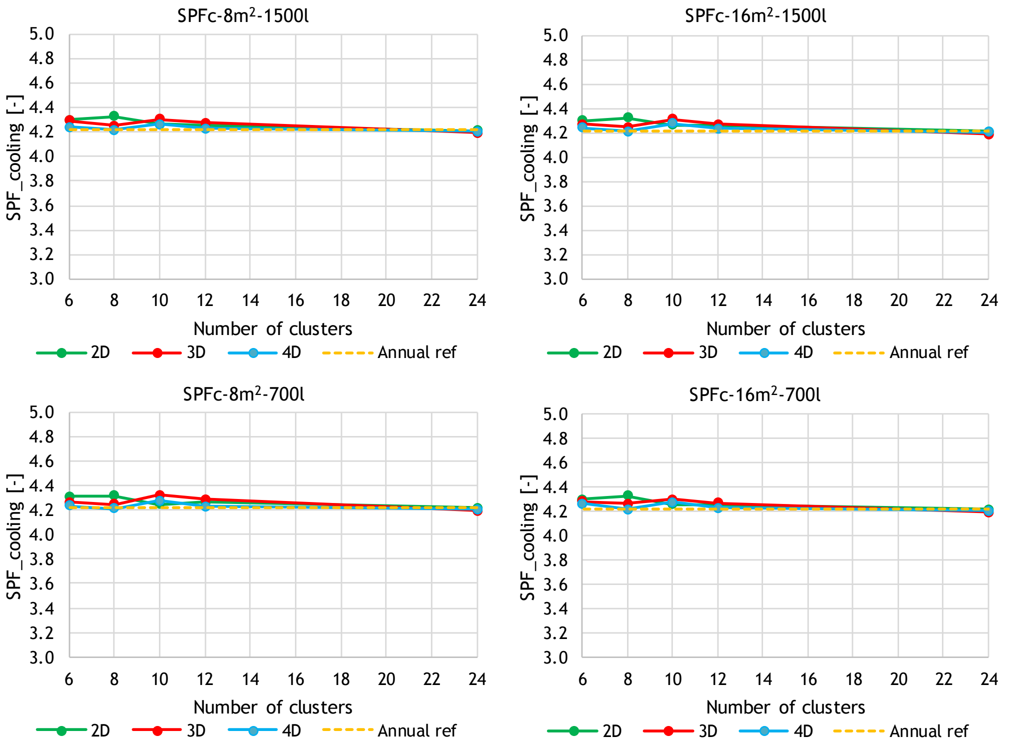

Figure D-10: Cooling seasonal performance factor as a function of number of clusters. Bolzano climate.

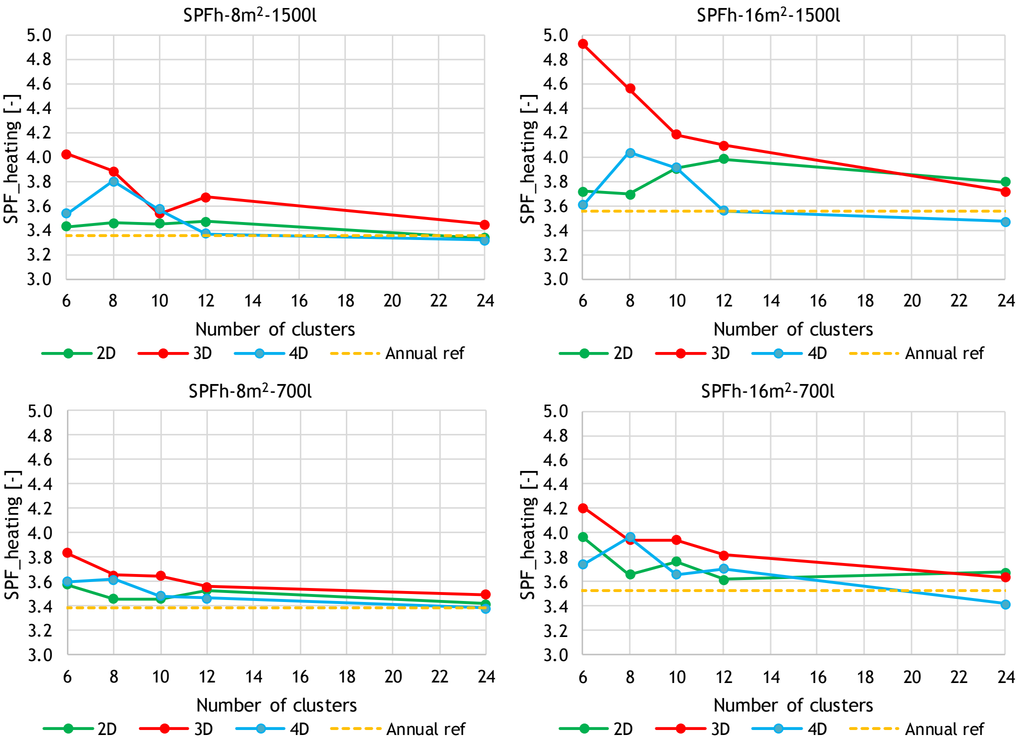

Figure D-11: Heating seasonal performance factor as a function of number of clusters. Zurich climate.

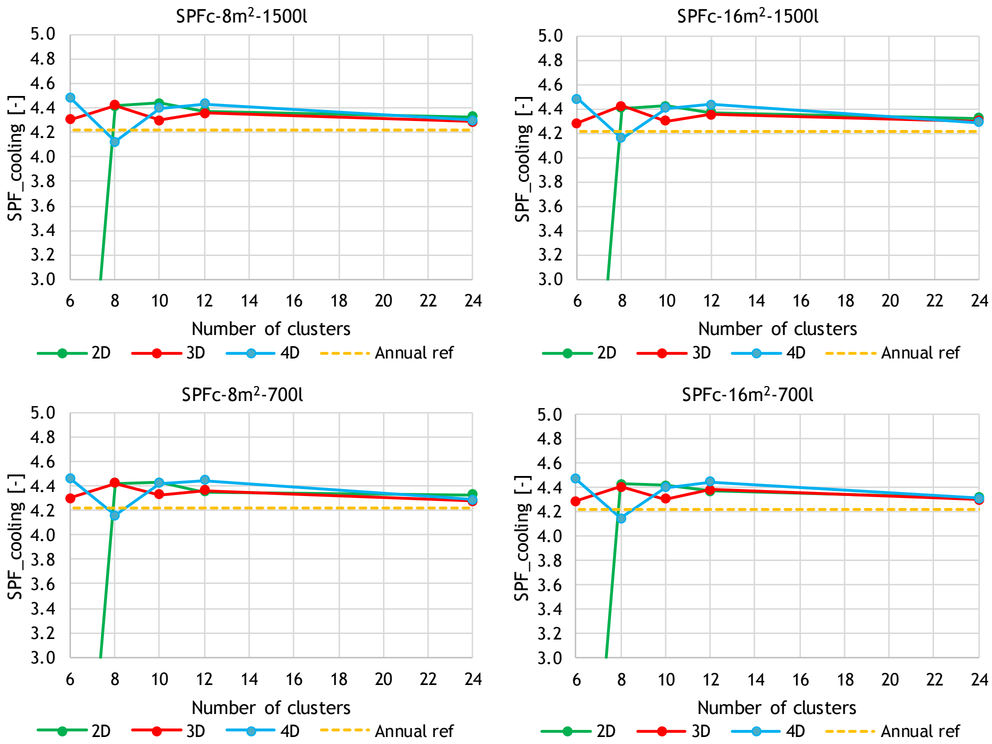

Figure D-12: Cooling seasonal performance factor as a function of number of clusters. Zurich climate.